THE INCLUSION BEHAVIOUR OF "WHEEL-AND-AXLE" HOST COMPOUNDS

Thesis submitted to the
University of Cape Town
for the degree of
Doctor of Philosophy

Louise Johnson

Department of Chemistry
University of Cape Town
Rondebosch
7700
South Africa

TABLE OF CONTENTS

ACKNOWLEDGEMENTS

I would like to extend thanks to the following people:

Prof Nassimbeni for brainstorming supervision,
Prof Mino Caira and Dr Diane Bond for all their help,
Susan for brain picking and other things,
Janet for all sorts of other things both otherwise and ordinary,
Lennid for car and computing help,
Stephen, Bridget & Graham for support,
the Foundation for Research Development for funding
and AECI Ltd. for a Postgraduate fellowship.

PARTS OF THIS THESIS HAVE BEEN PUBLISHED:

- "Complexation with Diol Host Compounds. Part 6. Structure and Dynamics of enclathration by 1,1,6,6-tetraphenyl-hexa-2,4-diyne-1,6-diol"
DR Bond, L Johnson, LR Nassimbeni & F Toda, J.Sol. State Chem., 92, 1991, 68-79.

- "Complexation with Diol Host Compounds. Part 8. Structures and Thermal Analysis of 1,1,6,6-tetraphenyl-hexa-2,4-diyne-1,6-diol with selected ketones", Acta Cryst. B, in press.

- "Complexation with Hydroxy Host Compounds. Part 4. Structures and Thermal Stabilities of Inclusion Compounds with dioxane as guest", SA Bourne, L Johnson, C Marais, LR Nassimbeni, K Skobridis, E Weber & F Toda, J.Chem.Soc, Perkin Trans. II, in press.

PARTS OF THIS THESIS HAVE BEEN PRESENTED AT:

XIIth European Meeting of the Union of Crystallographers, Moscow, USSR, 22-25 August 1989.

XVth Congress of the International Union of Crystallographers, Bordeaux, France, 19-28 July 1990.

AECI Seminar for young chemists
3-4 October 1990
3-4 October 1991

ABSTRACT

The inclusion behaviour of three "wheel-and-axle" host molecules was investigated. By virtue of their shape and the way in which they pack these host molecules are able to entrap guest molecules into a host-guest array. The host compounds were :
1,1,6,6-tetraphenyl-hexa-2,4-diyne-1,6-diol (HOST1),
4,4'-bis(diphenylhydroxymethyl)biphenyl (WEB11),
4,4'-bis(diphenylmethyl)biphenyl (WEB10).
The WEB11 host compound was found not to include guest molecules. The crystal structures of the non-porous α-phases of these three host compounds and the inclusion compounds were elucidated using single crystal X-ray diffraction methods. Both the diol hosts were found to form hydrogen bonded host-guest inclusion compounds with guests able to accept hydrogen bonds such as ketones. In these compounds there was host-guest hydrogen bonding and the hydroxy moieties of the host molecules adopted a trans conformation.

Host-host intermolecular hydrogen bonding existed in inclusion compounds containing guests unable to function as hydrogen bond acceptors. The host hydroxy moieties adopted a gauche conformation in order to allow host-host hydrogen bonding. Hydrogen bond formation was the directing force determining the form of the host-guest molecular array. The mechanism and kinetics of a solid-solid reaction between the host1 compound and benzophenone were investigated and electron microscopy showed the external habit of host1 α-phase to play an important role in propagating the reaction. The kinetics of the reaction occurring between solid host1 and acetone vapour was studied and an activation energy calculated. The kinetic behaviour of host1 could be explained in terms of exposed hydroxy moieties on the bc plane of the host1 α-phase.

Thermal analysis techniques were used to investigate the stability of these host-guest compounds. Thermogravimetry was used to evaluate the precise stoicheoimetry of the host-guest compounds as well as the complexity of their thermal decay. DSC was used to measure the enthalpies of thermal decomposition and to evaluate the strength with which the guest was held in the lattice. Correlation between thermal stability and the structure of these compounds was attempted and the results were encouraging. The problem lay in obtaining reliable values of the enthalpies of the guest release, a difficult task when dealing with compounds which are highly unstable at room temperature.

CHAPTER ONE

INTRODUCTION

The ability of a molecular component the host, to accommodate another component the guest, in a crystal lattice, exemplifies an inclusion compound. The inclusion of organic and inorganic guests in the lattices of hosts such as the hydroquinones, urea and bile acids had been recognised during the nineteenth century and new discoveries in the field of inclusion compounds burgeoned with the quantum leap in scientific knowledge and modern experimental techniques which have occurred this century **(1)**. The raison d'être and structural characteristics of these anomalous compounds were not fully understood until the pioneering work of HM Powell elucidated the crystal structure of quinol-sulphur dioxide compound using X-ray crystallography. A single molecule of sulphur dioxide was located within a cage formed by the quinol. This provided the fundamental insight and the experimental means that were required to comprehend the three-dimensional structural and bonding features of inclusion compounds **(2)**.

The way was paved for the understanding of structural frameworks of inclusion compounds comprised of hosts such as Dianin's compound, tri-o-thymotide, urea, the gas hydrates, intercalates of layer structures for example graphite, zeolites and the bile acids **(3)**. Later discoveries were the crown hosts, calixarenes, cavitands and carcerands **(4)**. These host compounds which may be regarded as 'classics' in the field of inclusion chemistry will not be discussed further as they have been repeatedly reviewed. This introduction will concentrate on the more recent host compounds which have been studied in the last twenty or so years. Powell subsequently coined the term "clathrate" in order to name compounds he described as possessing "an association in which molecular imprisonment was an essential element" **(5)**. Thus hosts would be molecular entities capable of forming closed cavities, channels or interlayer spaces, and thermodynamic stability and dense packing in the crystal lattice would be achieved if the voids or interstices were occupied by guest species **(6)**.

---

1 F Diederich, *Angew.Chem.Int. Ed.*, 27, 1988, 362

2 JED Davies, W Kemula, HM Powell & NO Smith, *J.Inclusion Phenomena*, 1, 1983, 3-44

3 JL Atwood, JED Davies & DD MacNicol (Eds), "*Inclusion Compounds*", Vol 1, Oxford University Press, Oxford, 1987, 13
E Weber (Ed), E Weber in "*Topics in Current Chemistry*", Vol 140, Springer-Verlag, Heidelberg, 1987, 3

4 JED Davies, W Kemula, HM Powell & NO Smith, *J.Inclusion Phenomena.*, 1, 1983, 3-44

5 JED Davies, W Kemula, HM Powell & NO Smith, *Ibid.*, 7

6 JL Atwood, JED Davies & DD MacNicol (Eds), "*Inclusion Compounds*", Vol 1, op. cit., 1987,15
E Weber (Ed), I Goldberg in *Topics in Current Chemistry*, Vol 149, Springer-Verlag, Heidelberg, 1988, 3
RM Barrer, *Pure & Appl.Chem.*, 58, no 10, 1986, 1317-1322

Such systems were of great interest and were pursued because of the possibilities which lay in molecular separation, inclusion polymerisation, enantiomer resolution, thermal-/photo-isomerisation and crystal engineering **(7)**. In addition to these, parallels with certain biological ion transport processes had been observed, and in vitro attempts to mimic these systems were intended. In many biological systems, functional groups attached to cavities provide reactive surfaces at which the selective binding of substrates occurs **(8)**.

Such applications are possible because of the selectivity and discrimination which occur upon incorporation of a guest species into a particular host lattice. Topological control could be exercised when forming a host-guest clathrate, and thus structures of clathrate-forming hosts could be extended either by constructing new hosts, or else by modifying the architecture of existing host compounds. A logical extension was to vary the size and nature of the inclusion lattice cavities in order to force selective inclusion of guest entities. The pursuit of a uniquely discerning host molecule which will form predictable stereospecific biologically relevant host-guest compounds has been tackled in a variety of innovative ways spanning the last three decades **(9)**.

---

7 E Weber in *Topics in Current Chemistry*, Vol 140, op. cit., 1988, 4-7

8 J-M Lehn, *Nobel Lecture*, 1988
F Diederich, *Angew.Chem. Int.Ed.Engl.*, 27, 1988, 362-386

9 JL Atwood, JED Davies & DD MacNicol, "*Inclusion Compounds*", Vol 4, Oxford University Press, Oxford, 1991

In pursuit of the perfect Host

Dianin's compound, shown in figure 1, proved to be a versatile candidate for host fine-tuning, since modification of ring substituents resulted in a change in the size and shape of the cavity in the clathrate, as illustrated in figure 2 **(10)**.

Figure 1 Dianin's compound

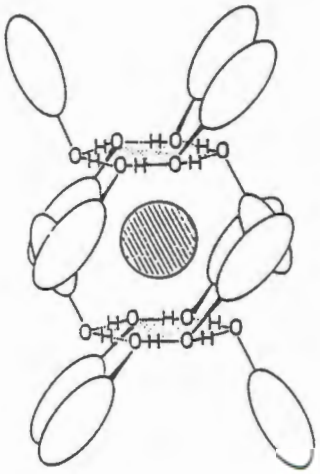

Figure 2 Modifying the size and shape of the cavity

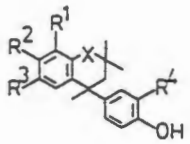

2a X=S, R^1-R^3= H

2b X=S, R^1= CH_3, R^2-R^4=H

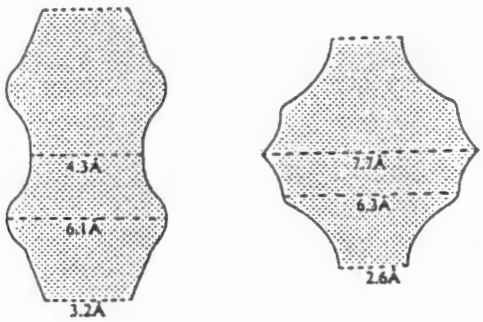

2a **2b**

Hexagon building blocks were identified as the main structural characteristics of such clathrates and this feature had also been observed in the packing of the quinol clathrates whose structures are characterised by hydrogen-bonded hexamers. Figure 3a shows a hydrogen bonded hexamer unit typical of phenolic hosts such as Dianin's compound. The concept of the hexagon as a template for clathrate formation was utilised by

---

10 JED Davies, W Kemula, HM Powell & NO Smith, *J.Inclusion Phenomena*, 1, 1983, 3-44

MacNicol **(11)**, who designed a new class of hosts (hexahosts), which were characterised by a hexa-substituted benzene constitution, see figure 3b . Fine-tuning hosts of this type was effective via the adjustment of the bulk of the side arms. This meant that the dimensions of the inclusion cavity could be engineered on an ad hoc basis so as to meet the geometric requirements of each guest.

Figure 3a A hydrogen bonded hexamer unit:

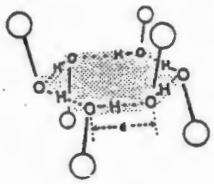

Figure 3b The hexa-host design:

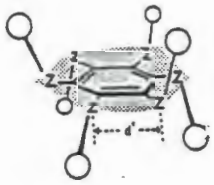

Thus, experiments in controlled clathration were under way and novel hosts were synthesized in accordance with predicted clathrating behaviour in order to influence inclusion by means of their shape, flexibility and functionality.
Non-polar inclusion compounds are stabilized by weak van der Waals forces and molecular arrangements dominated by steric factors. On the other hand, the presence of polar species in an inclusion compound implies that directional influences will stem primarily from interactions between polar functions, in addition to the influence of dispersion forces occurring between hydrophobic fragments **(12)**. Figure 4 illustrates schematically how the components possessed by a host entity would form a host-guest inclusion compound in which there are two main types of stabilizing influences: coordinative interactions and steric hindrance.

Figure 4 Design features of a host molecule

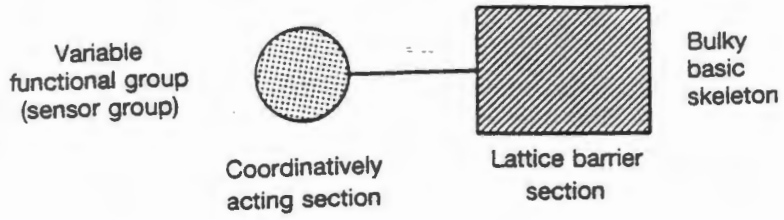

---

11 E Weber in "*Topics in Current Chemistry*", Vol 140, op. cit., 1987, 7-8
G Desiraju (Ed), G Tsoucaris in "*Organic Solid State Chemistry*", Elsevier, Amsterdam, 1987

12 JL Atwood, JED Davies & DD MacNicol (Eds), "Inclusion Compounds", Vol 4, op. cit., 1991

NOMENCLATURE

The types of host-guest inclusion compounds may be classified using a nomenclature devised by Weber and Josel **(13)** which is described below.
The main criteria are
- the type of interaction between host and guest if any
- the topology of the host-guest aggregate.

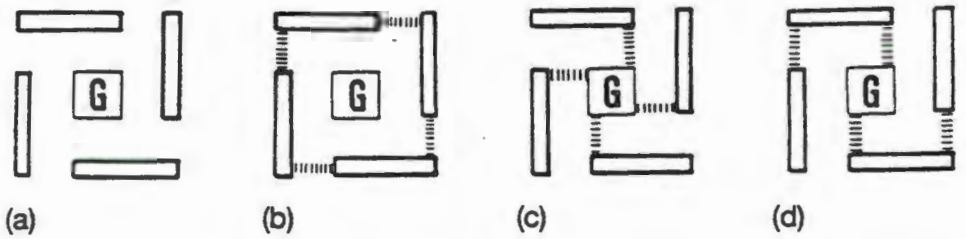

Figure 5

5a This is considered to be a true **clathrate** in which there are no coordinative interactions. Stabilization is due to the topology of the clathrating components in which the guest is retained by the steric barriers of the host lattice alone.
5b As for 1a, but there is additional stabilization owing to functional interactions between host components, this is called a **coordination-assisted clathrate host lattice.**
5c This is a **coordinato clathrate** in which there are only coordinative host-guest interactions.
5d **Coordinato clathrate in a coordination-assisted host lattice** in which there are both coordinative host-host and host-guest interactions.

---

13 E Weber & HP Josel, *J.Incln.Phenomena*, 1, 1983, 79-85

Figure 6 schematically illustrates the coordinatoclathrate concept.

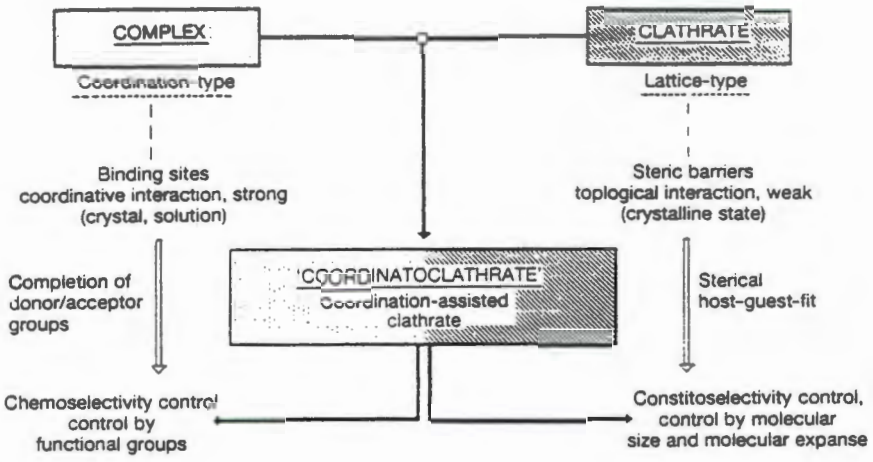

Further terms which are used to describe the type of cavitate are:
intercalate = a two-dimensional open-standing, layer or sandwich-type inclusion compound,
tubulates = one-dimensional open, channel inclusion compounds,
ædiculates = inclusion compounds containing cavities or niches,
cryptates = totally enclosed cage inclusion compounds,
coronates = ring-shaped hosts,
podates = open-chained hosts.
(14)

---

14 E Weber & HP Josel, *J.Incln.Phenomena*, 1, 1983, 79-85
E Weber in "*Topics in Current Chemistry*", vol 140,op. cit., 3-20
E Weber in "*Inclusion Compounds*", Vol 4, op. cit., chapter 5,

How is a successful host compound designed ?

A molecule possessing bulky groups will be unable to form close packing and will therefore be unable to reach the energy minimum corresponding to crystal lattice formation. It will therefore be energetically favourable for guest molecules to occupy the voids (which exist as a consequence of inefficient packing), in order to achieve stabilization. In addition to the requisite steric features, the host entity should have sufficient rigidity to support the clathrate lattice. Extra stabilization would result from suitably appended functional groups. Figure 7 shows how a coordinatoclathrate forms **(15)**. Thus a versatile host requires certain intrinsic features, in order to be conducive to inclusion compound formation.

Figure 7 Coordinatoclathrate formation

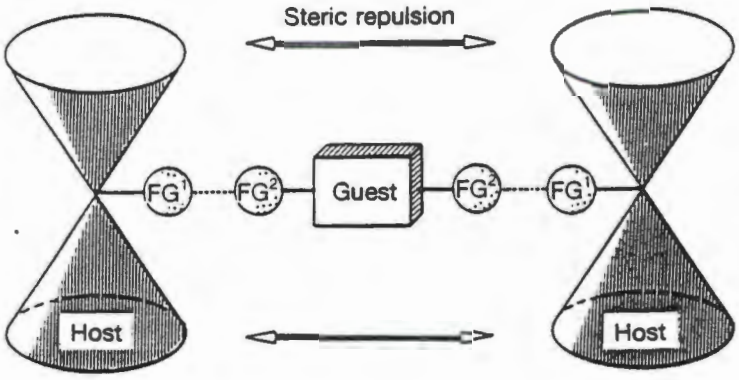

What are some examples of host compounds?

Toda **(16)** devised a structural class of host compounds which contain 'planar' elements as well as bulky groups. The 'planar' elements act as a rigid frame for the lattice aggregate and, in combined effect with the bulky spacer groups, spaces within the crystal lattice are effectively portioned off **(17)**. Host compounds of this type are termed "wheel-and-axle" hosts by virtue of their molecular shape which consists of a long axis with bulky groups at either end **(18)**.

---

15 E Weber in "*Inclusion Compounds*", Vol 4, op. cit., chapter 5

16 F Toda & K Akagi, *Tetrahedron Letters*, 1968, 3695

17 E Weber & M Czugler in "*Topics in Current Chemistry*", vol 149, op. cit., 54

18 F Toda, DL Ward & H Hart, *Tetrahedron Letters*, 22, no 39, 1981, 3865-3968

In the crystal phase, the concave sites along the molecular axis may be occupied either by a convex fragment of an adjacent host molecule, or else by a complementarily shaped guest molecule with which the host compound co-crystallizes **(19)**.
In order to enhance selectivity of a geometrically favourable host, directional control in the form of functional groups was introduced. Thus effective molecular binding not only depends on the "goodness of fit" of guest within a lattice, but also upon favourable functional group interactions. Therefore, in the light of the coordination-assisted clathrate tenet, the introduction of functional groups to act as sensors may provide sites for guest binding, as well as encouraging host-host interactions, thus achieving improved inclusion selectivity **(20)**. Effective host-guest interactions usually occur via hydrogen bond formation. Thus functional group candidates are hydroxyl, carbonyl and amide moieties.

"Wheel-and-axle" compounds, some examples

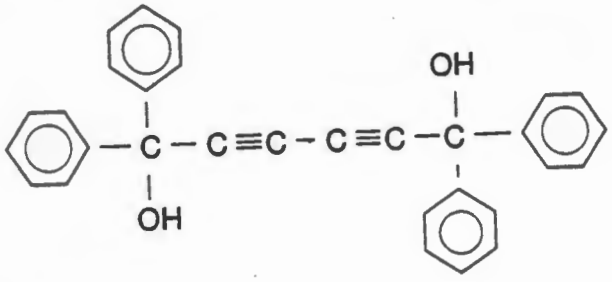

1a

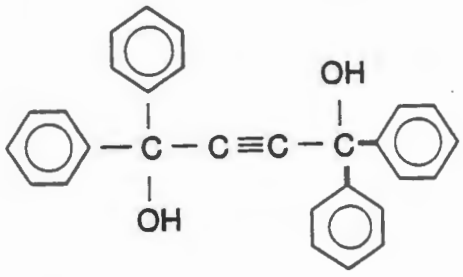

1b

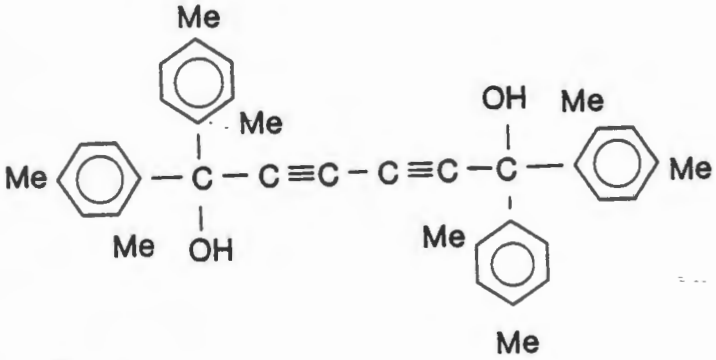

2

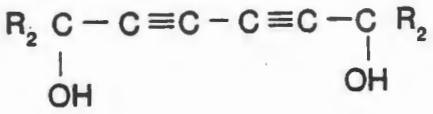

3a R=Me
3b R=Et
3c R=Bu-t

---

19 H Hart, L-T W Lin & I Goldberg, *Mol.Cryst. Liq.Cryst.*, 137, 1986, 277-286

20 I Goldberg in *"Inclusion Compounds"*, Vol 4, op. cit., 415
E Weber & M Czugler in *"Topics in Current Chemistry"*, Vol 149, op. cit., 1989, 47-55

Host compounds 1a and 1b are able to include a wide variety of guest compounds and form crystalline inclusion compounds **(21)**. In the majority of the cases, inclusion is mediated via hydrogen bond formation. Host compound 2 contains bulkier spacer groups, the phenyl rings having been dimethylated. Enhanced inclusion ability is obtained owing to the larger voids that such a host compound is able to create in the crystal phase. If, on the other hand, the spacer groups are decreased in size, little inclusion (3c), or no inclusion (3a and 3b) is obtained **(22)**.

Host 1a was able to separate isomeric mixtures **(23)**. For example, it complexed with the keto tautomer from the 2-mercapto substituted tropane tautomeric mixture **(24)**. Host 1a also proved to be successful in the isolation of natural products, by selectively complexing with brucine from a mixture of strychnine and brucine, as well as in the efficient isolation of nicotine and caffeine from their natural products **(25)**. One of the most important recent innovations in organic chemistry has been the study of solid-solid reactions in pursuit of higher yields and better selectivities. Thus Dieter Seebach, in his recent review entitled "Organic Synthesis - Where now?", highlights the work of Toda in this area **(26)**. Some organic reactions were found to proceed faster and/or more selectively in the solid state, for example, pinacol rearrangements, Grignard reactions, Baeyer-Villiger oxidation reactions and reductions of ketones with $NaBH_4$ using β-cyclodextrin as the chiral host **(27)**. Recently Toda has described a new method of synthesizing unsymmetrical ethers by co-crystallizing secondary alcohols and subsequent treatment with toluene-p-sulphonic acid **(28)**.

---

21 F Toda & K Akagi, *Tetrahedron Letters*, 33, 1968, 3695-3698

22 F Toda in "*Topics in Current Chemistry*", Vol 140, op. cit., 1987, 43-47

23 I Goldberg, Z Stein, A Kai & F Toda, *Chem. Letters*, 1987, 1617-1620
F Toda, K Tanaka, Y Wang & G-H Lee, *Chem. Letters*, 1986, 109-112

24 F Toda, K Tanaka, T Asao, Y Ikegami, N Tanaka, K Hamada & T Fujwana, *Chem. Letters*,1988, 509-512

25 K Fukawa, S Harada, N Kasai, M Toda, K Mori & F Toda , *Bull.Chem.Soc.Jpn.*, 62, 1989, 2714-2716
F Toda in "*Inclusion compounds*", vol 4, op. cit., 143-147

26 D Seebach, *Angew.Chem.Int.Ed.Engl.*, 29, 1990, 1320-1367

27 F Toda, In "*Inclusion compounds*", vol 4, op. cit., 182
F Toda, K Tanaka & A Sekikawa, *J.Chem.Soc. Chem.Commun.*, 1987, 279-280
F Toda, M Yagi & K Kiyoshige, *J.Chem.Soc. Chem.Commun.*, 1988, 958-959

28 F Toda & K Okuda, *J.Chem.Soc. Chem.Commun.*, 1991, 1212-1214

Moreover, certain "wheel-and-axle" hosts , for example the versatile host 1a, were able to act as reaction frameworks within which appropriately oriented guests could be irradiated in the solid state and form stereospecific chiral photoproducts **(29)**. This is possible because reactions in the solid state proceed with minimum atomic and molecular movement. According to the topochemical postulate, a conformationally sensitive reaction will proceed in the crystal only if the molecular conformation is conducive to reaction **(30)**, which means that a photoreaction involving guests will be governed by the manner of packing in the crystal structure **(31)**. Compound 1a formed a 1:2 host-guest inclusion compound in which molecules of chalcone were entrapped at a certain distance apart (< 4Å which proved to be the prerequisite maximum separation for photoreactions of this sort), as shown in figure 8. The *syn* head-to-tail photodimer was formed upon irradiation because of the specific conformation and molecular orientation that the chalcone adopted as a guest **(32)**. Photochemical reactions such as this may be described in terms of reactant guest molecules being introduced within a matrix formed by the host molecules, where the host provides "hanging sites through hydrogen bonding for organization of the guest molecules" **(33)**.

Figure 8 The conformation of the reacting centres of the chalcone molecules

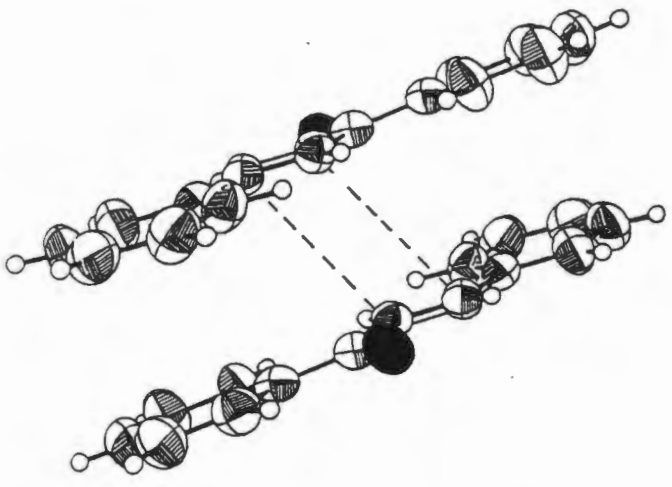

---

29 F Toda, in "*Inclusion compounds*", vol 4, op. cit., 166-180
F Toda, K Tanaka & M Yagi, *Tetrahedron*, 43, no 2, 1987, 1495-1502

30 MD Cohen, *Tetrahedron*, 43, no 2, 1987, 1211-1222

31 R Lamartine, *Bull.Soc.Chimique France*, 2, 1989, 237-246

32 K Tanaka & F Toda, *J.Chem.Soc. Chem.Commun.*, 1983, 593-594

33 M Kaftory, K Tanaka & F Toda, *J.Org.Chem.*, 50, 1985, 2154-2158
M Kaftory, *Tetrahedron*, 43, no 2, 1987, 1503-1511

Host compound 5, shown in figure 9a , is an example of a chiral host which was effective in resolving a variety of racemates both in the crystal form as well as in solutions of its host-guest inclusion compound. This host complexes with guests such as 2,3-epoxycyclohexanones and 5-methyl-γ-butyrolactone so as to produce an optically pure product **(34)**. The influence of the rigidity of the molecular axis was investigated by synthesizing the host containing an alkyl backbone as shown in figure 9b. Since it did not exhibit any inclusion properties, it was concluded that rigidity of the host moiety, ie limited degrees of freedom, is important if a molecule is to function effectively as a host.

Figure 9a

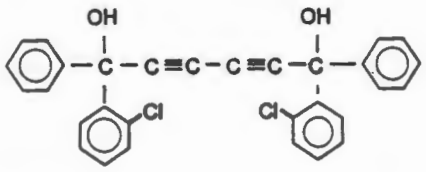

9b

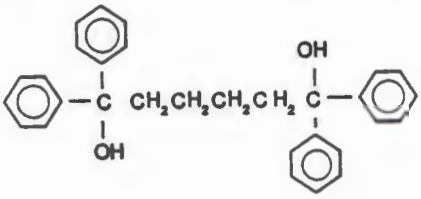

Hart and co-workers extended and generalised this concept using Toda's hosts as a basic design but with altered structural details. They eliminated hydrogen bonding functionality by replacing the hydroxyl group of 1a with a third aryl group, as shown in figure 10, and found that inclusion was still achieved with a significant degree of success. Host-guest complexation was also observed when the molecular backbone was altered in length and linearity. The hosts packed so that their molecular axes were aligned and the structures typically contained channels **(35)**.

Figure 10 A host molecule with no functionality

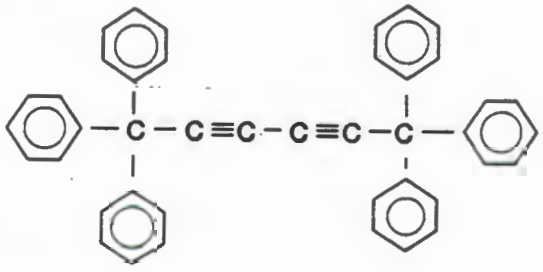

---

34 F Toda in "*Inclusion Compounds*", vol 4, op. cit.,
F Toda, K Tanaka & M Yagi, *Tetrahedron*, 43, no 2, 1987, 1495-1502

35 H Hart L-T W Lin & DL Ward, *J.Amer.Chem.Soc.*, 106, 1984, 4043-4045
H Hart L-T W Lin & I Goldberg, *Mol.Cryst.Liq.Cryst.*, 137, 1986, 277-286

Weber and coworkers used a similar host molecular shape concept , but in their case the rigid backbone comprised an allene moiety and the spacer units were large aromatic substituents. Figure 11 shows a typical example of such a host; it has a relatively rigid and non-bulky backbone and bulky aromatic substituents **(36)**.

Figure 11

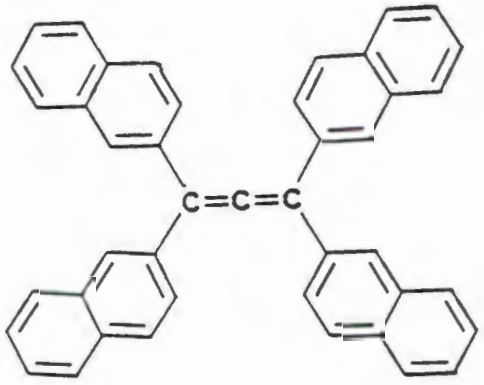

These hosts were able to include a variety of alicyclic , aromatic and heterocyclic similarly proportioned guest compounds. Modification of the channel size may be achieved by using large aryl substituents in the host compound and in this way altering the steric barrier and forcing inclusion selectivity. Lengthening the molecular axis created additional space for the inclusion of guest molecules.

Scissor-like host compounds

Hosts designed with the shape of scissors have two-fold symmetry and were found to be amenable to inclusion compound formation. Furthermore, since such hosts are chiral , they may enantioselectively include guests. The host compound illustrated in figure 12 exhibits interesting inclusion properties and can selectively include a guest component from a solvent guest mixture. Such hosts readily form stoicheiometric crystalline inclusion compounds with a variety of small, often polar, organic molecules **(37)**.

---

36 I Goldberg in "*Inclusion Compounds*", Vol 4, op. cit., 1991
E Weber, W Seichter, I Goldberg, G Will & H-J Dasting, *J.Incln.Phenomena*, 10, 1991, 267-282

37 I Csöregh, A Sjögren, M Czugler, M Cserzö & E Weber, *J.Chem.Soc. Perkin Trans 2*, 1986, 507-513
I Csöregh, M Czugler, A Ertan, E Weber, J Ahrendt, *J.Incln. Phenomena*, 8, 1990, 275-287
I Csöregh, M Czugler, E Weber, J Ahrendt, *J.Incln. Phenomena*, 8, 1990, 309-322

Depending on the spatial requirements of the guest and on the number of functional groups, different host-guest stoicheiometries were obtained.

Figure 12 1,1'-Binaphthyl-2,2'-dicarboxylic acid - the prototype scissor-like host

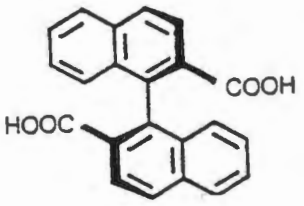

It was possible to vary the position and type of functional groups in order to create modified binaphthyl hosts such as those shown in figures 13a, 13b and 13c. Increasing the distance of the carboxylic acid moiety from the anchoring naphthyl moiety, by introducing a methylene moiety as shown in figure 13a and b, proved to be detrimental to inclusion behaviour as it introduced too much conformational flexibility and functional group dimerisation and dense crystal packing. The position of the carboxylic acid group has been moved in the host compound shown in figure 13c. This compound exhibited modest clathrate-forming ability and formed organic salt-like associations containing pyridine and a variety of non-basic solvents including cyclic ethers, dipolar aprotic compounds and acids. These compounds were characterised by an intramolecular hydrogen bond between the carboxylic moieties **(38)**.

Figure 13a

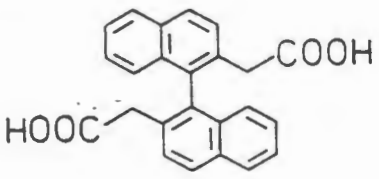

13b

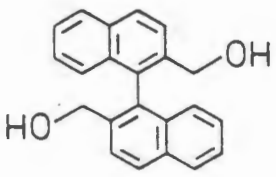

13c

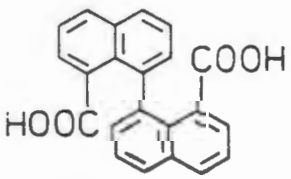

---

38 E Weber,"Inclusion Compounds", Vol 4, *op.cit.*, 223-228

The scissor-like hosts possess rigid or semi-rigid molecular skeletons, and since a preformed receptor site is important in order for the complexation and recognition of a substrate, the concept of preorganization of the binding site was extrapolated to apply to these host compounds as a design feature **(39)**. Crystal structures of these roof and scissor-like hosts have indicated that host-to-host and guest-to-guest interactions occur preferentially over host-guest bonding **(40)**.
Extension of the "roof" and "scissor" concepts led to the creation of host compounds in which the central axis had been expanded to three or four atoms. Additional functionality and spacers could then be attached to the three- or four-membered rings and these small ring inclusion hosts could be specifically modified to suit individual guest entities by varying the nature, number and position of functional groups as well as the substituents and ring size. The extension of the linear molecular axis into a three or four-membered ring is shown schematically in figure 15 **(41)**.

Figure 15 The design concept of small-ring inclusion hosts
(the spheres are replaceable groups)

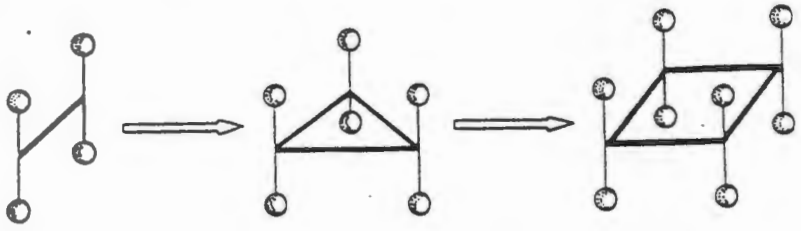

Recently Weber and coworkers have synthesized an extensive family of new lattice-forming hosts which are simple yet highly variable in structure : the singly bridged triarylmethane host frameworks form inclusion compounds with a number of uncharged organic molecules, both polar and apolar. Inclusion compound formation depends on the structural features of the hosts: the size and shape of the substituents, the bridging group, the spacer and the functional groups **(42)**. Figure 16 illustrates the host design concept as well as some examples of hosts of this type.

---

39 E Weber, Inclusion Compounds", Vol 4, *op.cit.*, 251

40 I Csöregh, M Czugler, E Weber & J Ahrendt, *J.Incln.Phenomena*, 9, 1990, 309-322

41 E Weber, M Hecker, I Csöregh & M Czugler, *Mol.Cryst.Liq.Cryst.*, 187, 1990, 165-174
E Weber, M Hecker, I Csöregh & M Czugler, J.Am.Chem.Soc., 111, no 20, 1989, 7866-7872

42 E Weber, N Dörpinghaus & I Csöregh, *J.Chem.Soc. Perkin Trans 2*, 1990, 2167-2177

Figure 16

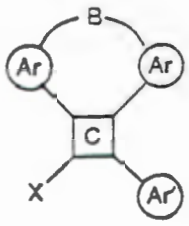

Ar = aryl unit
B = bridge element
X = functional group

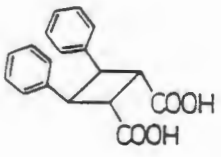

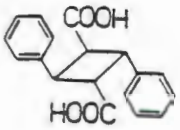

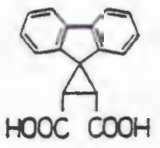

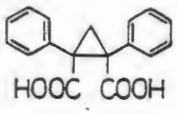

Bishop and Dance prepared novel diol host compounds which were able to form a unique type of clathrate architecture **(43)**. Figure 17 shows the double helical sequence of hydrogen bonded diol molecules which form a tube upon clathrate formation. A number of molecules aggregate to leave a channel which may be occupied by many different guests.

Figure 17

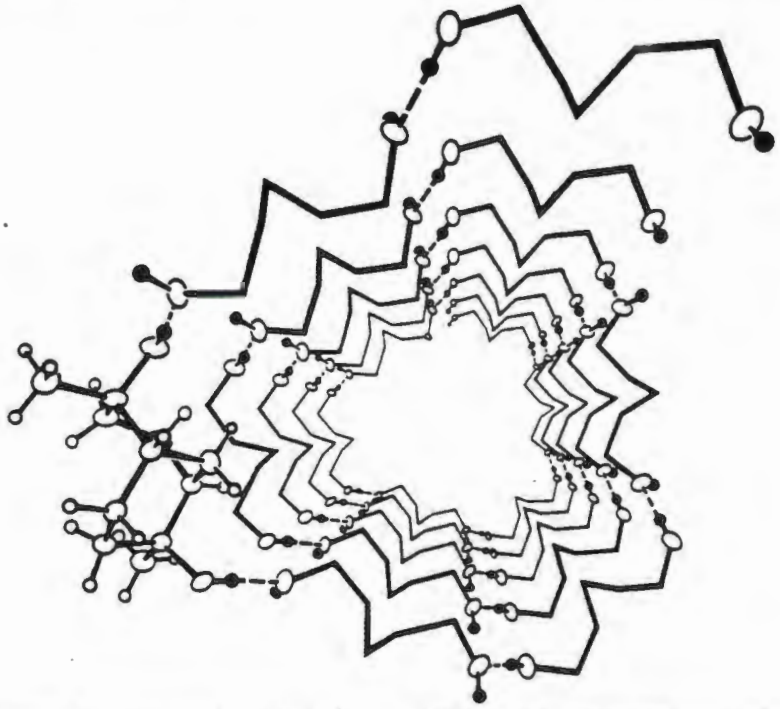

The figure below shows a prototype of this host which was appropriately derivatised and other compounds which formed similar clathrate structures were obtained.

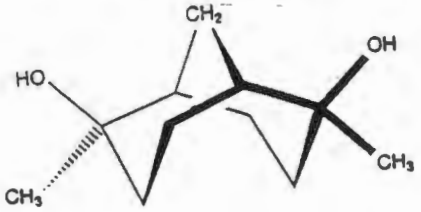

---

43 R Bishop & IG Dance in "*Topics in Current Chemistry*", op. cit., Vol 149, 1988
R Bishop & IG Dance in "*Inclusion Compounds*", Vol 4, op. cit., 1991

AIM OF THIS WORK

Studies of three "wheel-and-axle" host compounds were carried out in an attempt to contribute to the existing knowledge in the field of crystal engineering.
Bearing in mind that the formation of host-guest inclusion compounds is both complicated and subtle, we sought to identify whether there were patterns evident in the crystal packing of these compounds which could be related to host, and to variations in guest. We also aimed to perform stability studies on the host-guest compounds in order to obtain an insight into the manner and strength with which guest molecules were held. Thus the inclusion compounds formed were subjected to thermal analysis, with the aim of measuring the enthalpy of the guest-release reactions and thereby to correlate host-guest interaction with structure. This process was further studied by carrying out a kinetic study on a solid-vapour system and a solid-solid system.

The three "wheel-and-axle" host compounds

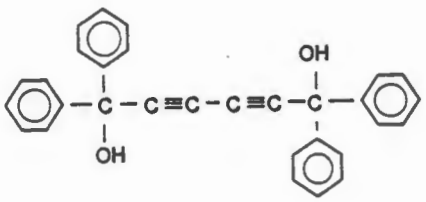

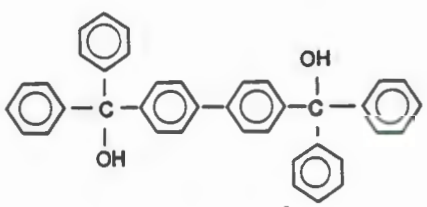

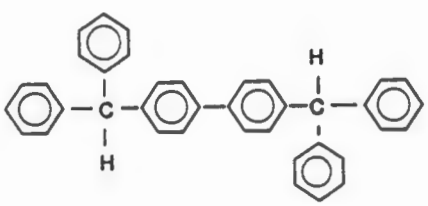

CHAPTER TWO

PREPARATION OF THE HOST COMPOUNDS

1) 1,1,6,6-Tetraphenylhexa-2,4-diyne-1,6-diol - **Host1**

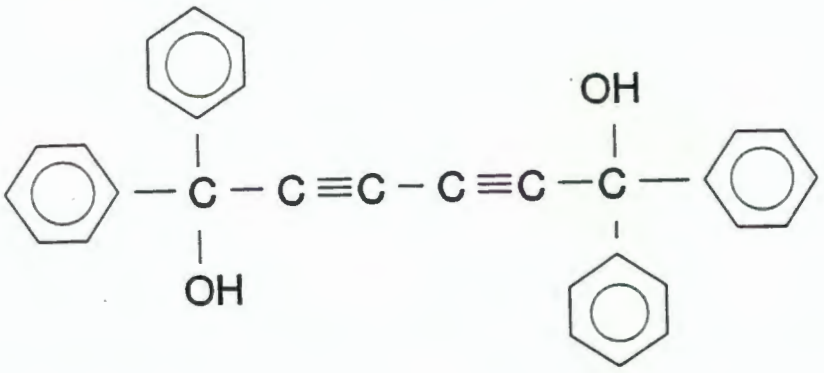

This compound was synthesized by Fumio Toda of Ehime University in Japan according to the oxidative coupling method as performed by W. Ried, W. Schlegelmilch and S. Piesch. They dissolved 0.1g of sodium metal in liquid ammonia whilst stirring at -40°C. 200mg of crystalline Fe(III)nitrate hydrate was used as catalyst and sodium amide was produced. After the blue colour disappeared, 0.05mol of hexadiynediol dissolved in ether, which had been obtained from a rearrangement of disodiumdiacetylene, was added dropwise, and this solution was stirred for two hours. 0.05 mol of benzophenone, dissolved in ether, was then added at -40°C. The suspension that was obtained was stirred at -35°C to -40°C for twenty hours. The solution was then neutralised with solid ammonium chloride and the ammonia was evaporated off. The ether extract was dried with sodium sulphate and recrystallisation was carried out in petroleum ether **(1)**.

2) 4,4'-bis(diphenylhydroxymethyl)biphenyl - **WEB11**

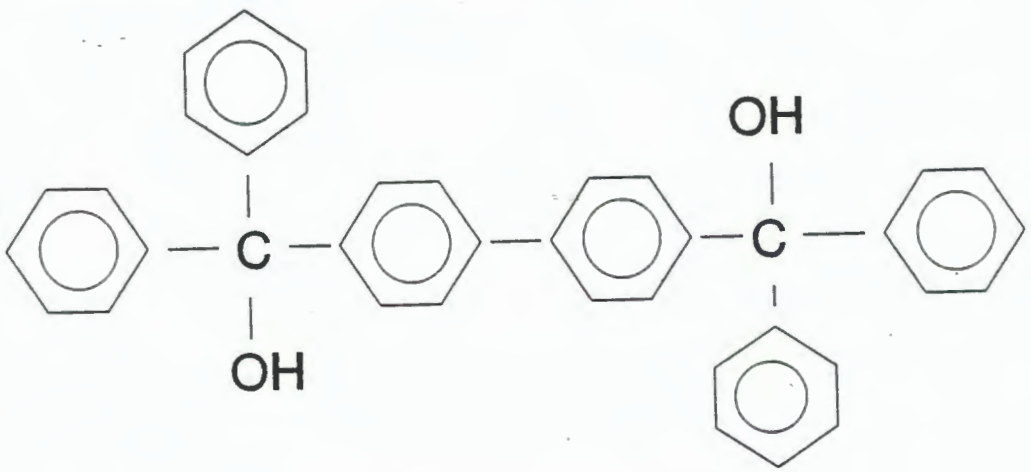

---

1 W. Ried, W. Schlegelmilch & S. Piesch, *Chem.Ber.*, 96, 1221, 1963

WEB11 and WEB10 host compounds were synthesized by Edwin Weber at Bonn University. The precursor, 4,4'-dibenzoylbiphenyl, was synthesized as follows. Twenty grams of biphenyl was added to a stirred suspension of 50g $AlCl_3$ in 50g benzoyl chloride and heated until a solid mass formed. After standing overnight, the mixture was quenched with ice and the solid separated by vacuum suction. Any residual benzoyl chloride was removed by heating with ethanol and separated off. 4,4'-dibenzoylbiphenyl was recrystallized from chloroform in a 65.8% yield.

WEB11 was then prepared as follows: A Grignard solution prepared from 12.0g bromobenzene and 1.95g Mg cuttings in 100 ml of dry diethylether, was dropped into a stirred suspension of 9.0g 4,4-dibenzoylbiphenyl in 100 ml benzene. The violet coloured solution thus formed, was then refluxed for three hours. After cooling to room temperature, 100 ml benzene was added, and the mixture was separated, dried with Na_2SO_4 and evaporated to 100 ml. Upon cooling in a refrigerator, the product precipitated out as a solid which was recrystallized from benzene to give the 1:1 benzene solvate. The benzene was desorbed from this inclusion compound by vacuum drying at 100°C, 15 Torr, and there was a 73.3% yield of the pure product which had a melting point of 160-161°C **(2)**.

3) 4,4'-bis(diphenylmethyl)biphenyl - **WEB10**

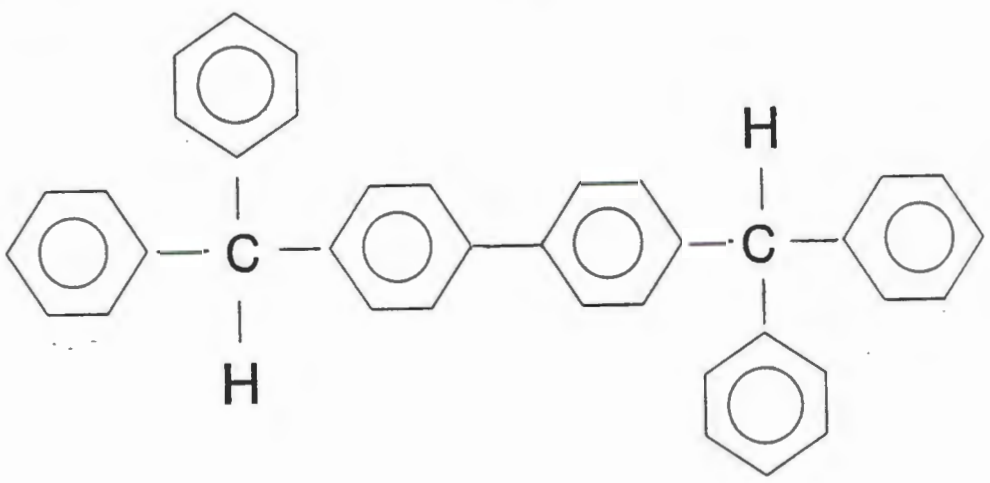

WEB10 was prepared by dissolving 8g of WEB11 in 120ml of hot acetic acid. This was refluxed with 16g Zn-powder for three hours. Excess zinc and solid zinc acetate were filtered off and washed with hot acetic acid. Cooling of the filtrate yielded a solid precipitate which was treated with hot water to complete removal of the zinc acetate. Recrystallization was carried out in acetone giving a 91% yield.

---

2 W Schlenk, M Brauns, *Ber.Dstch.Chem.Ges.*, 48, 1915, 716

PREPARATION OF HOST-GUEST CRYSTALS

Concentrated solutions of the host compound dissolved in the guest or with the guest in a mutual solvent, were allowed to evaporate slowly. Crystals were obtained on standing for a period that ranged from 1-30 days. The quality of these crystals was then rated by their ability to extinguish plane polarised light. This was carried out using a Nikon Stereoscopic microscope SMZ-10.

MELTING POINTS

The melting points of the compounds were measured on a Linkam CO600 Hotstage and Controller. The Nikon Z-10 Stereo Microscope had a photographic extension onto which a Nikon FX-35 camera was attached. Photographs of the melting process could then be taken using this apparatus in conjunction with a Nikon Microflex AFX-II Photomicroscopic Attachment. Melting points were confirmed using the Differential Scanning Calorimeter which will be discussed in more detail later in this chapter.

DENSITY MEASUREMENTS

Density measurements were made using the principle of flotation, and readings were taken with a Paar DMA 35 Digital Density meter. This was done as follows: The density of a water/saturated aqueous potassium iodide solution was read at the point at which the crystal concerned remained suspended within the fluid. This was repeated with a fresh crystal in order to eliminate any error owing to crystal deterioration, and an average value was taken.

NMR

^{1}H NMR scans were performed using a Varian 200 multinuclear spectrometer and were carried out in order to characterize the inclusion compounds. However, this method was not sufficiently accurate to establish precise host-guest ratios. ^{13}C NMR solid state scans were performed on a Brüker 300 mHz instrument at the CSIR in Pretoria.

INFRA RED SPECTROSCOPY

Infra Red spectra were recorded on a Perkin-Elmer 983 IR Spectrophotometer (double beam). Samples were prepared by mixing with NUJOL and then scanned in KBr windows. Preliminary Infra red techniques involved KCl discs which were prepared by compressing the sample and KCl into a disc using a special mould and a hydraulic press.

RAMAN SPECTROSCOPY

Raman spectra were recorded using a DILOR Raman spectrometer in conjunction with a coherent INNOVA 90 laser source at the University of Pretoria.

X-RAY POWDER DIFFRACTION

The apparatus used was a Philips X-Ray Powder Diffraction Assembly which consisted of a Philips vertical goniometer PW1050/80 mounted on a Phillips PW1130/90 X-ray generator. This was operated at 40 mA and 45 kV and was controlled by a Phillips 1394 motor control unit in conjunction with a Phillips PW1390 channel control unit. A mortar and pestle were used to crush the samples which were then compacted into the sample holders. The 2θ range scanned was 8^{o} to 36^{o} as outside this range the organic materials did not appear to diffract significantly. Divergence and receiving slits had apertures of 1^{o} each and no anti-scatter slit was used. X-ray powder scans were carried out in a continuous step mode at a scan speed of 2^{o} (2θ) per minute.

ELECTRON MICROSCOPY

Electron microscope photographs were taken on a Cambridge 5200SEM at the Electron Microscope Unit at the University of Cape Town. Samples were mounted on stops with MGIB proprietry glue and were coated firstly with graphite, and finally with a gold-palladium coating under low heat conditions at an operating voltage of 5 kV.

GAS-SOLID APPARATUS

Apparatus to study a gas-solid reaction was designed and constructed as illustrated in figure 1. The host compound was placed in the bucket attached to a silica spring. The increments by which the spring extended were measured by means of a cathetometer. The silica spring was precalibrated using known masses and yielded an excellent linear extension-weight calibration, as shown in figure 2. Liquid acetone was placed in a reservoir and was introduced into the bottom of the reaction vessel when desired. The system was connected to a vacuum line, illustrated in figure 3, which was connected to a Pfeiffer TVS 250 vacuum pump. In this way the reaction environment could be evacuated and the sample suspended in the bucket exposed to acetone vapours. The vapour pressure of the acetone was controlled by maintaining the water flowing through the double-walled tube at a certain temperature, the latter being recorded by a thermocouple which was inserted in a glass finger in the bottom of the reaction chamber. In order to determine optimal reaction temperatures and general conditions, an initial set of kinetic runs was performed using a less sensitive spring.

Figure 1

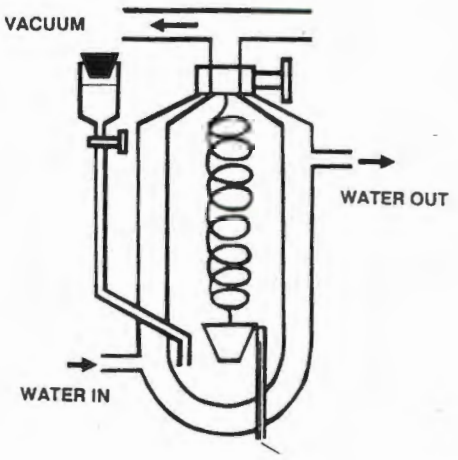

Figure 2

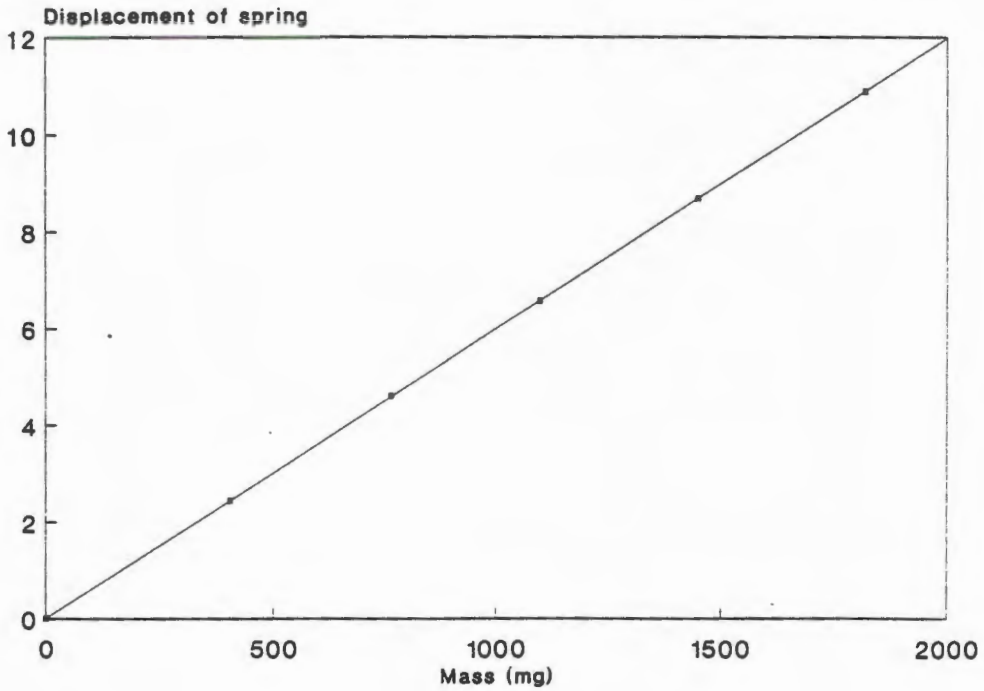

Figure 3

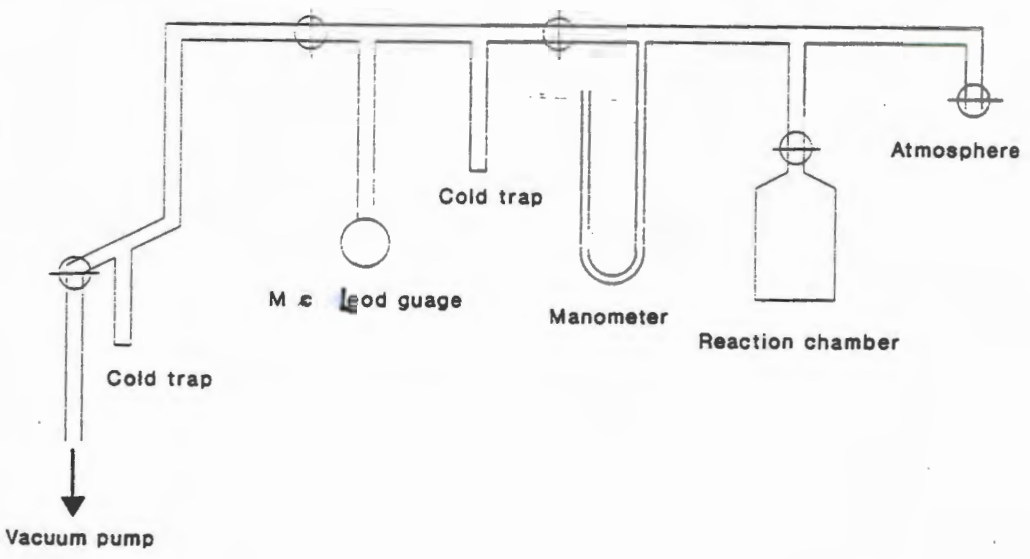

X-ray photography

Suitable crystals were selected and then mounted in Lindemann capillary tubes with mother liquor so that decomposition owing to guest desorption would be avoided. This was particularly important in host-guest compounds for which the guest had a significant vapour pressure at room temperature. Since the majority of these host-guest compounds decomposed rather rapidly swift mounting in the presence of mother liquor was vital even though this made subsequent crystal photographic alignment rather awkward. Figure 4 shows a crystal that is mounted in a Lindemann capillary tube. X-ray photography was performed using Nickel-filtered CuK_{α} radiation ($\lambda = 1.5418$Å) and single crystals were photographed using either a STOE Weissenberg goniometer **(3)** or a STOE Reciprocal Lattice Explorer. The latter instrument yields undistorted photographs of the reciprocal lattice using either the normal precession mode or the De Jong-Baumann arrangement **(4), (5)**. The X-ray generators (PW1120 and PW1008) operated at 20 mA and 40 kV **(6)**.

Figure 4

3 MJ Buerger, "*Crystal Structure Analysis*", John Wiley & Sons Inc., New York, 1967

4 MJ Buerger, "*Contemporary Crystallography*", Mc-Graw-Hill, New York, 1970.

5 T Hahn (Ed.), "*International Tables for Crystallography*", Vol A, D Reidel Publishing Co., Dordrecht, 1983

6 MJ Buerger, "*The Precession Method*", John Wiley & Sons Inc., New York, 1964

INTENSITY DATA COLLECTIONS

An ENRAF-NONIUS CAD4 Diffractometer was used to collect the reflection intensities. This instrument consisted of a Kappa axis goniometer, X-ray generator with graphite-monochromated molybdenum radiation (MoK_α λ= 0.7107Å), interface, computer system and controlling software **(7)**. A single crystal was aligned by manual centering and an automatic peak search was performed to identify twenty-five strong reflections (a discrimination factor of 1.2) at $\theta = 10^o$. Once a preliminary cell had been determined it was refined by collecting 24 peaks at $16^o < \theta < 17^o$. Cell refinement was carried out by subjecting the setting angles, θ, φ, κ and ω, of the 24 reflections to least-squares analysis. A data collection was then performed using a zigzag routine. Crystal quality was monitored by measuring the intensities of three reflections every hour, and centering was checked after every hundred reflections. If crystal decay was observed, a linear decay correction would be applied **(8)**. Data were collected in the ω-2θ scan mode and the final acceptance limit was 20σ at $20^o min^{-1}$ and a maximum measuring time of forty seconds per reflection.

Data reduction of the collected intensities included Lorentz factor and polarization corrections. The vertical aperture length was fixed at 4 mm for each data collection. The aperture width (mm) was set according to the formula: x+1.05tanθ, and the scan width ($\Delta\omega/^o$), according to y+0.35tanθ. Empirical absorption corrections were not applied because the absorption correction factor A^* did not vary in the θ range. This was because all the compounds comprised only C, H and O and had small μR_{min} and μR_{max} values, where μ = linear absorption coefficient and R_{min} and R_{max} are the minimum and maximum dimensions of a crystal **(9)**.

STRUCTURE SOLUTION

Direct methods, as performed by the program SHELXS86 **(10)**, provided automatic structure solutions for the crystals structures studied. Reflections which were unobserved ie F< 4σF or systematically absent were rejected. The unique data as a

---

7 ENRAF-NONIUS CAD4 *Diffractometer Manual*

8 *Program Decay*, ENRAF-NONIUS CAD4 Diffractometer Manual

9 NFM Henry & K Lonsdale, *"International Tables for Crystallography"*, Vol 3,The Kynoch Press, Birmingham, 1969, 166
GH Stout & LH Lensen, *"X-ray Structure Determination"*, 2nd Edition, John Wiley & Sons, New York, 1989, 79-83

10 GM Sheldrick SHELXS86, *"Crystallographic Computing 3"*, GM Sheldrick, C Kruger & R Goddard (Eds.), Oxford University, 1985, 175

function of resolution was then examined in the range 1.2Å to 1.1Å because in order for the direct methods to have a reasonable chance of solving it is necessary for the number of observed reflections to be greater than one-quarter of the theoretically possible reflections in a centrosymmetric structure. In the case of non-centrosymmetric structures, the critical fraction increases to the value of a half. Mean $|E^2-1|$ values of approximately 0.97 indicated a centrosymmetric structure and values of approximately 0.74, a non-centrosymmetric one. Subset reflections are selected on the basis of the number of negative quartets that they generate and the value of the estimated values of α the phase angle. The chosen subset phase permutations are refined and subjected to further cycles of tangent refinement. Extra E values are used to calculate which subset permutations are "best". The "best" phase permutation is then extended by further tangent expansion and is then subjected to one cycle of E-Fourier recycling. In most cases, consideration of the highest peaks observed in the E-map above a definite cutoff point allowed for assignment of a chemically feasible molecular model. In those cases where there was uncertainty owing to thermal motion or guest disorder, refinement invariably allowed for sensible structure interpretation.

Figures of merit calculated for the reflection data set using equivalent reflections are described in terms of R_σ and R_{int} and are defined as :

$$R_\sigma = \Sigma\sigma(F^2)/\Sigma F^2$$

$$R_{int} = \Sigma|F^2-(F^2)_{mean}|/\Sigma F^2$$

Figures of merit calculated for all refined phase permutations :

$$R_\alpha = \Sigma w[(\alpha-\alpha_{est})]^2/\Sigma w[(\alpha_{est})]^2 \quad \text{where } w=1/[\alpha_{est}+5]$$

$$NQUAL = \frac{\Sigma[\Sigma(E_{-1}{}^*E_{-2})^*\Sigma(E_{-3}{}^*E_{-4}{}^*E_{-5})]}{\Sigma[|\Sigma(E_{-1}{}^*E_{-2})|^*|\Sigma(E_{-3}{}^*E_{-4}{}^*E_{-5})|]}$$

The combined figure of merit is a minimum for the "best" solution:

$$CFOM = [0 \text{ or } (NQUAL-wn), \text{ whichever is larger}]^2$$

STRUCTURE REFINEMENT

SHELX76 **(11)** performs refinements using a full-matrix-least squares routine in which the function shown below is minimised :

$$D = \Sigma_{hkl} w_{hkl} (|F_o| - |kF_c|)^2$$

summing over all the observed reflections. The value k is a scaling factor and w is the weight associated with an observed reflection.
Since the version of SHELX76 used could only cope with 500 parameters during refinement, blocked matrix least-squares methods were used to refine structures in which the number of parameters overstepped this limit. Complex neutral atom scattering factors for non-hydrogen atoms were taken from Cromer & Mann **(12)** and those for hydrogen atoms, from Stewart, Davidson & Simpson **(13)**. Reflections suffering from secondary extinction were omitted during structure refinement **(14)**. There was a reasonable convergence of parameters in all cases.
Non-hydrogen atoms were refined with anisotropic temperature factors. Aromatic hydrogen atoms were constrained to 1.0Å from their parent carbons, their positions being dictated by the geometry of the molecule, and they were refined with a common isotropic temperature factor. Methyl hydrogen atoms were refined as rigid groups with a common isotropic temperature factor. Hydroxyl hydrogen atoms were located on difference electron density maps and refined as constrained to their parent oxygen atoms with estimated standard deviations and individual isotropic temperature factors. The distance at which hydroxyl hydrogen atoms were fixed was obtained from a plot of O-H distances versus O---O distances **(15)** which is shown in figure 5.
Any extraordinary treatment of structure refinement will be discussed individually at a later point. In structures where atoms lay on special positions, symmetry restrictions on thermal parameters were applied according to Peterse & Palm **(16)**.

---

11 SHELX76 GM Sheldrick in "*Computing in Crystallography*", H Schenk, R Olthof-Hazekamp, J von Koningsveld & GC Bassi (Eds), Delft University Press, 1978, 34.

12 DT Cromer & JB Mann, *Acta Crystallogr.*, A, 1968,24,321

13 RF Stewart, ER Davidson & WT Simpson,*J.Chem.Phys.*, 42, 1970, 3175

14 GH Stout & LH Jensen, "*X-ray Structure Determination*", op. cit., 183

15 JC Speakman, "*The Hydrogen Bond*", The Chemical Society, London, 1975, 13

16 WJAM Peterse & JH Palm, *Acta Crystallogr.*, 20, 147, 1966

Figure 5

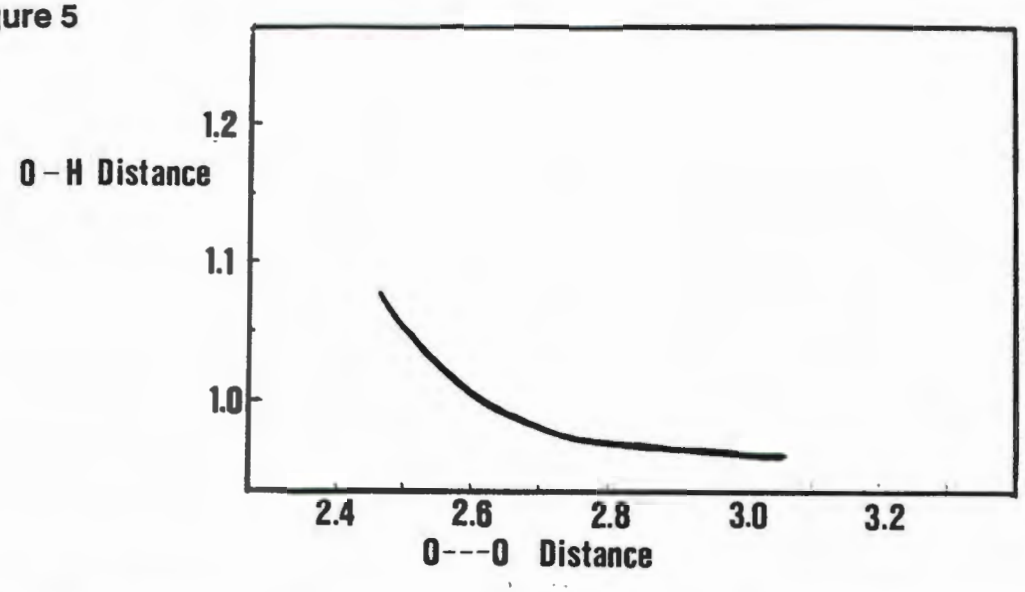

The residual factor, R reflects the agreement between observed and calculated structure factors. It is defined as:

$$R=(\Sigma||F_o|-|F_c||)/(\Sigma|F_o|)$$

The weighted residual R factor is given by:

$$R_w=(\Sigma/w||F_o|-|F_c|)/(|\Sigma/w|F_o|)$$

where the weighting scheme is $w=(\sigma^2(F_o)+gF_o^2)^{-1}$.
Unit weights yielded satisfactory convergence in the early stages of structure refinement, but in the final stages the weighting was extended to include $\sigma(F_o)$ to correct for systematic trends in $\Sigma w(\Delta F)^2$. Values of g between 0 and 1 were chosen in order to attain minimal variation in $\Sigma w(\Delta F)^2$ with respect to $\sin\theta$, $(F/F_{max})^{½}$, parity groups and Miller indices. The value of the "goodness of fit" parameter was also taken into account when choosing a weighting scheme. Additional parameters which were considered with respect to an optimal weighting scheme were the values of the standard deviations of the atomic coordinates.
Relevant atomic coordinates and thermal parameters may be found at the end of chapters three, five and six. The latter as well as bond lengths, bond angles and torsion angles for all the structures may be found in Appendices 1,2 and 3. Torsion angles may be found in Appendix 4.

COMPUTATION

Initial computing was carried out on the SPERRY 1100181 network but the majority was carried out using the VAX/VMS NETWORK version 5.4 at the University of Cape Town

Computing Centre. Plotting was carried out using the program PLUTO89 **(17)** and a similar PC version thereof. Torsion angles and least squares-planes were calculated using PARST **(18)**.

OPEC is a program able to ~~calculate~~ calculate molecular volumes therefore the unoccupied regions of a crystal can be studied. It takes into account molecular volumes based on molecular geometries and standard atomic radii thus in this way the shapes of cavities and channels may be mapped by computing molecular volumes **(19)**.

The program EENY **(20)** was used to evaluate non-bonded van der Waals interactions using empirical atom-pair potential curves. A Lennard-Jones type equation is used to express the coefficients of the atom-atom potentials :

$$U(r) = a \exp((-br/r^d) - c/r^6)$$

The distance r represents the separation between any pair of atoms (in Å) and the coefficients (a, b, c and d) are those given by Giglio **(21)**, and reviewed by Pertsin & Kitaigorodsky **(22)**. In this way the energy environment of the guest molecule was simulated by completely surrounding it with host molecules. The positions of the host moieties were held constant whilst the guest molecule was allowed to find its minimum energy environment by incremental translations and rotations.

A hydrogen bonding potential has recently been incorporated into the EENY calculations in a program called HEENY **(23)**. This is a simplified version of that used by Vedani & Dunitz **(24)**, using the potential:

$$U_{H\text{-}bond} = (A/R^{12} - C/R^{10})\cos^2\theta$$

A hydrogen bond is defined in this program as Donor-H----Acceptor and the angle θ is described by these three atoms. The donor-acceptor angle was allowed to scale the interaction with $\cos^2\theta$ for $90^o \leq \theta \leq 180^o$, the main drawback being that a hydrogen bond detected at 90^o is permitted to make a close contact without penalty. R is the distance

---

17 WDS Motherwell, "*PLUTO & PLUTOX-programs for plotting molecular and crystal structures*", Cambridge University, UK, unpublished

18 M Nardelli, *Comput.Chem.*, 7, 1983,95

19 A Gavezotti, *J.Am.Chem.Soc.*, 105, 1983, 5220-5225
A Gavezotti, "*OPEC- Organic Packing Energy Calculations manual*", Milan University, Italy, unpublished

20 WDS Motherwell, "*EENY Potential Energy Program*", Cambridge University, UK, unpublished

21 E Giglio, *Nature*, 222, 1969, 339.

22 AJ Pertsin & AI Kitaigorodsky,"*The atom-atom potential method*", Chemical Physics 43, Springer-Verlag, Berlin, 1987,Chapter 3

23 CF Marais, "*HEENY*", 1990, University of Cape Town, 1990, unpublished

24 A Verdani & JD Dunitz, *J.Am.Chem.Soc.*, 102, 1987, 7653

between the hydrogen atom and the acceptor atom. At $\theta = 180^{o}$, the constants A and C are related to U_{min} (the depth of the energy well) and the equilibrium distance R_o by $A = -5R_o^{12} U_{min}$ and $C = -6R_o U_{min}$. The program employed the mixing scheme:

$$U_{tot} = U_{H\text{-}bond} + (1-\lambda)\, U_{normal} \qquad ,\lambda = \cos^2\theta$$

In this way the full non-bonded potential U_{normal} can be progressively augmented as the angle deviates from the ideal hydrogen bonding geometry.

THERMAL ANALYSIS TECHNIQUES

DIFFERENTIAL SCANNING CALORIMETRY

Differential Scanning Calorimetry (DSC) was performed on a Perkin-Elmer DSC7 Dynamic Differential Calorimeter and a PETA77/PC Thermal Analysis Instrument Controller, controlled by means of an Epson PCAX2 personal computer. Hardcopies of thermal data were obtained from a Hewlett-Packard Color Pro plotter which was connected to the thermal station. DSC calibration was carried out by measuring the melting point of a standard, in this case Indium. Samples were blotted dry on filter paper, crushed to ensure consistency in particle size and then weighed in a vented, sealed aluminium pan of capacity 30μl-50μl. A five-place Sartorius Micro Balance was used for weighing. The host-guest compounds studied were very unstable when removed from their mother liquor and great haste was necessary when preparing samples for thermal measurements. Thus, sample sieving was not performed because the volatile guests desorbed from the host-guest lattice.

The DSC operates as a power-compensated null balance comprising a sample and reference furnace which are embedded in a large aluminium heat sink. The furnaces are made of a Platinum-Iridium alloy and are maintained at the same temperature by the addition or subtraction of appropriate amounts of electrical energy by a heater located in the sample holder. The reference furnace would typically contain an empty sealed pan of the same type as that containing the sample. Both the sample and reference pan were covered by vented Platinum lids which were purged with high purity nitrogen gas at a flow rate of 40ml min^{-1}.

The Platinum resistance heaters and thermometers performed temperature and energy measurements and the continuous adjustment of heater power to maintain $T_{sample} = T_{reference}$. This provided an electrical signal which varied directly with the thermal behaviour of the sample **(25),(26)**. Since the measured signal is observed as a

---

25 PERKIN-ELMER, *DSC7 Manual*

deviation from a baseline, reproducibility of the latter was paramount. A reference baseline was created by carrying out a DSC run in which both the sample and reference furnace contained similar empty sample pans. The resultant reference baseline could then be subtracted from each DSC run.

Figure 6 Schematic diagram of the heating and temperature sensing mechanism beneath the sample (S) and reference (R) furnaces.

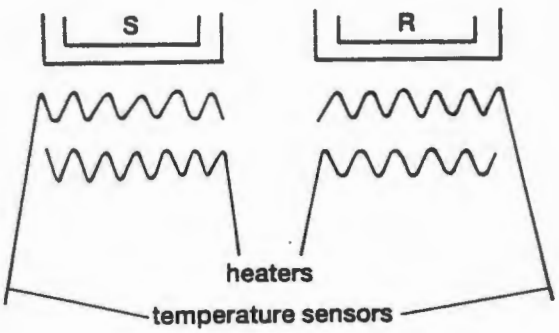

Figure 7 Diagram of the Perkin Elmer DSC 7 sample holder and sample holder cover.

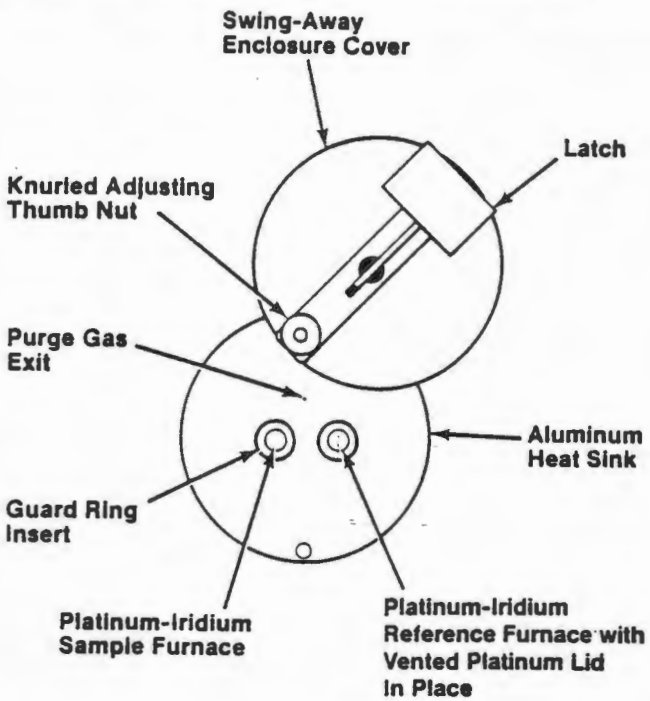

The application to the compounds studied as well as theory of Differential scanning calorimetry are discussed in detail in chapter four.

---

26 ME Brown, "*Introduction to Thermal Analysis*", Chapman & Hall Ltd., Cambridge, 1988

THERMOGRAVIMETRIC ANALYSIS

Thermogravimetric analysis (TG) measures change in mass of the sample with temperature **(27)**. Instrumentation consisted of a PETGA7 Thermogravimetric Analyser and a PETAC7/PC Thermal Analysis Instrument Controller in conjunction with an Epson PCAX2 personal computer. The analyser comprises two components, a sensitive microbalance and a furnace element. This balance consists of a null-point weighing mechanism which ensures the sample remains in the same part of the furnace in spite of any changes in mass **(28)**. The null balance operates by a servo-controlled torque motor which compensates for weight changes in the spring.

Figure 9a depicts a scheme of a thermobalance. The beam supporting the sample pan is deflected when a crystal sample, which had been quickly blotted dry and crushed, is placed in the pan. A beam position detector detects this by means of an optical sensor and current compensation takes place to restore the balance to its null point. The actual amount of current required to restore the beam is directly related to the weight of the sample, the minimum detection limit being 0.1μg. Figure 9b illustrates the weighing mechanism of a thermobalance. Throughout the scan the sample chamber was purged with high purity dry nitrogen at a rate of 40ml min^{-1}.
The small thermal mass furnace consists of an aluminium cylinder which is wound with Platinum wire. The Platinum wire functions both as a heater and as a temperature sensor. This resistance thermometer senses the temperature of the wire during one half cycle and compares it to the desired program temperature. Power is then applied during the second half of the cycle to negate any difference between actual and desired program temperature. Thermal lags between the heater and sensor do not occur because they are same element, and coupling between the wire and the furnace body is via a highly conductive material **(29)**.

---

27 ME Brown, *Op cit.*

28 PERKIN-ELMER, *TGA7 Manual*

29 WWM Wendlandt, "*Thermal Analysis*", 3rd Edition, New York, 1986, 118

Figure 9a A diagram of the scheme of a thermobalance

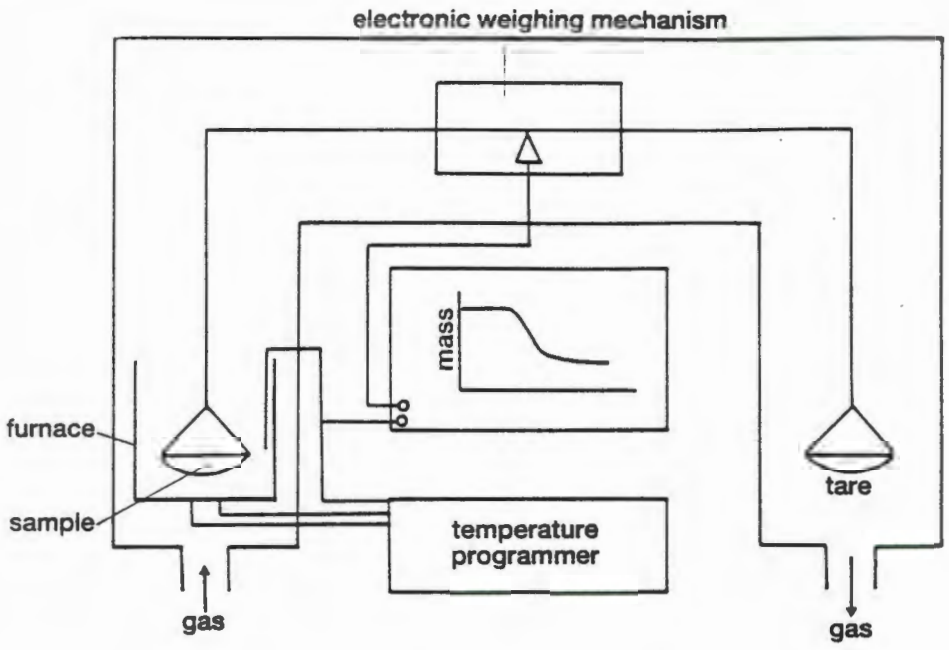

Figure 9a The weighing mechanism of a thermobalance

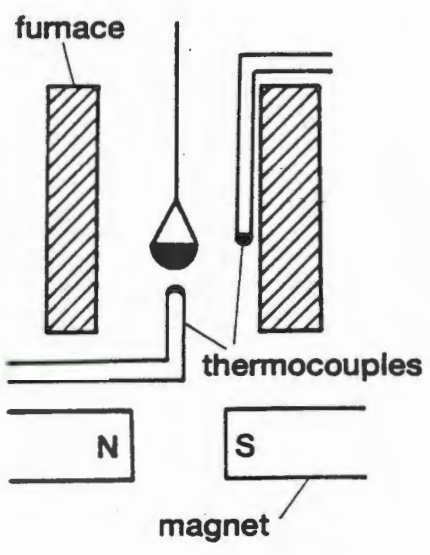

CHAPTER THREE

THE STRUCTURE OF THE HOST1 COMPOUND

The host1 compound is an ideal example of a "wheel-and-axle" compound. On either end of a thin carbon chain are bulky groups able to create voids which may be occupied by guest molecules **(1)**. In addition to this, a molecule of host1 possesses hydroxy groups capable of forming hydrogen bonds with appropriate guests. Owing to the propensity of host1 to entrap a wide variety of solvent molecules it was of interest to determine whether the host1 compound was able to crystallize without guest inclusion occurring.
Atomic coordinates of the host1-guest inclusion compounds may be found in tables at the end of this chapter.

A molecule of host1

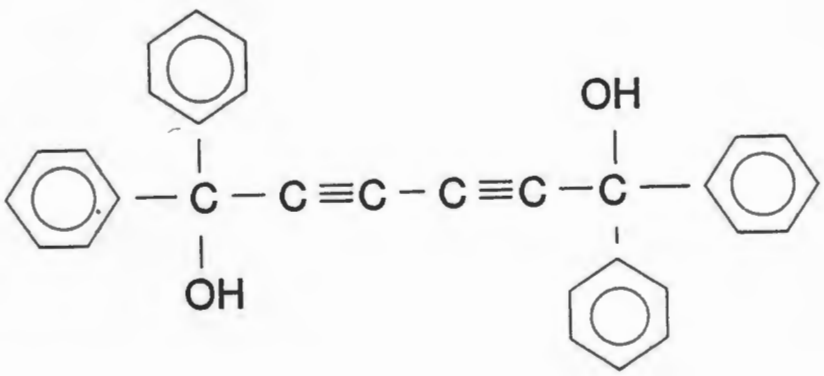

The numbering scheme of host1

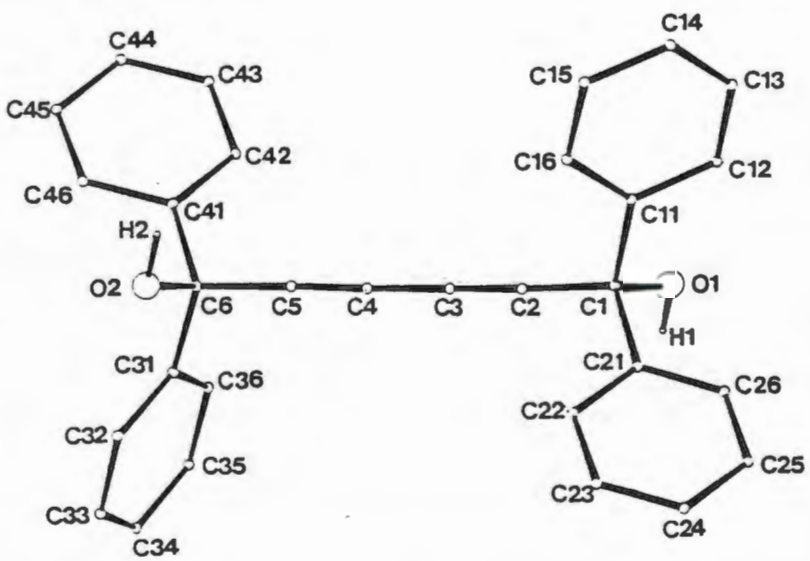

---

1 F Toda & K Akagi, *Tetrahedron Lett.*, 1968, 3395

EXPERIMENTAL

It proved to be very difficult to obtain diffraction quality crystals of the unclathrated form of the host1 because the host co-crystallized with many of the solvents attempted. Suitable crystals were eventually obtained by dissolution of host1 in 2:1 (vol/vol) diethyl ether:petroleum ether (boiling fraction 100°-120°C). Slow evaporation of such a solution over 2-4 weeks yielded low-quality, needle-like crystals. X-ray powder diffraction and Infra red scans were carried out to fingerprint this form.

Solution and refinement

No symmetry other than $\bar{1}$ was detected on oscillation and zero-layer Weissenberg photographs which indicated that the space group was P1 or $P\bar{1}$. The structure was successfully solved in $P\bar{1}$ using direct methods. The values for mean $|E^2-1|$ statistics were close to the theoretical value of 0.968 for the okl, h0l and hk0 projections as well as the remainder of the reflections implying that the choice of space group was correct . The combined figure of merit was 0.085 and the R_E value which is based on the E values used was 0.322. Successful refinement confirmed the choice of the centric space group. The temperature factors of all non-hydrogen atoms were anisotropically refined. The hydroxyl hydrogen atoms were located in difference electron density maps as were as some phenyl hydrogen atoms; all of the latter were geometrically constrained to their parent carbon atoms. The crystal parameters are shown in Table 1. A g-factor of 0.005 was decided upon in the weighting scheme after temperature factors and their standard deviations and analysis of variance had been considered. The maximum shift/e.s.d. was 0.068 and a final residual factor of 0.0635 was obtained.

DISCUSSION

There was no intermolecular hydrogen bonding between host1 molecules implying that the α-form of the host1 was stabilized by van der Waals forces. The packing of the crystal is illustrated in figure 1a and 1b, which show the packing along [1 0 0] and [0 1 0] respectively. Surprisingly, the centrosymmetric host1 does not lie on a crystallographic centre of symmetry. Molecules of host1 are packed in staggered rows, the hydroxy moieties lie trans to one another and are exposed in the bc plane.

Torsion angles and the conformation of host1 will be discussed later.

Figure 1a The molecular backbones of host1 aligned parallel to one another

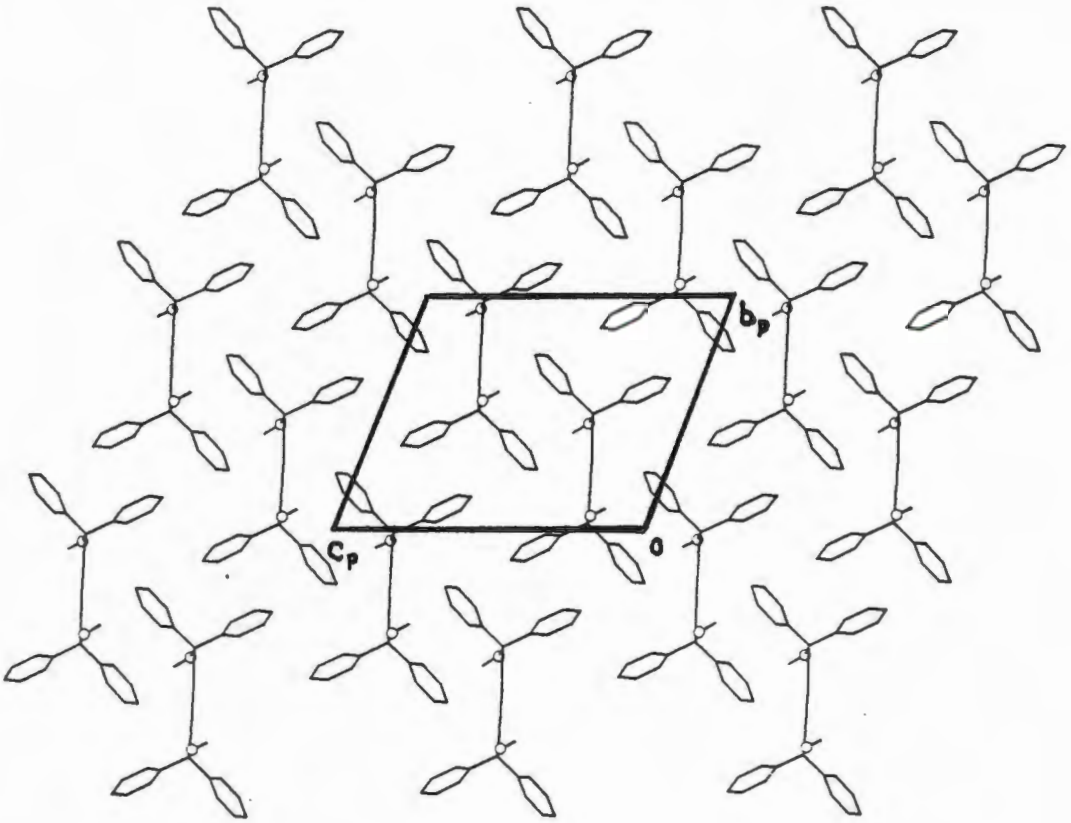

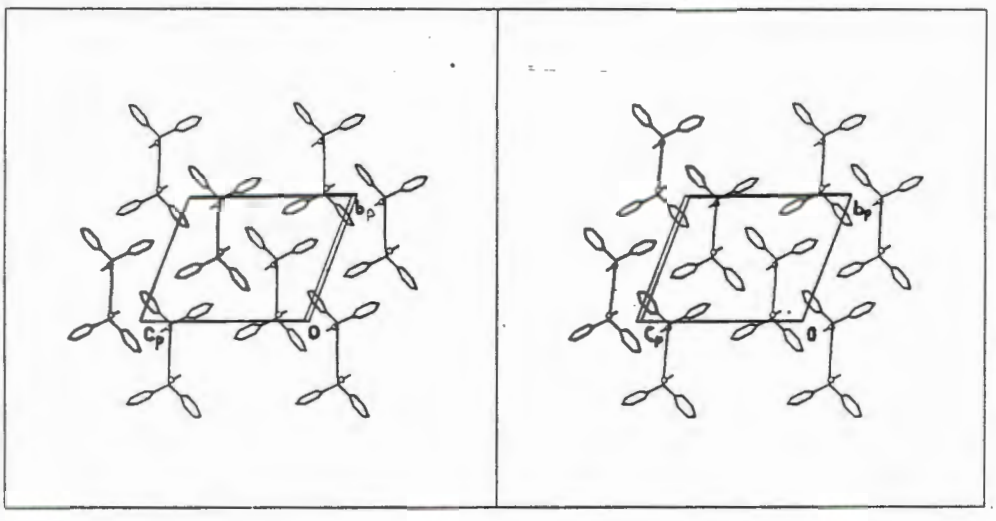

Figure 1b

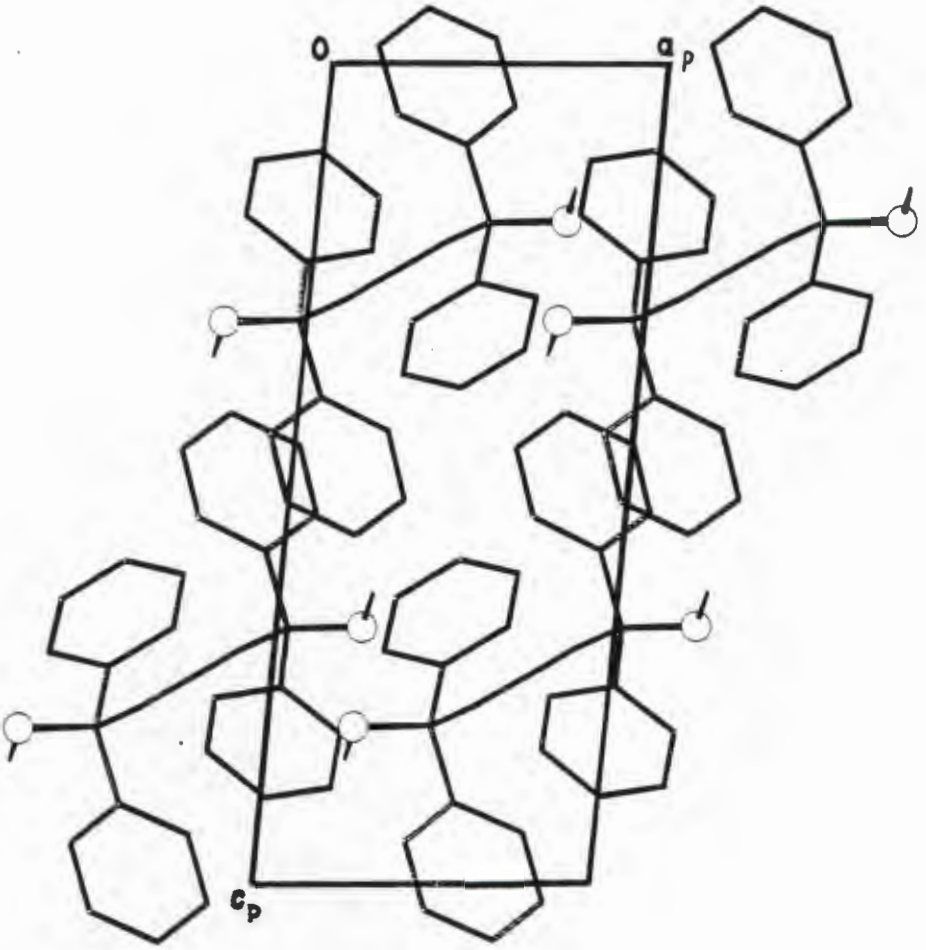

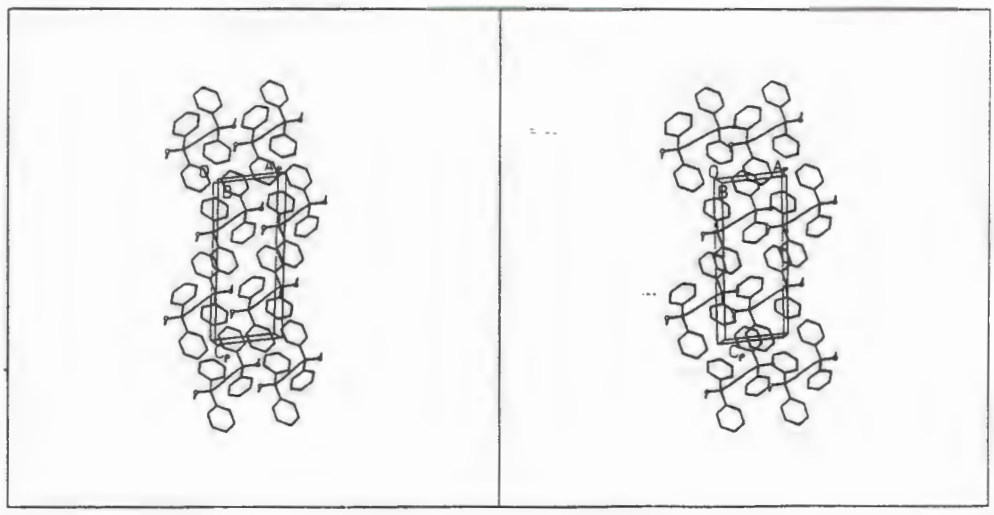

TABLE 1 CRYSTAL DATA AND EXPERIMENTAL DETAILS FOR α-FORM OF HOST1.

Compound	**α-form of host1**
Molecular formula	$C_{30}H_{22}O_2$
Molecular weight ($gmol^{-1}$)	414.50
Space group	$P\bar{1}$
a (Å)	6.051(7)
b (Å)	12.606(1)
c (Å)	15.708(1)
α (°)	111.20(7)
β (°)	94.19(8)
γ (°)	92.96(10)
Z	2
V ($Å^3$)	1110(2)
D_c (gcm^{-3})	1.24
D_m (gcm^{-3})	1.23(3)
$\mu(MoK_\alpha)$ (cm^{-1})	0.41
F(000)	436
Data collection (21°C)	
Crystal dimensions (mm)	0.25x0.38x0.47
Range scanned θ (°)	1-25
Range of indices *h,k,l*	±7,±15,+18
Reflections for lattice parameters no.,θ range (°)	24,16-17
Instability of standard reflections (%)	1.9
Scan mode	(ω-2θ)
Scan width in(°)	(0.90+0.35tanθ)
Vertical aperture length (mm)	4
Aperture width (mm)	(1.12+1.05tanθ)
Number of reflections collected (unique)	3052
Number of reflections observed with $I_{rel} > 2\sigma I_{rel}$	1863
Final refinement	
Number of parameters	358
R	0.064
wR	0.071
w	$(\sigma^2(F_O)+0.005F_O^2)^{-1}$
S	1.27
Max. shift/e.s.d.	0.68
Max. height in difference electron density map ($eÅ^{-3}$)	0.23
Min. height in difference electron density map ($eÅ^{-3}$)	-0.22

THE STRUCTURE OF THE HOST1-ACETONE (1:2) INCLUSION COMPOUND

SOLUTION AND REFINEMENT

The structure of host1-acetone had already been solved by Toda, Ward and Hart but had been poorly refined **(2)**. Collection of a new data set and crystal solution were therefore carried out because more accurate atomic parameters were required for molecular mechanics calculations. The structure solution was performed using direct methods and the combined figure of merit was 0.188. Half a host1 molecule on a centre of symmetry, Wyckoff *b*, and one acetone molecule in a general position were located. Since the acetone guest was not unambiguously located in the direct methods, initial refinement runs with $I_{rel} > 3\sigma I_{rel}$ were used to allow for the location of the rather volatile guest (the vapour pressure of acetone at 25°C is 230.0 mmHg). The host1 hydroxyl hydrogen atom was located in difference electron density maps and constrained to its parent oxygen at 0.98Å. Relatively high values of 0.83 for the shift/e.s.d. were due free rotation of the guest methyl moieties. The bond angles and lengths refined to acceptable values and there was satisfactory convergence in the refinement cycles. All the non-hydrogen atoms were refined anisotropically and the hydrogens were subjected to constrained refinement. The maximum electron density that existed in the final electron density map was 0.22 $eÅ^{-3}$ and a g factor of 0.001 was used in the weighting scheme since this resulted in a satisfactory analysis of variance and standard deviations after the last cycle of refinement. Details of intensity data collection and refinement details may be found in Table 2.

DISCUSSION OF STRUCTURE

This type of host-guest inclusion compound is called a tubulato coordination assisted inclusion compound. Two acetone molecules are hydrogen bonded to each host1 molecule. The O---O hydrogen bonding distance between the host hydroxyl and the guest carbonyl oxygen is 2.726(3)Å characterising this as a medium strength hydrogen bond. The hydrogen bonding and molecular packing are shown in figure 2.

---

2 F Toda, DL Ward & H Hart, *Tetrhedron Lett.*, 22, 1981, 3865-3868

Figure 2 Crystal packing and hydrogen bonding in the host1-acetone inclusion compound

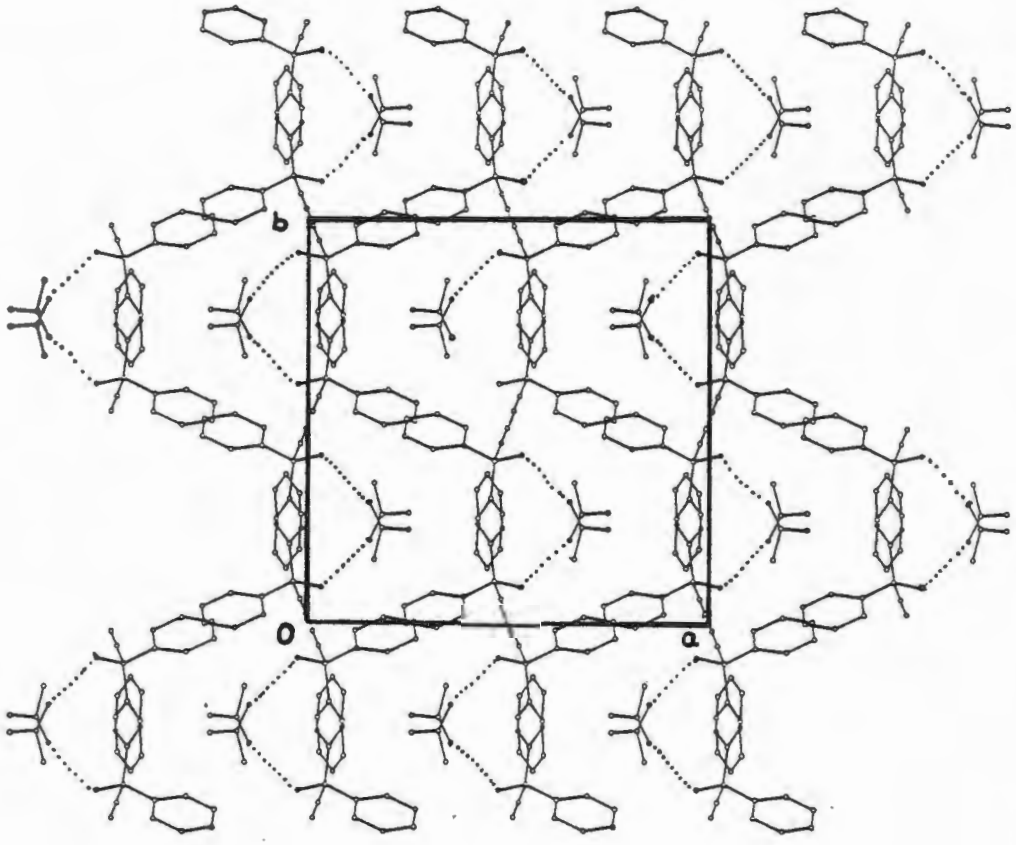

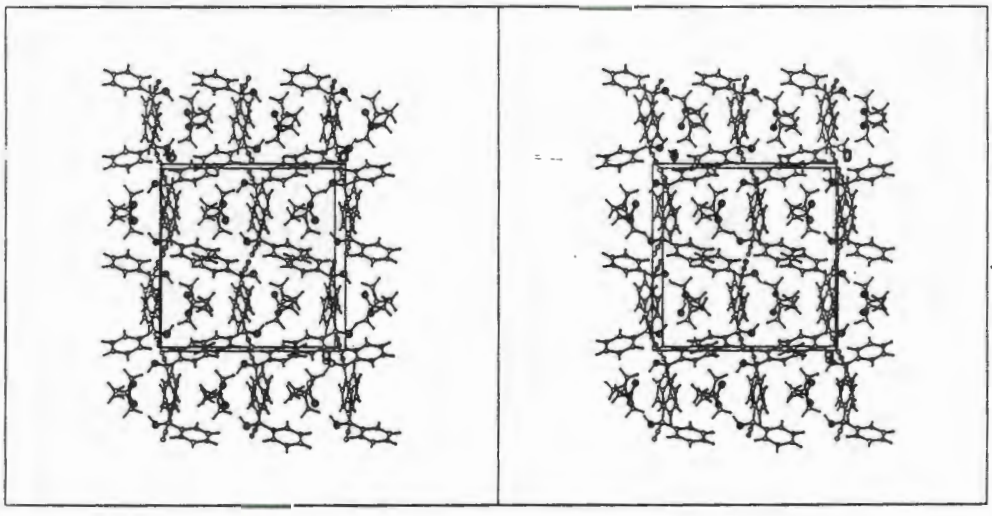

The acetone guest lies in channels which run in the [0 0 1] direction. The channels are illustrated in figure 3 in which the acetone molecules have been omitted for purposes of clarity. The host1 phenyl rings are roughly at right angles and the torsion angles will be discussed later in this chapter.

Figure 3

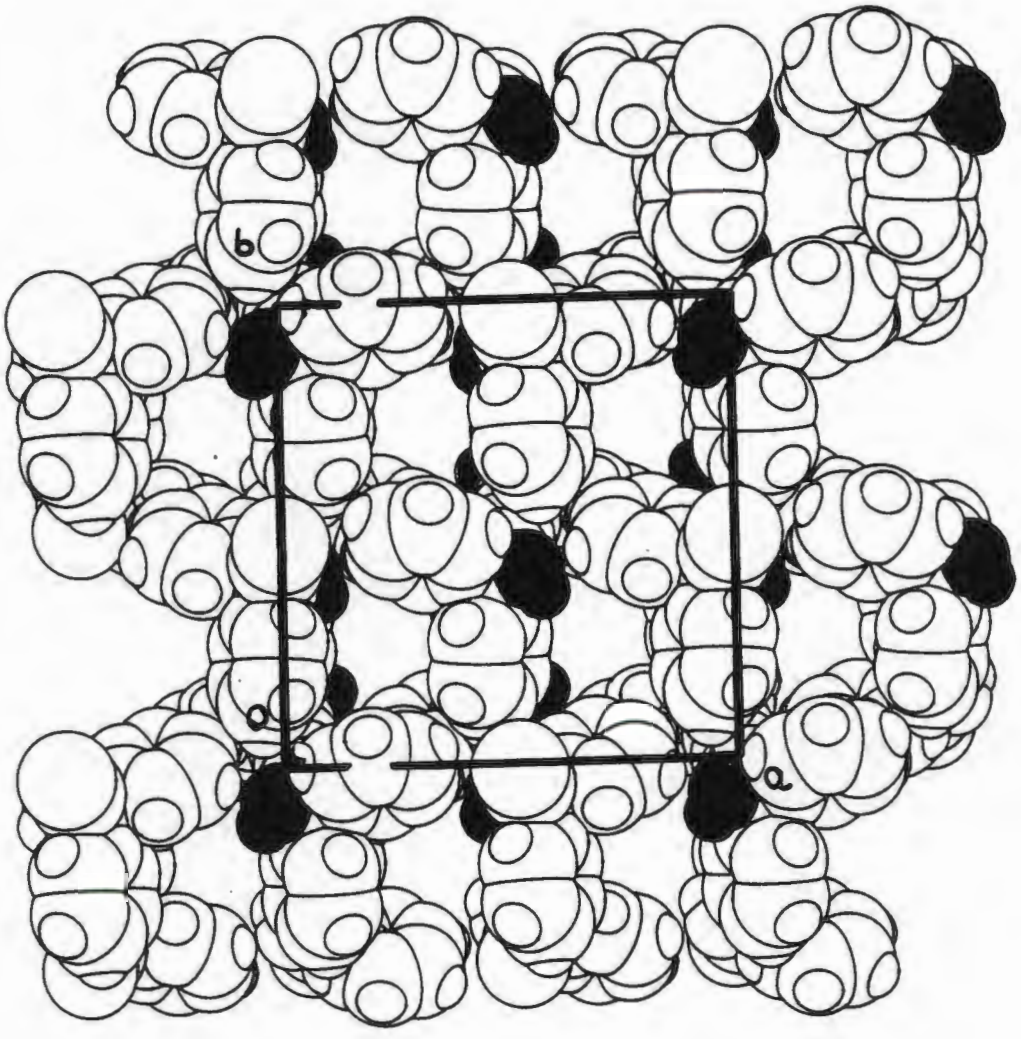

TABLE 2 CRYSTAL DATA AND EXPERIMENTAL DETAILS FOR HOST1-ACETONE STRUCTURE.

Compound	**Host1-Acetone**
Molecular formula	$C_{30}H_{22}O_2.2C_3H_6O$
Molecular weight ($gmol^{-1}$)	530.64
Space group	Pbca
a (Å)	16.078(3)
b (Å)	16.182(5)
c (Å)	11.517(4)
Z	4
V ($Å^3$)	2996(2)
D_c (gcm^{-3})	1.18
D_m (gcm^{-3})	1.16(2)
$\mu(MoK_\alpha)$ (cm^{-1})	0.49
F(000)	1128
Data collection (21°C)	
Crystal dimensions (mm)	0.44x0.50x0.53
Range scanned θ (°)	1-30
Range of indices *h,k,l*	+22,+22,+16
Reflections for lattice parameters no.,θ range (°)	24,16-17
Instability of standard reflections (%)	0.4
Scan mode	(ω-2θ)
Scan width in(°)	(0.85+0.35tanθ)
Vertical aperture length (mm)	4
Aperture width (mm)	(1.12+1.05tanθ)
Number of reflections collected (unique)	4355
Number of reflections observed with $I_{rel}>2\sigma I_{rel}$	2315
Final refinement	
Number of parameters	192
R	0.065
wR	0.071
w	$(r^2(F_o)+0.001F_o^2)^{-1}$
S	2.44
Max. shift/e.s.d.	0.83
Max. height in difference electron density map ($eÅ^{-3}$)	0.22
Min. height in difference electron density map ($eÅ^{-3}$)	-0.24

The program OPEC calculated packing and potential energies of molecules in a crystal by taking into account van der Waals radii. In this way the total occupied volume in the cell was calculated and any channels or cavities existing in the structure located. Thus inspection of packing density maps (down each cell axis) revealed any unoccupied spaces. The channels, see figure 4, ran parallel to the c axis and had approximate dimensions of 4.5Å by 2.6Å.

Figure 4

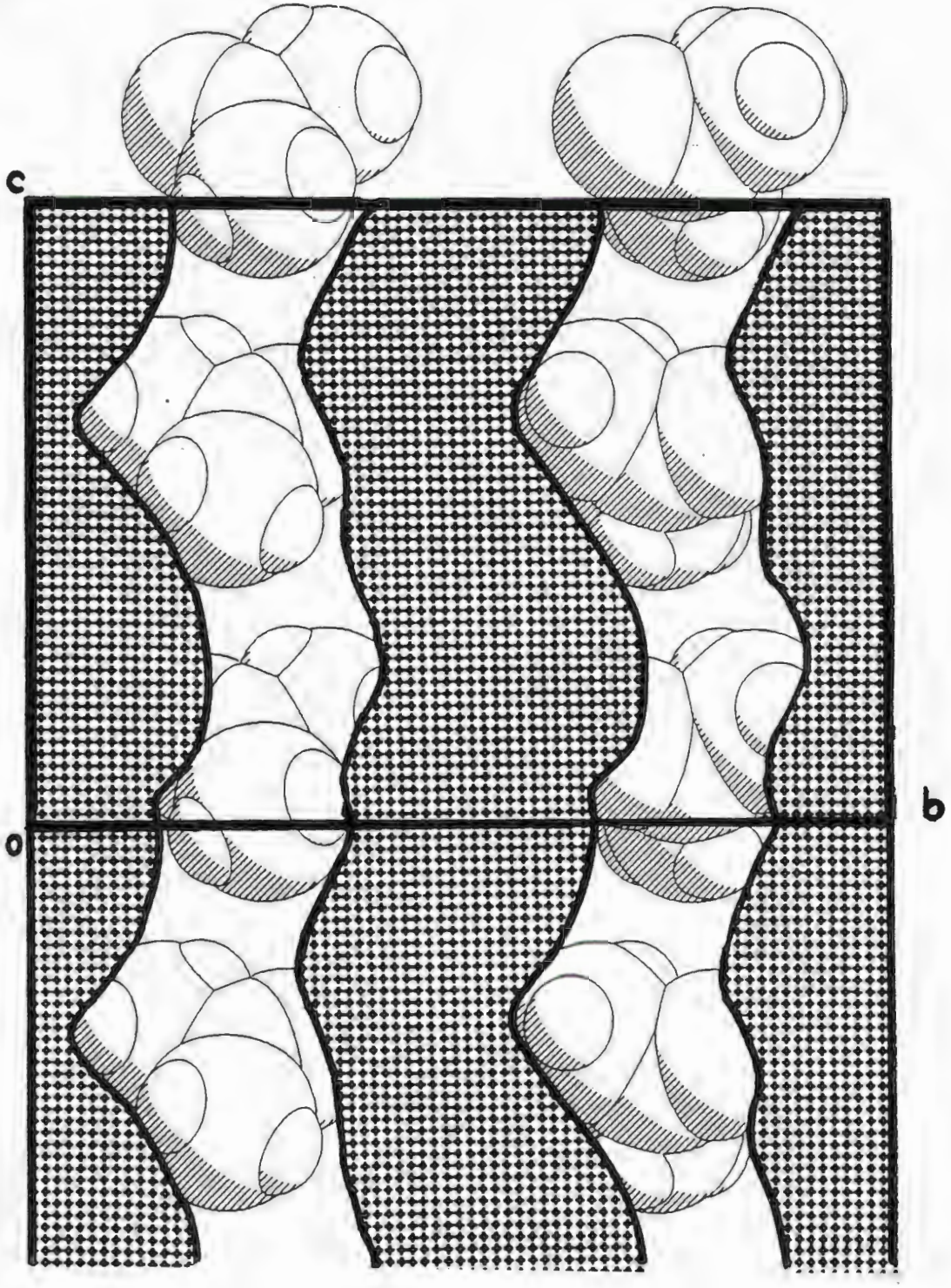

DECOMPOSITION OF INCLUSION COMPOUNDS

The decomposition of an inclusion compound may follow three fundamentally different paths (this is illustrated below). Molecules of a host compound may be reacted with molecules of guest (typically by dissolution of the host in the guest liquid) to form a new phase, which is the clathrate or β phase. When this inclusion compound decomposes and the guest molecules allowed to escape, there are three possible products that may form. Either the host may revert to its former α phase; or the host framework may be retained giving rise to an 'empty' clathrate - the β_o phase, which occurs in the case of zeolites. Thirdly there may occur some loss of guest (and probable shrinkage of the crystal lattice) with subsequent formation of a third phase, the γ phase **(3)**.

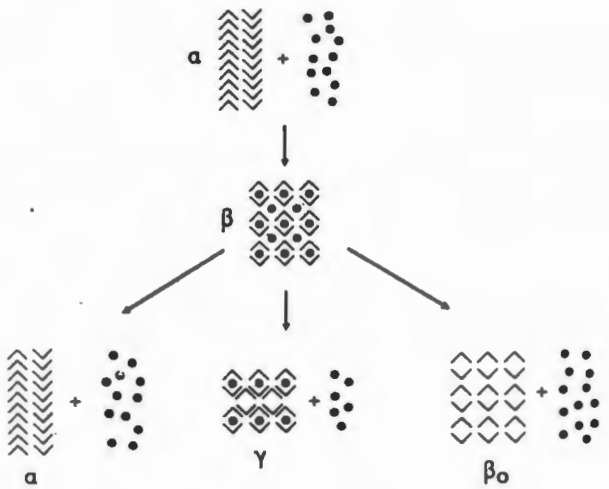

The β_o-phase would be a phase possessing the structure of the host1-acetone complex minus the guest. Since the host1-acetone contained guest channels we undertook to investigate whether in fact the β_o-phase could be obtained by desorption of acetone from the host1-acetone inclusion compound. The resultant compound was found to be the α-phase which is not unexpected since removal of the guest from these types of compounds usually results in collapse of the inclusion compound channel phase **(4)**. X-ray powder diffraction diagrams, shown in figure 5 are of: the host1-acetone compound, 5 (i), the host1 compound from which the acetone had been desorbed by gentle heating (60°C) under vacuum, 5 (ii), and the

---

3 DR Bond, MR Caira, GA Harvey, LR Nassimbeni & F Toda, *Acta Crystallogr.*, B46, 1990, 771-780

4 GR Desiraju, "*Organic Solid State Chemistry*", Elsevier, Amsterdam, 1987, 180

host1 α-form grown from ether, 5 (iii). This indicated that desorption of the acetone left α-form host1 and not the cage-like β_o-phase.
All the host1-ketone inclusion compounds were found using X-ray powder diffraction to decompose in this way, ie no evidence was found for the existence of a β_o-phase for the host1 inclusion compounds to be discussed.

Figure 5

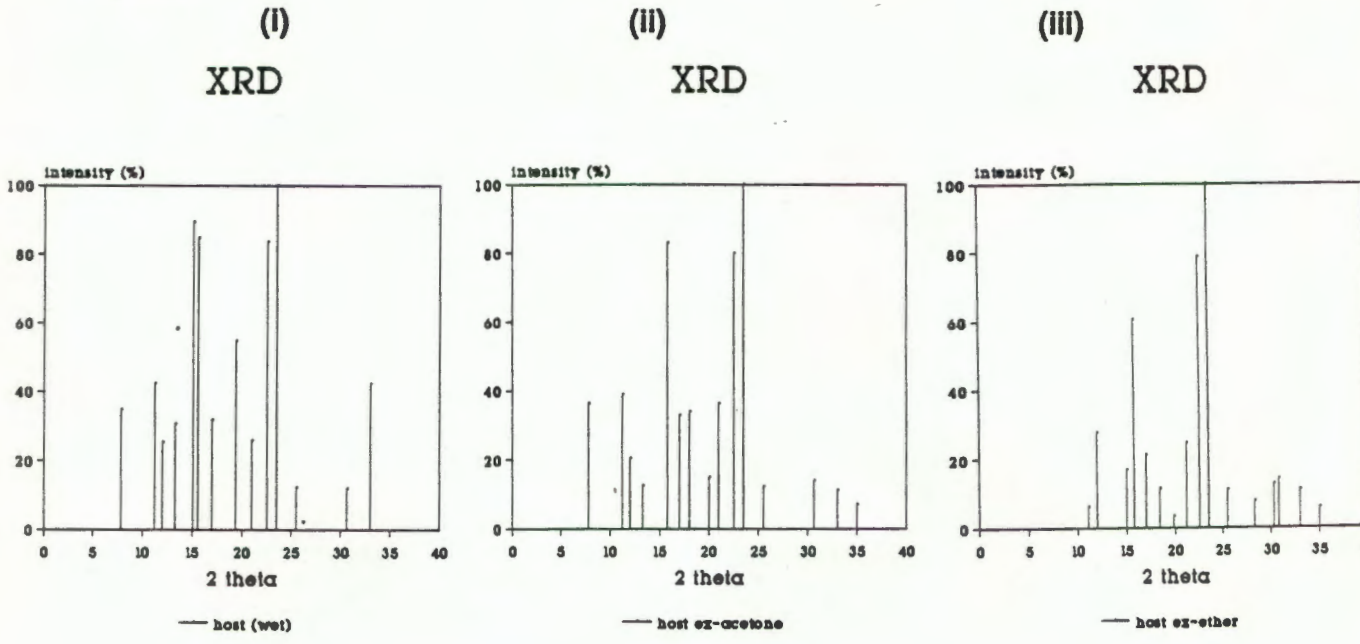

Could the α-phase be reverted to the β-phase? The question as to whether α-phase host would transform to the host1-acetone β-phase if exposed to acetone vapour warranted further investigation. It was for this reason that the gas-solid reaction behaviour of acetone and host1 was investigated .

THE GAS-SOLID REACTION

EXPERIMENTAL

The vapour-solid reaction:

$$Host1_{(s)} + 2\ Acetone_{(g)} \longrightarrow [Host1\ (Acetone)_2]_{(s)}$$

involves a change of phase, α to β, with hydrogen bonds being formed between the hydroxyl groups (donors) and the acetone carbonyl groups (acceptors).
The α-phase was obtained by recrystallizing host1 from acetone and then heating the host1-acetone crystals at 60°C under vacuum for 6 hours.

RESULTS AND DISCUSSION

The fractional reaction, α, is directly proportional to the extent of the reaction and is defined as gain in weight as a fraction of total weight gain **(5)**. Typical characteristics of α-time curves are: an induction period (since there is a finite time period involved before reactants reach the reaction temperature when the acetone is first introduced into the bottom of the reaction chamber); an acceleratory period and a region of deceleration and reaction completion.

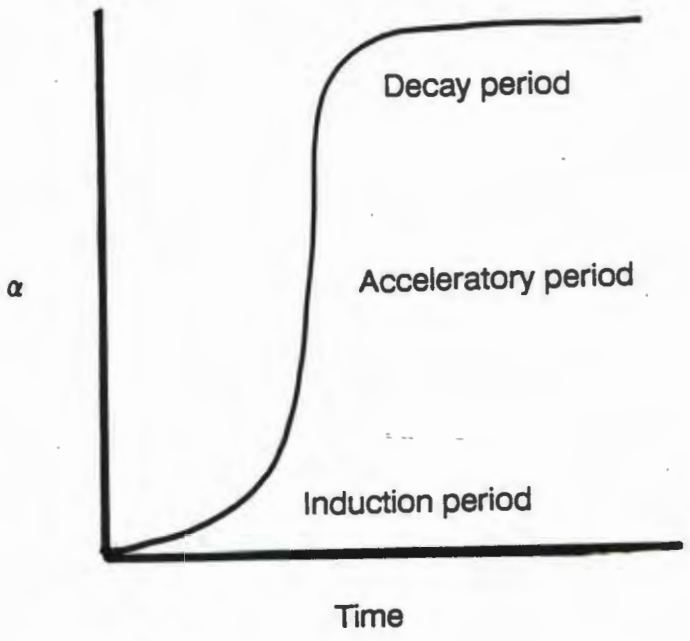

(6)

---

5 CH Bamford & CFH Tipper, (Eds.), "*Comprehensive Chemical Kinetics*", Vol 22, Elsevier Press, Amsterdam, 1980, Vol 22, 41

6 W Ng, *Aust.J.Chem.*, 28, 1975, 1169-1178

The results of the kinetics of acetone absorption are shown overleaf. The plot shows the extent of guest absorption α, with time. The reaction was performed at six different temperatures and considerable effort was made to obtain acceptable, reproducible results. The temperatures lay in the range 23°C to 48°C and each run was repeated a minimum of three times. The data used in calculating the rate constants excluded the induction period because only the acceleratory region of the kinetic curve is deemed to be relevant to the kinetic analysis **(7)**. A data fitting program which calculated nineteen rate equations was used to evaluate rate constant values and their corresponding correlation coefficients.

RATE EQUATIONS TO WHICH DATA FOR THE GAS-SOLID REACTION WERE FITTED

1.	$f(\alpha) = 1-(1-\alpha)^{1/2}$	contracting area
2.	$f(\alpha) = 1-(1-\alpha)^{1/3}$	contracting volume
3.	$f(\alpha) = \alpha^2$	one dimensional diffusion
4.	$f(\alpha) = (1-\alpha)\ln(1-\alpha) + \alpha$	two-dimensional diffusion
5.	$f(\alpha) = (1-2/3\alpha)-(1-\alpha)^{2/3}$	three-dimensional diffusion
6.	$f(\alpha) = [1-(1-\alpha)^{1/3}]^2$	Jander
7.	$f(\alpha) = -\ln(1-\alpha)$	Avrami-Erofe'ev, n=1
8.	$f(\alpha) = [-\ln(1-\alpha)]^{2/3}$	Avrami-Erofe'ev, n=3/2
9.	$f(\alpha) = [-\ln(1-\alpha)]^{1/2}$	Avrami-Erofe'ev, n=2
10.	$f(\alpha) = [-\ln(1-\alpha)]^{1/3}$	Avrami-Erofe'ev, n=3
11.	$f(\alpha) = [-\ln(1-\alpha)]^{1/4}$	Avrami-Erofe'ev, n=4
12.	$f(\alpha) = \ln[\alpha/(1-\alpha)] + C$	Prout-Tompkins
13.	$f(\alpha) = \ln\alpha$	Exponential Law
14.	$f(\alpha) = \alpha$	power law, n=1
15.	$f(\alpha) = \alpha^{1/4}$	power law, n=4
16.	$f(\alpha) = \alpha^{1/3}$	power law, n=3
17.	$f(\alpha) = \alpha^{1/2}$	power law, n=2
18.	$f(\alpha) = 1/(1-\alpha)-1$	Second order
19.	$f(\alpha) = 1/(1-\alpha)^{1/2}-1$	Third order

(8)

---

7 CH Bamford & CFH Tipper, *op. cit.*, 21, 42

8 CH Bamford CFH Tipper (Eds.), *op. cit.*,22, 57-61
CJ Keattch & D Dollimore, "*An Introduction to Thermogravimetry*", 2nd Edition, Heyden & Son ltd., London, 62-65
JH Sharp, GW Brindley, BN Narahari Achar, *J.Amer.Chem.Soc*, 49, 1971, 379-387

Gas-solid reaction
kinetic runs

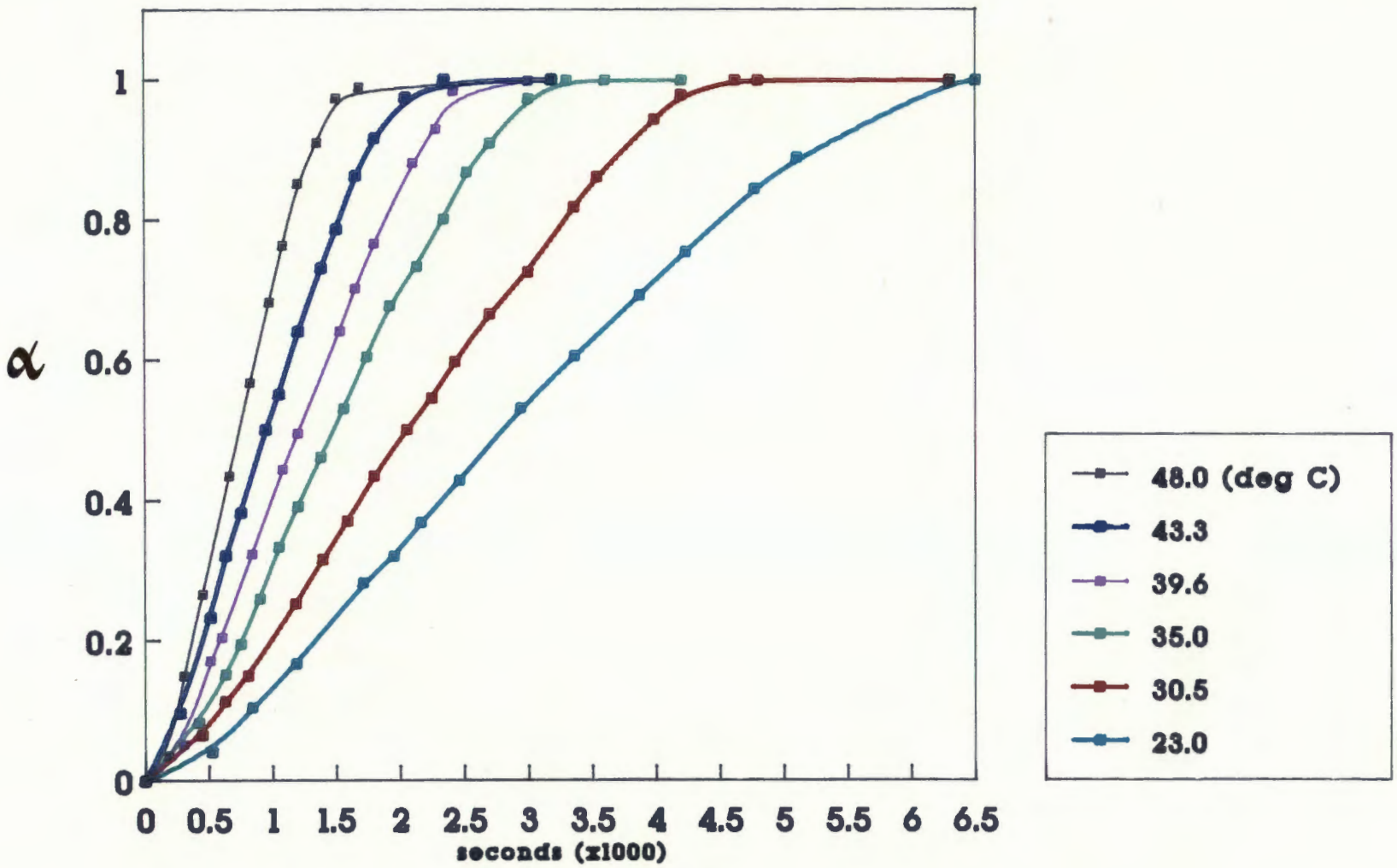

Each of the above rate laws describe a particular gas-solid reaction mechanism. Rate equations 1 and 2 are based on geometric models: $1-(1-\alpha)^{1/n}=kt$ where n is the number of dimensions through which the interface advances. The reaction is controlled by the advancement of phase boundaries from the outside of a crystal inwards, reaction at the edges of a disc or plate-like particle. This has found applications in studies of the dehydrations of certain substances containing layer-type lattices, for instance, some clathrate hydrates **(9)**.
Rate laws 3, 4, and 5 govern the behaviour of reactions in which there is diffusion of a volatile reactant towards one less volatile. The advance of the interface obeys the parabolic law, in contrast to decomposition reactions. The Jander equation, 6, deals with diffusion proceeding in a spherical particle. It combines one dimensional diffusion with the rate law for contracting volume because there is an increase in thickness in the barrier layer of the spherical particle. Reactions involving nucleation would be governed by the sigmoid rate equations 7-12. The Avrami-Erofe'ev equations apply if the rate of a solid state reaction is governed by random nuclei that grow in a specific dimension/s and ingest other nuclei. They hold for many solid phase decompositions, phase transformations and recrystallizations of alloys.

The Prout-Tompkins equation considers the special case where the rate of a solid state reaction is controlled by linearly growing nuclei that branch into chains and are terminated according to the number of nuclei present. It has applications to many systems, for example the thermal decomposition of potassium permanganate. The power laws, 13-16 are acceleratory rate equations. The rate equations that are based on order of a reaction are not always as applicable for solid state reactions because the concept of molecularity of a reaction is not necessarily well defined for solid state reactions **(10)**.

The purpose of the kinetic study was to establish the reaction mechanism by determining which rate equation provided the most accurate fit to the experimental data. Several of the kinetic equations gave good fits to the data according to their correlation coefficients. It was thus necessary to consider the relevance and applicability of possible mechanisms in conjunction with good correlation. Bearing these factors in mind this resulted in the choice of the rate law for one-dimensional

---

9 O Yamamuro & H Suga, *J.of Thermal Analysis*, 35, 1989, 2025-2064

10 CH Bamford CFH Tipper (Eds.), *op.cit.*, 61-67
SR Byrn, "*Solid-State Chemistry of Drugs*", Academic Press, New York, 1982, 61-62
CJ Keattch & D Dollimore, "*An Introduction to Thermogravimetry*", 2nd Edition, Heyden & Son ltd., London, 1975

diffusion, where diffusion through the reacted zone is the rate determining step **(11)**. The correlation coefficients obtained varied between 0.98 and 1.00.

$$f(\alpha) = kt = \alpha^2$$

CORRELATION COEFFICIENTS OF THE KINETIC ANALYSIS

Temperature(^{o}C)	Ln k	Correlation Coefficient
23.0	-8.686	0.984
30.5	-8.194	0.983
35.0	-7.946	0.990
39.6	-7.689	0.986
43.3	-7.469	0.991
48.0	-7.277	0.983

The rate determining step of the gas-solid reaction may be described either in terms of diffusion of the acetone, or else in terms of chemical reaction involving bond redistribution at the reaction interface, ie the phase change from α to β **(12)**. In a diffusion-limited reaction, the overall rate is determined by the movement of the reacting species to the reaction interface **(13)**. The former mechanism seemed most probable after considering the structure of the host1, the vapour pressure of the acetone and confirmational experimental evidence. One-dimensional diffusion would correspond to the movement of acetone through the channels which run parallel to the c-axis. Increases in reaction rate with temperature obey the Arrhenius equation and hence an activation energy may be calculated. An Arrhenius plot of ln k versus the inverse of time, yielded a satisfactory straight line, from which was obtained an activation energy of 45.3 kJmol-1 as shown in figure 6.

---

11 JH Sharp, GW Brindley & BN Narahani Achar, *J.Amer.Ceram.Soc.*, 49(7), 1966, 370-383
SR Byrn, *op. cit.*, 65
G Wilkinson, D Gillard & JA McCleverty (Eds.), HE leMay in "*Comprehensive CoordinationChemistry*", Pergamon Press, Oxford, Vol.1, 1987, 464
W Jander, *Z.anorg.allg.Chem.*, 166, 1927, 31-51

12 CH Bamford & CFH Tipper (Eds.), *op. cit.*, Vol. 22, 41

13 CH Bamford & CFH Tipper (Eds.),*op. cit.*, Vol. 22, 41

Figure 6

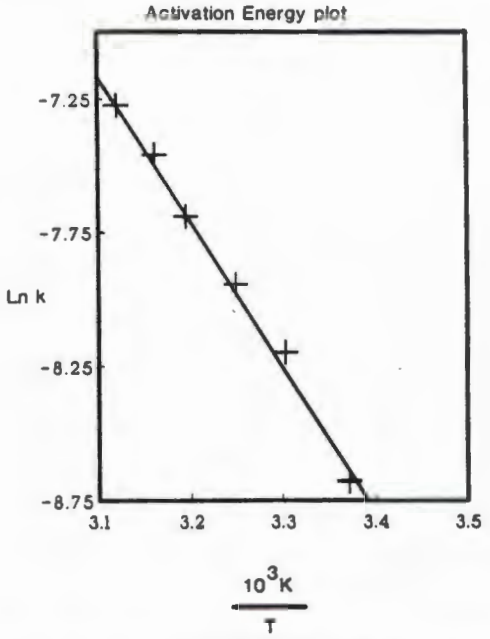

In attempting to explain the phenomenon of this solid-vapour reaction, the crystal structure of both the host1-acetone compound, and the α-form of host1 should be considered.

The acetone guest molecules are known to hydrogen bond to host1 and to lie in channels which run parallel to the c axis in the host1-acetone compound. Figure 7 illustrates a van der Waals radii packing diagram of α-form host1 with the hydroxyl moieties which are exposed on the bc face are shaded. The accessibility of the hydroxy moieties favours possible reaction with incoming acetone carbonyl groups. Reaction causes a change in phase so that the new host1-guest product compound thus formed, separates from the reactive surface of the α-phase. In this way, diffusing guest molecules are able react with exposed reactive host1 hydroxy groups of the next layer of host1 molecules **(14)**.

Figure 7

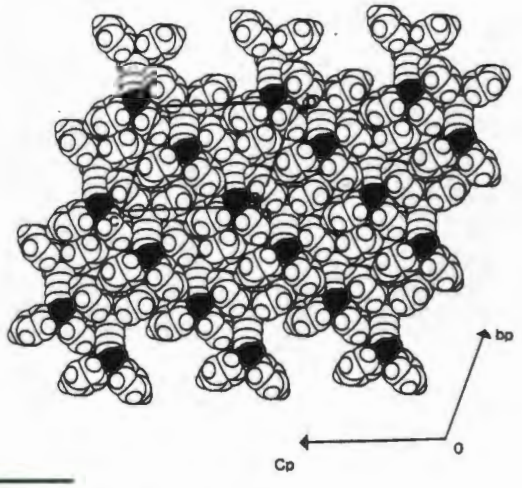

14 CH Bamford & CFH Tipper (Eds.),*op. cit.*, Vol 22,41

Figure 8 illustrates the way in which acetone molecules (dotted) interact with the exposed hydroxy groups (striped) located on the bc plane of the host1-acetone structure.

Figure 8

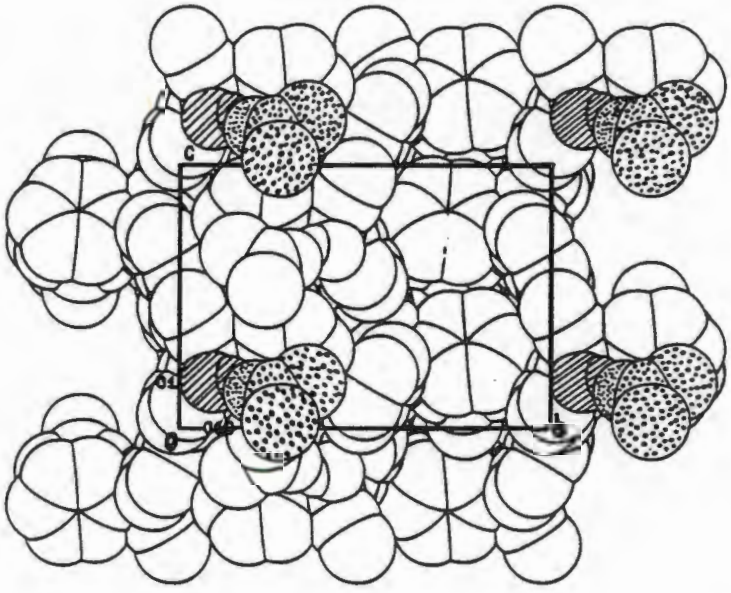

When the α-form is exposed to acetone vapour visible physical swelling occurs as the α-phase reacts and converts into the β-phase. A series of photographs shown overleaf illustrates this. Photograph (a) shows a crystal of α host1 under polarised light which had been grown from ether. After 20 minutes of exposure to acetone vapours, these crystals become opaque, photograph (b). Photograph (c) shows how after six hours exposure to acetone, the crystalline form of α host1 has undergone a phase change to the β form, host1-acetone compound. X-ray powder diffraction was used to confirm the phase obtained.

In some cases the products of a gas-solid reaction can be controlled by exposing a particular face of a crystal to encourage anisotropic migration **(15)**. A reaction of this type has been proposed for the analogous reaction of p-chlorobenzoic acid with ammonia gas by Miller, Paul and Curtin **(16)**. They observed that there is preferential attack by the ammonia at those faces where the carboxyl groups of the acid are accessible **(17)**.

---

15 SR Byrn, *op. cit.*, 228

16 RS Miller, IC Paul & DY Curtin, *J.Am.Chem.Soc.*, 96, 1974, 6334

17 GR Desiraju (Ed.), "*Organic Solid State Chemistry*", Elsevier, Amsterdam, 1987

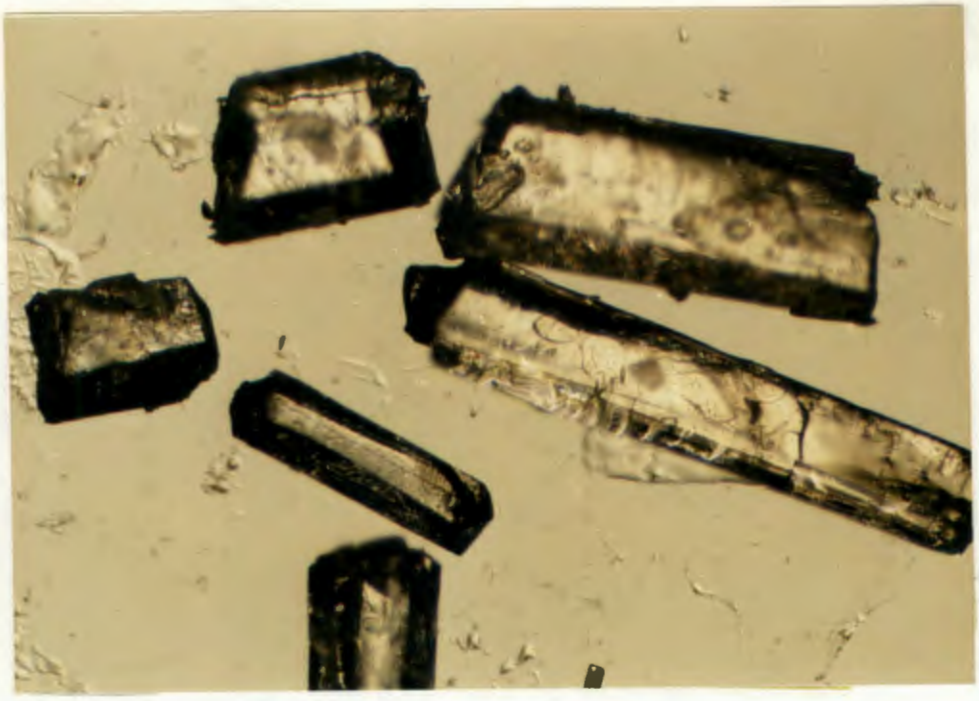

a

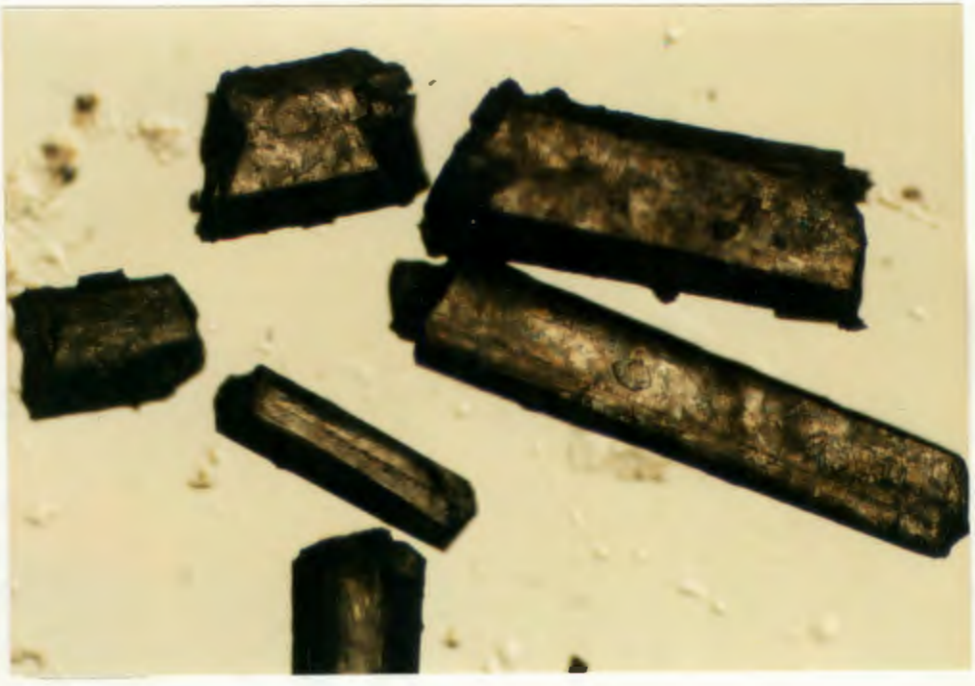

b

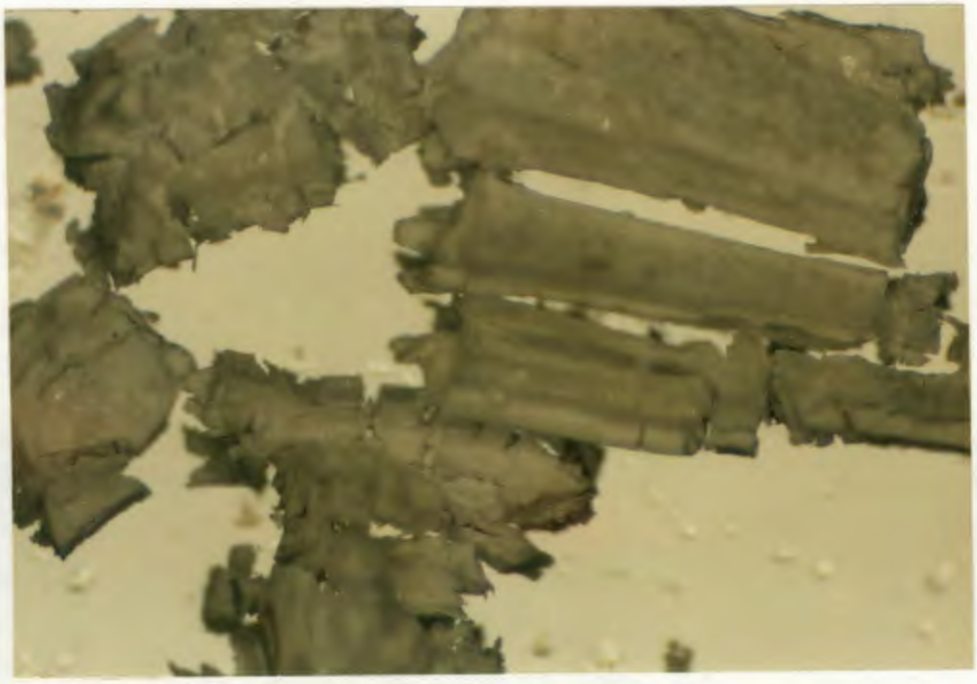

c

THE STRUCTURE OF THE HOST1-BENZOPHENONE (1:1) INCLUSION COMPOUND

Host1 undergoes a solid phase reaction when it is shaken together with benzophenone (which will be discussed in detail later in this chapter). In order to perform a comprehensive study of the organic solid state chemistry of such a system, it was of interest to determine the structure of the host1-benzophenone.

EXPERIMENTAL

Suitable crystals of Host1-benzophenone were obtained by dissolving equimolar quantities of both components in cyclohexane and evaporating this solution for approximately 6 days or until crystals were observed to form.

SOLUTION AND REFINEMENT

Oscillation and Weissenberg photographs established that the host1-benzophenone compound belonged to the monoclinic space group $P2_1/c$ and the crystal reflection data exhibited non-extinction reflection conditions confirming this.
h0l: l=2n
0k0: k=2n
(00l: l=2n)
The structure was solved using direct methods with an R_{int} value of 0.0447, indicating the internal consistency of reflection intensities for merged pairs, for the data set and 5783 unique reflections. The combined figure of merit had a value of 0.251 for forty-six surviving atoms which corresponded to one host1 molecule and one benzophenone. The temperature factors of all non-hydrogen atoms were refined anisotropically. Hydroxyl hydrogen atoms were located from difference electron density maps and were refined with individual temperature factors. Some of the phenyl hydrogens emerged in the difference electron density maps but all were refined with a common temperature factor and placed in calculated positions. The weighting factor g, in the weighting scheme was allowed to refine to 0.0048 since this yielded a satisfactory analysis of variance and acceptable temperature factors. The final residual factor was 0.0446 and there was 0.142 $eÅ^{-3}$ residual electron density. Reflections (1 0 0) and (-1 0 2) were omitted because they are reflections at low θ and suffered from secondary extinction which was indicated values of F_o being much lower that those of F_c. Details of the intensity data collection and refinement may be found in Table 3.

DISCUSSION

Figure 9 illustrates the stoicheiometry of the 1:1 host1-benzophenone compound, the hydrogen bonding scheme involves two host molecules and one guest molecule. The hydroxyl oxygen atom O1A of the host1 molecule, located on Wyckoff position *c*, acts as a hydrogen bond donor to the carbonyl oxygen atom of benzophenone (O---O = 2.670(2)Å). O1A also acts as a receptor for the hydroxyl oxygen atom O1B of the host1 molecule located on Wyckoff position *d* (O---O = 2.786(3)Å). The dual capacity of hydroxy groups is well known and Goldberg describes it as " providing the main driving force for clathrate formation" **(18)**. In the crystal this results in alternating rows of hydrogen-bonded host1 molecules which are illustrated overleaf in figure 11. The guest lay in cavities which were approximately of 7.1Å by 9.7Å in dimensions.

Figure 9 the hydrogen bonding observed in the host1-benzophenone inclusion compound

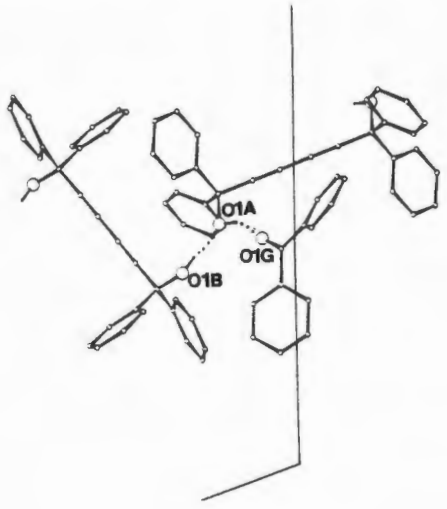

The bulky phenyl groups prevent close packing and create molecular voids which guest molecules may occupy. This is example of an ædiculate host-guest arrangement and is depicted in figure 10. Functional group assisted inclusion is influential and the coordinative interactions between the hosts on one hand, and the host and guest on the other, are the main stabilizing forces in the crystal lattice. Conformational aspects and torsion angles will be discussed at the end of this chapter.

---

18 I Goldberg in " Inclusion Compounds", JL Atwood, JED Davies & DD MacNicol (Eds), Oxford University Press, Oxford, 1991, 427

Figure 10

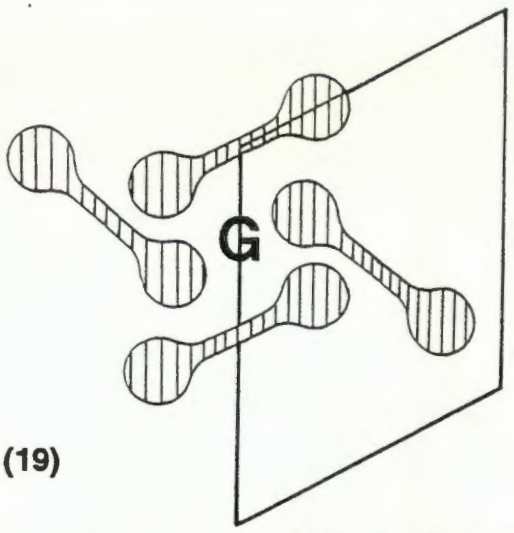

Guest occupies voids
created by host1 molecules **(19)**

Figure 11 contains packing diagrams showing the way in which the backbone ie. the long carbon chains of the 2 host1 molecules have a zigzagged packing motif due to the orientating influence of hydrogen bond formation.

Figure 11 Packing diagrams along [0 1 0] of host1-benzophenone compound

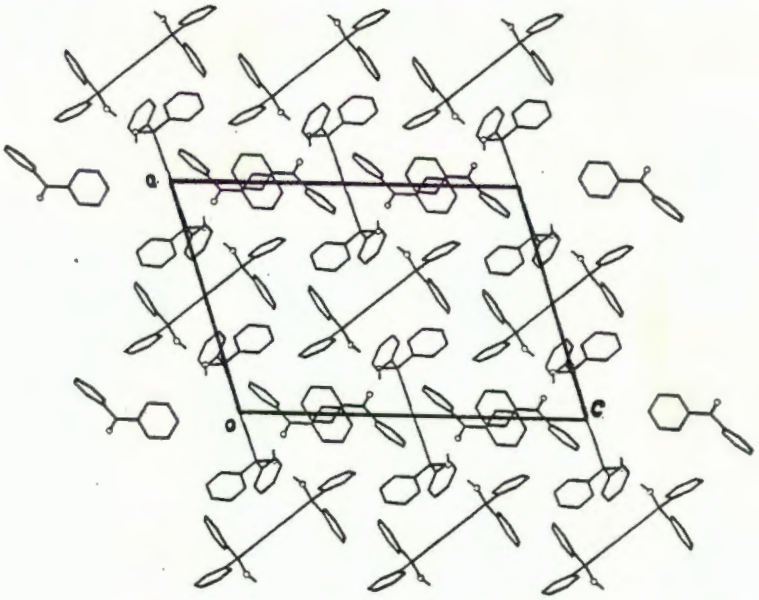

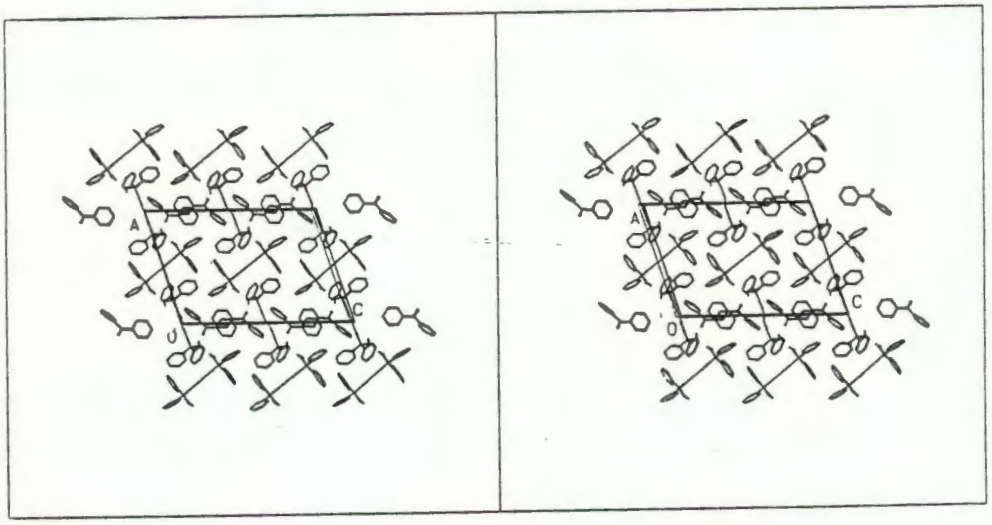

19 JL Scott, private communication, 1991

TABLE 3 CRYSTAL DATA AND EXPERIMENTAL DETAILS FOR HOST1-BENZOPHENONE STRUCTURE.

Compound	**Host1-Benzophenone**
Molecular formula	$C_{30}H_{22}O_2 \cdot C_{13}H_{10}O$
Molecular weight ($gmol^{-1}$)	596.7
Space group	$P2_1/c$
a (Å)	16.119(3)
b (Å)	9.181(3)
c (Å)	23.541(3)
β (°)	108.62(1)
Z	4
V ($Å^3$)	3302(1)
D_c (gcm^{-3})	1.20
D_m (gcm^{-3})	1.19(2)
$\mu(MoK_\alpha)$ (cm^{-1})	0.40
F(000)	1256
Data collection (21°C)	
Crystal dimensions (mm)	0.47x0.25x0.31
Range scanned θ (°)	1-30
Range of indices *h,k,l*	±19,+10,+28
Reflections for lattice parameters no.,θ range (°)	24,16-17
Instability of standard reflections (%)	1.0
Scan mode	(ω-2θ)
Scan width in(°)	(0.90+0.35tanθ)
Vertical aperture length (mm)	4
Aperture width (mm)	(1.12+1.05tanθ)
Number of reflections collected (unique)	5783
Number of reflections observed with $I_{rel} > 2\sigma I_{rel}$	3345
Final refinement	
Number of parameters	425
R	0.045
wR	0.052
w	$(\sigma^2(F_o)+0.0048F_o^2)^{-1}$
S	0.849
Max. shift/e.s.d.	0.001
Max. height in difference electron density map ($eÅ^{-3}$)	0.14
Min. height in difference electron density map ($eÅ^{-3}$)	-0.23

SOLID-SOLID REACTION

Toda, Tanaka and Sekikawa had performed solid-solid reactions by mixing a host and a guest together to obtain complexes with no charge transfer interactions. Using host1, they were able to obtain inclusion complexes with solid guests such as benzophenone, chalcone, 2-pyridone and p-dimethylaminobenzaldehyde **(20)**. Further studies of this kind led them to deduce that "the movement of molecules in host1-guest complex formation" was favourable in the solid state **(21)**.
The host1 compound is able to undergo a solid state reaction with benzophenone, since when the host1 and guest are shaken together at room temperature, they react to form a hydrogen-bonded complex.

$$HOST1_{(s)} + BENZOPHENONE_{(s)} \xrightarrow{\text{shaking}} [HOST1\ BENZOPHENONE]_{(s)}$$

EXPERIMENTAL

The host1 and guest were pre-dried in a vacuum oven at 30°C and then sieved to ensure that particle size lay in the range 75μm to 150μm. Equimolar quantities of the two reactants were then mixed together in a sealed tube and shaken together at a constant frequency. The reaction was effectively completed after 16 minutes of shaking at room temperature and samples of the reaction mixture were withdrawn at 2 minute intervals for analysis.

RESULTS AND DISCUSSION

The reaction was followed using a variety of analytical techniques. However reproducibility problems became significant when attempts were made to quantify the results accurately . This was due to the fact that the reaction could not be analysed *in situ* over time because a "new" sample had to be withdrawn from the reaction mixture for analysis at each reaction time and this rendered results insufficiently reproducible for quantitative analysis. Infra Red spectroscopy proved to be the most successful analytical technique attempted. Spectra were recorded in the 3000-4000 cm^{-1} range **(22)** because bands in this region arising from symmetrical and anti-symmetrical O-H stretching modes **(23)** may be assigned. This proved to be

---

20 F Toda, K Tanaka & A Sekikawa, *J.Chem.Soc.,Chem.Commun.*, 1987, 279

21 F Toda, M Yagi & K Kiyoshige, *J.Chem.Soc.,Chem.Commun.*, 1988, 959

22 RC Weast, MJ Astle & WH Beyer, CRC Handbook of Chemistry & Physics, 66th Edition *op. cit*, F197-205

23 M McNamara & NR Russel, *J.Inclusion Phenomena*, 10, 1991, 485-495

successful because these modes could be used as qualitative criteria for hydrogen bond formation detection **(24)**. The value of the O-H stretching frequency has been used as a test for, and measure of, the strength of hydrogen bonds:- the stronger the hydrogen bond the longer the O-H bond and the lower the frequency of vibration **(25)**

The α-phase of host1 which does not exhibit hydrogen bonding absorbed strongly at 3525cm^{-1} corresponding to free O-H stretching at reaction time=0. Infra red spectra determined that mixing alone was unable to initiate any reaction and shaking was required in order to start and propagate the reaction. As the reaction proceeds with shaking, the absorption band at 3525cm^{-1} is seen to decrease in size whilst there is concomitant increase in intensity of a peak at 3400cm^{-1} which is illustrated below. The latter absorption peak is due to weakening of the O-H bond which results in infra red absorption at a lower frequency. Even at the beginning of the reaction; a small shoulder at 3400cm^{-1} was observed due to the O-H stretching absorption of water which was a constant problem encountered. Despite considerable precautions to carry out the whole analysis under rigorously dry conditions, this was never in fact achieved. The presence of the band due to the absorption of the O-H stretching of water was however always small and diffuse.

Infra red spectra following the course of the solid-solid reaction:

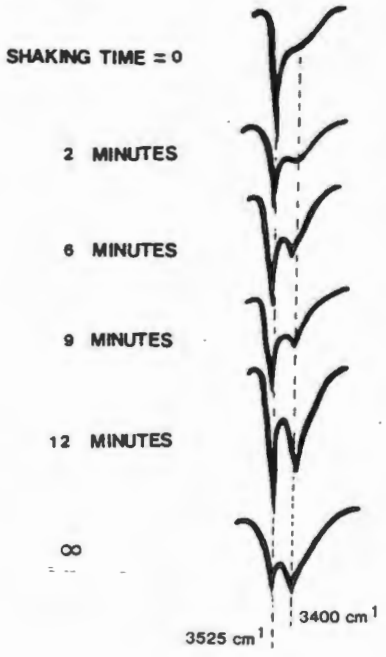

---

24 GC Pimentel & HL McClellan, "*The Hydrogen Bond*", WH Freeman & Co., New York, 1960, 70

25 D H Williams & I Fleming,"*Spectroscopic methods in Organic Chemistry*", 3rd edition, Mc-Graw-Hill ltd., London, 1980
AO Patil, DY Curtin & IC Paul, *J.Amer.Chem.Soc.*, 106, 1984, 348-353
NB Singh, NN Singh & RK Laidlaw, *J.Sol.State.Chem.*, 71, 1987, 530-539

Despite extensive efforts to quantify the kinetics of this solid-solid reaction, attempts in this regard were not entirely successful. Although pre-massed quantities of sample and NUJOL or KCl were analysed, the fact that a 'different' sample corresponding to each reaction time was placed in the spectrophotometer, meant that peak intensity was too unreliable as a quantitative measure of the extent of reaction. Figure 11 shows a plot of reaction time versus the ratio of infra red absorption peaks $3400cm^{-1}$:$3520cm^{-1}$ for the solid state reaction. It shows the observed trend as the hydrogen bonded hydroxyl absorption peak at $3400cm^{-1}$ increases due to solid state reaction. This is illustrative of the quality of kinetic data obtained from Infra red spectroscopic analysis.

Figure 11

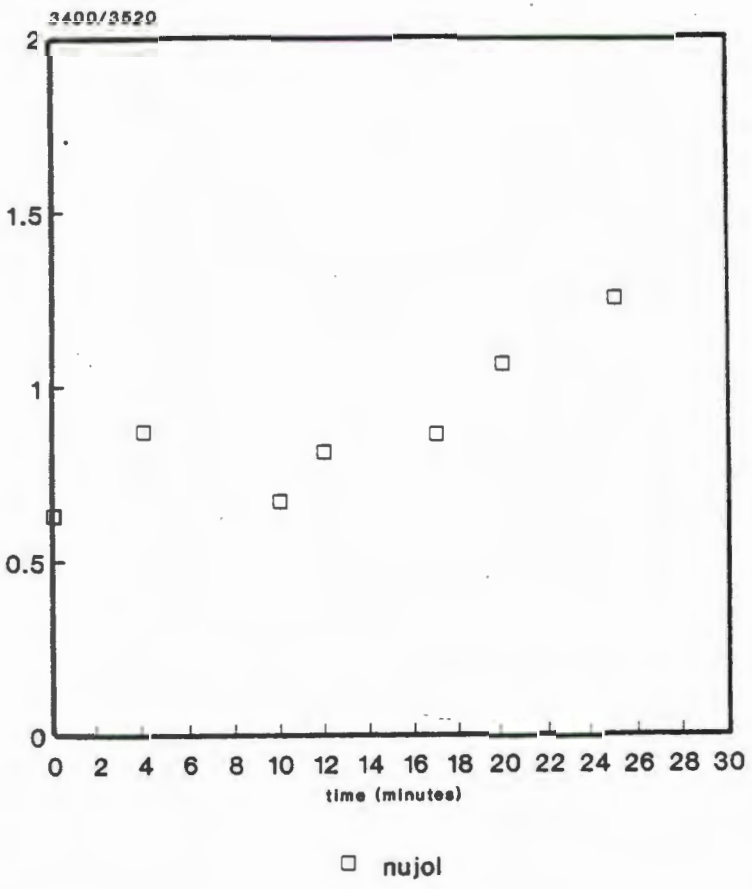

^{13}C NMR

In principle, solid state NMR is predicted to detect small differences in the environment of functional groups which in a normal NMR, would only be seen as a broad featureless spectrum **(26)** because of strong interactions between observed nuclei with neighbouring nuclei with subsequent coalescence of peaks. Samples were sent away to the CSIR, Pretoria, for solid state ^{13}C NMR and the spectra obtained showed that the :-*C-C- of host1 ie the sp^3 carbon atom experienced a field perturbation after undergoing the solid-solid reaction. The NMR spectra of the host1, benzophenone and the host1-benzophenone complex may be found in figure 12. The signal (δ = 80.6 ppm) arising from the *C-OH of the host1, is split into a doublet (δ = 82.5 & δ = 78.5 ppm) after it was shaken together with the benzophenone **(27)**. Shifts in the resonance due to hydrogen bonding have been reported on studies involving the linkage positions of glucose oligomers and polymers **(28)** and alcohols **(29)**. This angle could not be comprehensively pursued owing to lack of access to the solid state NMR probe necessary for these types of experiments as well as the prohibitive cost of each experiment.

---

26 SR Byrn, *op. cit.*,323

27 E Breitmaier & W Voelter, "*Carbon-13 NMR Spectroscopy*", 3rd Edition, VCH, Weinhem, 1987
AE Derome, "*Modern NMR Techniques for Chemistry Research*", Pergamon Press, Oxford, 1987

28 JD Roberts, FJ Weigert, JI Kroschwitz & HJ Reich, *J.Amer.Chem.Soc.*, 92, 1976, 1343

29 T Usui, N Yamaoka, K Matsuda, K Tuzimara, H Sugiyama & S Seto, *J.Chem.Soc Perkin I*, 1973, 2425-2432

Figure 12

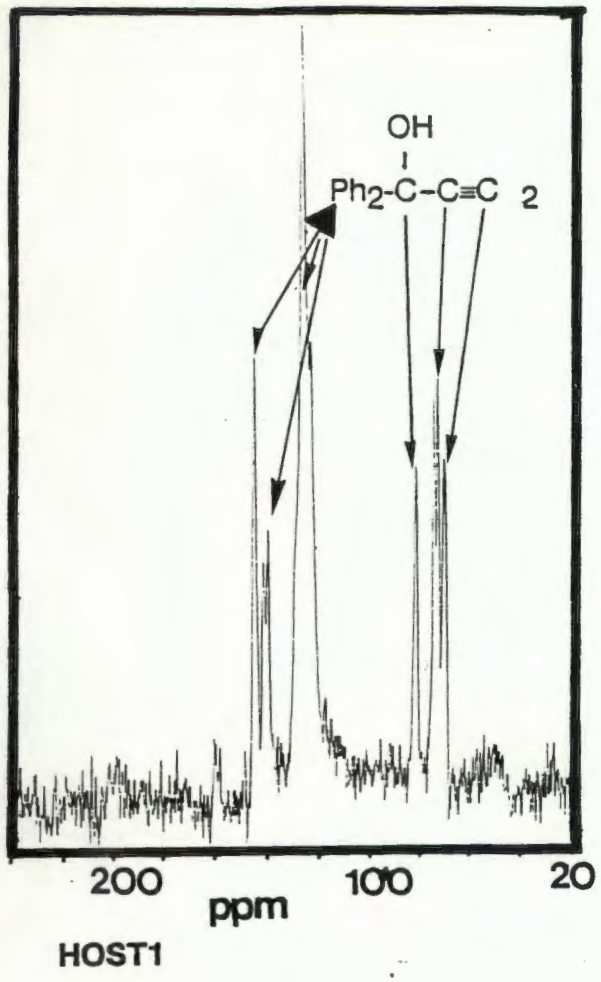

HOST1

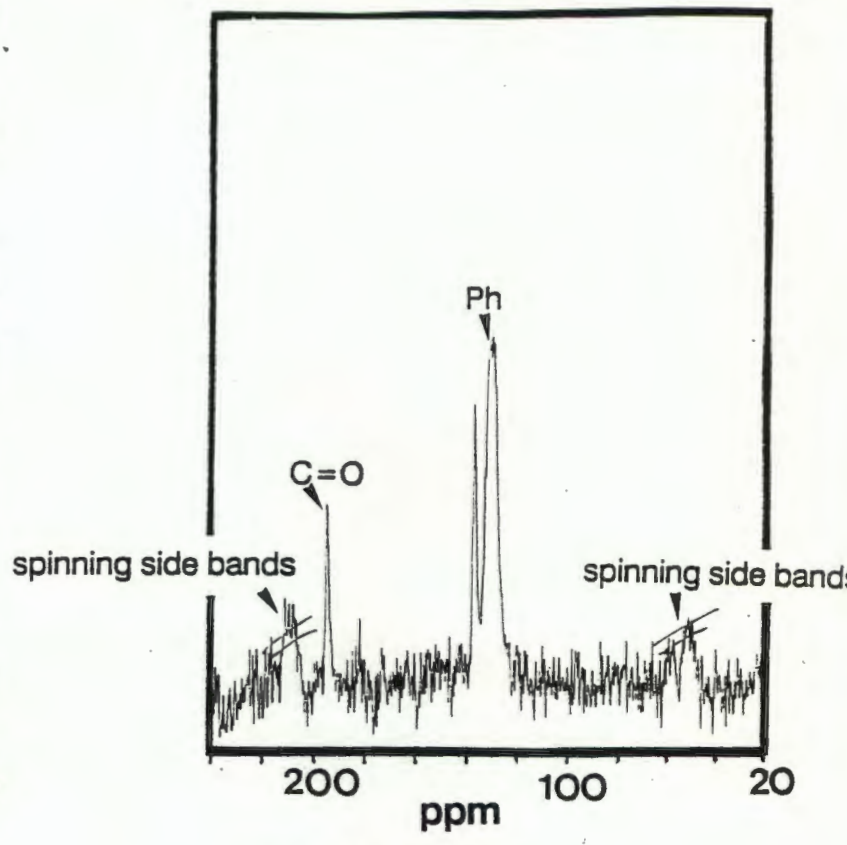

BENZOPHENONE

(^{13}C Benzophenone by Bloch decay, ω_r=6000 Hz)

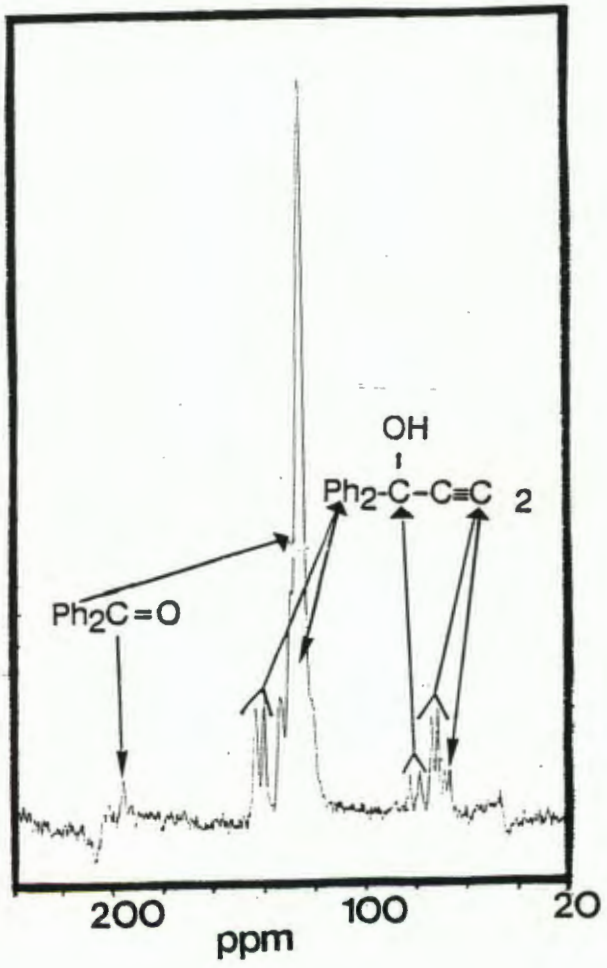

X-RAY POWDER DIFFRACTION STUDIES OF THE SOLID STATE REACTION

X-ray powder diffraction studies were performed by scanning samples withdrawn from the reaction mixture every two minutes. Peak shifts were observed but despite extensive attempts, this technique proved to be insufficiently quantitative as a kinetic monitor owing to difficulties in packing the samples and severe static in the sample particles. Several modes of packing the samples were tried but the results were not sufficiently reproducible to warrant attempts at quantifying the results obtained **(30)**.

RAMAN SPECTROSCOPY

Raman spectroscopy is able to detect symmetrical stretching that is inactive and hence unobservable in the Infra red. Moreover, water is a only a weak scatterer of Raman radiation and for this reason it was tried as an analytical tool for the solid state reaction. Once again reproducibility was poor, and dependence upon intensity changes as a quantitative measure of rate proved to be ~~quantitatively~~ unreliable. The C≡C stretch was examined and the decrease in intensity of the 2263.1 cm^{-1} symmetrical stretching band as the solid-solid reaction proceeds may be seen below **(31)**.

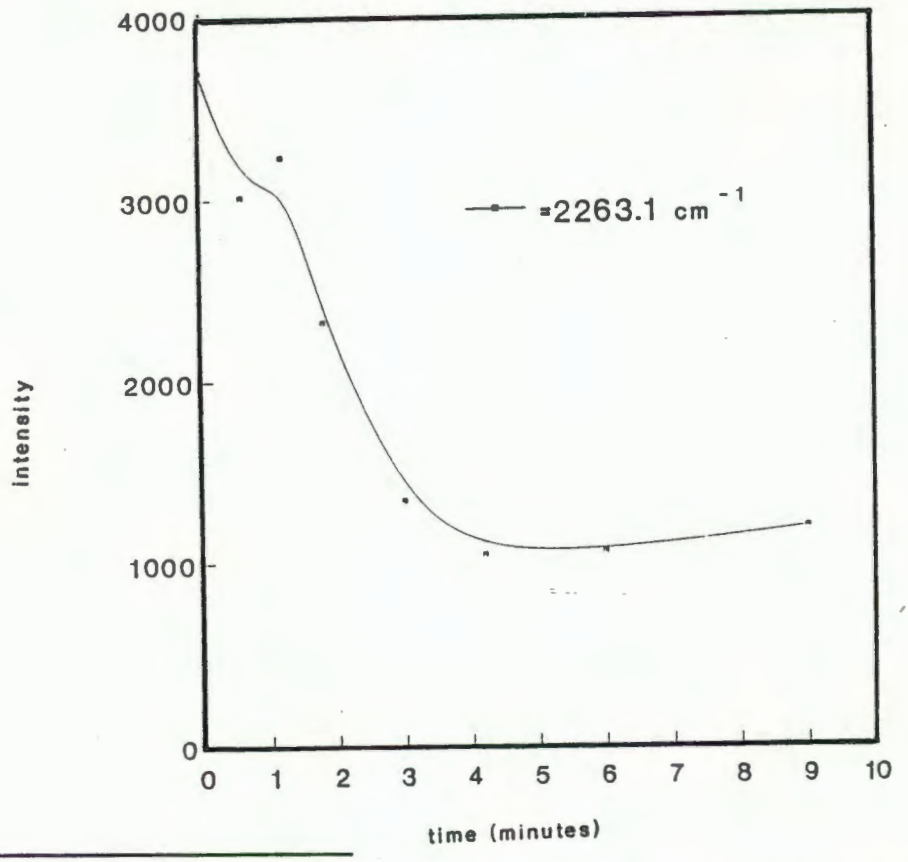

30 PJ Brown & JB Forsyth, "*The Crystal Structure of Solids*", Edward Arnold, London, 1973

31 DA Skoog, "*Principles of Instrumental Analysis*" 3rd Edition, CBS College Publishing, 1985

REACTION MECHANISM

When considering solid state reactions it is important to bear in mind that, in contrast to liquid and gas phase reactions, the reactant molecules in solid-solid reactions are unable to move freely. Thus reaction occurs within the constraining environment of the crystal lattice. The reactant crystal lattice can control the kinetic features of a reaction and the nature of the products, ie topochemical features must be considered **(32)**. Propagation of the reaction is complex, and ideally, when trying to quantify the kinetics of a solid phase powder reaction, one should be concerned with grain size, grain size distribution, grain shape, the contact area between these grains as a function of time and vapour pressure of the reactants **(33)**. Thus, the large number of parameters and the fact that reactions between powders are localized, mean that quantitative analysis of the kinetic features and elucidation of the mechanism of a solid-state reaction are very complicated indeed **(34)**.

One successful quantitative method of following a solid phase reaction is the capillary method which was first reported by Rastogi, Bassi and Chadha in 1962 **(35)**. According to their method, two organic reactants are placed separately in a glass capillary so that the two components are in contact with each other. By observing the boundary of contact they were able to measure the thickness of the growing product as a function of time. Since this method requires colour differentiation at the reaction boundary, this procedure was unsuitable for the solid-state reaction considered and could not be employed because the host1 compound, benzophenone and solid reaction product are all white in colour **(36), (37)**.

---

32 G Wilkinson, D Gillard & JA McCleverty (Eds.),*op.cit.*, 463-473

33 H Schmalzried, "*Solid State Reactions*", 2nd edition, Verlag Chemie, Basel, 1981

34 NB Hannay, "*Solid-State Chemistry*", Prentice-Hall Inc., New Jersey, 1967
NB Hannay (Ed.), "*Treatise on Solid State Chemistry*", Vol.4, Plenum Press, New York, 1976
RN Barrer, "*Zeolites and Clay Minerals as Sorbents and Molecular Sieves*", Academic Press, London, 1978
JS Anderson, MW Roberts & FS Stone (Eds.), "*Reactivity of Solids*", Chapman & Hall, London,1972
MM Labes, HW Blakeslee & JE Bloor, *J.Amer.Chem.Soc.*, 87, 1965, 4251-5255
P O'Brien, *Polyhedron*, 2, no 4, 1983, 233-243
CG Savelyev, AA Medvinskii & YV Mitrenin, *J.Sol.State Chem.*, 26, 1978, 69-77

35 R.P. Rastogi, P.S. Bassi & S.L. Chadha, *J.Phys.Chem*, 66,1962, 2707-2710

36 R.P. Rastogi, P.S. Bassi & S.L. Chadha, *J.Phys.Chem*, 67,1963, 2569-2573

37 GR Desiraju (Ed.), "*Organic Solid State Chemistry*", Elsevier, Amsterdam, 1987
H Schmalzried, *op. cit.*

Figure 13 shows the possible reaction mechanism scheme, figure 13a represents reaction of guest (G) with host1 (H) at the reaction interface. This is followed by molecules of G crossing the product boundary by surface migration or grain boundary vapour phase diffusion which is initiated by lattice disturbances, as indicated in figure 13b. In figure 13c, the reaction is propagated by turbulent shaking. Reaction between the powders only occurs upon shaking during which time G is able to penetrate the lattice and diffuse through cracks in the crystal and continue reacting **(38), (39).**

Figure 13

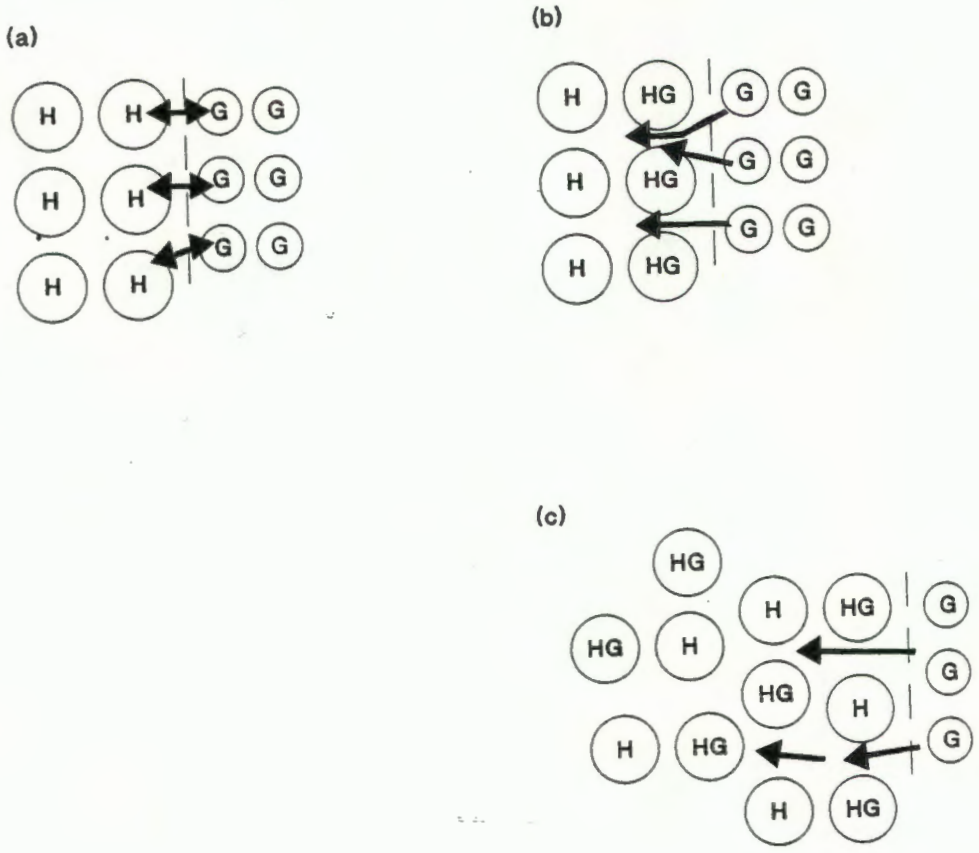

---

38 RP Rastogi, *J.Scient.Ind.Res.*, 29, 1970, 177-189
RP Rastogi & BL Dubey,*J.Amer.Chem.Soc.*, 89, 1967, 200-209

39 RP Rastogi, NB Singh & RP Singh, *J.Sol.State Chem.*, 20, 1977, 191-200

Reactivity of the host can be explained in terms of accessibility of the host hydroxy moieties and in terms of the relatively low $\Delta H_{sublimation}$ of 20kJmol^{-1} of benzophenone **(40)**. This is analogous to the gas-solid reaction, viz. access to the reactive sites on the ac plane of α-form host1. Therefore the host1 hydroxyl moieties are susceptible to reaction by forming hydrogen bonds with incoming carbonyl groups. Favourable geometry of the reactants and products is the driving force for the occurrence of solid state reactions **(41)**. The fact that the host-guest ratio of complex formed is 1:1 is significant in itself. This is noteworthy since, owing to the geometry of the guest and orientation of reacting functionalities, only one guest is involved in the formation of this coordination-assisted clathrate. The orientation of hydrogen bond forming moieties on the bc plane is illustrated in the figure below.

Illustration to depict the relative orientations of interacting host and guest moieties

(i) host1 molecule interacting with another host1 molecule, no guest molecule
(ii) a guest molecule is hydrogen bonded in place

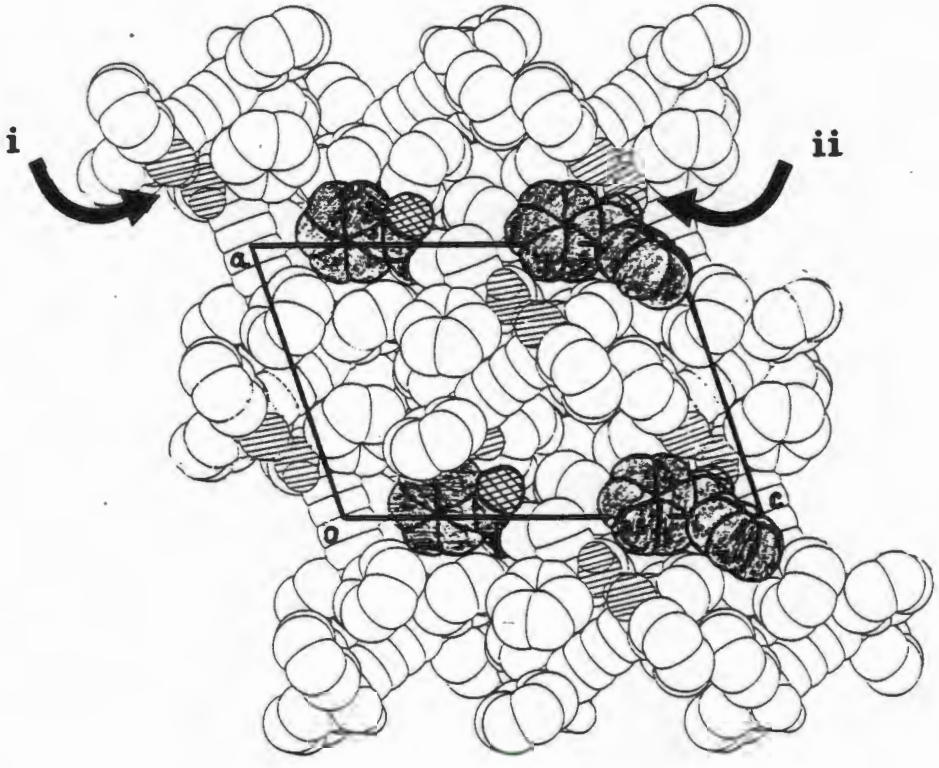

---

40 *CRC Handbook of Chemistry & Physics*, op. cit., 864

41 RP Rastogi, *J.Scient.Ind.Res.*, 29, 1970, 177-189
NB Singh & HC Singh, *J.Sol.State Chem.*, 38, 1981, 211-218
NB Singh & RJ Singh, *J.Sol.State Chem.*, 76, 1988, 375-390

Only one benzophenone molecule interacts with one host lattice molecule, resulting in self-association of the latter host molecule with another host1 molecule. The solid state reactivity of the crystal depends on a balance between steric packing factors and electronic properties **(42)**. Crystal packing is a function of recognition of molecular shapes and, via the hydrogen bonding scheme, there is effectively little host1 lattice disturbance since only one guest molecule reacts. There is reorientation of a second host molecule so that the overall host1 structural motif is relatively undisturbed (if the packing motif of this β form is compared to that of the α form).

Reaction will not occur if the two reactants are separated by an air gap because benzophenone has a very low vapour pressure at room temperature. This, combined with the fact that the reaction requires shaking in order to take place, implies that a vapour phase diffusion mechanism does not rule the rate determining step. The route by which reaction end point is attained most probably involves surface diffusion of the benzophenone molecules into surface cracks and imperfections with further reaction being propagated by the action of vigorous shaking.

---

42 M Pierrot, "*Structure and Properties of Molecular Crystals*", Elsevier, Amsterdam, 1990

ELECTRON MICROSCOPY

In order to provide experimental support for the proposed mechanism, the surfaces of the reacting solids were investigated using electron microscopy. Electron micrographs 1-3 at magnifications of 37, 616 and 2400 times respectively, show particles of the host1 grown from acetone and vacuum dried to result in desorption of the acetone.

Electron micrograph 3 reveals that the host1 grown from acetone and dried under vacuum at 60°C ie the α-phase, has a porous sponge-like crystal habit. This porosity implies a relatively large surface area and hence many possible reaction sites exist. Electron micrographs 4-6 (at magnifications of 37, 616 and 2400 times), show the solid state reaction product. Electron micrograph 6 shows the surface of this product at high magnification and it is obvious that the particle has become much less porous and that the pitted surface area has been "filled in" upon reaction with benzophenone. Thus it would appear that the existence of "pitting" in the surface of the host1 compound provides the critical surface area required for reaction to take place. Turbulence encourages the guest to penetrate ever further into lattice grain boundaries, eg. cavities and cracks, observed in the α–phase habit of host1.
Electron micrographs 7 and 8 show benzophenone particles at magnifications of 37.5 and 607 times respectively. The benzophenone is partially sublimed due to the energy of the incident electron beam.
The α-phase of the host1 was grown from solutions of host1 dissolved in diethyl ether as previously described and electron micrographs 9-10 taken at magnifications of 616 and 2400 times, show the external habit of this form. The surface of a particle of host1 is now distinctly non-porous and crystalline.
The solid-solid reaction was subsequently performed using this particular habit of α-form host1.

The product obtained by reacting host1 grown from ether with benzophenone is shown in 11-12. These electron micrographs show particles comprising of clusters of partially reacted materials and reaction product. This may be deduced if a comparison is made with photographs 4-6 which are of the solid state reaction product. In photographs 11-12 the observed particles show reaction of the benzophenone with the host1 at the points of contact only. Unreacted host and guest may also be observed because there is no further reaction with the non-porous form of the host1 other than at these points of contact.

1mm

(1)

1mm

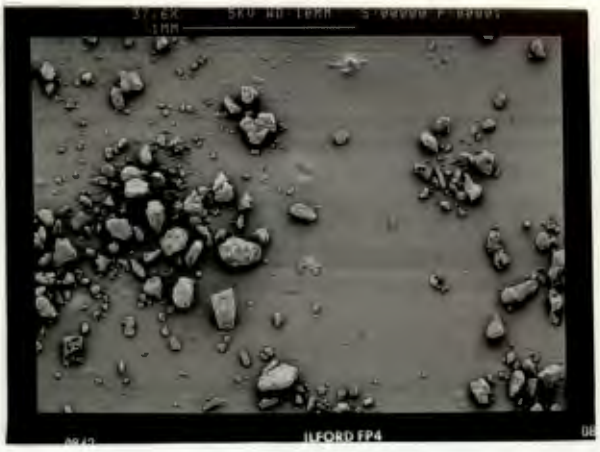

(4)

50μm

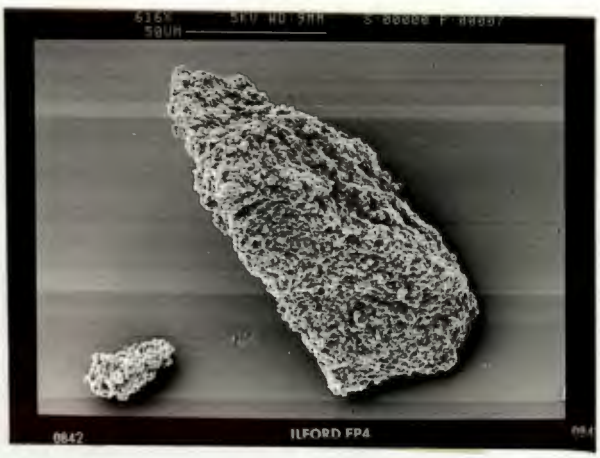

(2)

50μm

(5)

20μm

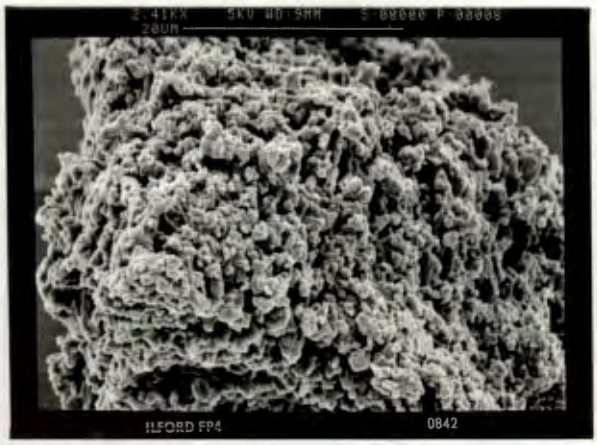

(3)

20μm

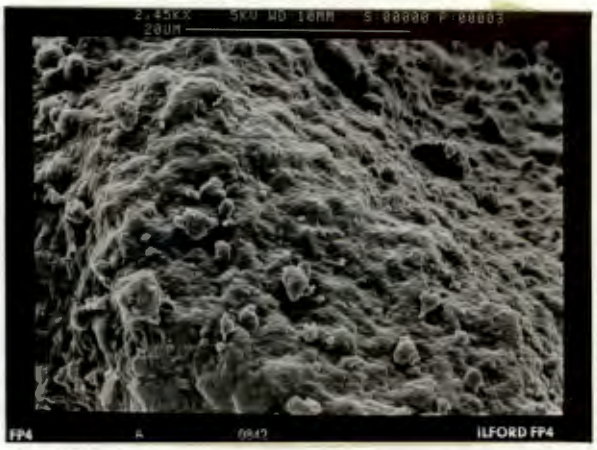

(6)

1mm

(7)

10μm

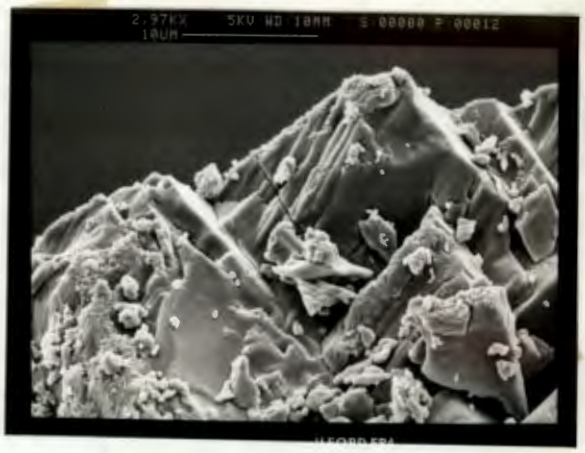

(10)

50μm

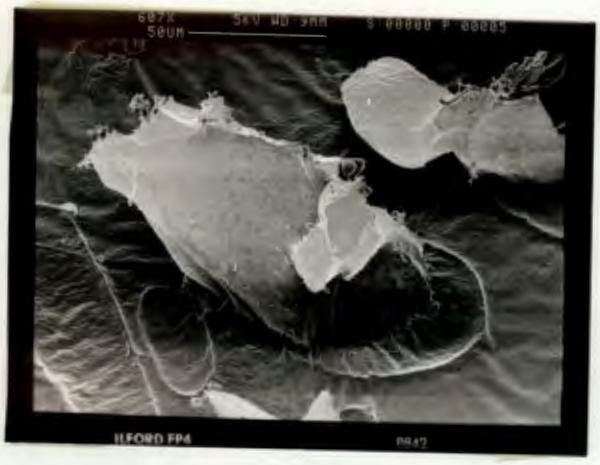

(8)

200μm

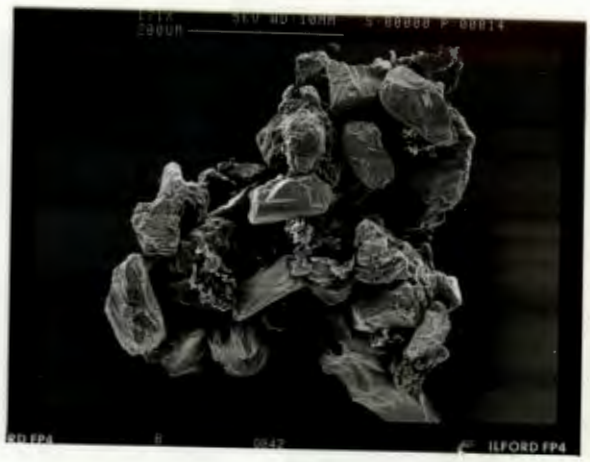

(11)

50μm

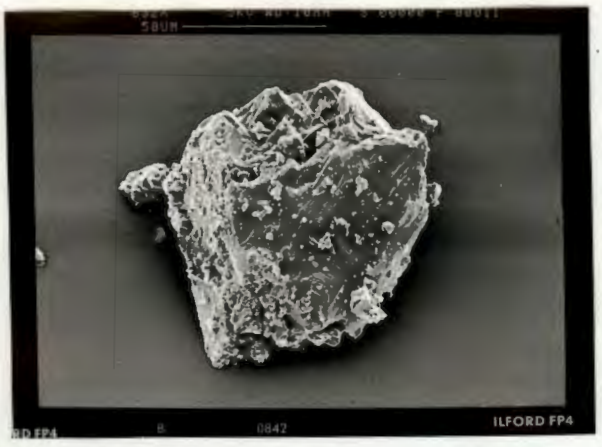

(9)

50μm

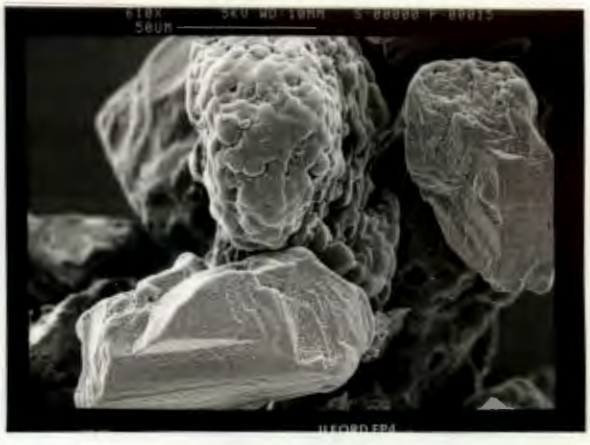

(12)

In order to test this hypothesis, the course of this particular solid-solid reaction was followed using infra red spectrophotometry and is illustrated in figure 14.
It was observed that some reaction occurs during the first five minutes of shaking, as evidenced by the growth of a peak at approximately 3400cm^{-1}. However, there is no further change in the relative peak heights even after forty minutes of shaking which is in contrast to the solid-solid reaction which occurred between the host1 (habit grown from acetone and vacuum dried), and benzophenone. After a reaction time of forty minutes, both the O-H stretching of host1 material, as well as the hydrogen-bonded O-H stretching of the reaction product can be observed. This can be explained if reaction occurred only at the surface of the non-porous host1 compound accompanied by no further reaction by the benzophenone. This would be the case if, according to the proposed mechanism, the benzophenone was unable to penetrate any further into the host1 particle owing to a paucity of cracks and lattice imperfections, ie a smaller available reactive surface area.

These experimental observations lend credibility to the proposed mechanism in which requisite crystal porosity, in conjunction with turbulence, propagate and advance reaction of the guest in the host1 lattice.

	HOST (GROWN FROM ACETONE) & BENZOPHENONE	HOST (GROWN FROM ETHER) & BENZOPHENONE
SHAKING TIME = 0		
2 MINUTES		
6 MINUTES		
9 MINUTES		
12 MINUTES		
17.5 MINUTES		
25 MINUTES		
40 MINUTES		

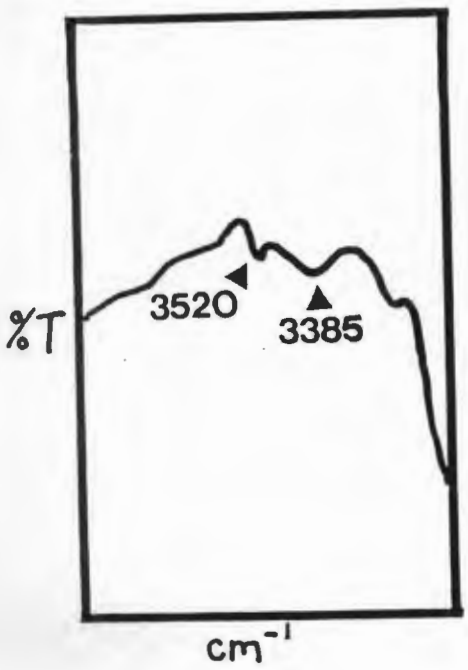

THE STRUCTURES OF OTHER HOST1-KETONE INCLUSION COMPOUNDS

The host1 compound showed a propensity to co-ordinate with guests with carbonyl functions (*n* donors) and in order to form a series for comparative purposes, the structural work was extended to include coordinato-clathrates of the host1 with methyl ethyl ketone (MEK), diethyl ketone (DEK) and acetophenone.

EXPERIMENTAL

Suitable crystals of the molecular complexes were obtained by slow evaporation of dilute solutions of the host1 in the various guest liquids. The time required ranged from 3 to 20 days. Single crystals were mounted inside Lindemann capillaries to prevent desorption of the guest and crystal deterioration. Accurate cell parameters were then obtained by least-squares analyses of the setting angles of twenty-five reflections. Crystal data and further experimental details can be found in Table 4.

THE HOST1-METHYL ETHYL KETONE (1:2) INCLUSION COMPOUND

DISCUSSION OF STRUCTURE

Oscillation and Weissenberg photographs identified the structural symmetry to be monoclinic and the intensity data exhibited non-reflection conditions corresponding to the space group $P2_1/n$.
h0l: h+l=2n
(h00: h=2n)
(00l: l=2n)
0k0: k=2n

A structure solution performed using direct methods yielded a combined figure of merit of 0.045 and R_E value of 0.342. The host molecule was required to reside on a special position and was located on a centre of symmetry at Wyckoff position *c* with the guest in a general position. The hydroxyl hydrogen atom was located from difference electron difference maps and was refined with an individual temperature factor. Phenyl hydrogen atoms were constrained to their parent carbon atoms as previously described, and the methy moieties were refined as rigid groups with a common temperature factor. Each of the hydroxyl moieties of host1 are hydrogen bonded to one methyl ethyl ketone carbonyl function with an oxygen-to-oxygen separation of 2.770 (6)Å. The guest molecule was anisotropically refined with high

temperature factor components which ranged from 0.17-0.33Å^2. The vapour pressure of MEK at 25^o is 90.2 mmHg, which implies considerable thermal motion of the MEK at the temperature of the data collection (21^{o}C).

Hydrogen bonding between the trans hydroxy groups of host1 and the carbonyl groups of two MEK molecules

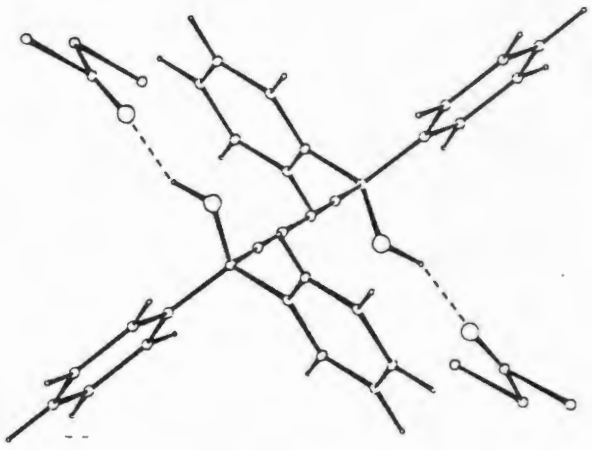

Crystal packing is shown in figure 15. The phenyl rings of the host molecule are at right angles to each other and the host1 molecular backbones are packed parallel to one another.

Figure 15

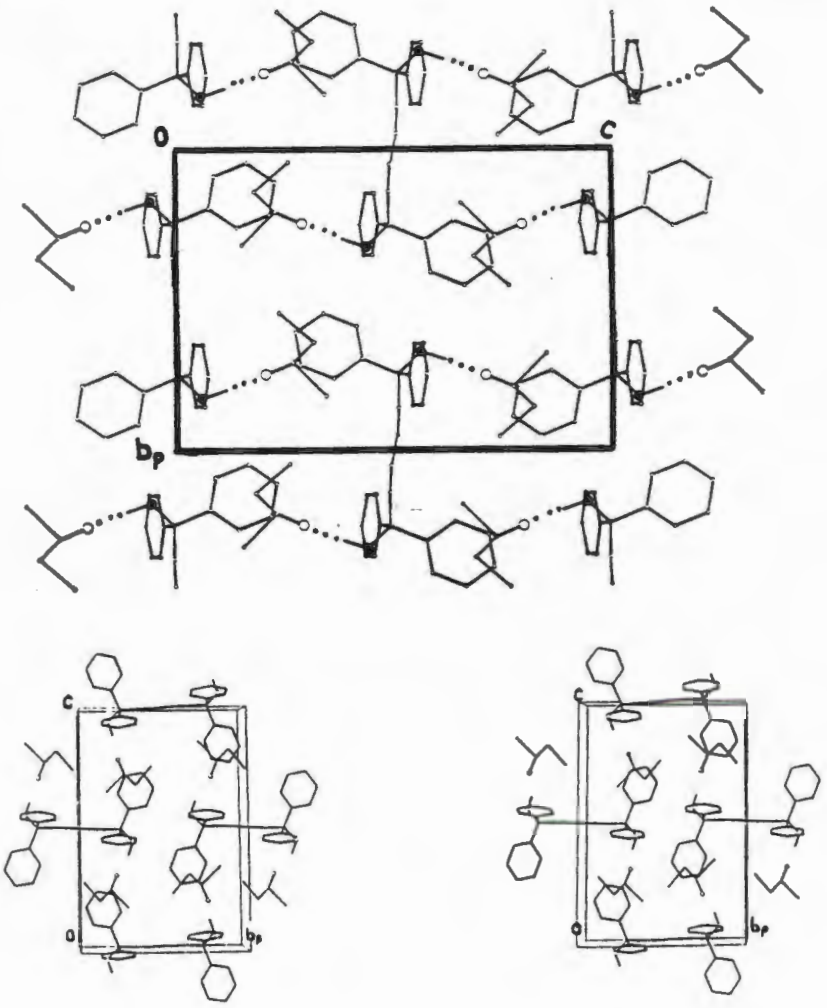

OPEC maps are shown in the figure below illustrating the guest MEK molecules lying in channels running parallel to [010] at x=0.25 (i) and x=0.75 (ii). The dimensions of the channels range from 4.3Å to 6.2Å.

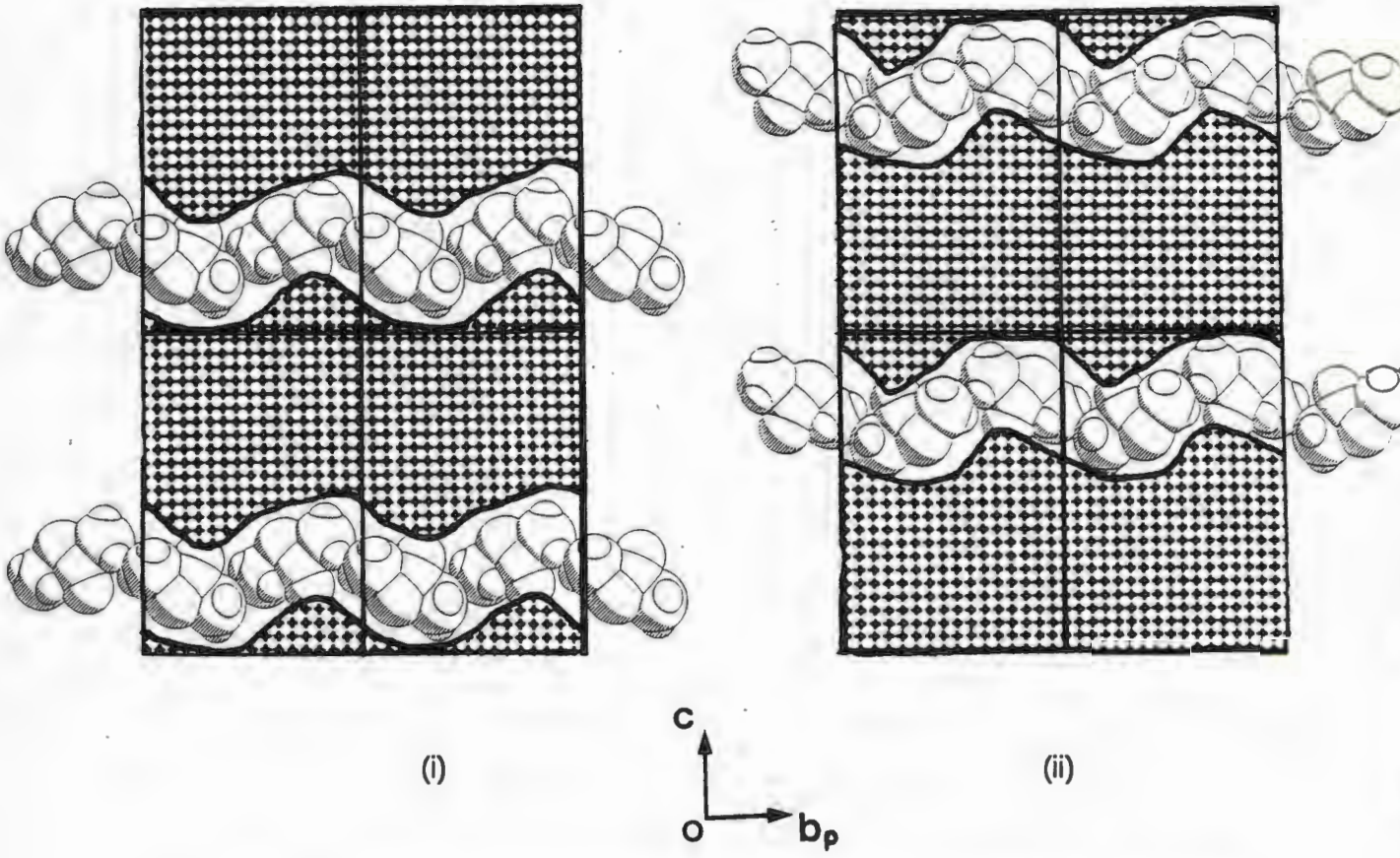

The packing diagram shown below, illustrates the way in which the host1 molecular backbones align in the crystal structure.

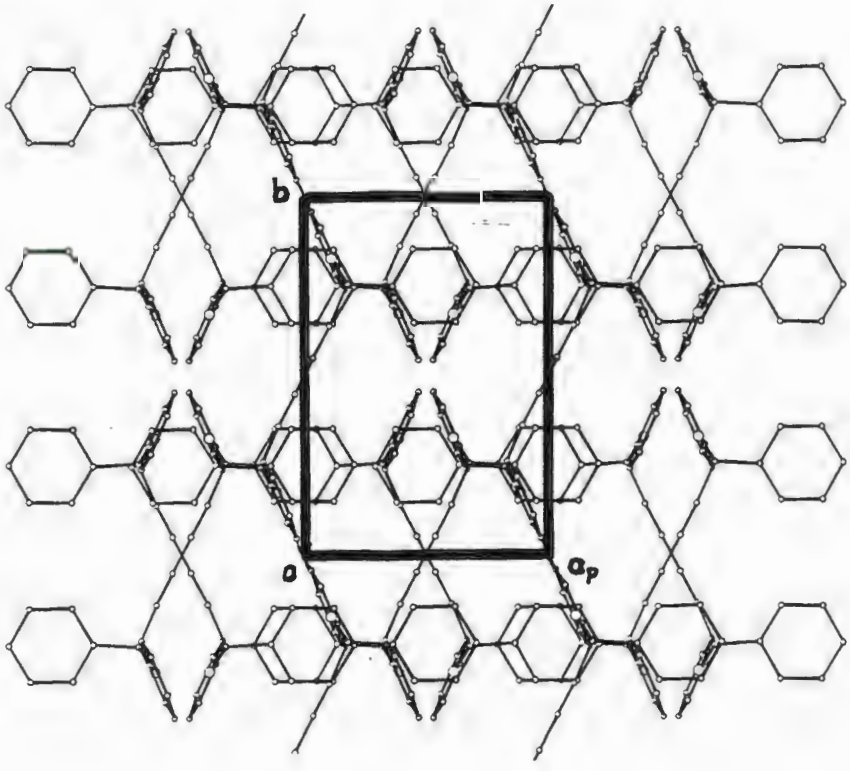

THE STRUCTURE OF THE HOST1-DEK (1:2) INCLUSION COMPOUND

During data collection a 22.4% loss in intensity over a 22.2 hour exposure period was measured and therefore a linear decay correction was applied **(43)**.

DISCUSSION OF CRYSTAL PACKING

X-ray photographs showed monoclinic symmetry and the reflection data set exhibited the non-extinction reflection conditions corresponding to $P2_1/n$. A structure solution carried out using direct methods yielded a CFOM of 0.033 and a R_E value of 0.28 resulted in and E-map from which a molecular model could be derived. A molecule of the guest was located in a general position and a molecule of centrosymmetric host1 on a centre of inversion (Wyckoff *d*). All non-hydrogen atoms were anisotropically refined with a common temperature factor for the phenyl hydrogen atoms which were constrained to ride on their parent carbon atoms. The methyl groups were refined as rigid groups and the positions of all guest hydrogens were calculated and refined with a common temperature factor. The hydroxyl hydrogen atom was unambiguously located and individually refined. Diethyl ketone has a vapour pressure of 35.2 mmHg at 25°C the guest had consistently higher thermal parameters than those of the host1 molecule. Figure 16 shows the hydrogen bonding scheme in which two guests molecules hydrogen bond to one host1 molecule, in a manner which is similar to that of the host1-MEK structure (previous structure). The O---O distance is 2.788 (6)Å.

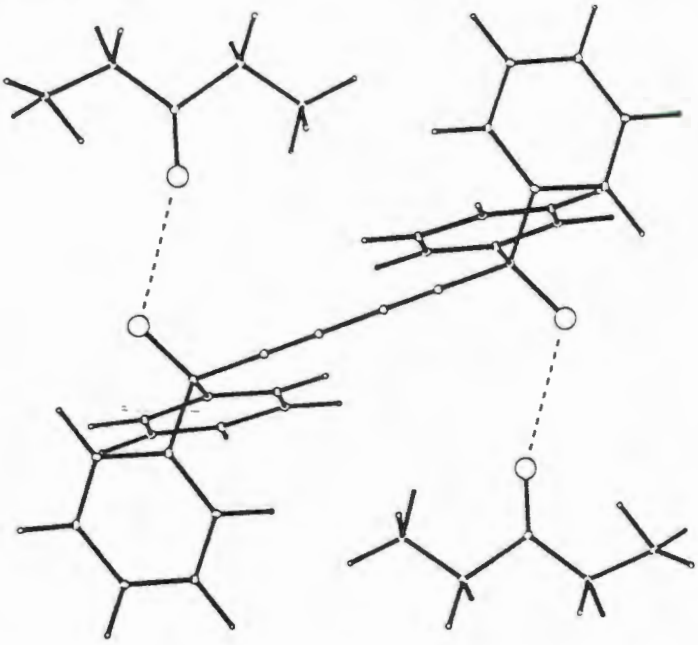

Figure 16
Hydrogen bonding of Host1 and DEK

---

43 PROGRAM DECAY, *Enraf-Nonius Structure Determination Package*, Delft, Holland, 1982.

The crystal packing of the host1-DEK structure viewed along [010], is shown below .

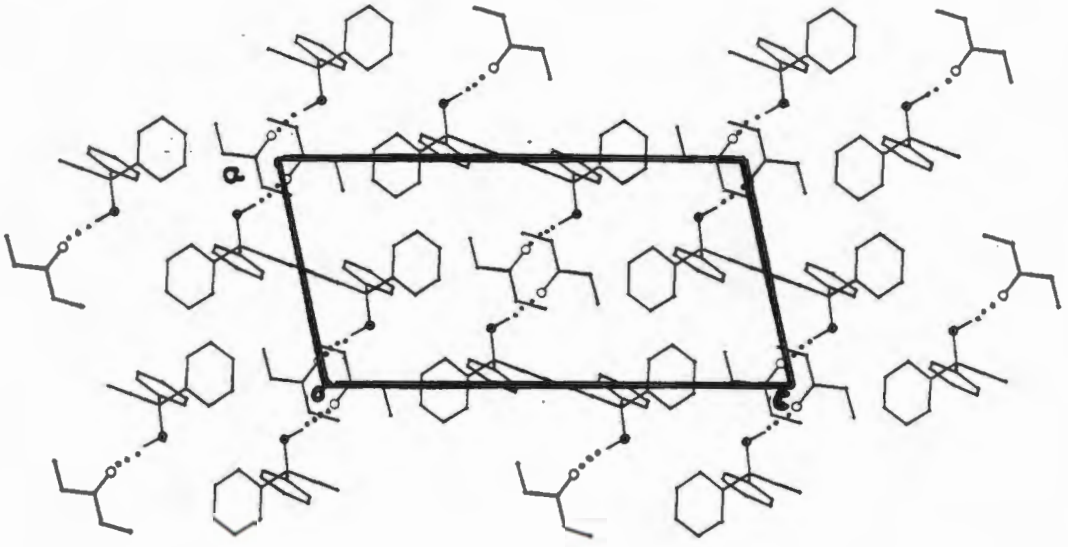

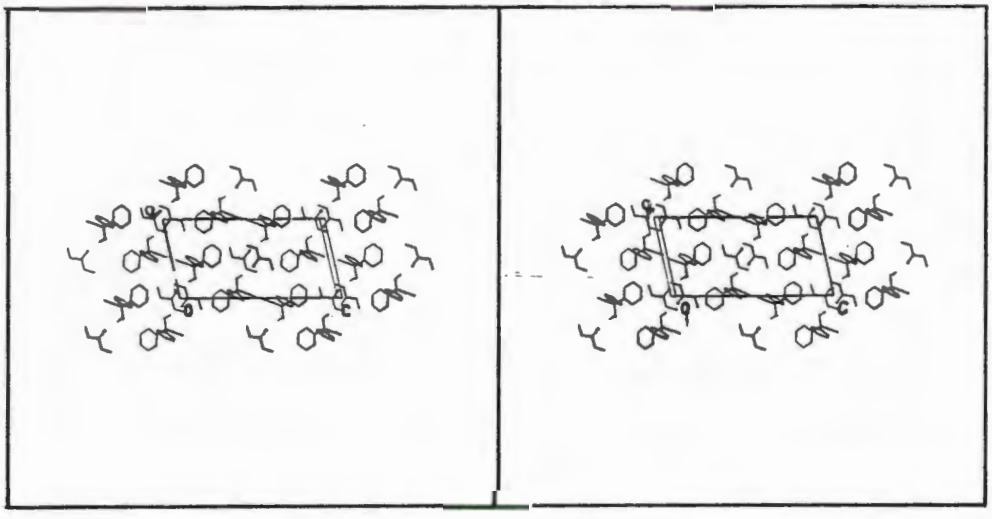

OPEC mapped the channels in which molecules of DEK lay. It ran parallel to b, at x= ½, 17 (i) and x= 0, 17 (ii). The channels range from 5.0Å to 8.2Å in dimension.

Figure 17

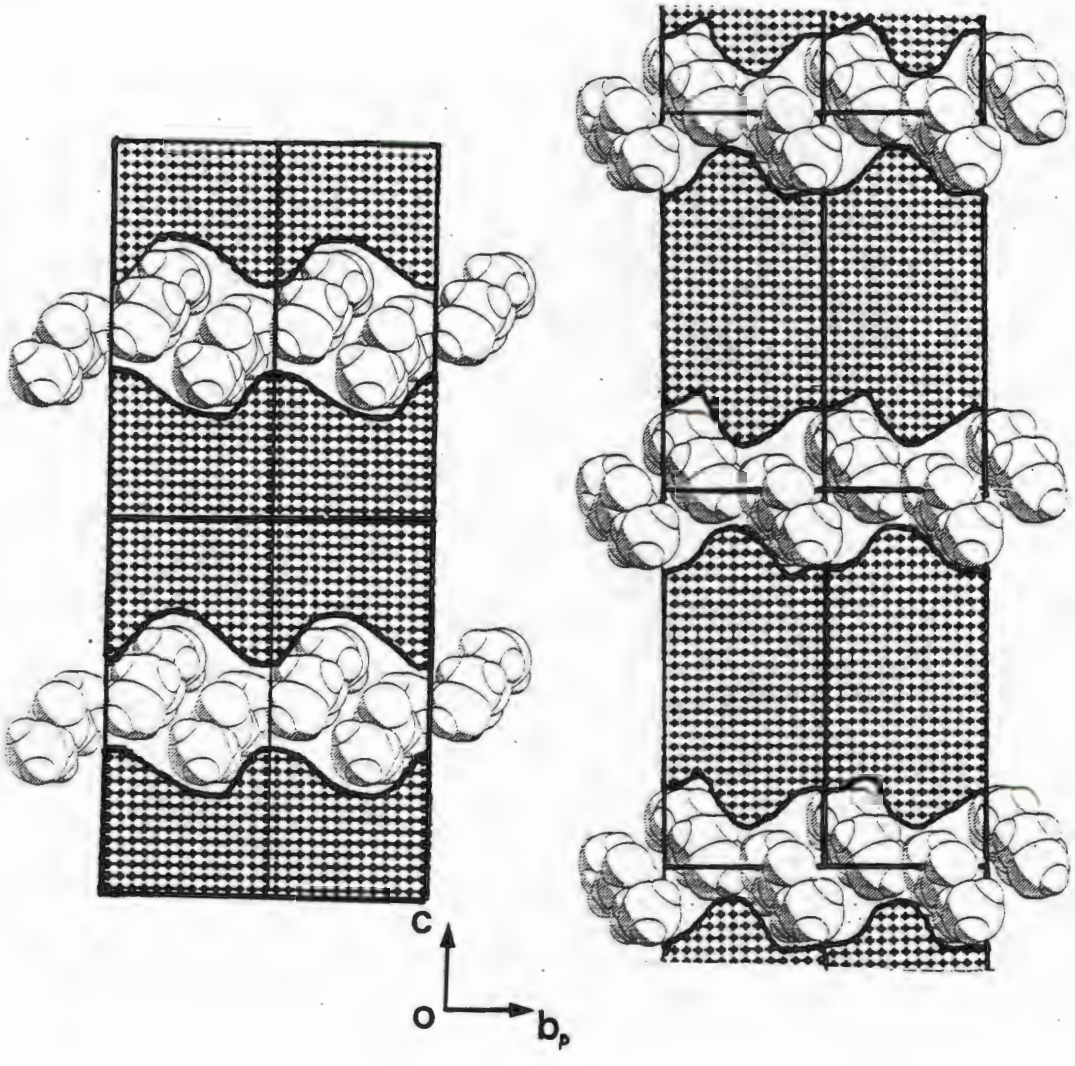

THE STRUCTURE OF THE HOST1-ACETOPHENONE (1:2) INCLUSION COMPOUND

DISCUSSION

Oscillation and zero-layer Weissenberg photographs found no symmetry other than $\bar{1}$. A structure solution was carried out in $P\bar{1}$, E-statistics supporting the centric choice which was vindicated by successful refinement and convergence of parameters. The E-map corresponding to the best solution contained electron density peaks which could be assigned to two crystallographically distinct host1 molecules located at Wyckoff *h* and *d*, as well as two individual guest molecules. All non-hydrogen atoms were anisotropically refined and the hydroxyl hydrogen atoms were successfully located from difference electron density maps and were refined with individual temperature factors. Most phenyl hydrogen atoms were located in difference electron density maps, and all were constrained a fixed distance from their parent carbon atoms and refined with a common temperature factor. The reflections omitted were : (-1 2 2), (0 1 0), (-1 4 0), (-1 6 0), (-1 5 7). This was because they are low θ reflections exhibiting extinction with values of F_o being much lower than those of F_c. The O---O separations between the host1 hydroxyl atoms and the acetophenone carbonyl functions are 2.885 (11)Å and 2.859 (11)Å. These are longer than those found in the host1-MEK and host1-DEK structures.

Two guest molecules hydrogen bond to each host1 molecule.

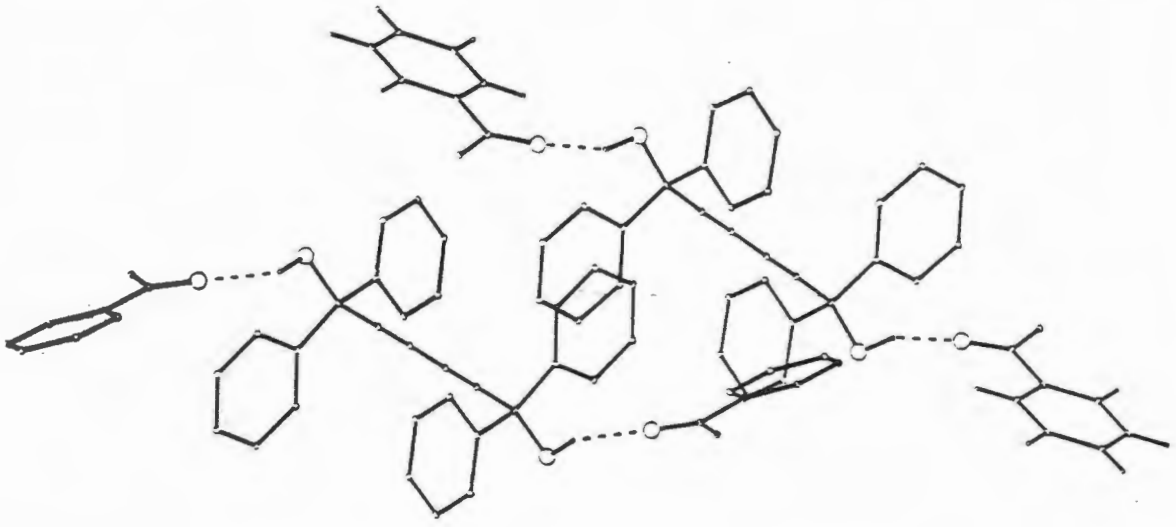

The molecular axes of the host1 molecules lie in staggered parallel rows. The packing diagram shown in figure 18 illustrates the stoicheiometry. There are two crystallographically distinct O-H---O=C interactions. Stereoscopic packing diagrams viewed along each axis are shown overleaf in figure 19.

Figure 18

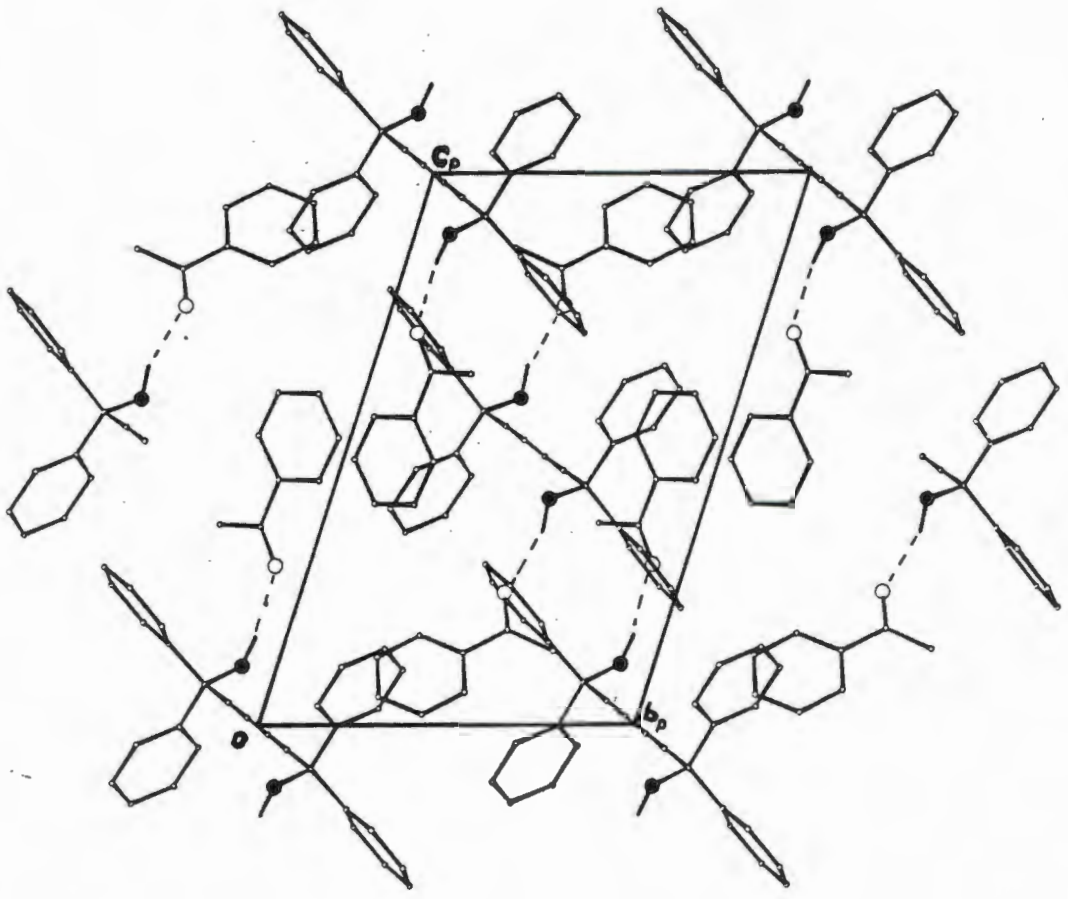

Figure 19

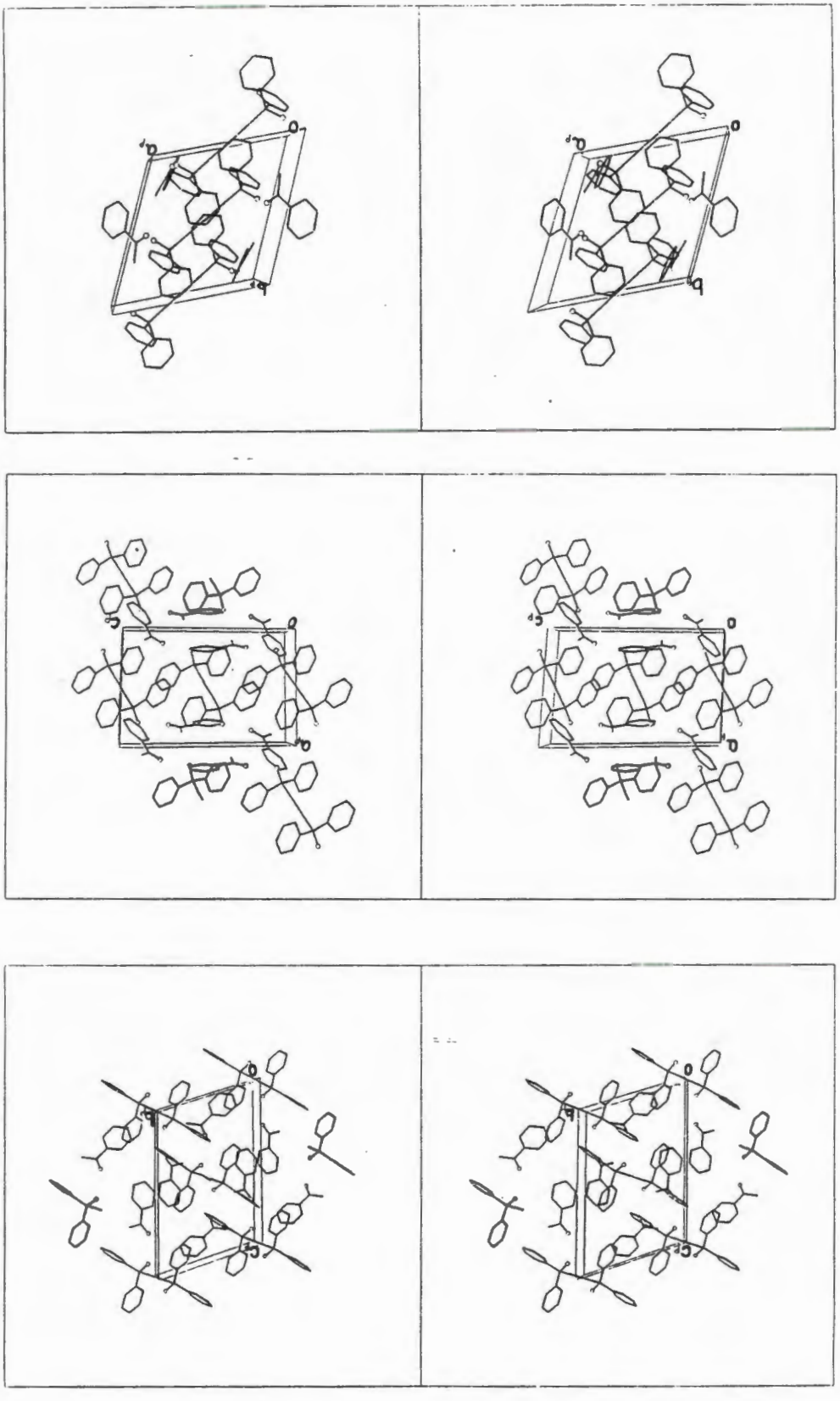

Mapping the occupied volumes in the crystal using OPEC located open ended cavities shown in figure 20. Guest 1 (O1G) is situated at y = 1 and guest 2 (O2G) at y = ½.

Figure 20

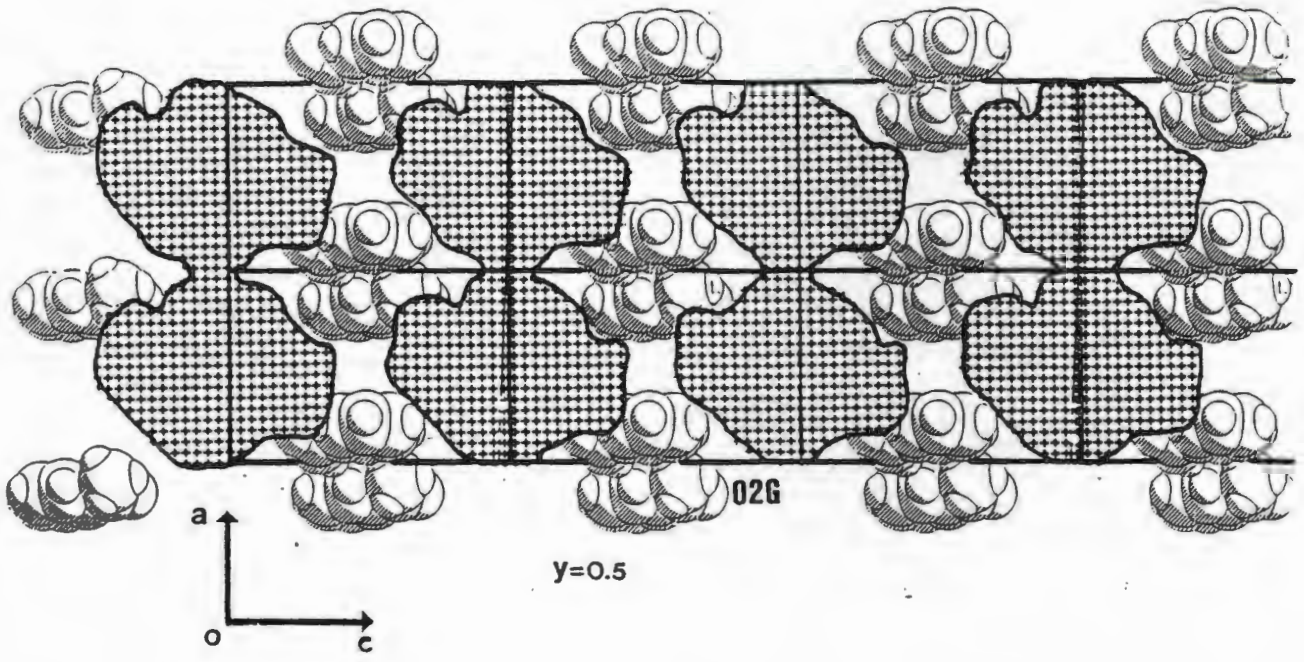

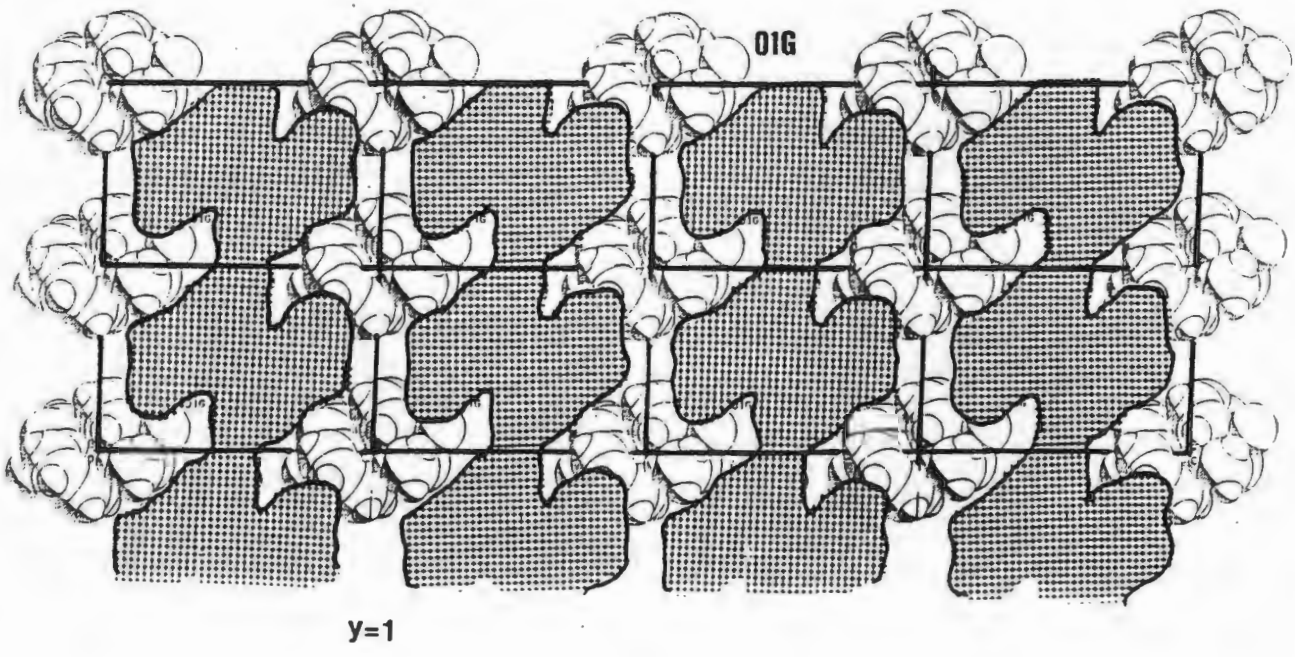

TABLE 4 CRYSTAL DATA AND EXPERIMENTAL DETAILS.

Compound	Host1-MEK	Host1-DEK	Host1-ACETOPHENONE
Molecular formula	$C_{30}H_{22}O_2.2C_4H_8O$	$C_{30}H_{22}O_2.2C_5H_{10}O$	$C_{30}H_{22}O_2.2C_8H_8O$
Molecular weight ($gmol^{-1}$)	558.72	586.77	654.80
Space group	$P2_1/n$	$P2_1/n$	$P\bar{1}$
a (Å)	8.321(3)	10.108(2)	11.204(4)
b (Å)	11.845(3)	8.579(1)	11.856(6)
c (Å)	17.153(4)	20.536(2)	16.236(6)
α (°)	90	90	69.50(4)
β (°)	100.35(2)	102.45	79.32(3)
γ (°)	90	90	62.98(4)
Z	2	2	2
V ($Å^3$)	1663(1)	1738.9(4)	1799(2)
D_c (gcm^{-3})	1.12	1.12	1.21
D_m (gcm^{-3})	1.09(3)	1.10(2)	1.20(1)
$\mu(MoK_\alpha)$ (cm^{-1})	0.39	0.33	0.41
F(000)	596	628	692
Data collection (21°C)			
Crystal dimensions (mm)	0.31x0.47x0.50	0.44x0.47x0.47	0.47x0.25x0.31
Range scanned θ (°)	1-25	1-25	1-22
Range of indices *h,k,l*	±9,+14,+20	±12,+10,+24	±11,±12,+17
Reflections for lattice parameters no.,θ range (°)	24,16-17	24,16-17	24,12-14
Instability of standard reflections (%)	-6.0	-22.4	6.0
Scan mode	(ω-2θ)	(ω-2θ)	(ω-2θ)
Scan width in(°)	(0.85+.35tanθ)	(0.85+.35tanθ)	(0.85+.35tanθ)
Vertical aperture length (mm)	4	4	4
Aperture width (mm)	(1.12+1.05tanθ)	(1.12+1.05tanθ)	(1.12+1.05tanθ)
Number of reflections collected (unique)	2266	2507	3251
Number of reflections observed with $I_{rel}>2\sigma I_{rel}$	1494	1818	2106
Final refinement			
Number of parameters	181	216	353
R	0.073	0.081	0.096
wR	0.084	0.0900	0.102
w	$(\sigma^2(F_o)+0.001F_o^2)^{-1}$	$(\sigma^2(F_o)+0.003F_o^2)^{-1}$	$(\sigma^2(F_o)+0.005F_o^2)^{-1}$
S			
Max. shift/e.s.d.	0.24	0.20	0.003
Max. height in difference electron density map (eA^{-3})	0.23	0.19	0.39
Min. height in difference electron density map (eA^{-3})	-0.24	-0.31	-0.37

THE STRUCTURE OF THE HOST1-PROPIOPHENONE (1:1) INCLUSION COMPOUND

After approximately three years, crystals of the (1:1) inclusion compound of host1 and propiophenone were obtained. The intensity data set exhibited the following non-extinction conditions:

h00: h=2n

0k0: k=2n

00l: l=2n

This corresponds the reflection conditions corresponding to the space group $P2_12_12_1$. The mean $|E^2-1|$ values for the special projections 0kl, h0l and hk0 were all centric and those for the remaining data acentric which supported the choice of space group and chemically feasible solution was derived. This is the only non-centrosymmetric host1 inclusion compound encountered and for this reason it will be separately considered. The structure refined poorly with a final R value of 0.127 since the propiophenone guest was partially disordered and exhibited high temperature factors due to rotational freedom of the ethylene arm. The residual electron density in the final electron density map amounted to 0.46 $e^-Å^{-3}$. The position of the host1 hydroxyl hydrogens could not be refined and they were not included in the model. Absolute configuration was not determined and the Hamilton test was not carried out because it was not warranted by the poor data quality and high R factor.

This inclusion compound has a packing factor of 17.11 $Å^3$/non-hydrogen atom, compared to that of the host1 α-form value of 17.35$Å^3$/non-hydrogen atom indicates an absence of channels and relatively tight packing. The hydroxy functions of the host hydrogen bond to the carbonyl function of a guest alternating along [1 0 0]. The hydrogen bonding distances are: O1G---O2 = 2.889Å and O1G---O1 = 2.994Å. The interesting feature of this structure is the cis conformation of the host1 hydroxy groups and this will be discussed later.

Crystal data and experimental details for the host1-propiophenone structure

Molecular formula	$C_{30}H_{22}O_2.C_9H_{10}O$
Molecular weight ($gmol^{-1}$)	548.67
Space group	$P2_12_12_1$
a (Å)	6.184(2)
b (Å)	18.497(2)
c (Å)	25.132(6)
Z	4
V ($Å^3$)	2874.6
D_C (gcm^{-3})	1.27

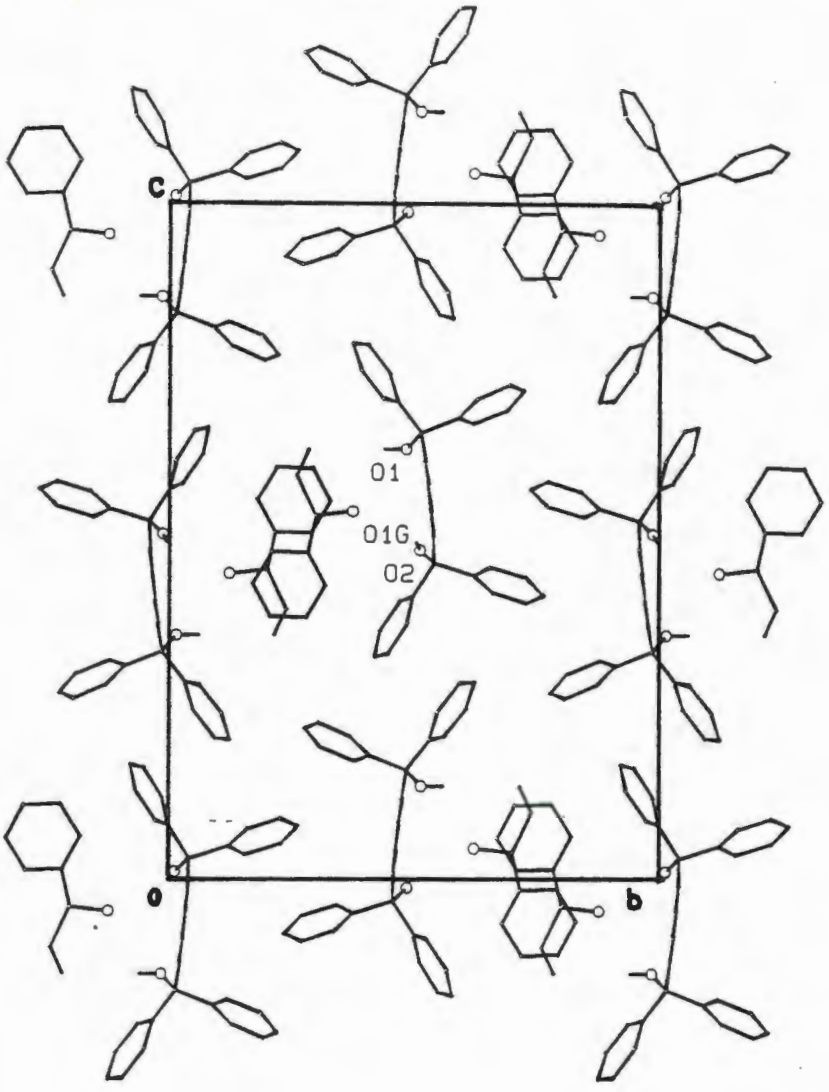
c
O1
O1G
O2
o
b

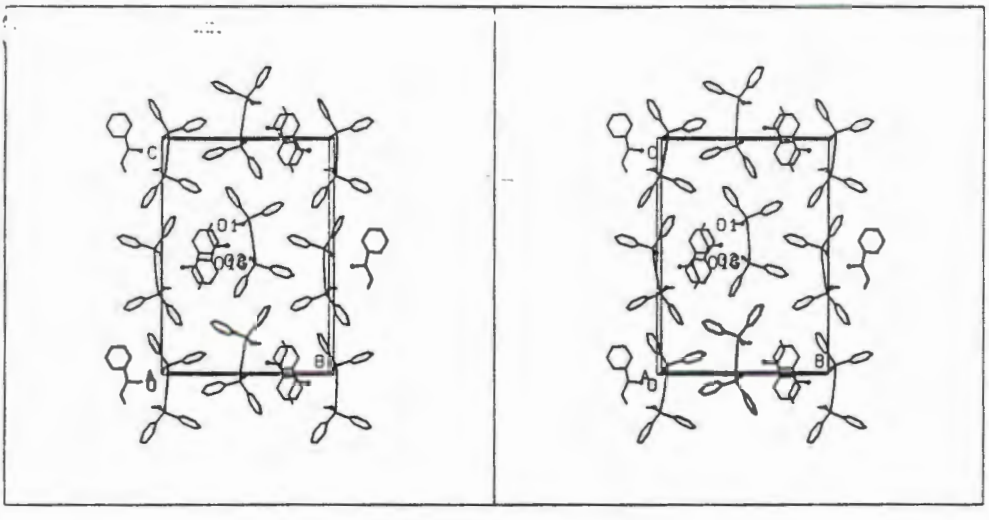

DISCUSSION OF THE HOST1-KETONE INCLUSION COMPOUND STRUCTURES

SALIENT BOND LENGTHS

	α-form		H1-Acetone	H-MEK	H-DEK
1)C1-C2	1.466(6)	1.474(6)	1.485(3)	1.479(5)	1.482(6)
2)C2-C3	1.195(6)	1.195(6)	1.191(3)	1.189(5)	1.201(6)
3)C3-C4	1.360(6)		1.378(3)	1.377(5)	1.373(6)
4)C1-C11	1.533(7)	1.539(7)	1.529(2)	1.520(5)	1.529(5)
C1-C21	1.533(5)	1.537(5)	1.528(3)	1.534(4)	1.530(5)
5)C1-O1	1.436(5)	1.430(5)	1.433(2)	1.425(5)	1.420(4)
6)ave.phenyl C-C length	1.375(8)		1.376(4)	1.395(6)	1.381(6)

The host1 α-phase does not lie on a centre of symmetry thus bond lengths corresponding to both 'halves' of the molecule are included in the above table.

	Host1-Acetophenone		H-Benzophenone	
	a*	b*	a*	b*
1)C1-C2	1.472(14)	1.491(15)	1.490(3)	1.481(3)
2)C2-C3	1.1814(14)	1.194(15)	1.192(3)	1.194(3)
3)C3-C4	1.398(14)	1.361(15)	1.382(3)	1.376(3)
4)C1-C11	1.525(8)	1.523(13)	1.530(4)	1.526(3)
C1-C21	1.516(12)	1.532(8)	1.528(3)	1.530(3)
5)C1-01	1.431(8)	1.453(9)	1.433(3)	1.431(3)
ave.phenyl C-C length	1.395(8)	1.395(8)	1.376(5)	1.380(5)

* a and b correspond to host1 molecules lying on centres of symmetry in the asymmetric unit.

The numbering scheme of the host1 molecule:

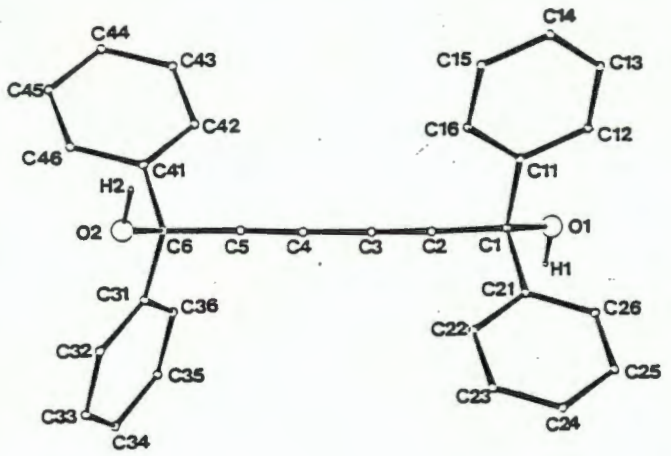

Literature values **(44)** reported for these bond lengths are:

	mean value	lower limit	upper limit
1)C-C≡C	1.466(1)	1.460	1.469
2)C≡C-C≡C	1.192(1)	1.187	1.197
3)C≡C-C≡C	1.378(1)	1.374	1.384
4)C-$C_{aromatic}$	1.513(1)	1.505	1.521
5)C-OH	1.432(1)	1.424	1.441
6)$C_{aromatic}$-$C_{aromatic}$	1.397(1)	1.392	1.403

The bond length values for the C-$C_{aromatic}$,C1-C11, C1-C21, C6-C31 & C6-C41, lie beyond the upper limit literature distances. The discrepancy lies in the second decimal place and is probably due to the fact that the pivotal carbon atoms C1 or C6 have two phenyl rings attached to them. The consequent crowding causes the bond lengths to increase in value. The bond length values for the C-C≡C, C1-C2 and C5-C6 lie in the range 1.466Å to 1.491Å. Once again the bond length values tend to be greater than those reported in the literature owing to the fact that there are two phenyl rings bonded to the tetrahedral sp^3 carbon which cause distortion. The values of the C-OH bond length lie in the range stipulated in the literature except for those of the host1 & acetophenone structure in which values of 1.431(8)Å and 1.453(9)Å are found. The bond lengths of the host1 & acetophenone structure exhibit higher standard deviations than those of the other host1-ketone compounds. In addition, the volatility of the guest molecules means that there are significant vibrations at the temperature of the data collection which would contribute towards deviations in the bond length values from reported ones.

Hydrogen bond stretching frequencies

Infra red spectra for host1 and MEK, DEK and acetophenone are shown in figure 21. The infra red spectrum of the host1 & benzophenone structure has been reported in the section on the solid-solid reaction in chapter 3. The spectra exhibited hydrogen bonded OH stretching and the values obtained are:

Host1-MEK	3443 cm^{-1}
Host1-DEK	3433 cm^{-1}
Host1-Acetophenone	3422 cm^{-1}
Host1-Benzophenone	3385 cm^{-1}

44 FH Allen, O Kennard, DG Watson, L Brammer, AG Orpen & R Taylor, *J.Chem.Soc.Perkin 2*, 1987, S6-S89

The absorption frequencies decrease in value with the decrease in vapour pressure of the ketones. Shoulder peaks in the region of 3525 cm^{-1} are due to the absorption of free OH which is due to desorption of the more volatile guests (MEK and DEK) and some decomposition of the host-guest complex.

Figure 21

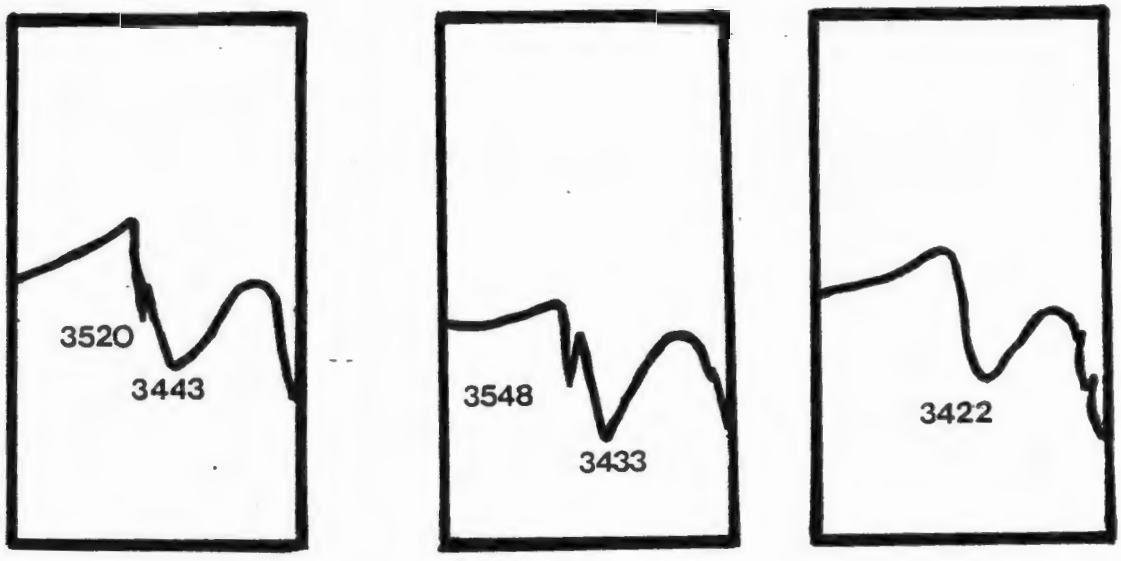

TORSION ANGLES

In order to study the conformation of the host1 molecule in each structure, torsion angles were examined. The backbone of the host1 molecule was in each case rigid and relatively inflexible. Thus phenyl ring orientation was the only indicator of the way in which a molecule of host1 might accommodate a guest. A labelled diagram of the host molecule is shown overleaf in figure 22. Bearing in mind that many of the host1 molecules lay at centres of symmetry, the labelling of the host1 molecules was arbitrary owing to great difficulty in unambiguously distinguishing between the two phenyl rings obtained per centrosymmetric host molecule as well as the unique ortho phenyl carbon atom in a ring.

The torsion angles were therefore defined as follows:

Atoms chosen to define the torsion angles - eg **C2-C1-C11-C12/16**

- C2 and C1 are backbone carbon atoms , C1 being the tetrahedral carbon atom to which the phenyl rings and hydroxy moiety are attached.
- C11 bonded to the C1 carbon.
- The ortho atom of the phenyl rings is reported as C12 or C16 as a consequence of the ambiguity of atom nomenclature.

How the value of the torsion angle was chosen:

- the smallest numerical value of the torsion angle for one phenyl ring was chosen. This was made positive if the host1 molecule lay on a centre of symmetry. Other angles were changed in sign accordingly.
- the torsion angles corresponding to the other phenyl ring were chosen so that both rings were in the same asymmetric unit.

Figure 22

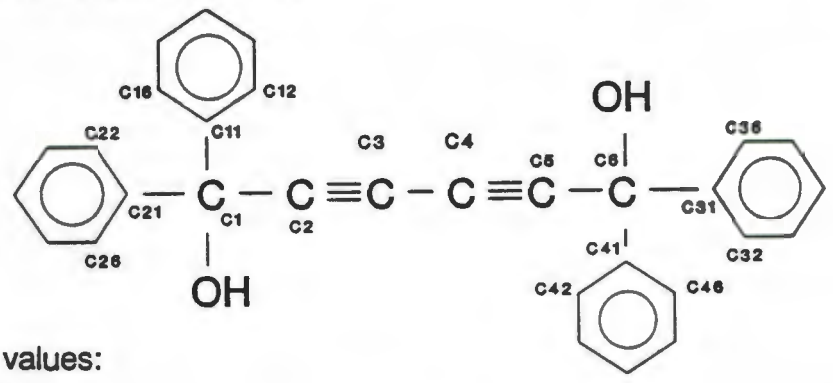

The torsion angle values:

	α-form	H1-Acetone	H-MEK	H-DEK	H-Acetophenone		H-Benzophenone		H-Propiophenone
A - Figure 22i									
C2-C1-C11-C12\16	33(1)	18(1)	-51(1)	3(1)	4(1)	75(1)	56(1)	62(1)	-67(2)
C2-C1-C21-C22\26	-25(1)	67(1)	10(1)	-58(1)	-68(1)	2(1)	47(1)	21(1)	3(2)
C5-C6-C31-C32\36	-67(1)								-67(2)
C5-C6-C41-C42\46	18(1)								10(2)
B - Figure 22ii									
O1-C1-C11-C12\16	-31(1)	74	11(0.4)	-56(0.5)	55(1)	11(1)	61(0.3)	2(0.3)	49(2)
O1-C1-C21-C22\26	38(1)	4	-50(0.4)	2(0.5)	7(1)	60(1)	18(0.3)	-76(0.3)	9(2)
O2-C6-C31-C32\36	-5(1)								55(2)
O2-C6-C41-C42\46	-44(1)								4(2)

Figure 22i

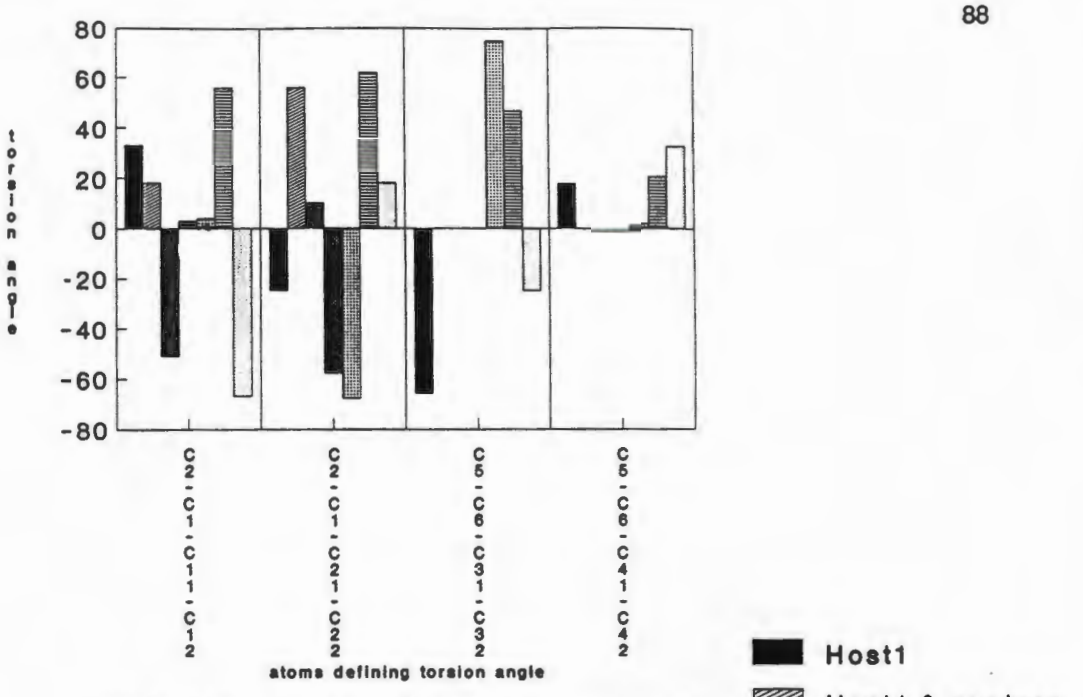

Figure 22ii

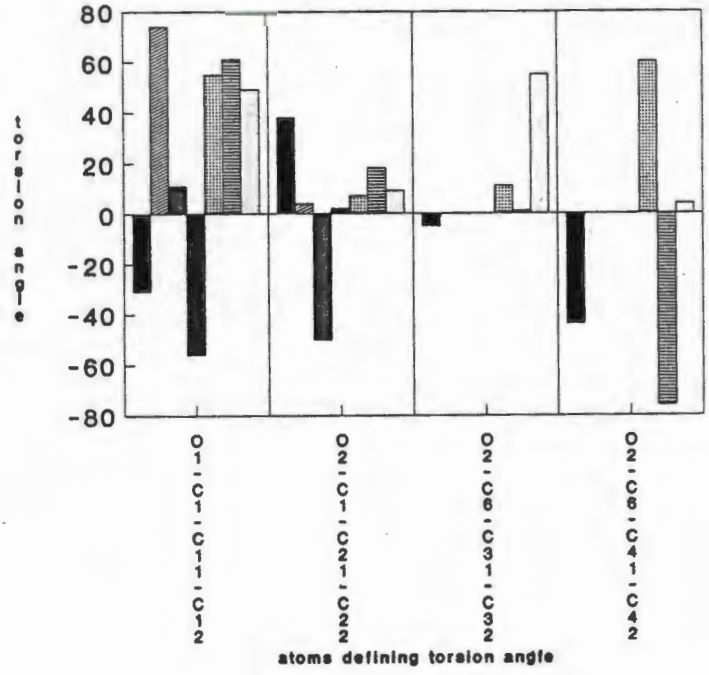

The host1 compound does not discriminate selectively with respect to the inclusion of ketone guests. The ability to act as a hydrogen bond acceptor not the size of the guest appears to be the driving force in inclusion compound formation. This is reflected in the torsion angles in which there is no set trend as would be the case if the size and shape of the guest were the dominating influence. The values of bond angle at the pivotal tetrahedral carbon atom O-C1-C2, lay in the range 107.6°-109.6° for the host1-ketone complexes which were studied.

Conformation of the host1 hydroxy moieties

The hydroxy groups always adopted the *trans* conformation in the inclusion compound, an exception being the host1-propiophenone compound in which the host1 molecule lay in a general position and some gauche character is observed in the molecular conformation as shown in figure 23 (i). Figures 23 (ii) and (iii) show the *trans* conformation obtained in the α-form of host1 as well as in the inclusion compounds formed with ketones respectively.

Figure 23 (i)

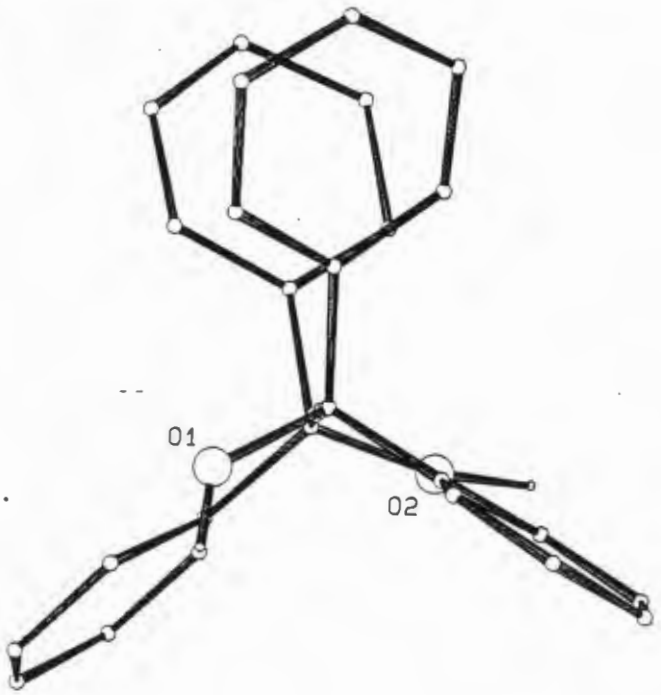

(ii)

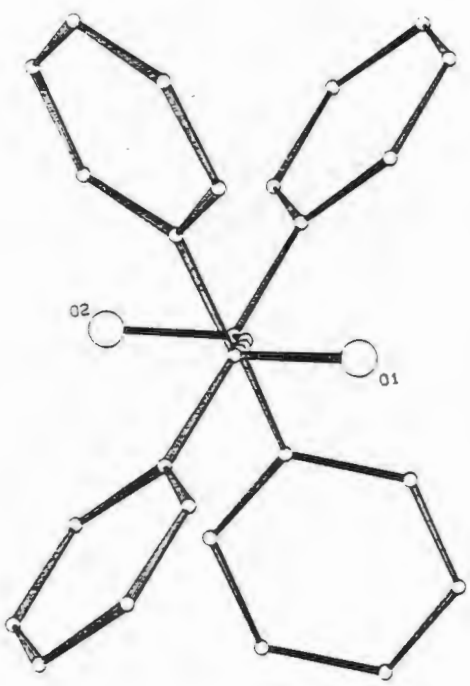

(iii)

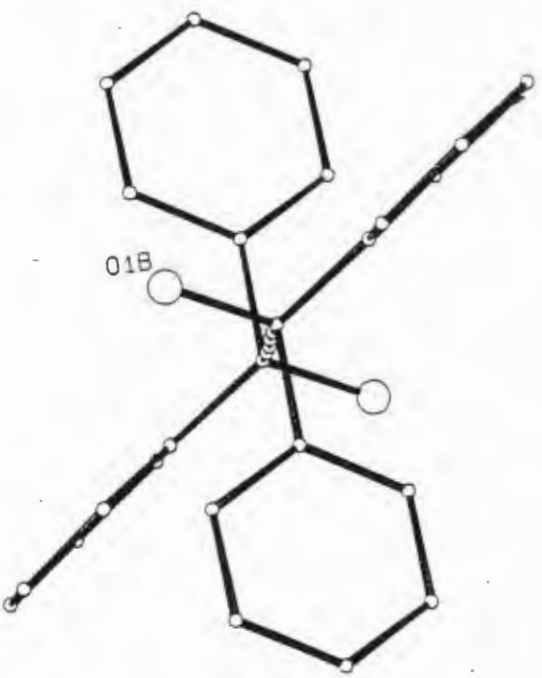

C(11)	-491(1)	1946(1)	2716(2)	37(1)
C(12)	-205(2)	2329(1)	3705(2)	62(1)
C(13)	-243(2)	3186(2)	3810(3)	74(1)
C(14)	-581(2)	3655(2)	2943(3)	68(1)
C(15)	-849(2)	3277(2)	1962(3)	75(1)
C(16)	-815(2)	2428(2)	1848(2)	60(1)
C(21)	-1174(1)	636(1)	1966(2)	35(1)
C(22)	-1128(2)	198(1)	937(2)	48(1)
C(23)	-1840(2)	-130(2)	441(3)	64(1)
C(24)	-2597(2)	-21(2)	958(3)	64(1)
C(25)	-2648(2)	403(2)	1993(3)	64(1)
C(26)	-1941(1)	728(2)	2493(2)	53(1)
O(1G)	1482(2)	2031(1)	1313(3)	131(1)
C(1G)	1791(2)	2666(2)	1106(3)	73(1)
C(2G)	2452(4)	2709(3)	222(6)	166(3)
C(3G)	1602(5)	3435(3)	1659(7)	189(4)

Fractional atomic coordinates ($x10^4$) and thermal parameters ($Å^2x10^3$) with e.s.d.'s in parentheses for Host1-Benzophenone structure

Atom	x/a	y/b	z/c	Uequiv/Uiso(*)
O(1A)	7967(1)	781(2)	5582(1)	46(1)
H(1A)	8413(16)	1543(26)	5651(14)	89(11)*
C(1A)	7941(1)	-48(3)	5061(1)	38(1)
C(2A)	8851(1)	-125(3)	5034(1)	42(1)
C(3A)	9579(1)	-46(3)	5014(1)	40(1)
C(11A)	7604(1)	-1557(3)	5156(1)	38(1)
C(12A)	6828(2)	-2109(3)	4786(1)	66(1)
C(13A)	6533(2)	-3455(4)	4901(2)	91(2)
C(14A)	7009(3)	-4278(4)	5376(2)	81(2)
C(15A)	7778(2)	-3725(4)	5751(2)	74(2)
C(16A)	8076(2)	-2371(3)	5643(1)	58(1)
C(21A)	7361(1)	680(3)	4488(1)	40(1)
C(22A)	7400(2)	245(3)	3934(1)	52(1)
C(23A)	6853(2)	863(4)	3414(1)	67(1)
C(24A)	6267(2)	1911(4)	3441(2)	78(1)
C(25A)	6215(2)	2338(4)	3987(2)	85(2)
C(26A)	6761(2)	1729(3)	4512(1)	61(1)
O(1B)	6973(1)	2142(2)	6203(1)	50(1)
H(1B)	7276(22)	1491(35)	6003(16)	114(13)*
C(1B)	6294(1)	1306(3)	6319(1)	41(1)
C(2B)	5726(2)	682(3)	5747(1)	47(1)
C(3B)	5265(2)	250(3)	5273(1)	50(1)
C(11B)	5734(1)	2349(3)	6546(1)	38(1)
C(12B)	5013(2)	1808(3)	6679(1)	48(1)
C(13B)	4491(2)	2727(4)	6880(1)	58(1)
C(14B)	4687(2)	4196(4)	6955(1)	63(1)
C(15B)	5402(2)	4730(3)	6827(1)	61(1)
C(16B)	5928(2)	3811(3)	6621(1)	50(1)
C(21B)	6709(1)	120(3)	6779(1)	42(1)
C(22B)	7070(2)	487(3)	7377(1)	54(1)
C(23B)	7485(2)	-540(4)	7799(1)	65(1)
C(24B)	7562(2)	-1946(4)	7633(2)	70(1)
C(25B)	7217(2)	-2335(4)	7038(2)	78(2)
C(26B)	6788(2)	-1314(3)	6615(1)	66(1)
O(1G)	10900(1)	-2102(2)	8917(1)	81(1)

COORDINATE TABLES

Table 5

$U_{eq} = (1/3)\Sigma\Sigma U_{ij} a_i a_i^* a_i \cdot a_j$

Fractional atomic coordinates ($x10^4$) and thermal parameters ($Å^2 x10^3$) with e.s.d.'s in parentheses for Host1

Atom	x/a	y/b	z/c	Uequiv/Uiso(*)
O(1)	7446(5)	515(3)	1904(2)	46(1)
H(1)	7578(94)	871(46)	1435(30)	83(20)*
O(2)	-2516(5)	4507(3)	3123(2)	49(1)
H(2)	-2893(109)	4072(53)	3520(40)	130(27)*
C(1)	5146(7)	190(3)	1913(3)	33(2)
C(2)	3943(7)	1224(4)	2148(3)	40(2)
C(3)	3059(7)	2092(3)	2364(3)	40(2)
C(4)	2031(7)	3079(4)	2613(3)	39(2)
C(5)	1102(7)	3939(4)	2848(3)	39(2)
C(6)	-267(7)	4918(3)	3111(3)	34(2)
C(11)	4961(7)	-333(3)	2651(3)	38(2)
C(12)	6724(9)	-920(5)	2832(4)	59(3)
C(13)	6536(15)	-1412(6)	3486(6)	89(4)
C(14)	4751(16)	-1358(6)	3947(5)	87(4)
C(15)	3010(13)	-772(6)	3781(5)	81(3)
C(16)	3146(9)	-280(5)	3127(4)	56(2)
C(21)	4245(7)	-699(3)	974(3)	34(2)
C(22)	2103(7)	-725(4)	600(3)	42(2)
C(23)	1328(9)	-1562(4)	-234(4)	50(2)
C(24)	2678(9)	-2366(4)	-699(4)	54(2)
C(25)	4800(9)	-2351(4)	-329(4)	59(2)
C(26)	5567(8)	-1526(4)	505(4)	50(2)
C(31)	-259(8)	5468(3)	2384(3)	39(2)
C(32)	-2161(10)	5424(5)	1831(4)	61(3)
C(33)	-2024(15)	5905(7)	1161(5)	92(4)
C(34)	-121(18)	6434(6)	1048(5)	94(4)
C(35)	1731(14)	6498(6)	1613(5)	87(4)
C(36)	1684(10)	6014(5)	2269(4)	66(3)
C(41)	585(7)	5806(3)	4060(3)	35(2)
C(42)	-798(8)	6619(4)	4506(4)	47(2)
C(43)	-102(11)	7449(4)	5344(4)	63(3)
C(44)	2031(11)	7479(4)	5748(4)	59(2)
C(45)	3388(9)	6681(4)	5321(4)	53(2)
C(46)	2709(8)	5835(4)	4469(4)	46(2)

Table 6

Fractional atomic coordinates ($x10^4$) and thermal parameters ($Å^2 x10^3$) with e.s.d.'s in parentheses for Host1-acetone structure.

Atom	x/a	y/b	z/c	Uequiv/Uiso(*)
O(1)	288(1)	875(1)	1745(1)	44(1)
H(1)	650(17)	1313(13)	1820(28)	88(10)*
C(1)	-398(1)	1017(1)	2514(2)	35(1)
C(2)	-228(1)	577(1)	3620(2)	41(1)
C(3)	-84(1)	211(1)	4494(2)	43(1)

C(1G)	10389(2)	-1188(3)	8623(1)	50(1)
C(11G)	10405(2)	-825(3)	8011(1)	46(1)
C(12G)	11149(2)	-1139(3)	7853(1)	61(1)
C(13G)	11167(2)	-846(4)	7287(2)	77(2)
C(14G)	10443(3)	-260(4)	6863(2)	80(2)
C(15G)	9702(2)	27(4)	7009(1)	72(1)
C(16G)	9676(2)	-245(3)	7578(1)	57(1)
C(21G)	9772(2)	-467(3)	8883(1)	47(1)
C(22G)	9575(2)	1001(3)	8802(1)	54(1)
C(23G)	9043(2)	1644(3)	9086(1)	66(1)
C(24G)	8684(2)	831(5)	9437(1)	78(2)
C(25G)	8871(2)	-629(5)	9517(1)	78(2)
C(26G)	9419(2)	-1274(3)	9247(1)	63(1)

Table 8

Fractional atomic coordinates ($x10^4$) and thermal parameters ($Å^2x10^3$) with e.s.d.'s in parentheses for Host1-MEK structure

Atom	x/a	y/b	z/c	Uequiv/Uiso(*)
O(1)	1116(3)	8264(2)	572(2)	74(1)
H(1)	1471(55)	7997(37)	1127(11)	115(16)*
C(1)	1800(4)	7541(3)	53(2)	60(1)
C(2)	1058(4)	6406(3)	52(2)	64(1)
C(3)	387(4)	5516(3)	22(2)	64(1)
C(12)	705(4)	9105(2)	-903(2)	89(2)
C(13)	326(4)	9541(2)	-1670(2)	10(2)
C(14)	617(4)	8899(2)	-2312(2)	12(3)
C(15)	1287(4)	7820(2)	-2187(2)	15(3)
C(16)	1667(4)	7384(2)	-1421(2)	15(2)
C(11)	1376(4)	8027(2)	-779(2)	53(2)
C(22)	4534(3)	6480(2)	400(2)	59(2)
C(23)	6233(3)	6496(2)	615(2)	606(3)
C(24)	7059(3)	7523(2)	741(2)	114(3)
C(25)	6186(3)	8534(2)	656(2)	118(3)
C(26)	4488(3)	8519(2)	441(2)	92(2)
C(21)	3662(3)	7492(2)	313(2)	64(1)
O(1G)	11190(6)	7474(5)	2098(3)	169(3)
C(1G)	11701(11)	8191(9)	3493(5)	184(5)
C(2G)	11162(8)	7095(10)	2727(6)	188(5)
C(3G)	10925(15)	6421(17)	3204(8)	305(12)
C(4G)	10385(14)	5443(9)	2402(8)	224(6)

Table 9

Fractional atomic coordinates (10^4) and thermal parameters ($Å^2x10^3$) with e.s.d.'s in parentheses for Host1-DEK structure.

Atom	x/a	y/b	z/c	Uequiv/Uiso(*)
O(1)	7431(2)	1608(3)	8807(1)	72(1)
H(1)	7882(45)	1993(56)	9240(12)	111(16)*
C(1)	6009(3)	1785(4)	8731(2)	54(1)
C(2)	5568(4)	1020(4)	9295(2)	61(1)

C(3)	5210(4)	365(4)	9744(2)	59(1)
C(11)	5625(3)	3512(4)	8687(2)	57(1)
C(12)	4902(5)	4222(5)	9106(2)	76(2)
C(13)	4616(6)	5815(5)	9030(2)	97(2)
C(14)	5062(5)	6657(5)	8547(3)	94(2)
C(15)	5741(5)	5954(5)	8128(3)	91(2)
C(16)	6028(4)	4388(5)	8194(2)	77(2)
C(21)	5306(3)	960(4)	8088(2)	56(1)
C(22)	3921(4)	900(5)	7919(2)	70(2)
C(23)	3262(5)	117(5)	7346(2)	89(2)
C(24)	4008(5)	-578(6)	6940(2)	89(2)
C(25)	5376(6)	-513(5)	7098(2)	88(2)
C(26)	6068(4)	244(4)	7677(2)	70(1)
O(1G)	9089(5)	2162(8)	10059(3)	192(3)
C(1G)	11658(11)	3278(15)	9932(5)	231(7)
C(2G)	11312(7)	2588(12)	10519(4)	163(4)
C(3G)	10002(6)	2054(7)	10525(3)	107(2)
C(5G)	8583(10)	828(17)	11251(6)	226(7)

TABLE 10

Fractional atomic coordinates (10^4) and Thermal Parameters ($Å^2 x 10^3$) with e.s.d.'s in parentheses for Host1 & Acetophenone structure.

Atom	x/a	y/b	z/c	Uequiv/Uiso(*)
O(1A)	1767(5)	4200(5)	5919(3)	49(3)
H(1A)	1823(102)	4114(104)	6516(21)	109(7)*
C(1A)	3072(7)	3335(8)	5683(5)	38(2)
C(2A)	3925(8)	4057(8)	5403(5)	38(2)
C(3A)	4592(7)	4659(7)	5149(5)	37(2)
C(12A)	2902(5)	1364(6)	6832(4)	54(5)
C(13A)	3371(5)	223(6)	7552(4)	68(6)
C(14A)	4607(5)	-196(6)	7898(4)	69(6)
C(15A)	5371(5)	526(6)	7524(4)	66(6)
C(16A)	4902(5)	1667(6)	6804(4)	51(5)
C(11A)	3667(5)	2085(6)	6458(4)	36(5)
C(22A)	4066(4)	2022(5)	4618(3)	49(5)
C(23A)	3986(4)	1666(5)	3904(3)	55(6)
C(24A)	2773(4)	2250(5)	3485(3)	56(6)
C(25A)	1641(4)	3190(5)	3781(3)	56(5)
C(26A)	1722(4)	3546(5)	4495(3)	42(5)
C(21A)	2935(4)	2962(5)	4913(3)	33(4)
O(1B)	1856(6)	9073(6)	1100(4)	64(4)
H(1B)	2023(105)	9187(105)	1611(40)	109(7)*
C(1B)	3141(8)	8256(8)	772(5)	44(2)
C(2B)	3957(8)	9036(8)	431(5)	45(2)
C(3B)	4614(8)	9657(8	156(5)	49(2)
C(12B)	3933(4)	6973(5)	-320(4)	53(5)
C(13B)	3721(4)	6659(5)	-1015(4)	67(6)
C(14B)	2465(4)	7321(5)	-1390(4)	71(6)
C(15B)	1421(4)	8298(5)	-1070(4)	75(7)
C(16B)	1632(4)	8612(5)	-374(4)	66(6)
C(11B)	2889(4)	7950(5)	1(4)	38(4)
C(22B)	3200(5)	6144(6)	1887(4)	63(5)
C(23B)	3779(5)	4987(6)	2578(4)	72(6)
C(24B)	5008(5)	4663(6)	2891(4)	61(5)

C(25B)	5659(5)	5496(6)	2513(4)	60(6)
C(26B)	5080(5)	6653(6)	1821(4)	54(6)
C(21B)	3850(5)	6977(6)	1508(4)	42(4)
O(1G)	1218(7)	15399(9)	2389(5)	195(6)
C(1G)	-636(12)	15793(12)	1716(8)	77(3)
C(1MG)	-884(14)	17178(13)	1344(9)	121(10)
C(12G)	1195(7)	15171(6)	603(4)	69(6)
C(13G)	2137(7)	14227(6)	211(4)	88(8)
C(14G)	2276(7)	12919(6)	530(4)	99(9)
C(15G)	1474(7)	12553(6)	1240(4)	95(8)
C(16G)	532(7)	13498(6)	1632(4)	78(8)
C(11G)	392(7)	14806(6)	1313(4)	57(6)
O(2G)	1643(8)	9108(8)	2890(5)	101(6)
C(2G)	1438(11)	8400(11)	3596(8)	80(3)
C(2MG)	1036(13)	7323(13)	3639(9)	109(9)
C(22G)	1881(6)	9546(6)	4414(4)	75(6)
C(23G)	2032(6)	9702(6)	5195(4)	70(7)
C(24G)	1935(6)	8796(6)	6001(4)	106(9)
C(25G)	1685(6)	7734(6)	6025(4)	87(7)
C(26G)	1535(6)	7578(6)	5243(4)	81(7)
C(21G)	1632(6)	8484(6)	4438(4)	61(5)

TABLE 11

Fractional atomic coordinates (x 10^4) and thermal parameters ($Å^2$ x 10^3) with e.s.d.'s in parentheses for Compound Host-propiophenone

Atom	x/a	y/b	z/c	Uequiv
O(1)	-166(0)	4847(0)	6383(0)	63(0)
O(2)	11125(0)	5134(0)	4879(0)	52(0)
C(1)	1808(0)	5141(0)	6626(0)	38(0)
C(2)	3441(0)	5220(0)	6207(0)	49(0)
C(3)	4691(0)	5289(0)	5862(0)	39(0)
C(4)	6256(0)	5362(0)	5457(0)	42(0)
C(5)	7451(0)	5391(0)	5098(0)	50(0)
C(6)	9081(0)	5402(0)	4683(0)	45(0)
C(11)	8367(0)	4975(0)	4196(0)	40(0)
C(12)	9788(0)	4859(0)	3792(0)	64(0)
C(13)	9340(0)	4492(0)	3355(0)	79(0)
C(14)	7397(0)	4197(0)	3288(0)	87(0)
C(15)	5641(0)	4328(0)	3689(0)	80(0)
C(16)	6269(0)	4728(0)	4132(0)	64(0)
C(21)	9542(0)	6222(0)	4508(0)	41(0)
C(22)	11428(0)	6536(0)	4627(0)	61(0)
C(23)	11710(0)	7278(0)	4477(0)	85(0)
C(24)	10032(0)	7627(0)	4215(0)	68(0)
C(25)	8326(0)	7278(0)	4107(0)	87(0)
C(26)	7832(0)	6578(0)	4259(0)	60(0)
C(31)	2579(0)	4663(0)	7077(0)	38(0)
C(32)	4505(0)	4368(0)	7105(0)	53(0)
C(33)	5053(0)	3937(0)	7522(0)	73(0)
C(34)	3674(0)	3781(0)	7926(0)	75(0)
C(35)	1750(0)	4057(0)	7903(0)	69(0)
C(36)	1054(0)	4523(0)	7481(0)	57(0)
C(41)	1254(0)	5906(0)	6847(0)	38(0)
C(42)	-687(0)	6215(0)	6763(0)	56(0)

C(43)	-1047(0)	6899(0)	6969(0)	76(0)
C(44)	548(0)	7232(0)	7248(0)	76(0)
C(45)	2446(0)	6942(0)	7325(0)	65(0)
C(46)	2780(0)	6273(0)	7118(0)	56(0)
O(1G)	10441(0)	3814(0)	5478(0)	172(0)
C(1G)	11727(0)	3125(0)	5414(0)	349(0)
C(2G)	12498(0)	2700(0)	6012(0)	325(0)
C(3G)	10807(0)	3043(0)	6406(0)	275(0)
C(11G)	10460(0)	2754(0)	4890(0)	200(0)
C(12G)	11048(0)	2027(0)	4868(0)	200(0)
C(13G)	11625(0)	1715(0)	4383(0)	200(0)
C(14G)	11615(0)	2130(0)	3920(0)	200(0)
C(15G)	11027(0)	2858(0)	3942(0)	200(0)
C(16G)	10450(0)	3170(0)	4427(0)	200(0)

CHAPTER FOUR

THERMAL ANALYSIS

Thermal analysis techniques may be used to measure changes in the physical properties of a material as a function of temperature. Investigating the thermal events that a compound undergoes on controlled heating, may yield valuable information as to bonding characteristics, thermodynamics and thermal stability. With respect to host-guest inclusion compounds, thermal analysis was undertaken in order to correlate structure and thermodynamics. This was a fairly novel approach since up to date, thermal analysis has not been extensively used to investigate the thermal behaviour and stabilities of inclusion compounds **(1)**. The thermal analysis techniques used were Differential scanning calorimetry (DSC) and Thermogravimetry (TG), which were described experimentally in Chapter 2.

Thermogravimetry - Theory

Dynamic TG exposes a sample to an environment in which there are controlled temperature changes. The inclusion compound is heated at a constant rate and the resulting mass change provides information as to the thermal stability and stoicheiometric composition of the starting material, intermediates formed as well as the residue. The change in mass may be due to a variety of factors, such as decomposition, chemical reaction and solvent or guest loss. The results obtained are temperature versus mass loss curves and typical examples of these are illustrated overleaf.

---

1 WWM Wendlandt, "*Thermal Analysis*", 3rd Edition, John Wiley & Sons, New York, 1986
B Wunderlich, "*Thermal Analysis*", San Diego, Academic Press, 1990
CJ Keattch & D Dollimore, *op. cit.*

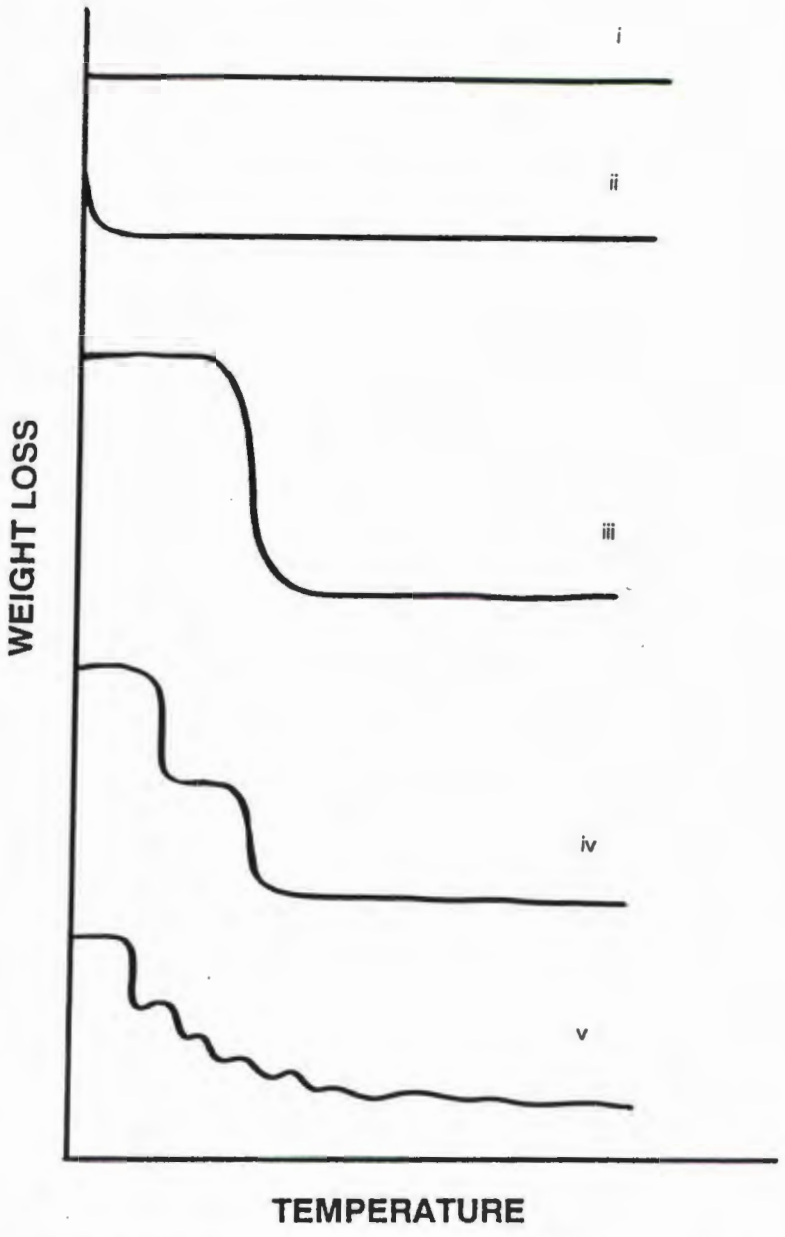

(i) There is no sample decomposition or loss of volatile products such as guests over the temperature range.

(ii) There is initial loss in mass due to evaporation of excess solvent or mother liquor but thereafter no mass loss is observed.

(iii) There is a one-step decomposition which reveals the stoicheiometry of the reaction as this mass difference corresponds directly to the stoicheiometric loss of guest.

(iv) This shows that there is a multi-step decomposition where relatively stable intermediates are formed at each stage. Once again the stoicheiometry may be determined although this is a much more complicated system than (iii).

(v) This is also a multi-stage decomposition but without stable intermediates.

(2)

---

2 ME Brown, "*Intoduction to Thermal Analysis*", Chapman & Hall, London, 1988

There are a multitude of variables influencing the shape of TG curves such as the rate of heating, atmosphere of the furnace, amount of gas evolved, particle size, heat of reaction and sample packing. Thus subsequent analysis of results may be complicated.

ACTIVATION ENERGY CALCULATIONS FROM TG CURVES

Flynn and Wall **(3)** devised a relatively simple method for determining activation energies directly from a series of weight loss versus temperature curves done at different heating rates. Their method was designed as an alternative to techniques such as differential analysis and curve fitting. The method of curve fitting desorption data does not work well if the order of the decay is not uniquely defined, which is often the case in solid state decompositions where concepts of molecularity and order of reaction cannot be necessarily pinpointed. Differential methods fail if the spread of data is too wide and are thus not always useful. Flynn and Wall established an alternative convenient method by relating the rate of decomposition to a function of the extent of decomposition, the rate of heating and the Arrhenius equation. This is expressed in the equation below:

$$dC/dT = (A/\beta)f(C)e^{-E/RT}$$

where C = degree of conversion
A = Arrhenius constant
E = activation energy
R = gas constant
T = temperature
β = heating rate

They rearranged this equation and differentiated with respect to C assuming A, f(C) and E to be independent of temperature, and A and E to be independent of f(C). In this way they arrived at:

$$\frac{d\log\beta}{d1/T} = \frac{0.457\,E}{R}$$

Thus for a constant weight loss, the corresponding temperatures can be read off thermograms for various rates of heating **(4)**. This is illustrated in figure 1.

---

3 JH Flynn & LA Wall, *Polymer Letters*, 4, 1966, 32

Figure 1

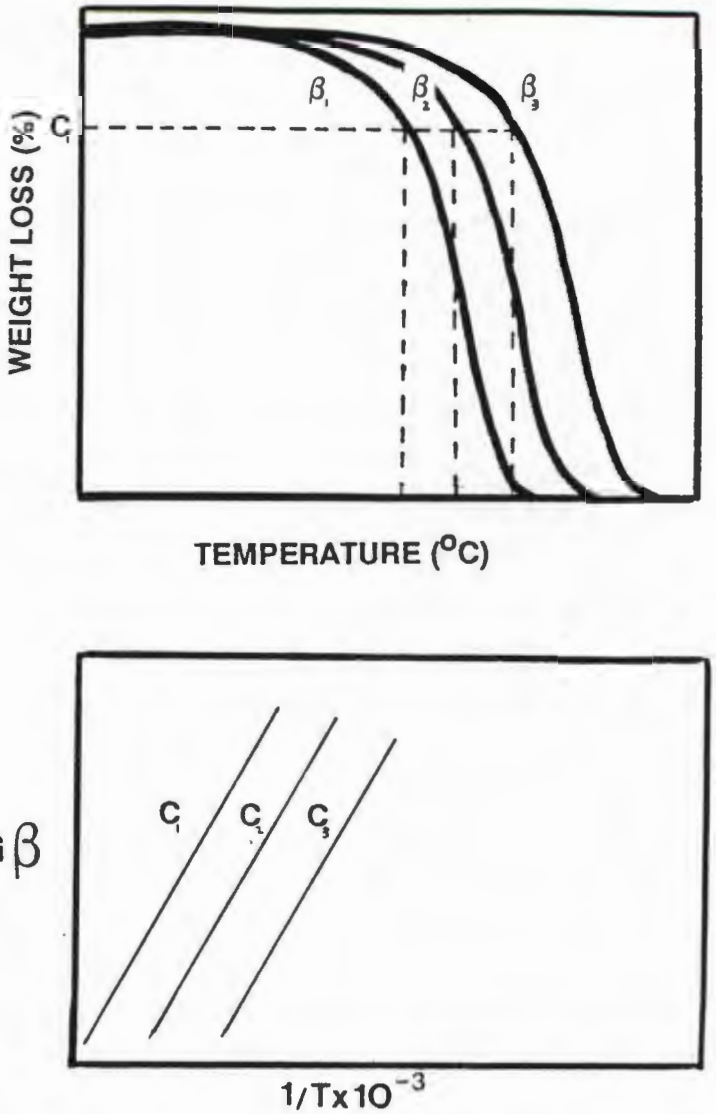

From plots of logβ versus the reciprocal of the absolute temperature, the activation energy can be calculated using the above equation. The gradients of these plots yield an approximate activation energy if multiplied by the constant 0.457/R. Plots resulting in parallel straight lines imply consistency in the manner of decay and hence indicate that the decomposition occurs in a single step. This method, originally developed for the study of the thermal decomposition of polymers has also been applied to the decomposition of inorganic coordination compounds **(5)**.
Owing to the fact that there are many variables influencing the shape and character of a TG curve, the approximate nature of the activation energy value should be emphasised. The main problem that affects curve reproducibility and shape is consistency of the particle size of each sample. While every effort was made to ensure that there was equality in particle size by crushing, sieving which would have been preferable, could not be done because the volatile guests desorbed rapidly from the host-guest compounds at room temperature.

---

5 MA Herman, H Hofmans & HO Desseyn, *Thermochimica Acta*, 85, 1985, 63-66

Theory - Differential Scanning Calorimetry (DSC)

DSC is a technique which measures the thermal energy per unit time transferred to or from the sample, as it is heated. Temperature changes in the sample are due to endothermic or exothermic enthalpic transitions. Therefore phase changes, destruction of crystalline lattice structure, boiling, sublimation, vaporrisation, dissociation or decomposition reactions, oxidation and reduction reactions and other chemical reactions can be examined using the DSC technique. DSC therefore provides a reliable way of detecting structural anomalies in crystals.

An example of DSC trace is shown in figure 2:

Figure 2

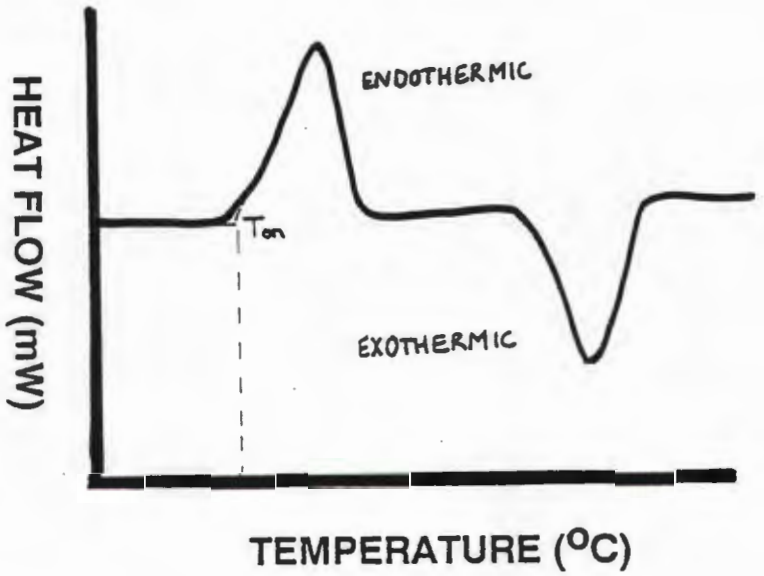

The magnitude of peak area is a measure of the enthalpy of a thermal event. Thus it should be possible to study crystal lattice rearrangements due to guest loss as well as recrystallizations and melts of host-guest compounds. In this way thermal analysis results may reconcile thermodynamics with structure. The degree to which the guest is held in the lattice of the β-phase crystal is reflected in the difference between the normal boiling point of the guest (T_b) and the temperature at which the guest release is observed (T_{on}). The greater the value for T_{on}-T_b that is obtained, the more stable the host-guest compound.

All single TG traces were performed at $10^{o}min^{-1}$ and all multi-heating rate TG traces were carried out at 2,5,10 and $20^{o}min^{-1}$.

All DSC runs were carried out at $10^{o}min^{-1}$.

APPLYING TG AND DSC TO INCLUSION COMPOUNDS

A typical decomposition of a host-guest inclusion compound in which the guest is relatively volatile may be expressed in terms of the scheme shown in figure 3.

Figure 3

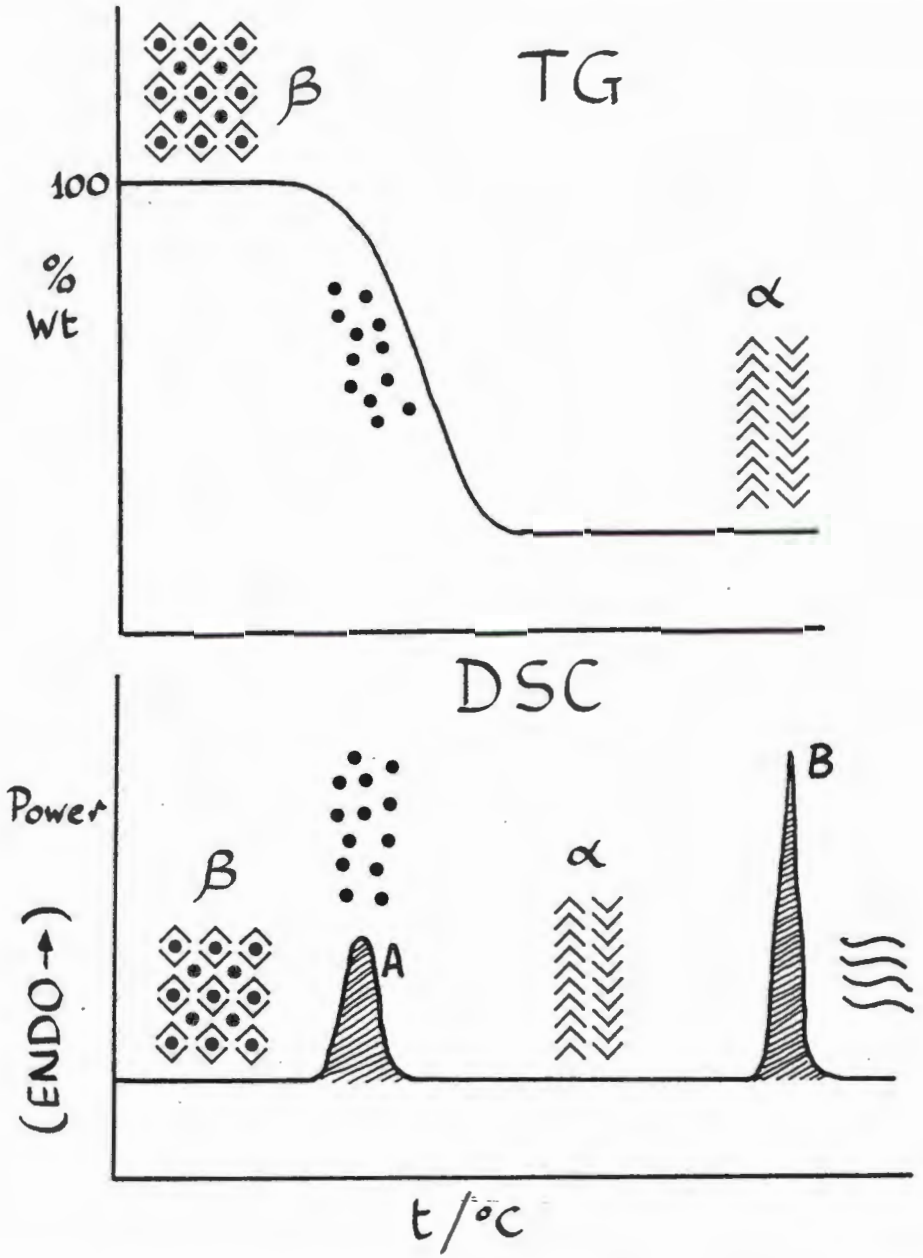

The TG trace follows the decay of the β host-guest inclusion complex, (dots within a diamond-like framework). The inclusion complex loses its guest (dots) as reflected by the weight loss curve, until the stoicheiometric limit corresponding to α-form of the host is reached. In order to detect the actual phase change however, the technique of DSC must be carried out on the same sample. The DSC trace shows the

desorption of the guest to be reflected by endotherm A and melting of α-form host by endotherm B.

A two-step TG thermogram is shown in figure 4. There is initial loss of guest to form intermediate or γ-phase which upon further heating results in desorption of the remaining guest and formation of α-form host. The corresponding DSC trace reflects two unique endotherms, A and B, which correspond to each guest desorption step. Peak C corresponds to the melting of α-phase host.

Figure 4

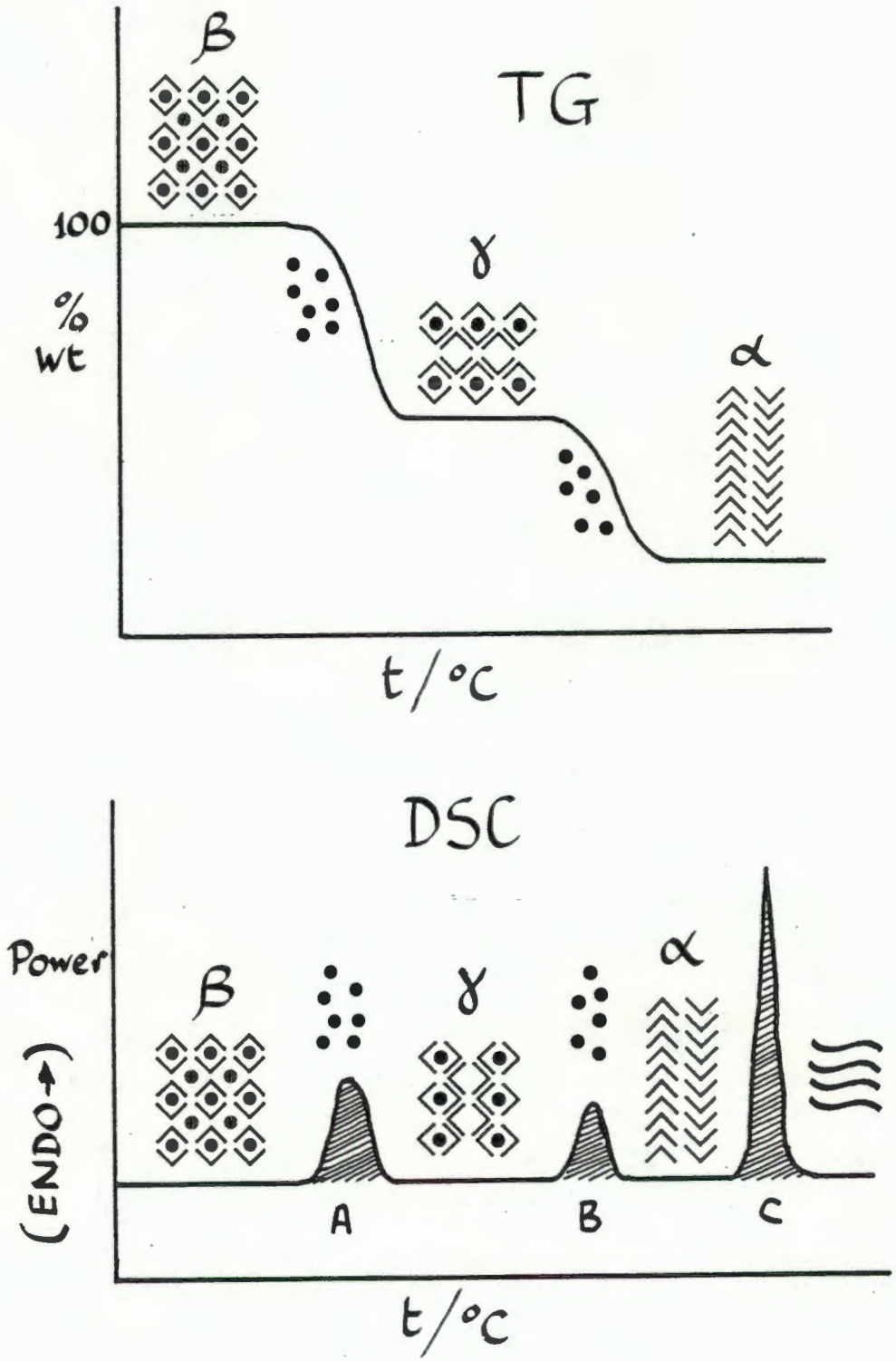

THERMAL ANALYSIS RESULTS

α-FORM OF HOST1

The TG trace predictably showed no loss in weight upon heating. The DSC, shown in figure 5, contains an endotherm at 148°C corresponding to the melting of the host1 compound.

Figure 5

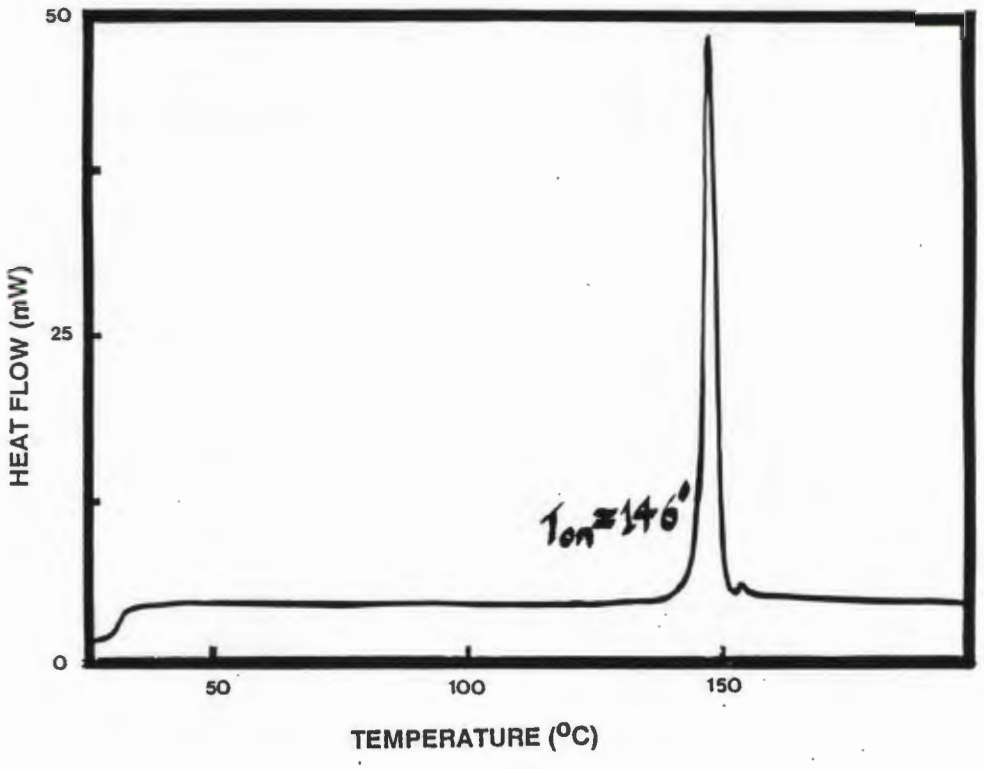

Host1-Benzophenone

The DSC trace, shown in figure 6, has a single endotherm at 98°C which corresponds to the collapse of the complex with concomitant dissolution of the host1 compound. The TG trace shows stoicheiometric loss of guest (calc % loss =30.5 and exptl % loss=30.1) which starts at 100°C for $\beta=2^{o}min^{-1}$ and 150°C for $\beta=20^{o}min^{-1}$. Benzophenone has a melting point of 48.5°C and boils at 305.4°C.

Figure 6

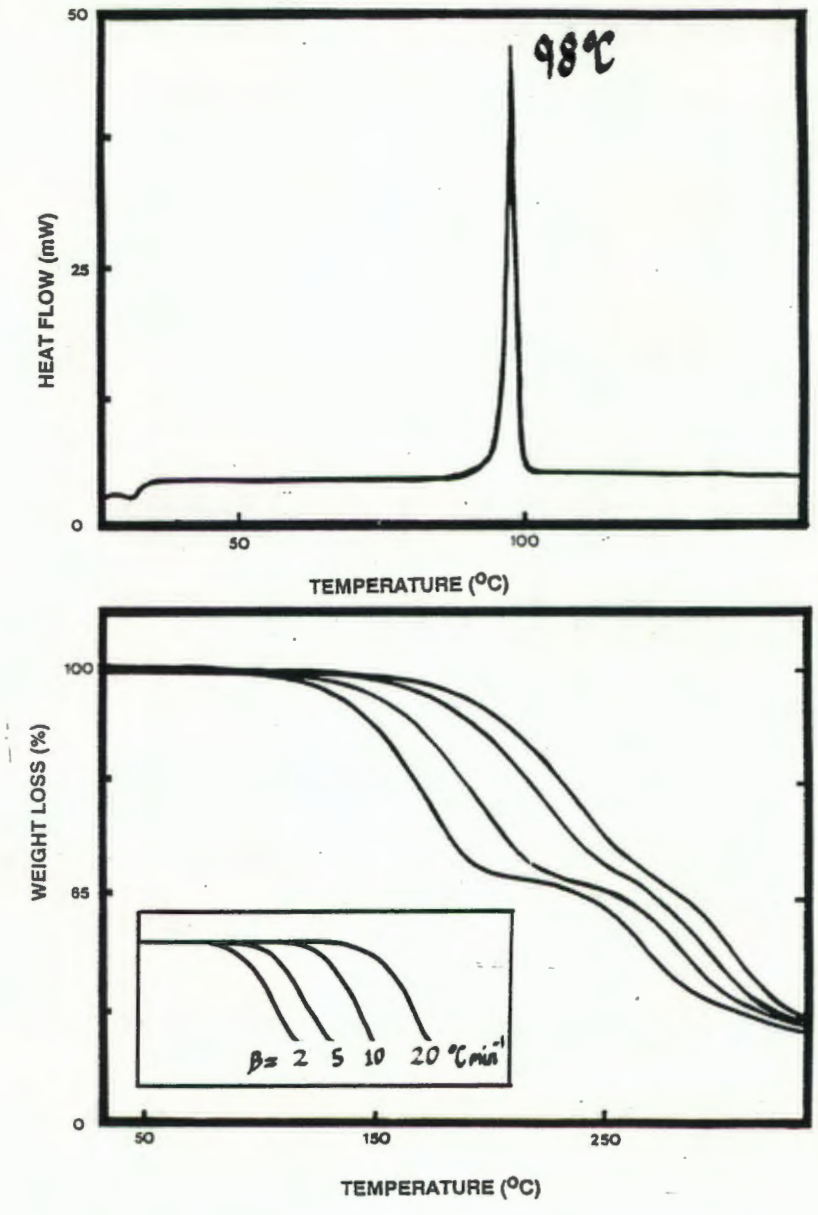

PHOTOGRAPHS OF THE MELTING OF THE HOST1-ACETONE INCLUSION COMPOUND

The thermal decomposition of this compound was followed photographically using a hotstage microscope **(8)**.

(i) Host1-Acetone compound at room temperature.

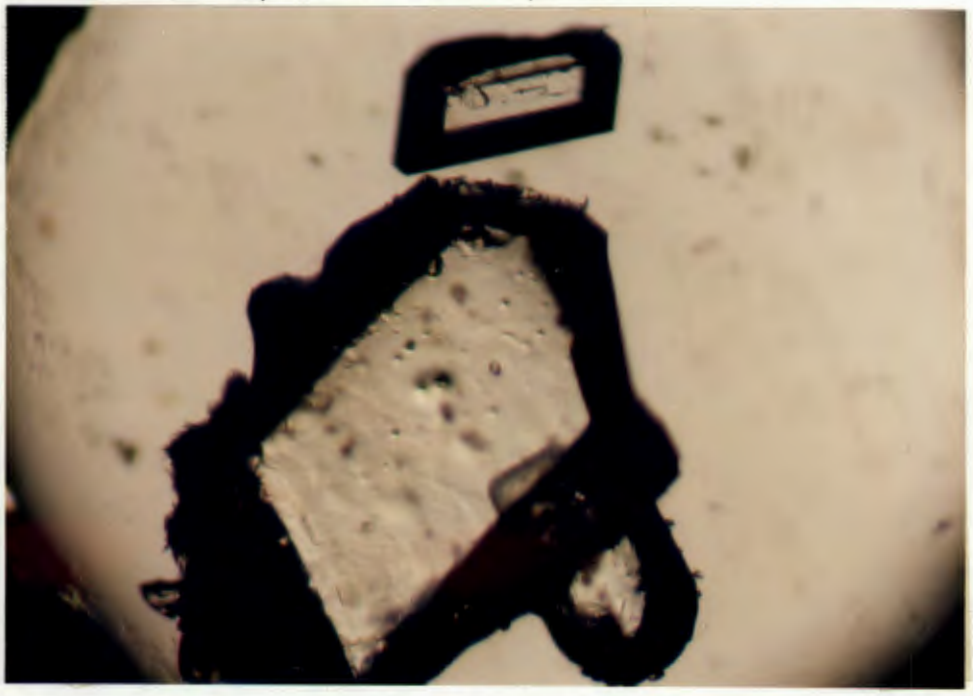

(ii) T=65°C, crystals are becoming opaque due to superficial loss of guest.

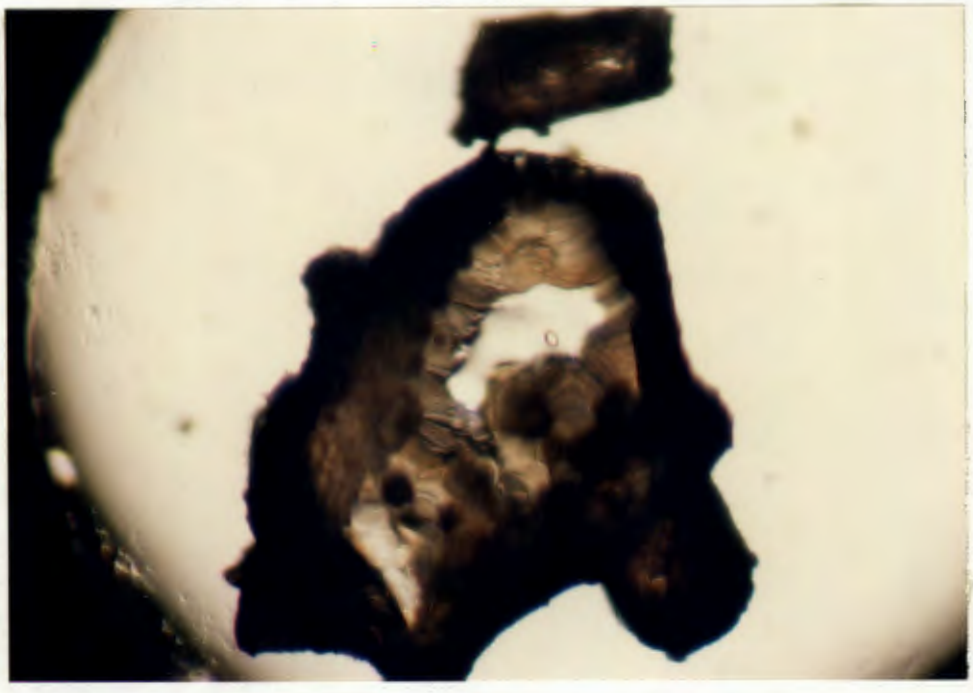

---

8 CT Lin, PY Siew & SR Byrn, *J.Chem.Soc Perkin 2*, 1, 1978, 957-962
CT Lin, PY Siew & SR Byrn, *op. cit.*, 963-968

(iii) T=82°C, the crystals are opaque.

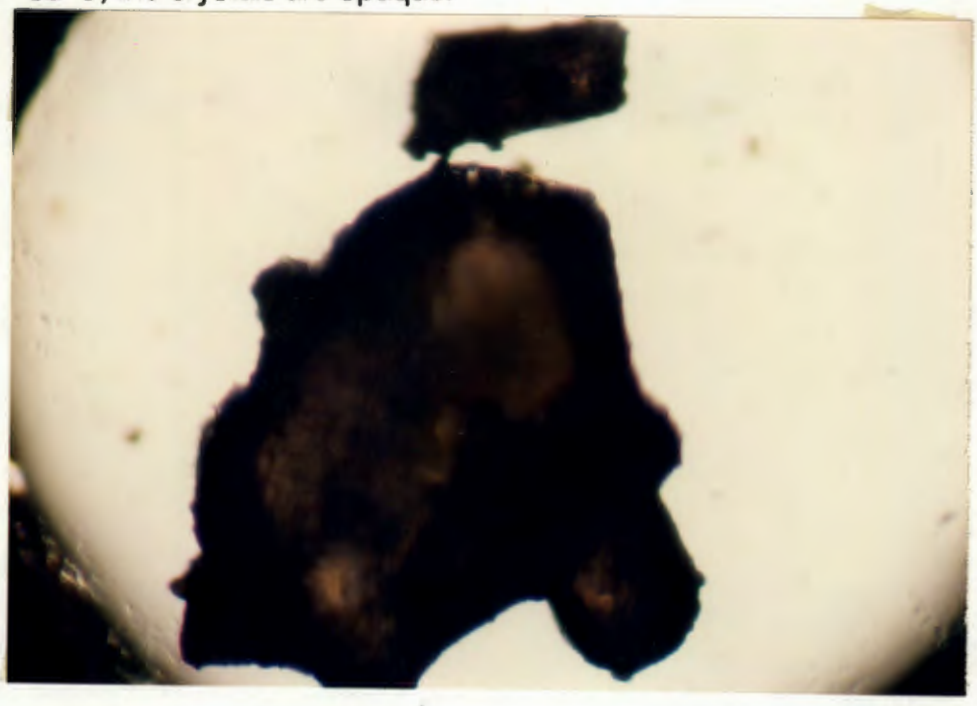

(iv) At 110°C, a vigorous boiling is observed as the acetone that is trapped within the channels escapes and the host1 recrystallizes (the small needle-like crystals).

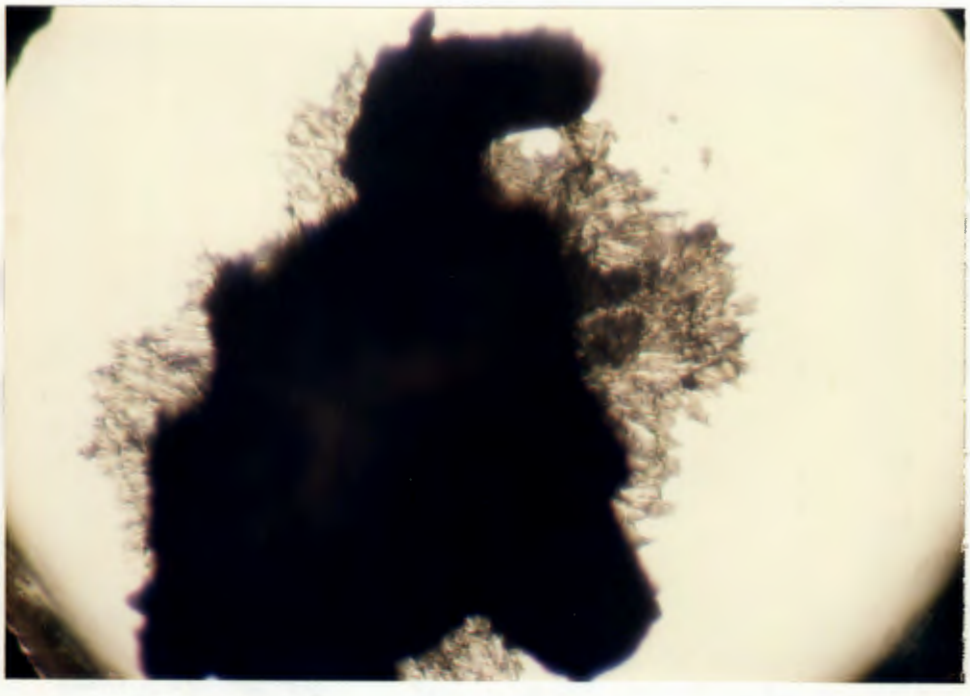

(v) Recrystallization of host1 is complete and at 146°C, melting occurs.

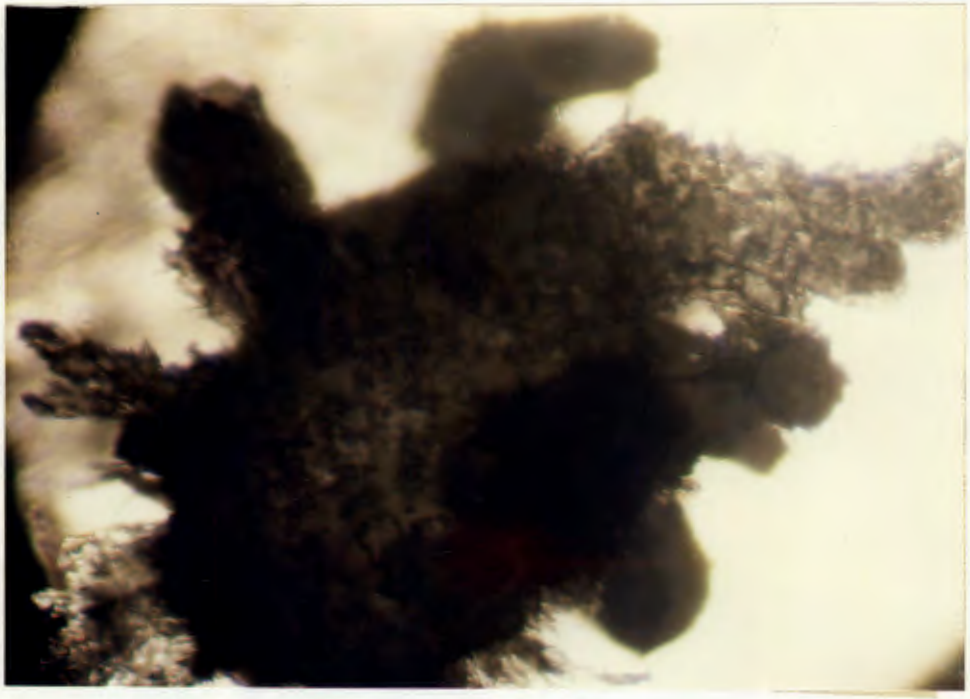

Figure 9A shows a DSC run carried out using an uncrushed crystal of the host1-acetone compound. There is a massive endotherm, B, corresponding to the energetic guest desorption process as was photographically observed.

Figure 9

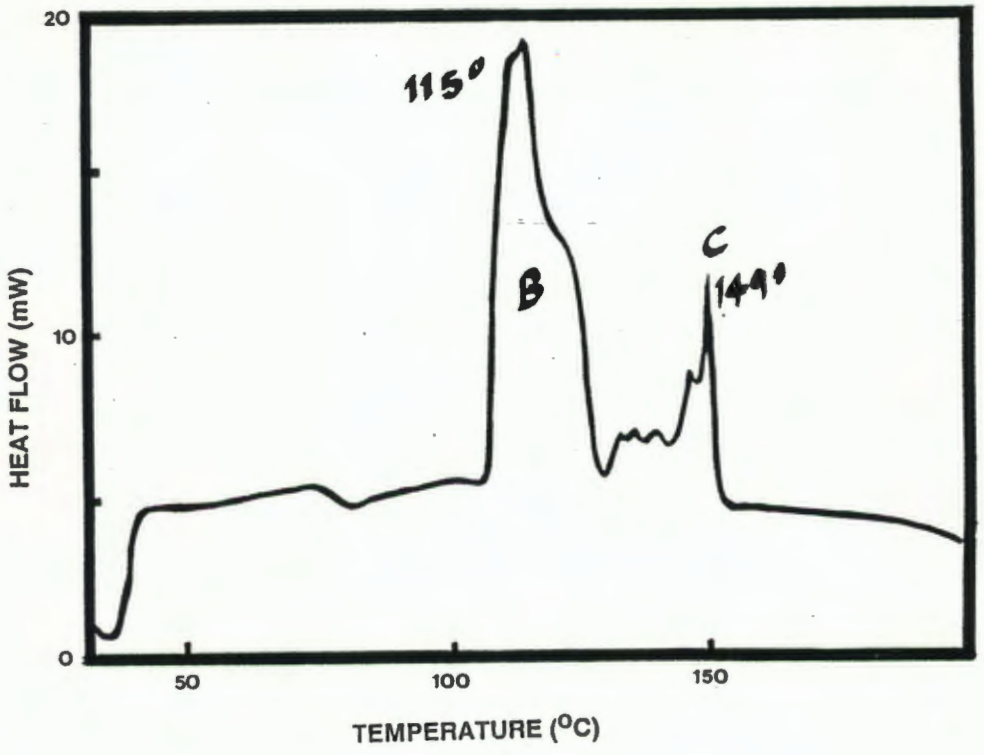

THERMAL ANALYSIS RESULTS OF HOST1-KETONE COMPOUNDS

Thermograms may be found overleaf in Figure 10

Compounds	h1-acetone	h1-MEK	h1-DEK	h1-acetophenone	h1-benzophenone
H:G	1:2	1:2	1:2	1:2	1:1
Calculated weight loss (%)	21.9	25.8	29.4	36.7	30.5
Experimental weight loss (%)	21.9	23.8	28.9	37.5	31.7

The agreement between observed and calculated weight loss is very good, the maximum difference being 2%. The host:guest ratios which were subsequently used in the crystallographic analyses are therefore confirms .

The decay of the host1-MEK compound, shown in figure 10i, results in two distinct endotherms on the DSC trace. The onset temperatures are T_{on} = 50°C and T_{on} = 143°C. The first peak corresponds to the collapse of the host1-guest complex at 50°C and the second endotherm to the melting of host1.
Host1-DEK behaves in a similar manner, the DSC, figure 10ii, shows a T_{on} at 72°C for the loss of DEK which is followed by the melting of the host1 at 146°C.
The host1-Acetophenone inclusion compound decomposes in a similar manner, shown in figure 10iii, to the host1-Benzophenone structure. There is a single endotherm with T_{on} = 73°C corresponding to dissolution of the host1 compound in the guest as the crystalline complex collapses.

Host1 & MEK

(i)

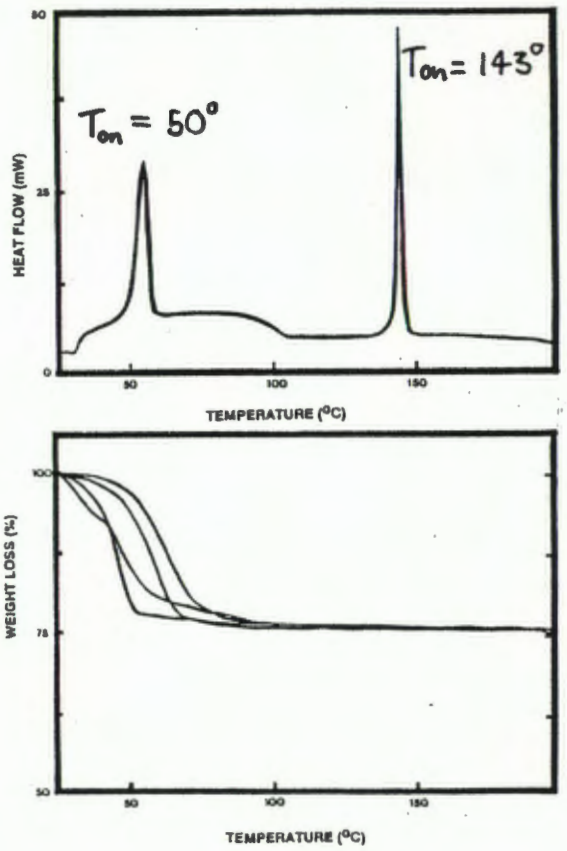

Host1 & DEK

(ii)

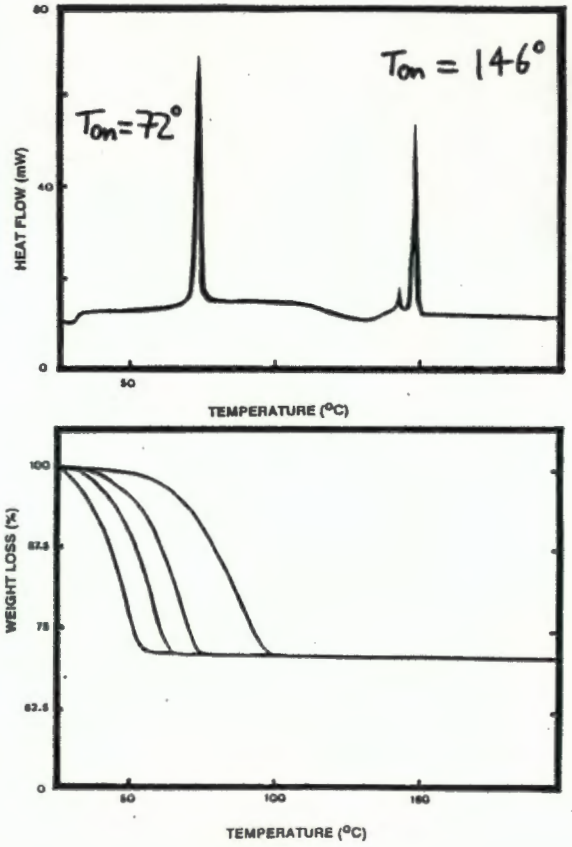

Host1 & Acetophenone

(iii)

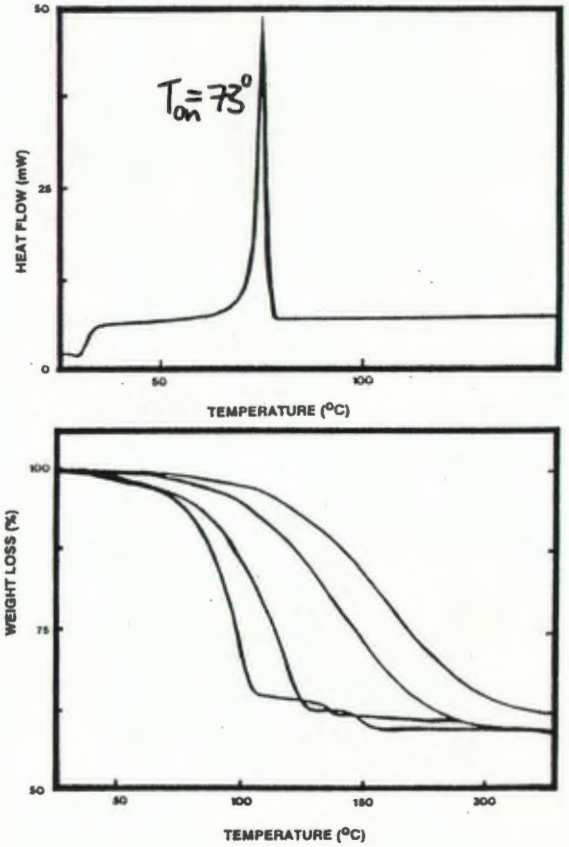

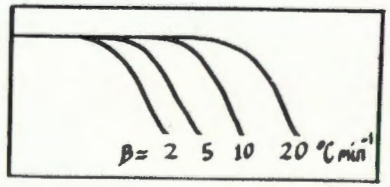

Figure 10

Host1-Propiophenone

The host-guest stoicheiometry of 1:1 was confirmed by the TG result. The calculated % guest loss is 24.5% and it was experimentally found to be 23.8%. The DSC exhibits a single endotherm corresponding to the melting of the compound at 57°C.

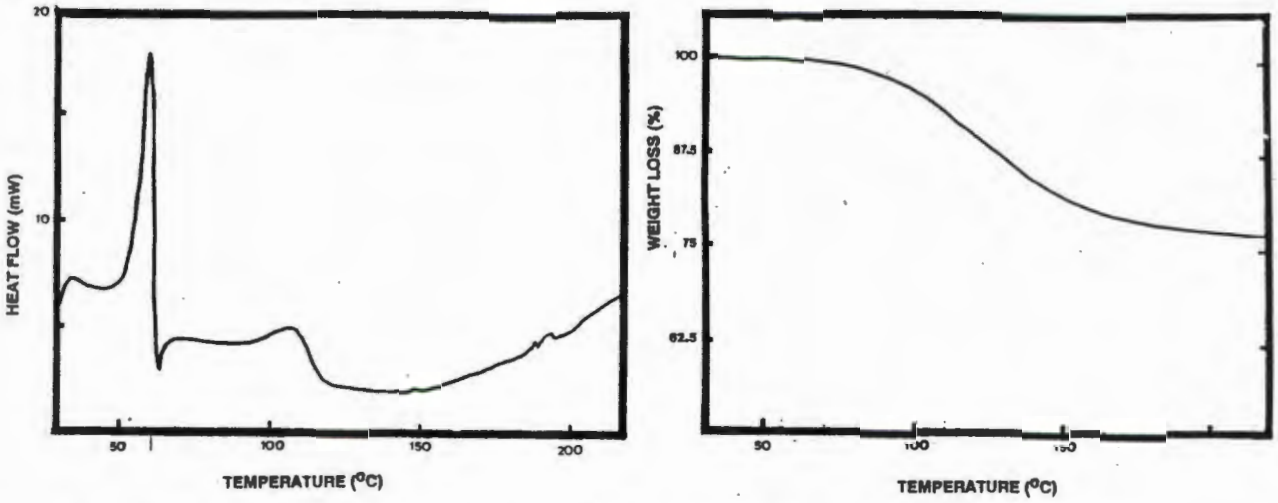

In order to calculate approximate activation energies for the guest desorption reactions, the method of Flynn & Wall **(9)** was employed. Analysis of the decomposition of host1-MEK was not carried out because a multi-step decomposition occurs as is evident by the presence of a point of inflection in the 2 $^{o}Cmin^{-1}$ trace. The semilogarithmic plots of host1-DEK, shown in figure 11, were not linear but distinctly curved which indicates that the mechanism of decomposition was temperature dependent.

Figure 11

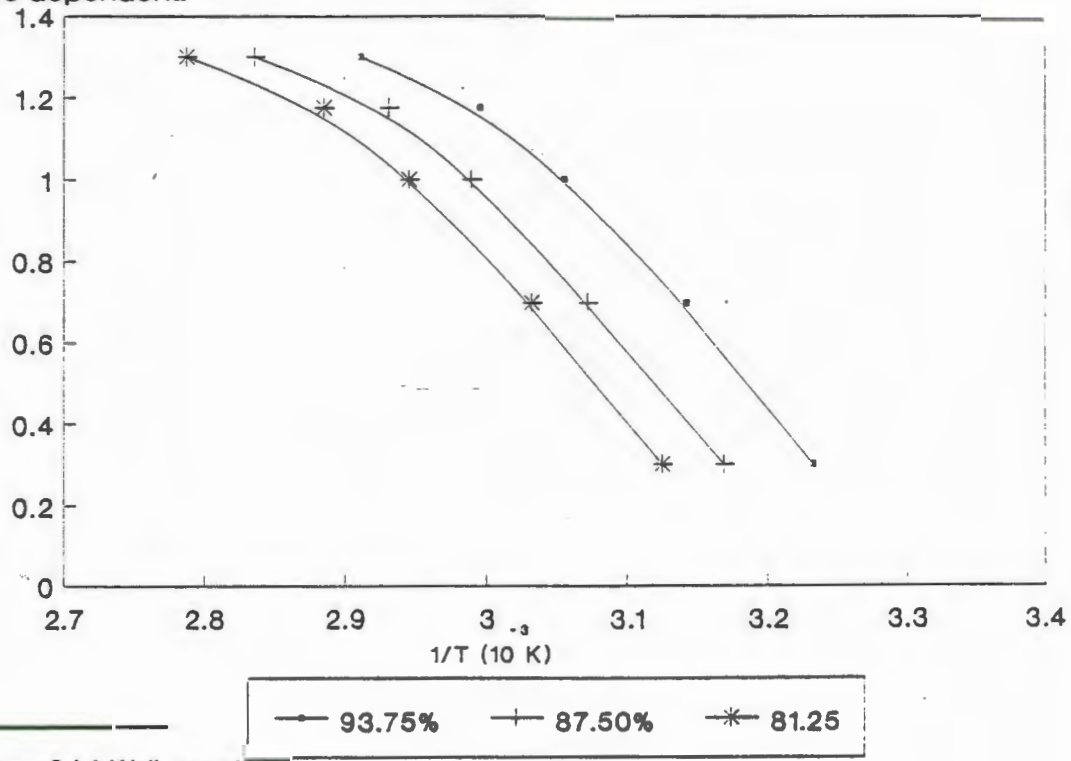

9 JH Flynn & LA Wall, *op. cit.*

The results for the decomposition of host1-acetophenone are shown in figure 12 and the semilogarithmic plots are reasonably straight lines and have activation energies varying from 42 $kJmol^{-1}$ to 51 $kJmol^{-1}$. Similar plots for host1-benzophenone may be found in figure 13. The values obtained for the decay of host1-benzophenone lie within the range 55.9-60.1 $kJmol^{-1}$.

Figure 12 (Host1-acetophenone)

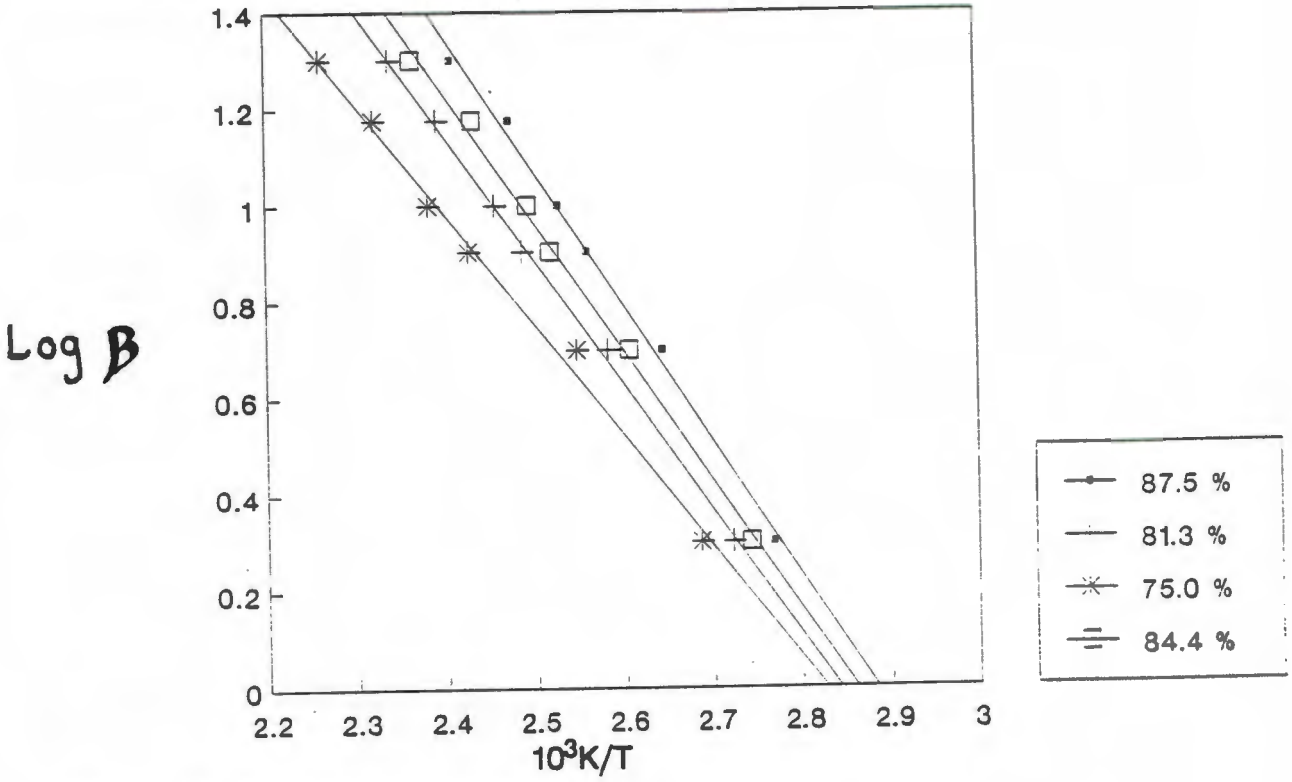

Figure 13 (Host1-benzophenone)

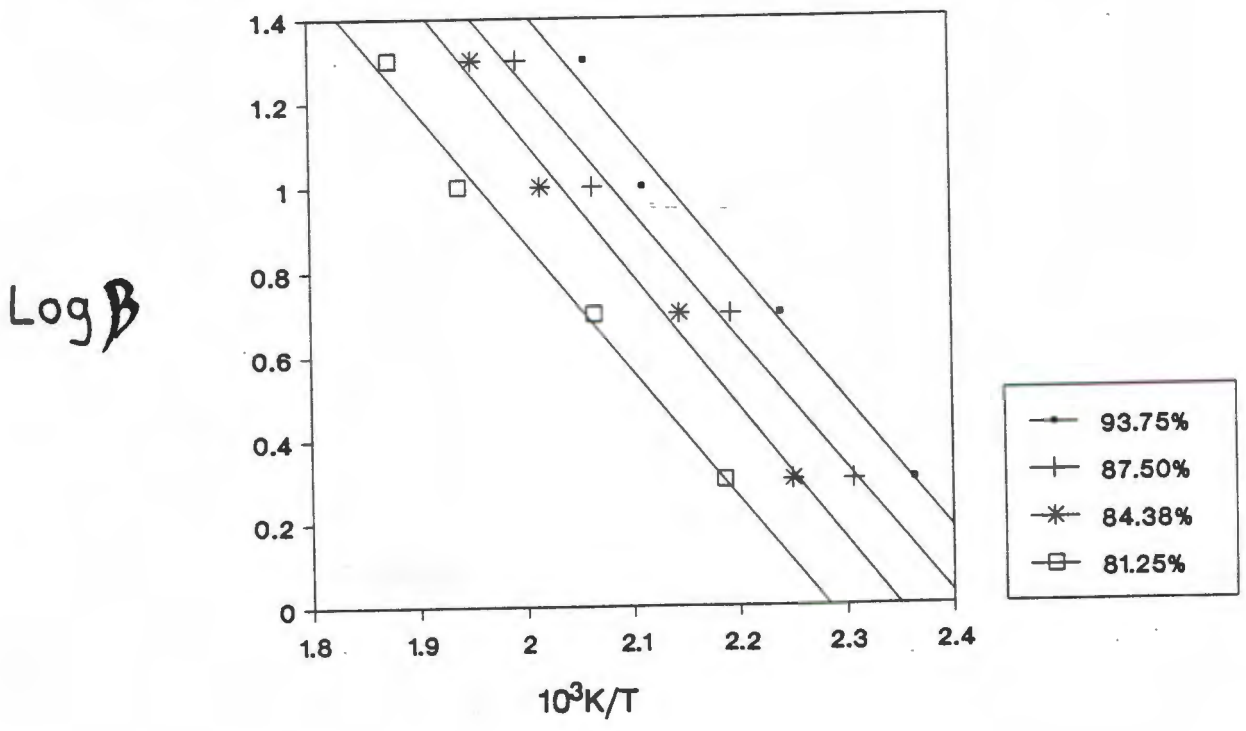

DISCUSSION OF THE HOST1-KETONE COMPOUNDS

The table shown overleaf is divided into parts **A** and **B**. Crystal structures in **A** contain guest molecules lying in channels. They exhibit multi-endotherm decays in their DSC traces - one endotherm corresponding to desorption of the guest as well as one corresponding to the melting of α-phase host1. Guests possessing high vapour pressures such as acetone, MEK and DEK fall into the above category. As guest molecules, they are particularly volatile and prone to desorption from the β-host-guest lattice if left exposed to the atmosphere. The two compounds classed as type **B** have one endotherm corresponding to the desorption of guest which occurs with concomitant dissolution of the host.

The packing mode of a structure may be expressed in terms of packing density. The packing factor is defined as the volume of the unit cell ($Å^3$) divided by the total number of non-hydrogen atoms present in the cell **(10)**. Thus a higher value implies that more space is available per atom and that the structure is loosely packed. The α-form of host1 has a packing factor PF of 17.35. The PF's of host1-acetone, host1-DEK and host1-MEK have values of 18.73, 19.80 and 19.75 respectively. These packing factors are higher than the packing factor of α-phase host1 and reflect the presence of channels in those structures which defines them as tubulato-coordinatoclathrates.

The PF's of host1-acetophenone and host1-benzophenone are 17.95 and 17.94 respectively and indicate the more efficient packing occurring in these compounds. The guests in column **B** structures have relatively low vapour pressures and as a consequence are less labile within a host-guest framework. These guests do not reside in channels and their thermal DSC decays exhibit single endotherms corresponding to collapse of the β-phase with concomitant dissolution of host1 in the guest liquid. These host-guest inclusion compounds may be described as ædiculato-coordinatoclathrates.

---

10 MH Moore, LR Nassimbeni, ML Niven & MW Taylor, *Inorganica Chimica Acta*, 115, 1986, 211-217

	A			B	
COMPOUNDS	H-ACETONE	H-MEK	H-DEK	H-ACETOPH	H-BENZOPH
Host1:Guest Packing Factor	1:2 18.73	1:2 19.80	1:2 19.75	1:2 17.95	1:1 17.94
No. of Endotherms	More than one endotherm tubulates			Only one endotherm adiculates	
VAPOUR PRESSURE OF GUEST DECREASING ---->					

Figure 14

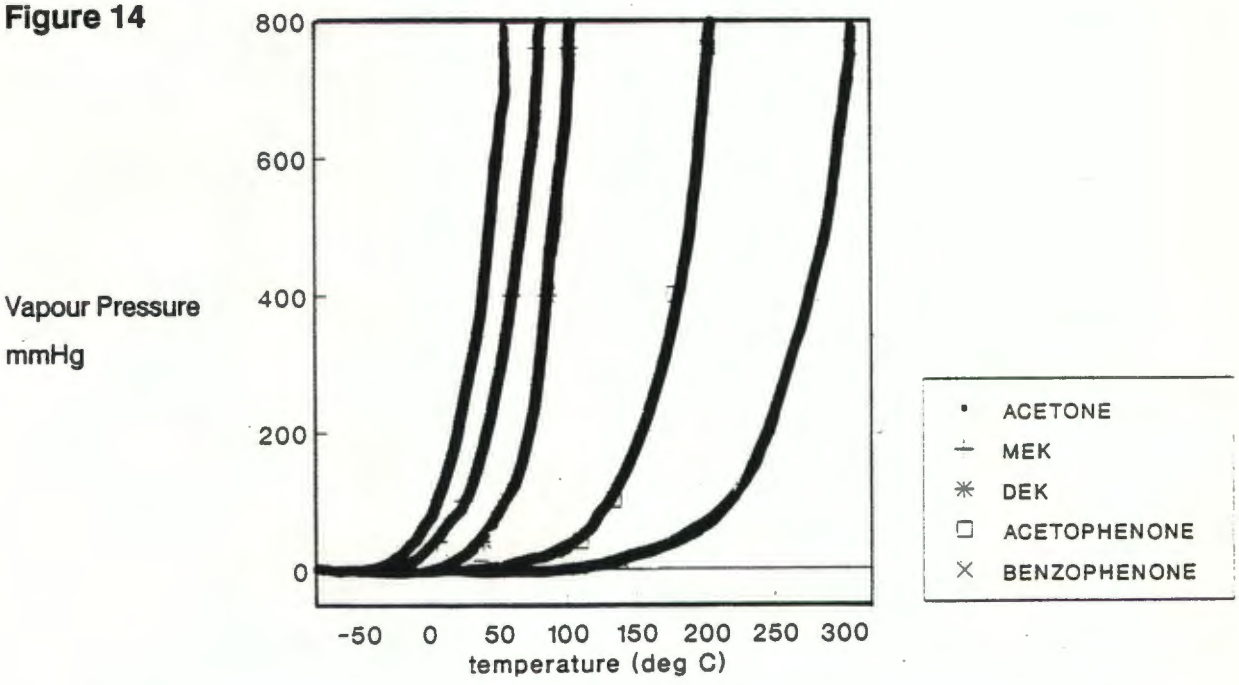

Figure 14 shows how the vapour pressure of these ketones (mmHg) varies with temperature **(11)**. It would appear that the host-guest compounds **A**, in which the guests are relatively volatile exhibit looser crystal packing and thermal decompositions which are characterised by guest release and α-phase host recrystallisation. Less volatile guests, on the other hand appear to pack more efficiently in a crystal and exhibit single endotherm decays corresponding to collapse of the β-complex.

---

11 CRC Handbook of Chemistry and Physics, *op. cit.*

The table below shows values of ΔH ($kJmol^{-1}$) which were calculated from the area under the curve of the DSC endotherms. The U_{min} ($kJmol^{-1}$) values were calculated using the program HEENY. HEENY, as has been described in Chapter 2, calculates the energy environment of a guest molecule which is surrounded by host molecules. The position of this guest is varied in incremental translations and rotations to attain an energy minimum taking into account energy contributions due to hydrogen bonding.

More stable compounds would probably have lower crystal energies U_{min} as well as higher values of T_{on}-T_b and of ΔH, the enthalpy change of the guest release reaction. It is necessary to be circumspect when considering the values of U_{min} because the HEENY calculation deals with severely simplified energy environments in a crystal. Comparisons between host-guest interactions should ideally only be carried out between guests which are geometrical isomers and between compounds which have the same host-guest ratio **(12)**.

The difference between the onset temperature observed in the DSC traces of the thermal decompositions of these compounds and the normal boiling point reflects the stability of these compounds when subjected to heating. For the two **B** host1-ketone compounds the difference displayed in the table below is T_{on} less the melting points of these ketones since they exhibit different thermal decompositions than those host1-ketone compounds in **A**.

	A			**B**	
Compounds	**H-Acetone**	**H-MEK**	**H-DEK**	**H-Acetophenone**	**H-Benzophenone**
ΔH($kJmol^{-1}$)	56.0	36.0	50.4	52.3	50.6
U_{min}($kJmol^{-1}$)	-67	-58	-48	-90	-99
T_{on}-T_b	4.0	-29.2	-29.2		
T_{on}-T_m				-52.5	-47.5
O---O (Å)	2.73	2.77	2.79	2.89 2.86	2.67 2.79

The host1-acetone compound displays a positive T_{on}-T_b difference and this indicates that the acetone is held within the lattice beyond its boiling point. This occurs despite

---

12 SA Bourne, LR Nassimbeni & E Weber, *J.Org.Chem.*,in press

the fact that acetone is the most volatile guest. The T_{on}-T_b difference for host1-MEK and host1-DEK exhibit the same value, which implies that they have the same order of stability. The number of host1-ketone structures considered prevents a conclusion being made concerning the ΔH and U_{min} values (kJmol-1). Disappointingly the results obtained do not appear to reflect a specific order but lie in the range of values expected for such organic molecules. These host-guest inclusion compounds are very unstable making sample preparation for precise and reproducible thermal analysis results extremely difficult. Further work in this area will have to be undertaken to establish ground work in this area of inclusion chemistry so that trends and stability orders can be precisely determined.

CHAPTER FIVE

COORDINATION-ASSISTED CLATHRATE COMPOUNDS FORMED WITH HOST1 AND NON-POLAR GUESTS

THE STRUCTURE OF THE HOST1-CYCLOHEXANE (2:1) INCLUSION COMPOUND

EXPERIMENTAL

An attempt to obtain the α-form of host1 by recrystallizing it from cyclohexane yielded a compound in which cyclohexane molecules had been trapped. Slow evaporation of dilute solutions of host in cyclohexane over a period of 60 days yielded needle-like crystals.

STRUCTURE SOLUTION AND REFINEMENT

Oscillation and Weissenberg photographs showed that the reflection conditions were:

hkl: $h+k=2n$
h0l: $l=2n$; $(h=2n)$
0k0: $(k=2n)$

This indicated that the space group was either C2/c or Cc. The structure was successfully solved in C2/c using direct methods, the combined figure of merit was 0.028 and the RE 0.283. E-statistics favoured the choice of the centrosymmetric space group, but in order to check and confirm the choice of C2/c, refinement of the structure was also attempted in Cc. Refinement in the non-centrosymmetric space group was carried out by placing two host1 molecules (no hydrogen atoms) and fixing the coordinates of one atom in x and z (the origin lay on the glide plane). Considerable correlation between corresponding atoms of the two host1 molecules via a centre of inversion was obtained and the guest did not refine successfully. These considerations, coupled with the fact that refinement in C2/c showed much better convergence and a lower conventional R value, led to the choice of C2/c as the correct space group.

The cyclohexane guest molecule was located in the difference electron density maps in which there were additional peaks beyond those attributed to a host1 molecule. This electron density was due to a molecule of cyclohexane which had been entrapped during recrystallization of host1. The asymmetric unit was found to contain one host1 molecule in a general position and a disordered cyclohexane molecule which lay on a diad at Wyckoff position *e*. It was necessary to contour electron density maps in order to locate the atomic positions of the guest molecule. Figure 1 shows the contour profiles

obtained from electron density maps by sectioning along [010].

$y_1 = 0.14$
$y_2 = 0.18$
$y_3 = 0.22$
$y_4 = 0.26$
$y_5 = 0.30$
$y_6 = 0.34$
$y_7 = 0.38$
$y_8 = 0.42$

Key for figure 1

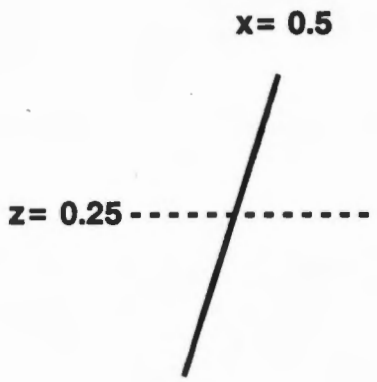

Figure 1

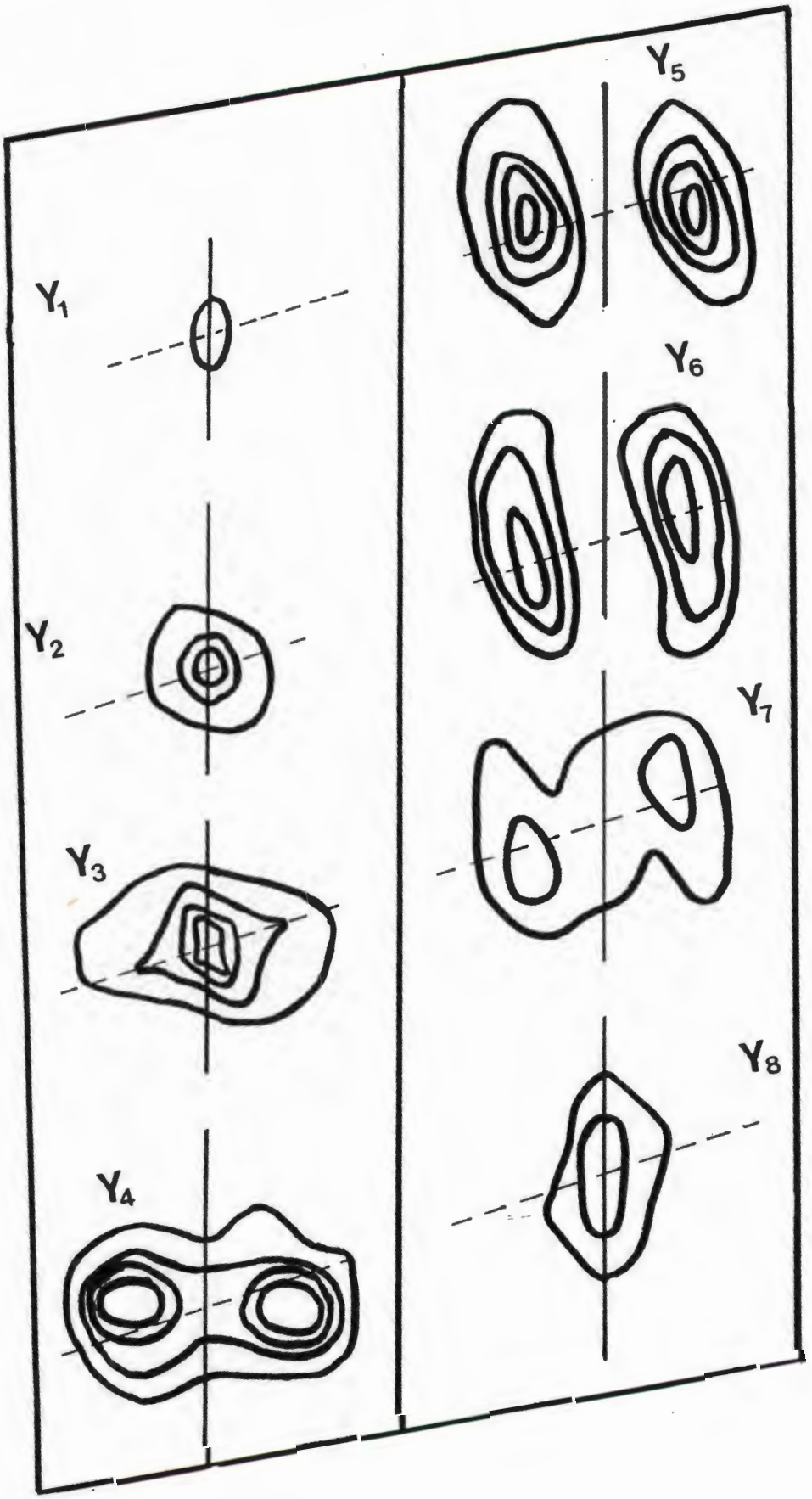

It was necessary to invoke disorder in order to model the guest because six guest atoms were assigned to the observed electron density. Atoms C1G and C4G were located on a special position of multiplicity 4 with a site symmetry of 2 (Wyckoff position *e*). They were refined isotropically **(1)**, **(2)** with site occupancy factors of 0.50. The remaining electron density was assigned to four atoms, C2, C3G, C21G and C31G which were refined isotropically with site occupancy factors of 0.50 each. The cyclohexane guest thus had the chair conformation, figure 2i and 2ii **(3)**. Figure 2iii shows the two disordered half molecules.

Figure 2

(i)

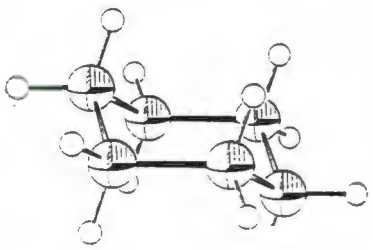

(ii)

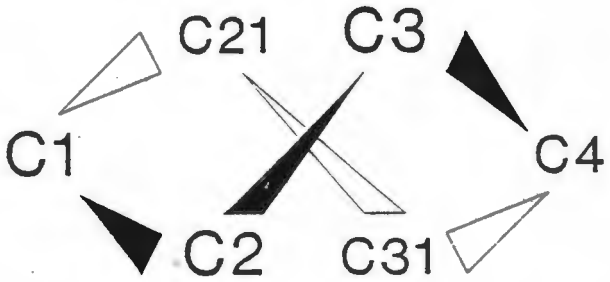

(iii)

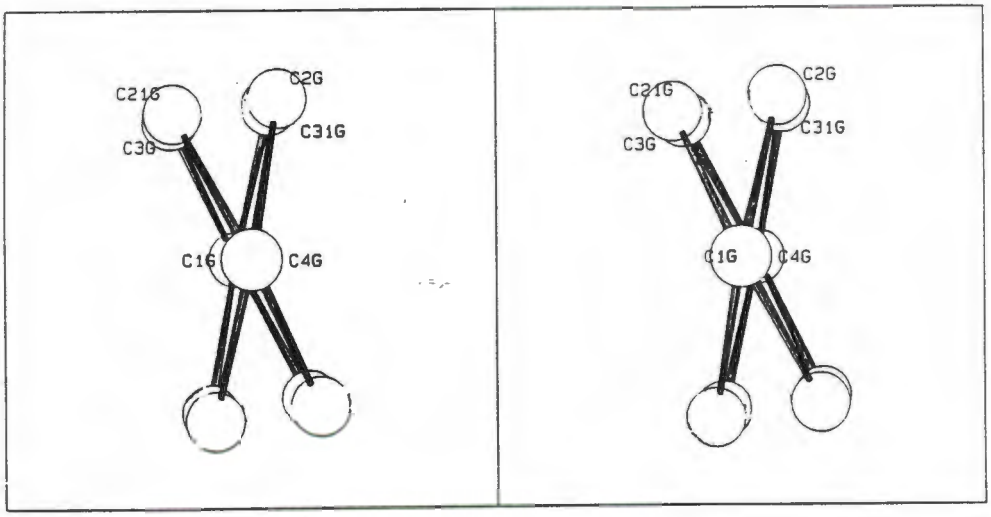

1 WJAM Peterse & JH Palm, *Acta Cryst*, 20, 1966, 147

2 R Kahn, R Fourne, D Andre & M Renaud, *Acta Cryst*, 1973, B29,131-138

3 P. Luger, "*Modern X-Ray Analysis on Single Crystals*", De Gruyter & co., Berlin, 1980, 21

The coordinates ($x10^4$) and isotropic temperature factors ($Å^3x10^2$) of the guest atoms are shown below.

Guest molecule

Atom	x/a	y/b	z/c	U_{iso}
C(1G)	5000(0)	2136(15)	2500(0)	179(8)
C(2G)	5604(8)	2707(13)	2910(13)	133(8)
C(21G)	5547(10)	2707(13)	2383(15)	203(14)
C(3G)	5547(10)	3556(18)	2383(15)	197(13)
C(31G)	5604(8)	3556(18)	2910(13)	225(16)
C(4G)	5000(0)	4202(19)	2500(0)	250(13)

During refinement the coordinates of the common atoms were linked. C1G and C4G were constrained to a non-bonded distance of 2.94Å and the other atoms were constrained to separations of 1.54(3)Å. The host1 hydroxyl hydrogen atoms were located on difference electron density maps and were refined with a common isotropic temperature factor. The positions of aromatic host1 hydrogen atoms were calculated and refined with a common temperature factor. Details of the data intensity collection and structure refinement may be found in Table 1.

Figure 3 - a projection along [010] with the guest shown as disordered.

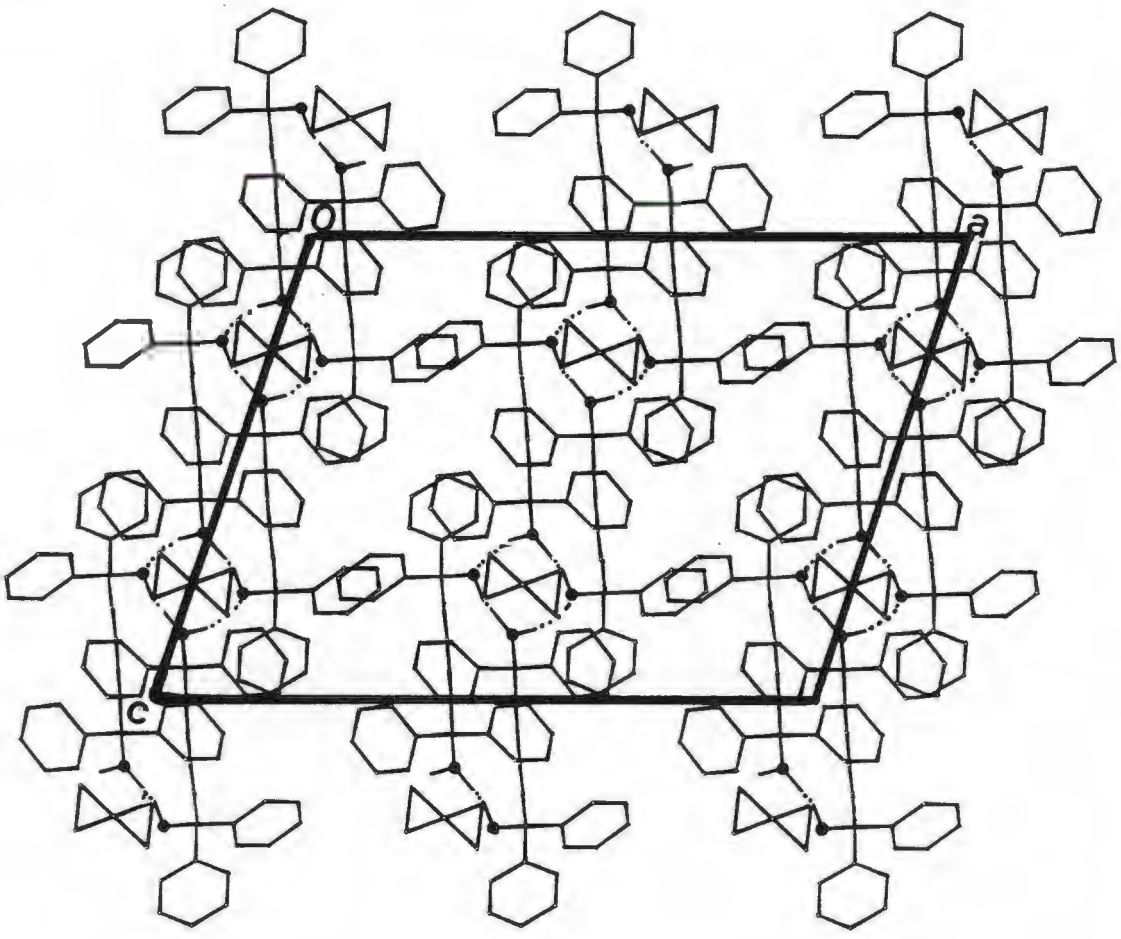

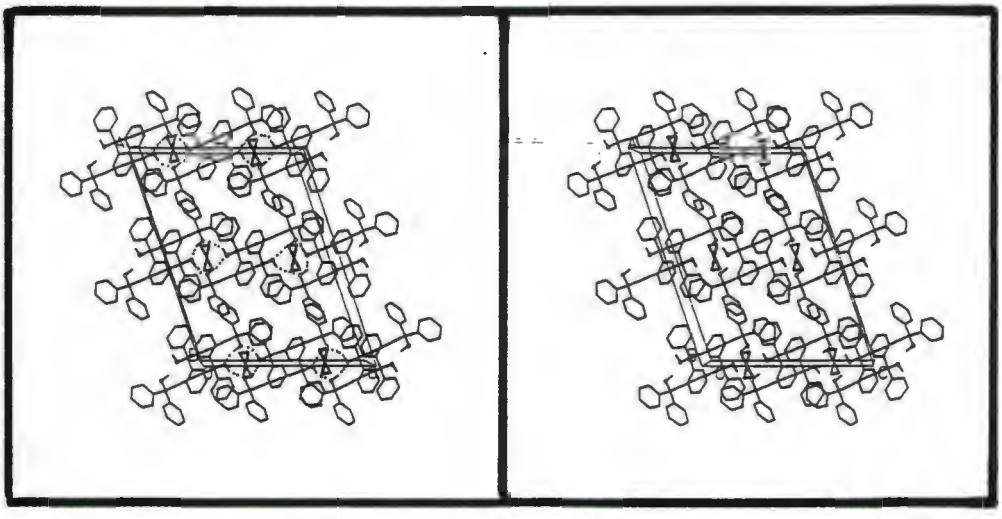

DISCUSSION

There are eight host1 and four cyclohexane molecules in the unit cell, resulting in a host1:guest ratio of 2:1. There is intermolecular hydrogen bonding between the hydroxy moieties of four host1 molecules. The O---O distances and corresponding symmetry operations are:

O2---O1	2.736(7)Å	x,-y,z+½
O1---O2	2.723(5)Å	-x+1,y,-z+1

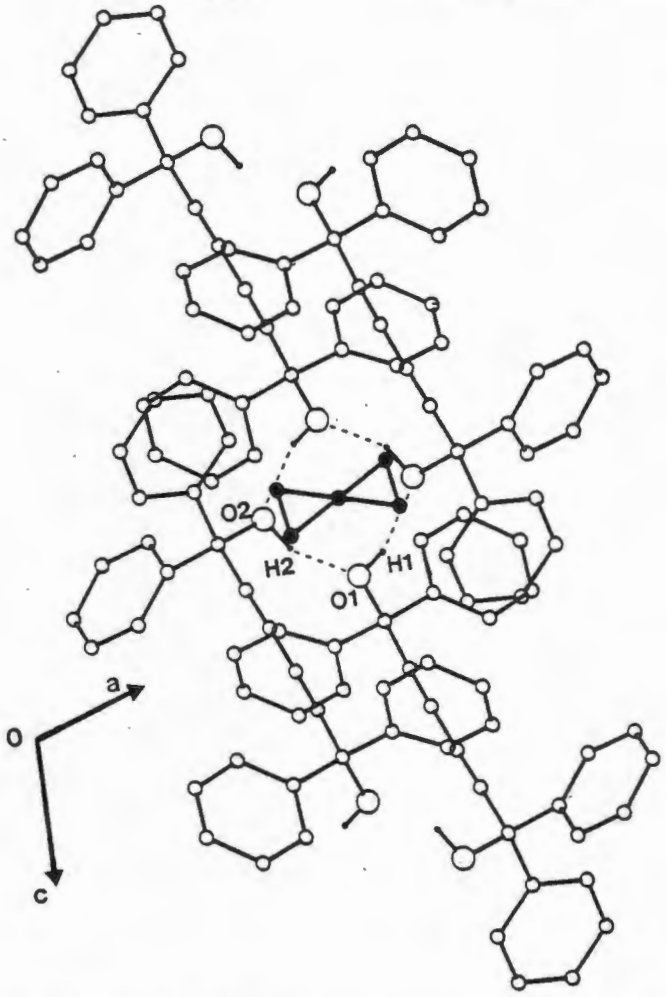

The usual way in which the host1 compound captures a guest, is by hydrogen bond formation involving the hydroxy functions of the host and the electron accepting moieties of the guests. In this particular complex, self-association between the host1 molecules creates a cavity in which the cyclohexane molecule is trapped. Thus this is an example of a true clathrate, analogous to the famous structure of quinol-sulphur dioxide which was elucidated by HM Powell, and which gave use to the name 'clathrate'. In terms of the nomenclature formulated by Weber and Josel, this compound has host-host hydrogen bonding but no strong bonds between host1 and guest and is therefore

classified as a coordination-assisted clathrate **(4)**.
Disordered guest species are not uncommon in inclusion structures which lack specific bindings between constituents and especially those in which the entrapped guest species has considerable volatility as well **(5)**. Figure 4 shows schematically how the guest lies sandwiched between host1 hydrogen bonded tetramers which are one unit cell apart along b.

Figure 4

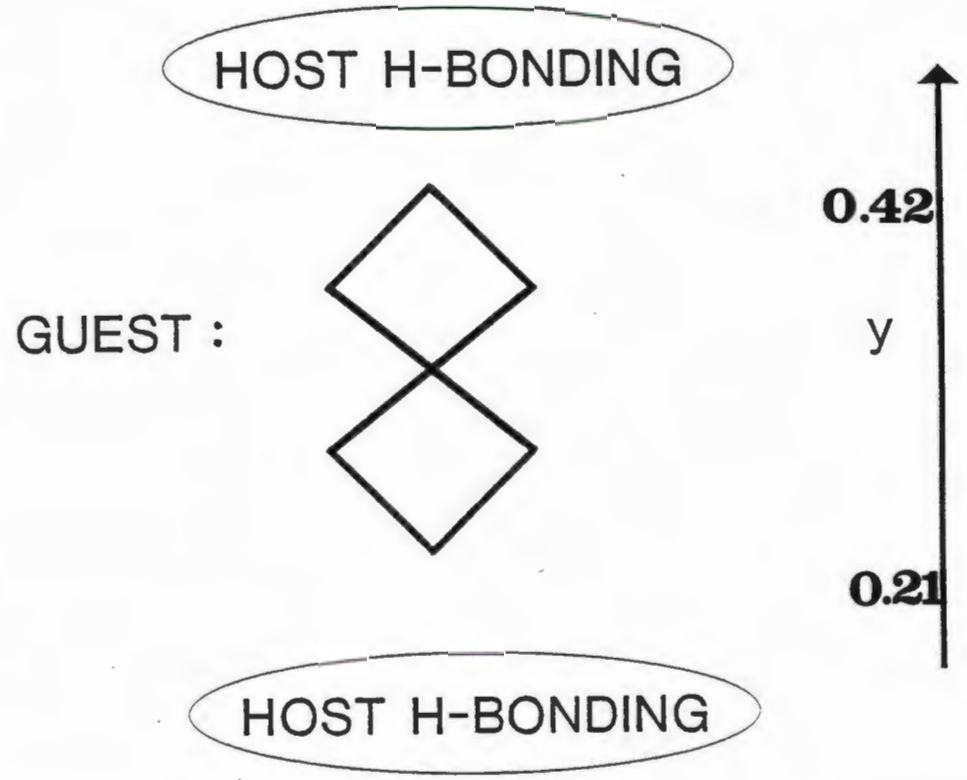

The torsion angles which were chosen according to the description given at the end of chapter 3 are as follows:

	host1	host1-cyclohexane
C2-C1-C11-C12/C16	33(1)	61(1)
C2-C1-C21-C22/C26	-25(1)	-13(1)
C5-C6-C31-C32/C36	-66(1)	-81(1)
C5-C6-C41-C42/C46	18(1)	21(1)

4 E Weber & HP Josel, *J.Incln.Phenomena*, 1, 79-85
5 I Goldberg in "*Topics in Current Chemistry*", Springer-Verlag, Berlin, 1988

The conformation of the hydroxy groups in a host1 molecule is gauche in character. This is illustrated in the figure below which shows a perspective view looking along the molecular backbone of a host1 molecule in this host-guest inclusion compound. The absence of a polar guest forces host1 molecules to form intermolecular hydrogen bonds in an attempt to achieve maximum stability in the crystal. In order to interact in this way, the trans conformation has transformed into a gauche conformation in order to achieve the host1 hydrogen-bonded close contacts.

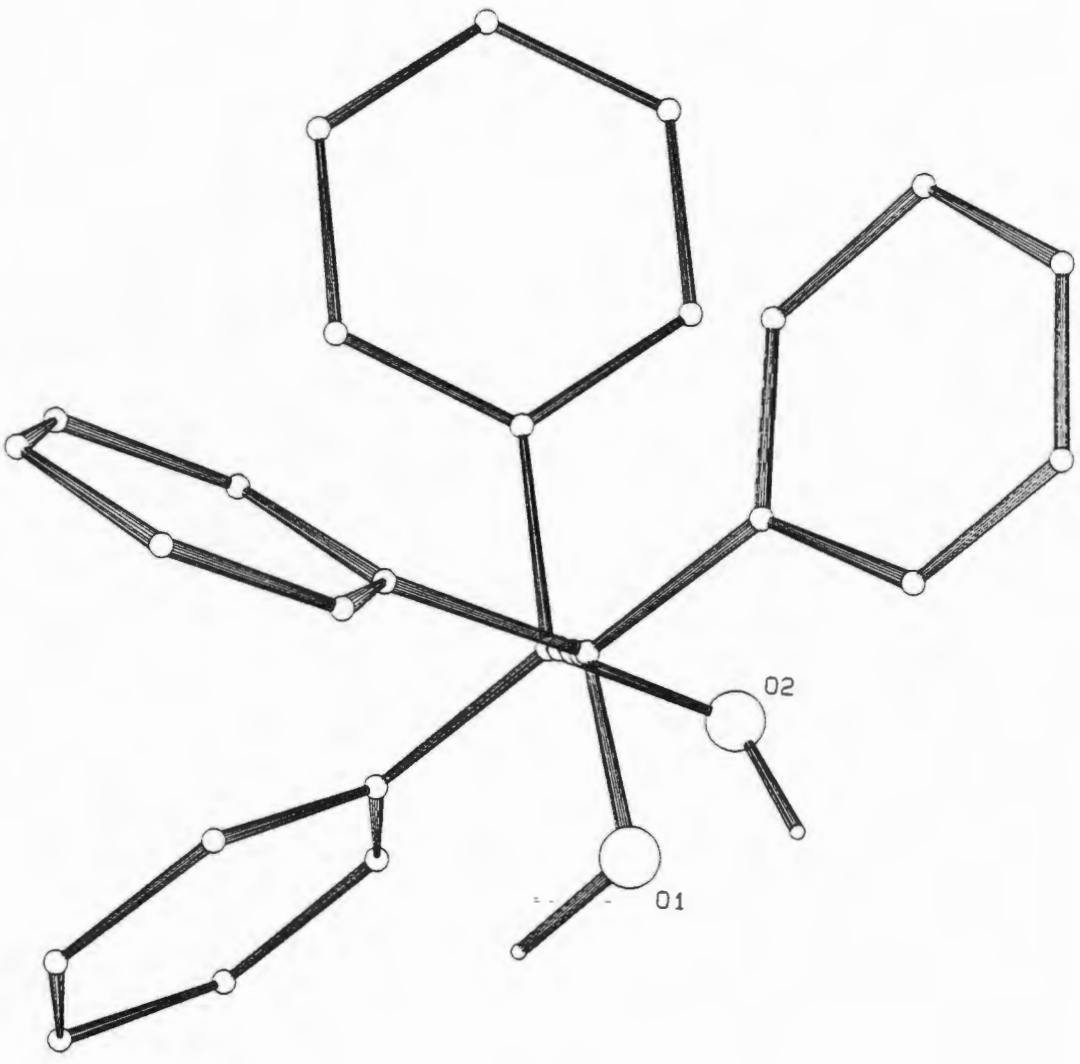

OPEC maps were calculated to determine the shape of the cavity. Figure 5i shows a cross-section of the cavity looking along [0 1 0] at y = 0.42. The shapes of the cavities viewed along [0 0 1] are shown in figure 5ii. The cavities are located at 0.25 and 0.75 along z.

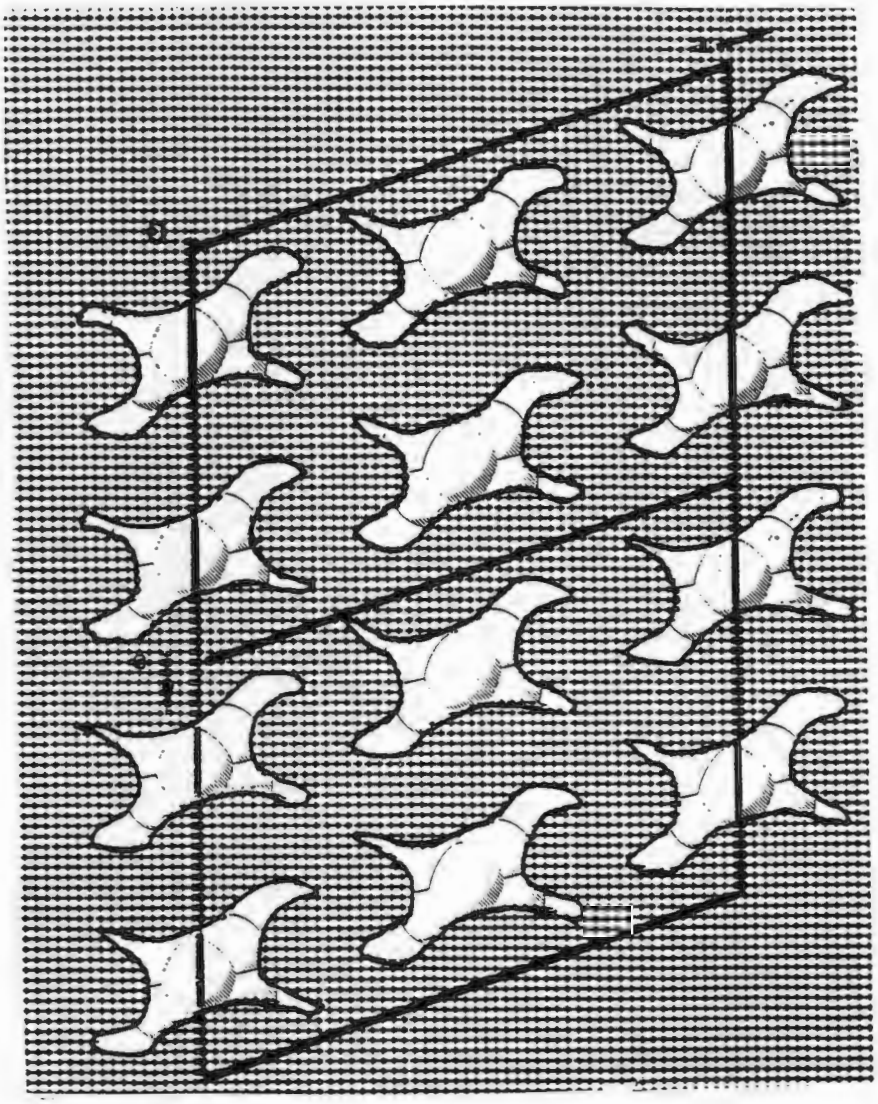

Figure 5(i)

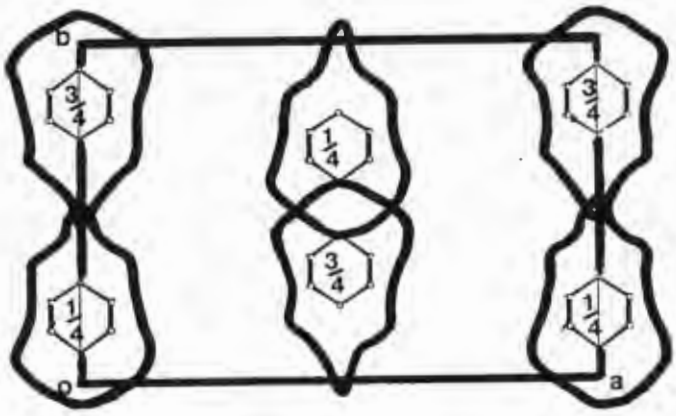

Figure 5(ii)

TABLE 1 CRYSTAL DATA AND EXPERIMENTAL DETAILS FOR HOST1-CYCLOHEXANE STRUCTURE.

Compound	**Host1-cylohexane**
Molecular formula	$2C_{30}H_{22}O_2 \cdot C_6H_{12}$
Molecular weight ($gmol^{-1}$)	913.20
Space group	C2/c
a (Å)	22.851(6)
b (Å)	14.010(2)
c (Å)	17.076(6)
β (°)	108.71(3)
Z	4
V ($Å^3$)	5178(2)
D_c (gcm^{-3})	1.17
D_m (gcm^{-3})	1.15(2)
$\mu(MoK_\alpha)$ (cm^{-1})	0.38
F(000)	1936
Data collection (21°C)	
Crystal dimensions (mm)	0.25x0.36x0.50
Range scanned θ (°)	1-25
Range of indices *h,k,l*	±27, +16, +20
Reflections for lattice parameters no.,θ range (°)	24,16-17
Instability of standard reflections (%)	-1.3
Scan mode	(ω-2θ)
Scan width in(°)	(0.85+0.35tanθ)
Vertical aperture length (mm)	4
Aperture width (mm)	(1.12+1.05tanθ)
Number of reflections collected (unique)	3326
Number of reflections observed with $I_{rel} > 2\sigma I_{rel}$	1937
Final refinement	
Number of parameters	312
R	0.092
wR	0.107
w	$(\sigma^2(F_o)+0.01F_o^2)^{-1}$
S	2.27
Max. shift/e.s.d.	0.011
Max. height in difference electron density map ($eÅ^{-3}$)	0.58
Min. height in difference electron density map ($eÅ^{-3}$)	-0.32

THERMAL ANALYSIS

The TG and DSC scans may be found in figure 6. The DSC shows a small diffuse endotherm corresponding to the guest release. The T_{on} is at 73°C which is lower than the boiling point of cyclohexane (80.7°C). This may be due to the fact that there is no host-guest hydrogen bonding holding the guest in place so this compound collapses fairly easily upon heating. After desorption of the guest, the host1 recrystallizes and melts at 150°C. The TGA trace confirms the host-guest ratio of 2:1. Owing to the fact that crystals of this compound are extremely difficult to obtain, TG runs ~~carried out~~ at different heating rates with the aim of calculating an activation energy were not carried out. The packing factor was calculated to be 18.49Å^3/non-hydrogen atom, which is higher than the value of 17.35 for the α-form of host1. This implies that the structure is loosely packed, which is confirmed by the presence of guest cavities.

H:G	% LOSS EXPTL	% LOSS CALC	T_{ON}	T_{ON}-T_B	ENTHALPY (kJmol^{-1})	PF
2:1	9.0	9.2	72.8	-7.9	23.1	18.49

Figure 6

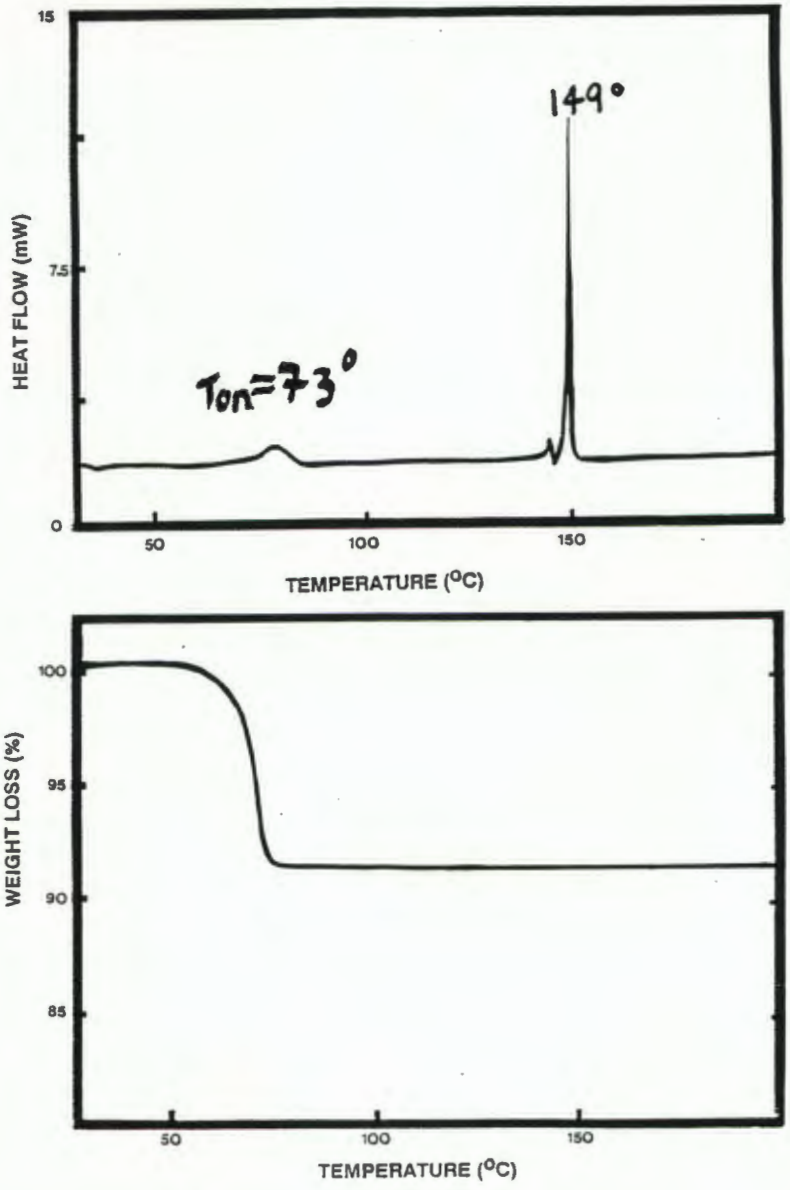

Potential energy calculations using EENY were carried out on host1-cyclohexane. Figure 7 shows the energy profile obtained as the cyclohexane molecule is moved along the y axis. At each increment in the unit cell the guest molecule was tumbled so as to attain a rotational energy minimum.

Figure 7

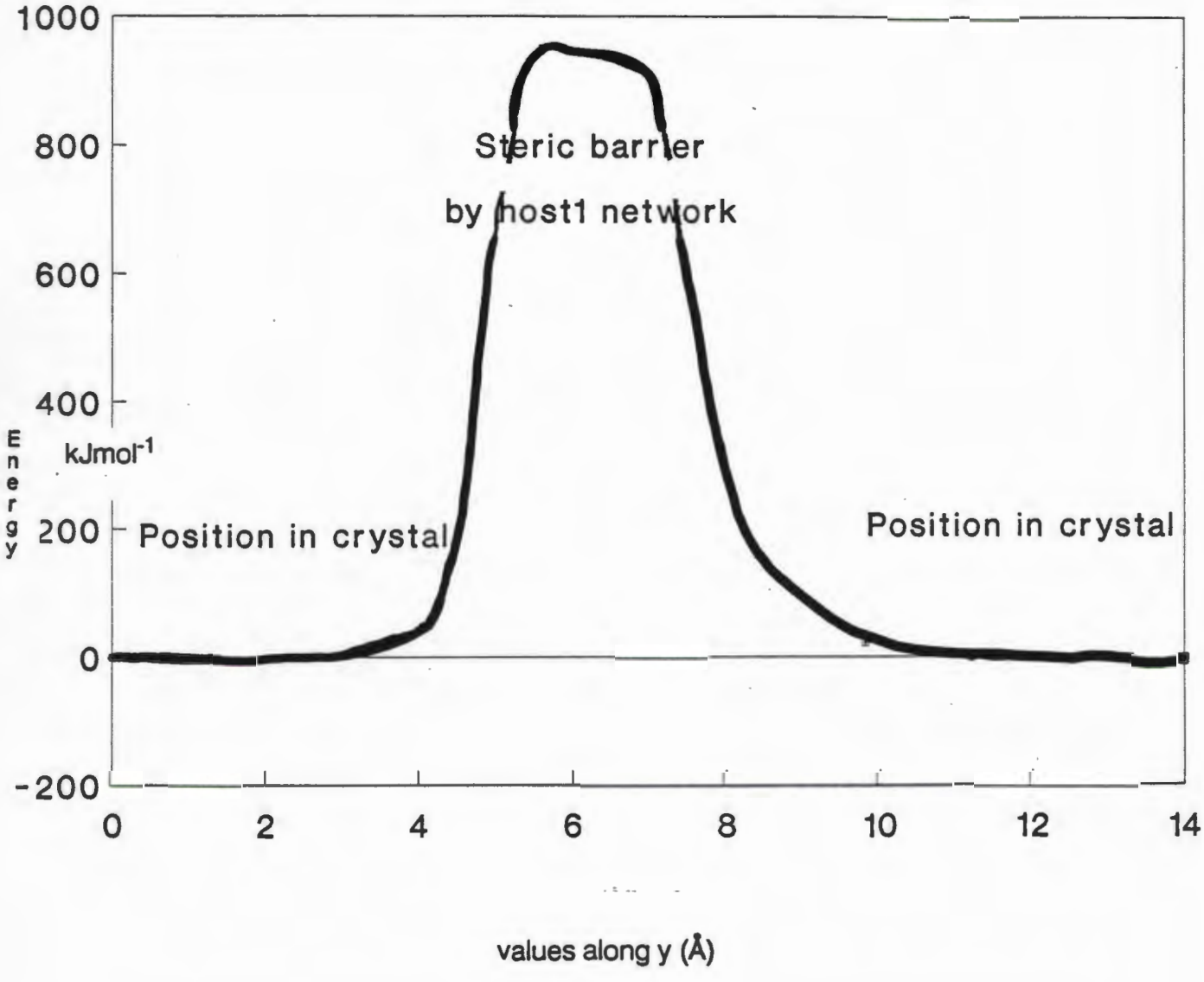

The position of the guest in the crystal is indicated at y=0 and y=14. The very high barrier is expected because the cyclohexane is located in a well defined cavity, and any attempt by the molecule to move outside this is effectively blocked by the host network.

THE STRUCTURE OF THE HOST1-1,4-DIOXANE (1:2) INCLUSION COMPOUND

SOLUTION AND REFINEMENT

No evidence of symmetry other than $\bar{1}$ was detected in oscillation and Weissenberg photographs implying P1 or P$\bar{1}$ as the space group. During intensity data collection three reflections were monitored for loss in intensity. After measuring 2883 reflections, a 35.6% loss in intensity was measured due to crystal deterioration and therefore a linear decay correction was applied **(6)**.

Structure solution was carried out in the space group P$\bar{1}$; mean $|E^2-1|$ statistics and subsequent successful refinement of the structure vindicated this choice. The asymmetric unit contained a host1 molecule and two crystallographically distinct half guest molecules (A and B), lying at crystallographic centres of inversion (Wyckoff *d*, *g* and *c* respectively). Details of the crystal parameters and data collection may be found in Table 2. All non-hydrogen atoms were refined with anisotropic temperature factors, and positions of the aromatic host1 hydrogens were calculated and refined with a common temperature factor. The guest molecules were refined isotropically owing to the higher thermal parameters observed. The hydroxyl hydrogen atom of host1 was located on a difference electron density map and was refined with an individual isotropic temperature factor.

Disorder was invoked for the oxygen atom of guest B during refinement. This was accomplished by modelling this oxygen as two atoms with site occupancy factors of 0.30 (O1GB) and 0.70 (O1BG).
Guest B has the conformation of a disordered chair,
viz.

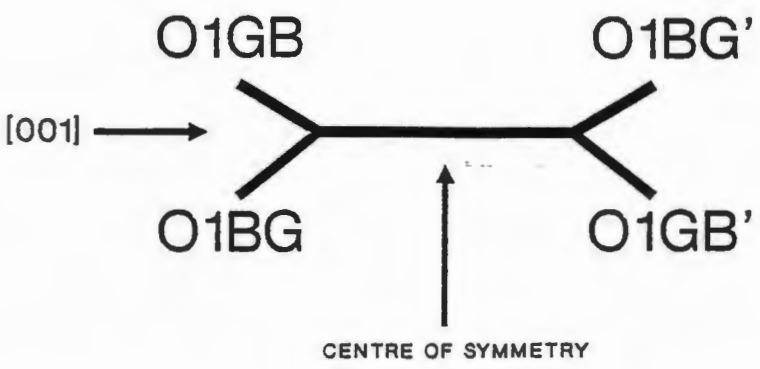

6 ENRAF-NONIUS, Structure Determination Package, "*Program Decay*"

CRYSTAL PACKING

The oxygen atoms of guest A are hydrogen bonded to the hydroxyl moieties of neighbouring host1 molecules as shown in figure 8. The second dioxane molecule, guest B, is not involved in hydrogen bonding and is held in place by van der Waals forces. 1,4-Dioxane has a similar conformation to a cyclohexane chair conformer but the presence of heteroatoms denotes that opportunity exists for hydrogen bond formation. Evidence of its hydrogen bond-forming ability was found for one guest molecule only. This is indicative of its inferior hydrogen bond-accepting ability if compared to that of ketone guests.

Figure 8

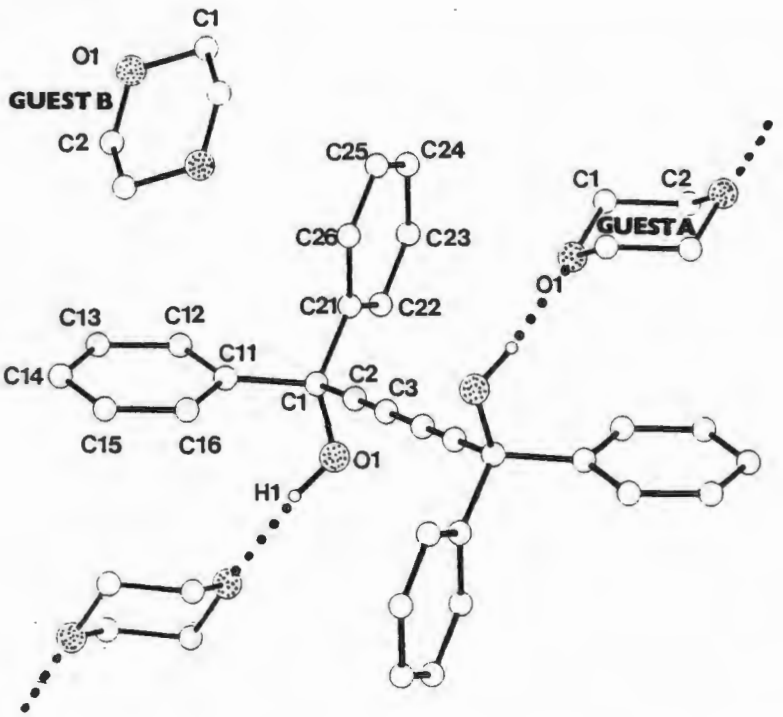

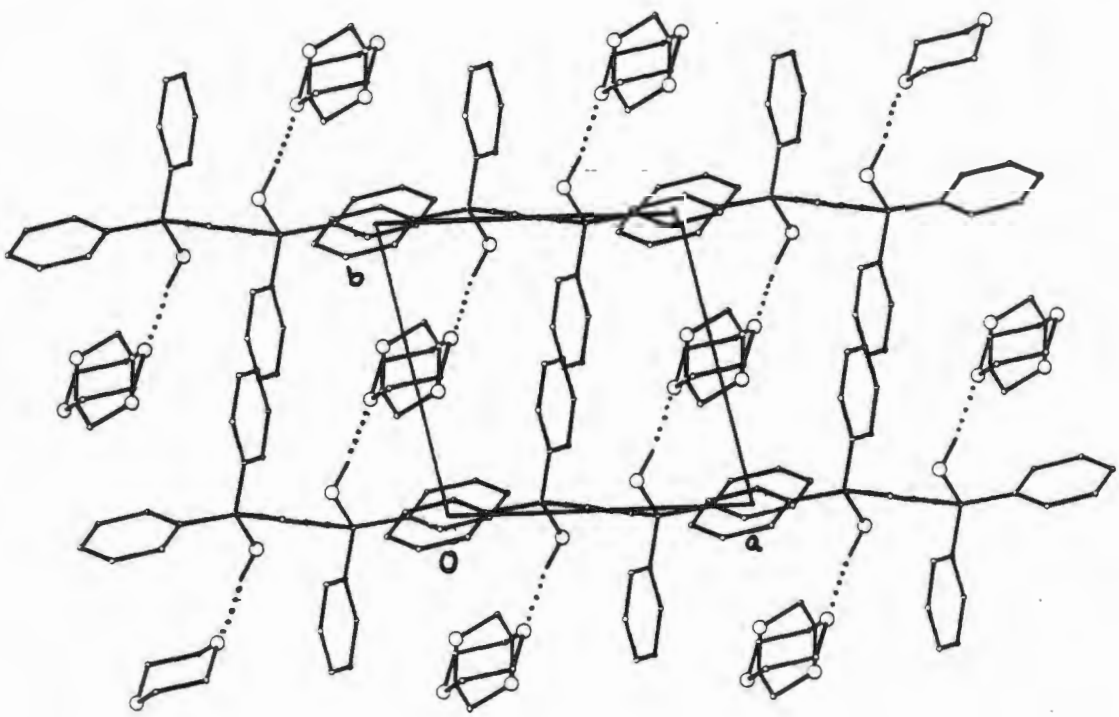

Figure 9 illustrates the crystal packing and hydrogen bonded ribbons of alternating host1 and guest molecules running parallel to [1 -1 0].

Figure 9

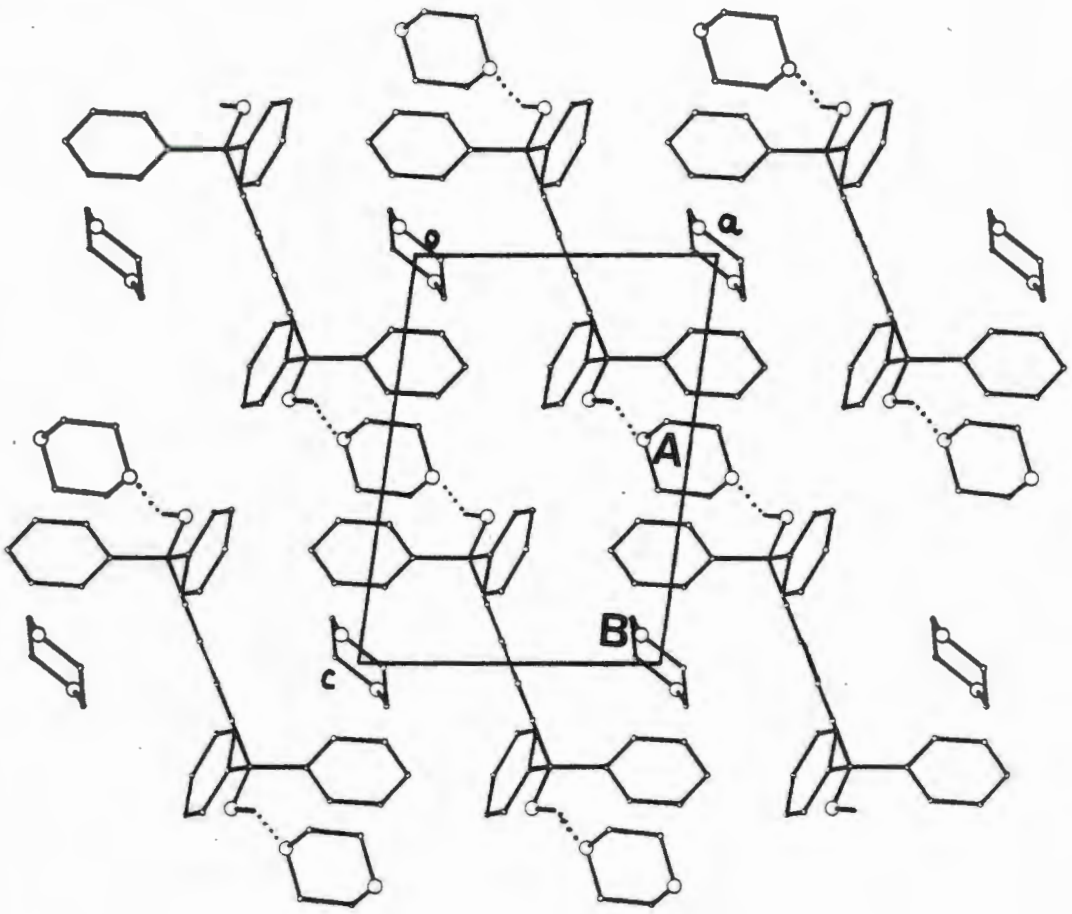

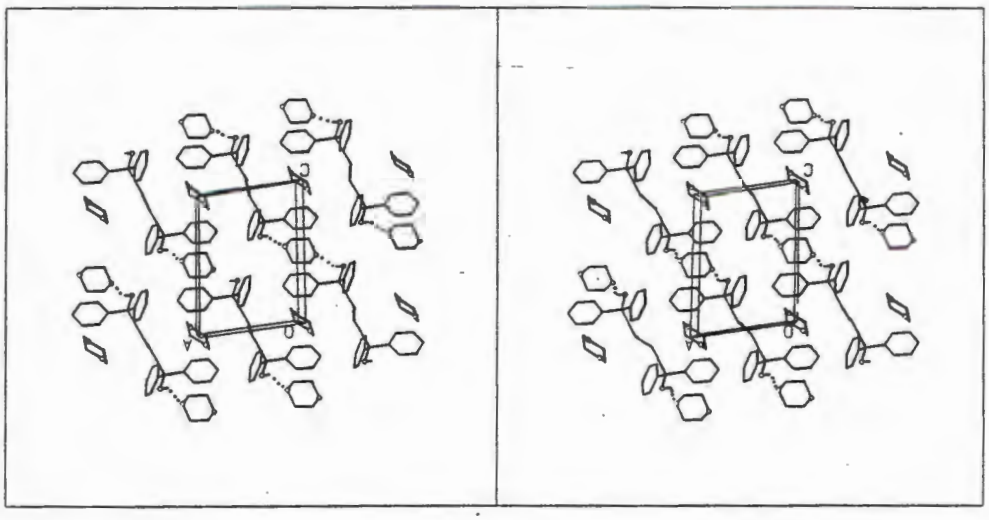

Both the dioxane molecules lie in channels running parallel to the c-axis. These channels were mapped using OPEC and are shown below.

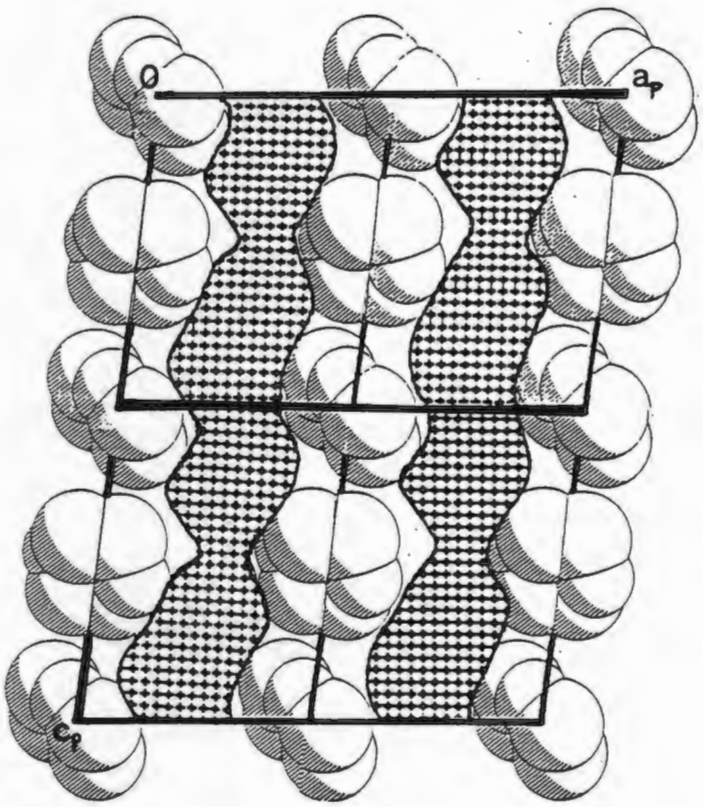

Torsion angles chosen according to the description given in chapter 3 are shown below.

	host1	host1-dioxane
C2-C1-C11-C12/C16	33(1)	21(1)
C2-C1-C21-C22/C26	-25(1)	54(1)
C5-C6-C31-C32/C36	-66(1)	/
C5-C6-C41-C42/C46	18(1)	/

TABLE 2 CRYSTAL DATA AND EXPERIMENTAL DETAILS FOR HOST1-1,4-DIOXANE STRUCTURE.

Compound	**Host1-1,4-Dioxane**
Molecular formula	$C_{30}H_{22}O_2.2C_4H_8O_2$
Molecular weight ($gmol^{-1}$)	590.72
Space group	$P\bar{1}$
a (Å)	8.337(1)
b (Å)	8.646(3)
c (Å)	11.700(3)
α (°)	108.33(3)
β (°)	94.22(2)
γ (°)	99.82(2)
Z	1
V ($Å^3$)	781.3(4)
D_c (gcm^{-3})	1.26
D_m (gcm^{-3})	1.25(2)
$\mu(MoK_\alpha)$ (cm^{-1})	0.48
F(000)	314
Data collection (21°C)	
Crystal dimensions (mm)	0.31x0.38x0.41
Range scanned θ (°)	1-25
Range of indices *h,k,l*	9, 10, +13
Reflections for lattice parameters no.,θ range (°)	24,16-17
Instability of standard reflections (%)	-35.6 (Decay correction applied)
Scan mode	(ω-2θ)
Scan width in(°)	(0.85+0.35tanθ)
Vertical aperture length (mm)	4
Aperture width (mm)	(1.12+1.05tanθ)
Number of reflections collected (unique)	2266
Number of reflections observed with $I_{rel} > 2\sigma I_{rel}$	1685
Final refinement	
Number of parameters	205
R	0.077
wR	0.088
w	$(\sigma^2(F_o)+0.001F_o^2)^{-1}$
S	2.39
Max. shift/e.s.d.	0.215
Max. height in difference electron density map ($eÅ^{-3}$)	0.51
Min. height in difference electron density map ($eÅ^{-3}$)	-0.45

THERMAL ANALYSIS

The TG and DSC traces are shown in figure 10. There is close agreement between the calculated and observed weight losses in the TG. The DSC exhibits a single endotherm implying that guest release is accompanied by dissolution of the host1 in the dioxane. This is possible in inclusion compounds in which the guest-to-host ratio is high and where the guest has a relatively high boiling point.

H:G	%WGHT LOSS EXPTL	% WGHT LOSS CALC	T_{ON}	T_{ON}-T_B	ΔH ($kJmol^{-1}$)	U_{min} ($kJmol^{-1}$)	PF
1:2	29.8	30.0	123	22	70.3	-93.2	17.76

Activation energies were calculated from a series of logβ versus the inverse of absolute temperature plots. Values ranged from 42.1 to 46.3$kJmol^{-1}$.

Figure 10

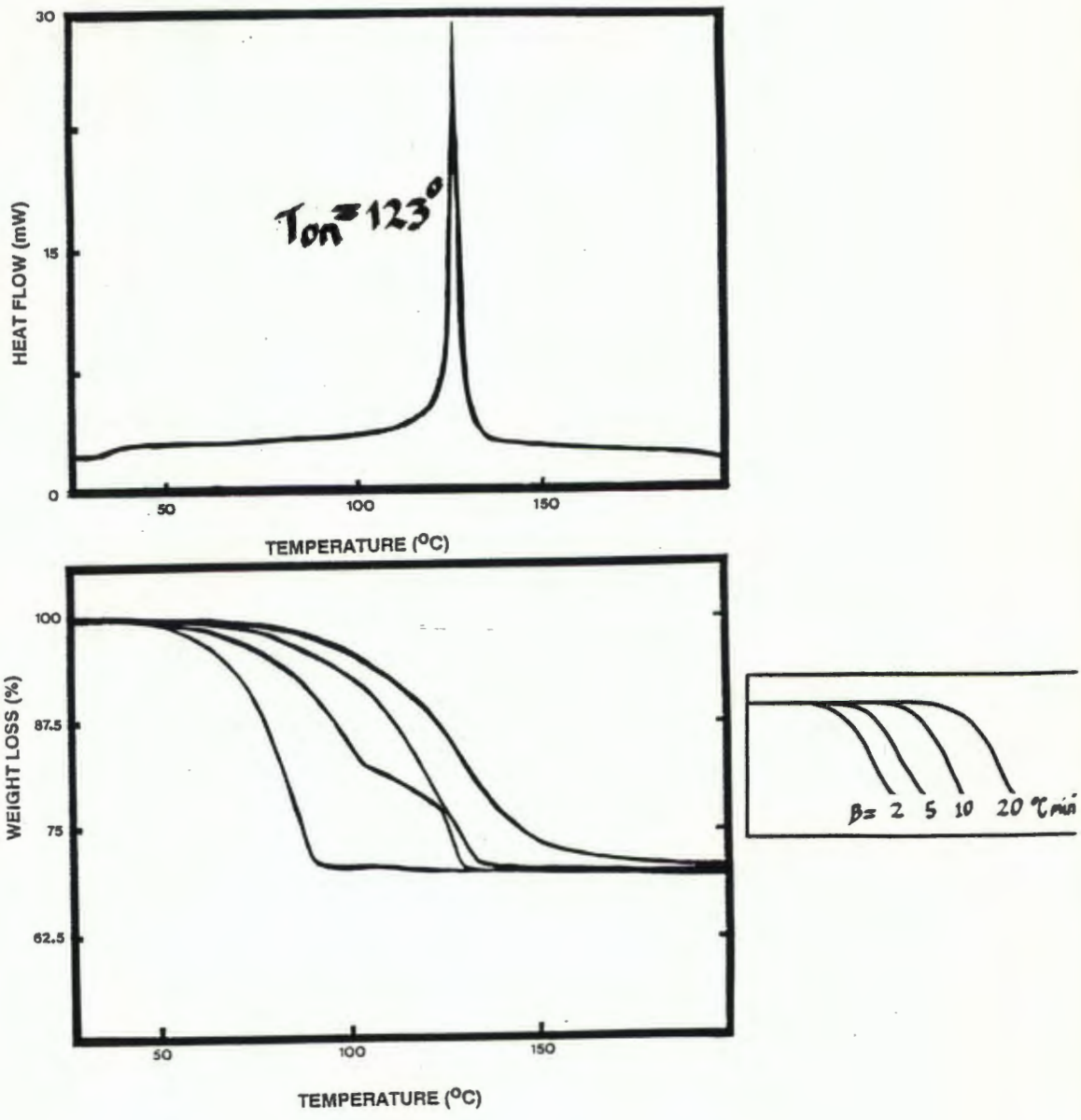

ENCAPSULATION OF XYLENES BY HOST1 - THEIR STRUCTURES

The inclusion behaviour of host1 indicated polarity not to be a requisite feature of a possible guest. A study was therefore initiated to examine the ability of host1 to capture apolar π-donors using xylenes as guest molecules.

EXPERIMENTAL

Crystals of host1-xylene were obtained by evaporating concentrated solutions of the host1 compound in a xylene. X-ray analysis and TG results showed that the host1 molecule was able to encapsulate xylene molecules as guests in a 4:3 host-guest ratio. Oscillation and Weissenberg photographs contained no evidence of symmetry other than $\bar{1}$. Direct methods performed successful structure solution on host1-o-xylene, host1-m-xylene and host1-p-xylene crystals. Mean $|E^2-1|$ statistics indicated that the space group was $P\bar{1}$ and not P1. The asymmetric unit contained two host molecules which in each case were located in general positions. Two guest molecules are in general positions and one is located on a centre of inversion: host1-o-xylene at Wyckoff *a*, host1-m-xylene at Wyckoff *b*, and host1-p-xylene at Wyckoff *c*.
Refinement was performed using blocked matrix least squares analysis owing to the large number of parameters. Details of the intensity data collections and crystal parameters may be found in Table 3. The absence of a hydrogen bond-accepting atom in these guest molecules resulted in self-association between host1 molecules with the creation of channels in which xylene molecules were located.
The host1-o-xylene and host1-m-xylene structures have almost identical cell parameters and as such are isomorphous. The host1-p-xylene structure only differs in the value of its α angle. The three structures were refined using different choices of origin but their mode of packing is the same, there is alignment of the molecular axes and clustering of the host phenyl rings to permit intermolecular host hydrogen bonding. The host1-p-xylene compound has skewed in one angle probably due to favourable packing and energy considerations.

DISCUSSION OF STRUCTURES

A schematic diagram illustrating the intermolecular hydrogen bonding between the two host molecules in asymmetric unit is shown below.

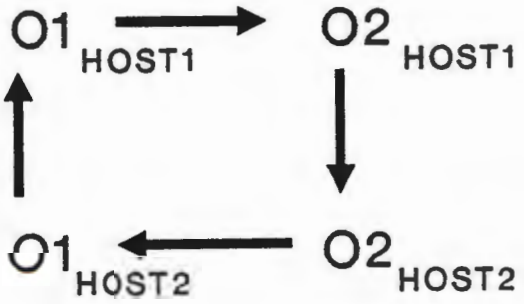

TABLE 3 CRYSTAL DATA AND EXPERIMENTAL DETAILS FOR HOST1-XYLENE COMPOUNDS

Compound	Host1-o-Xylene	Host1-m-Xylene	Host1-p-Xylene
Molecular formula	$2C_{30}H_{22}O_2.1½C_8H_{10}$	$2C_{30}H_{22}O_2.1½C_8H_{10}$	$2C_{30}H_{22}O_2.1½C_8H_{10}$
Molecular weight ($gmol^{-1}$)	1976.5	1976.5	1976.5
Space group	$P\bar{1}$	$P\bar{1}$	$P\bar{1}$
a (Å)	13.185(3)	13.267(5)	13.070(2)
b (Å)	15.466(3)	15.453(3)	15.348(3)
c (Å)	16.573(2)	16.654(5)	16.776(3)
α (°)	96.39(13)	97.12(2)	67.88(2)
β (°)	106.96(15)	107.09(30)	74.27(1)
γ (°)	114.94(18)	114.68(3)	65.29(1)
Z	2	2	1
V ($Å^3$)	2822(2)	2843(2)	2817(1)
D_c (gcm^{-3})	1.16	1.15	1.17
D_m (gcm^{-3})	1.15(1)	1.16(1)	1.16(1)
$\mu(MoK_\alpha)$ (cm^{-1})	0.33	0.33	0.33
F(000)	1046	1046	1046
Data collection (21°C)			
Crystal dimensions (mm)	0.31x0.31x0.34	0.31x0.34x0.44	0.47x0.47x0.50
Range scanned θ (°)	1-23	1-23	1-23
Range of indices *h,k,l*	±14,±17,+18	±14,±17,+18	±14,±16,+18
Reflections for lattice parameters no.,θ range (°)	24,15-17	24,15-17	24,16-17
Instability of standard reflections (%)	-1.1	16.1 (Decay correction applied)	21.1
Scan mode	(ω-2θ)	(ω-2θ)	(ω-2θ)
Scan width in(°)	(0.85+0.35tanθ)	(0.85+0.35tanθ)	(0.85+0.35tanθ)
Vertical aperture length (mm)	4	4	4
Aperture width (mm)	(1.12+1.05tanθ)	(1.12+1.05tanθ)	(1.12+1.05tanθ)
Number of reflections collected (unique)	6152	6505	6711
Number of reflections observed with $I_{rel}>2\sigma I_{rel}$	4060	4638	5249
Final refinement			
Number of parameters	600	596	711
R	0.075	0.083	0.050
wR	0.082	0.104	0.056
w	$(\sigma^2(F_o)+0.001F_o^2)$	$(\sigma^2(F_o)+0.05F_o^2)$	$(\sigma^2(F_o)+0.005F_o^2)$
S	3.82	1.09	0.90
Max. shift/e.s.d.	0.34	0.68	0.03
Max. height in difference electron density map ($eÅ^{-3}$)	0.55	0.63	0.21
Min. height in difference electron density map ($eÅ^{-3}$)	-0.29	-0.35	-0.30

The hydrogen bonding schemes are illustrated in figures 11(i), 11(ii) and 11(iii).

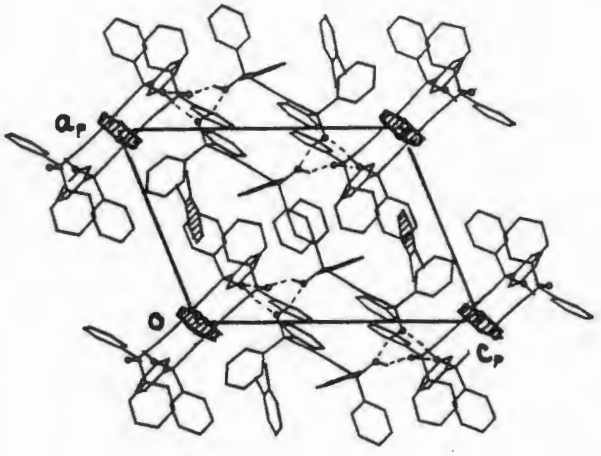

11(i)
Host1 & o-xylene

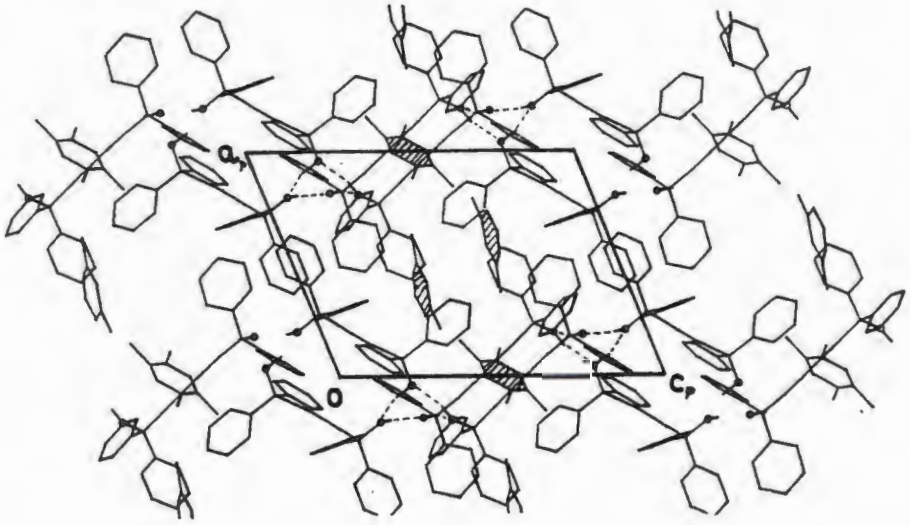

11(ii)
Host1 & m-xylene

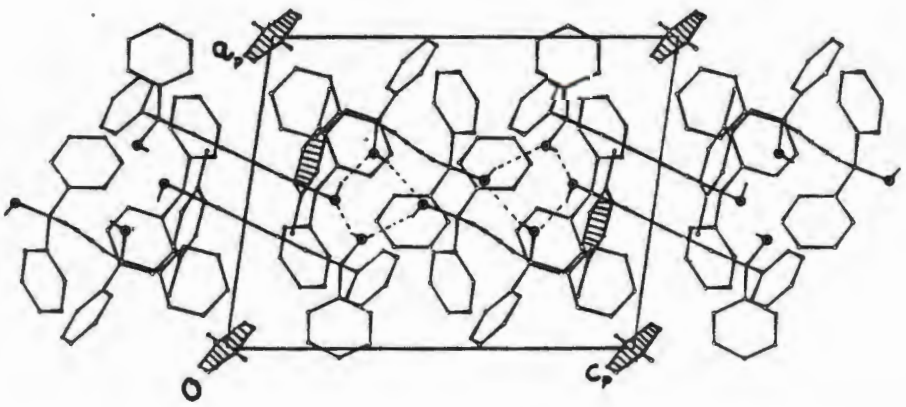

11(iii)
Host1 & p-xylene

Discussion

Host1-p-xylene: there was no disorder observed in guest atoms although their temperature factors were consistently higher than those of the aromatic carbon atoms in the host1 molecule.

Host1-o-xylene and Host1-m-xylene: Difference electron density maps were contoured to determine the location of the atoms of the ortho- and meta-xylenes. The positions were assigned on centres of symmetry. Since these xylene isomers are not centrosymmetric disorder was invoked. The model for refinement consisted of a regular hexagon of carbon atoms with methyl carbons having site occupancy factors of 0.50 to account for two carbon atoms **(7)**.
viz.

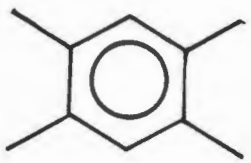

The oxygen-to-oxygen hydrogen bonding distances with their corresponding symmetry operations in parentheses are shown below.

	host1-o-xylene (Å)	host1-m-xylene (Å)	host1-p-xylene (Å)
$O1_{host1}$-->$O2_{host1}$	2.710(6)(-x,-y+1,-z)	2.708(5)(-x,-y+1,-z+1)	2.734(2)(-x,-y,-z)
$O1_{host1}$-->$O2_{host2}$	2.716(6)(-x,-y+1,-z+1)	2.725(6)(-x,-y,-z)	2.698(3)(-x+1,-y+2,-z)
$O1_{host2}$-->$O2_{host2}$	2.688(5)(-x,-y+1,-z+1)	2.689(5)(-x,-y+1,-z+2)	2.687(2)(-x+1,-y+2,-z-1)
$O1_{host2}$-->$O2_{host1}$	2.723(6)(-x,-y+1,-z)	2.728(5)(-x,-y+1,-z+2)	2.720(2)(-x+1,-y+2,-z-1)

Four hydroxyl moieties of four host1 molecules are involved in hydrogen bonding and the lipophilic bulky phenyl groups of the host are clustered together. This orientates the long axes so that a channel is formed around the apolar guests. The xylene molecules occupy these extramolecular channels in the lattice interacting weakly through dispersion forces with the surrounding molecules of the host **(8)**. The channels, which run parallel to [1 0 0], are shown in stereoscopic packing diagrams viewed along [1 0 0] in figures 12, 13 and 14.

---

7 MH Moore, LR Nassimbeni, ML Niven & MW Taylor, *Inorg.Chim.Acta*, 115, 1986, 211-217

8 E Weber, W Seichter, I Goldberg, G Will & HJ Dasting, *J.Incln Phenomena*, 10, 1991, 267-282

Figure 12

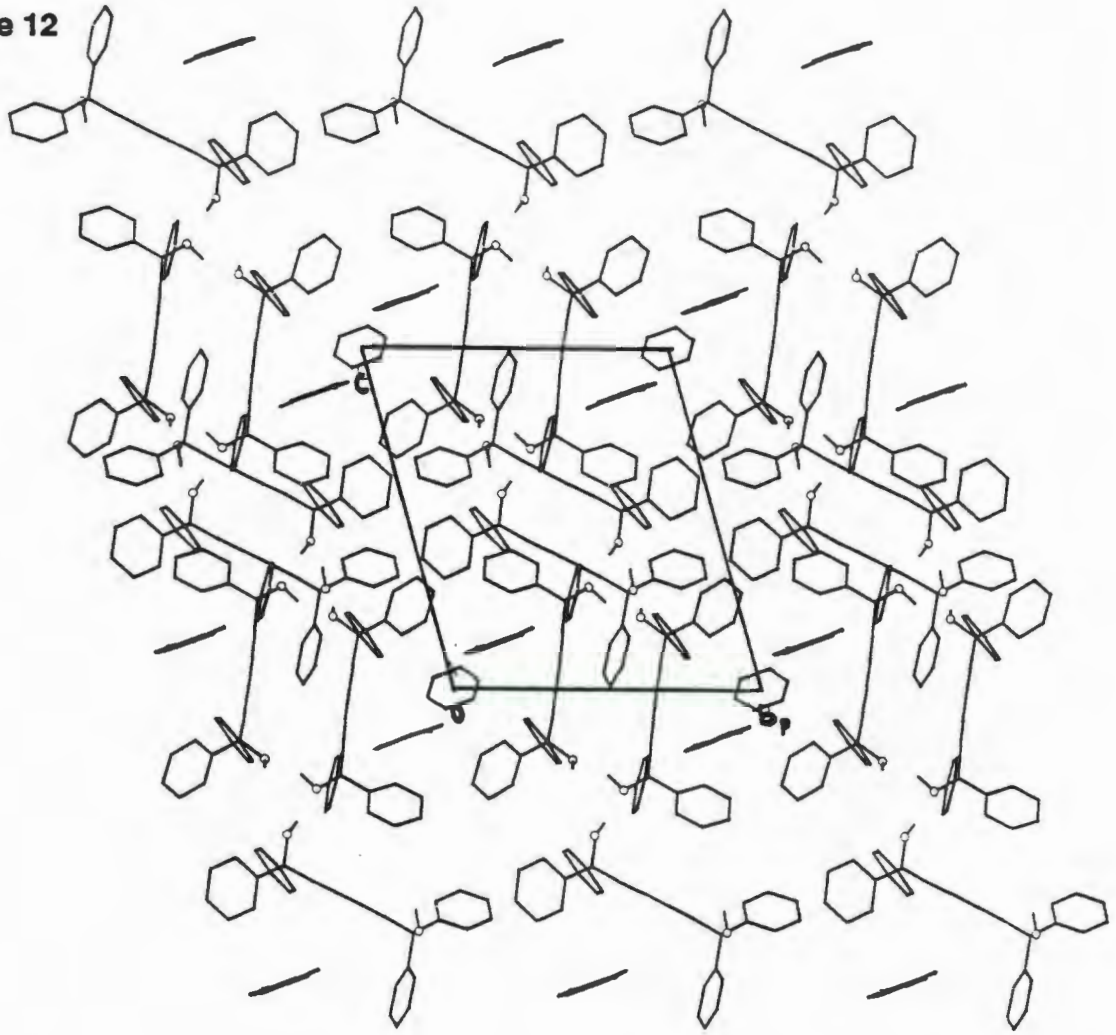

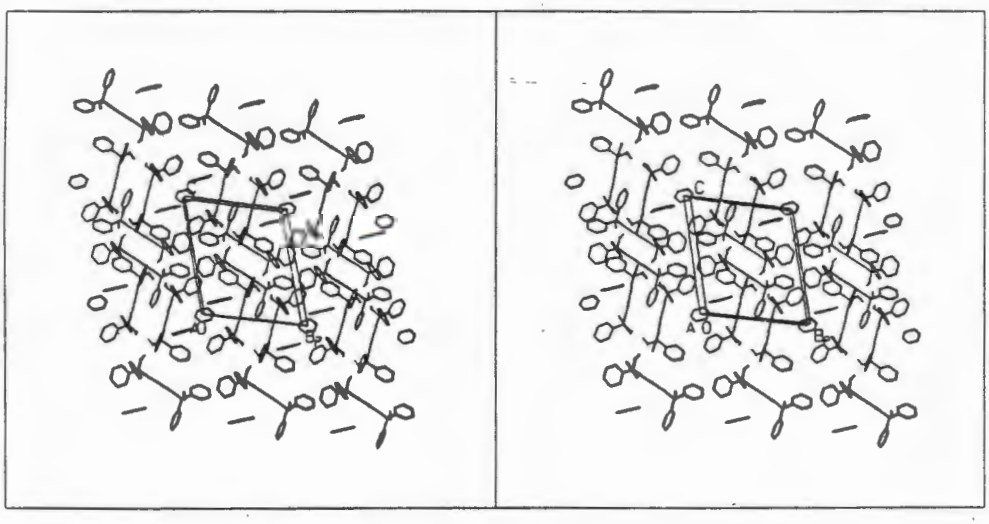

Figure 13

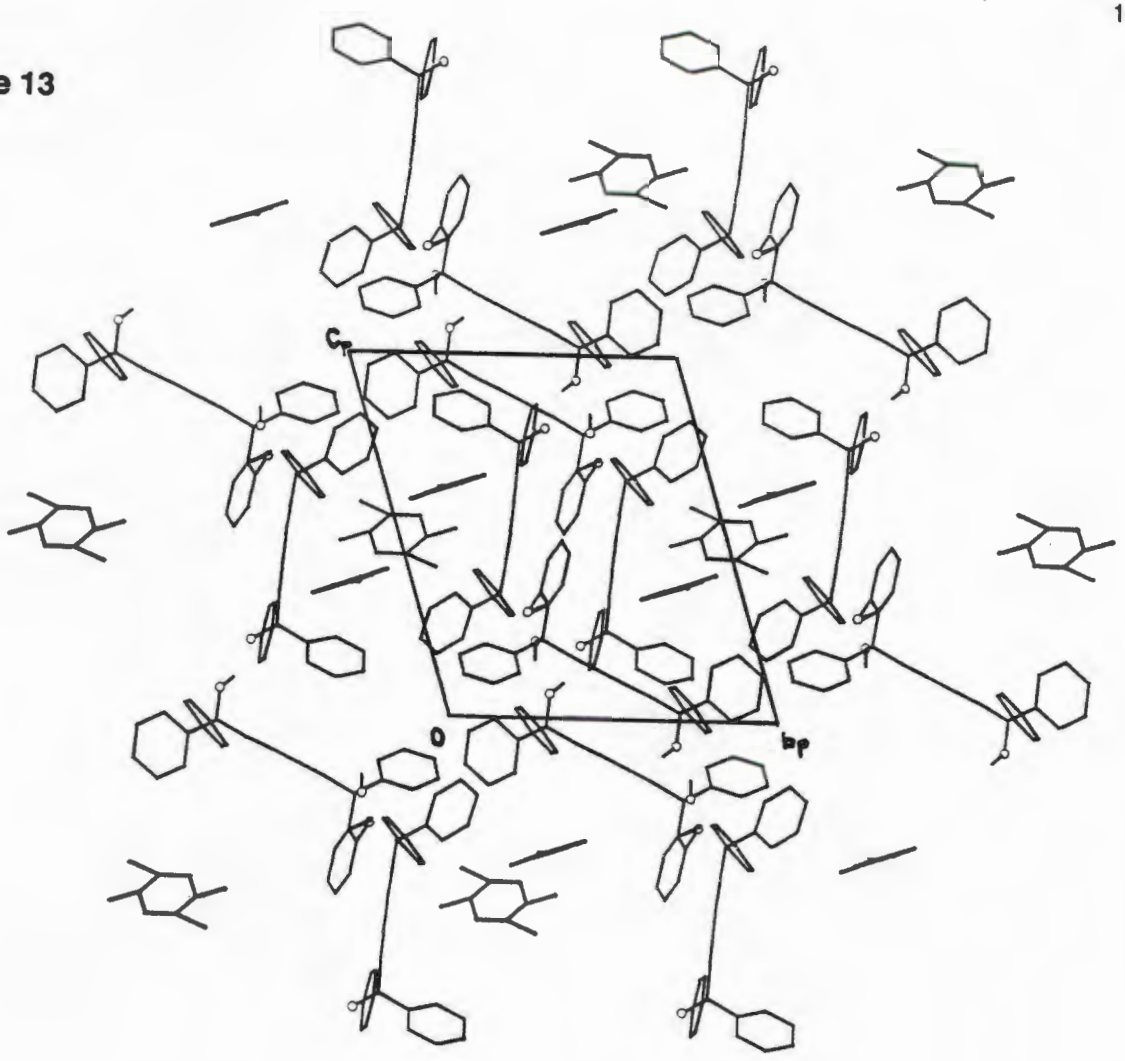

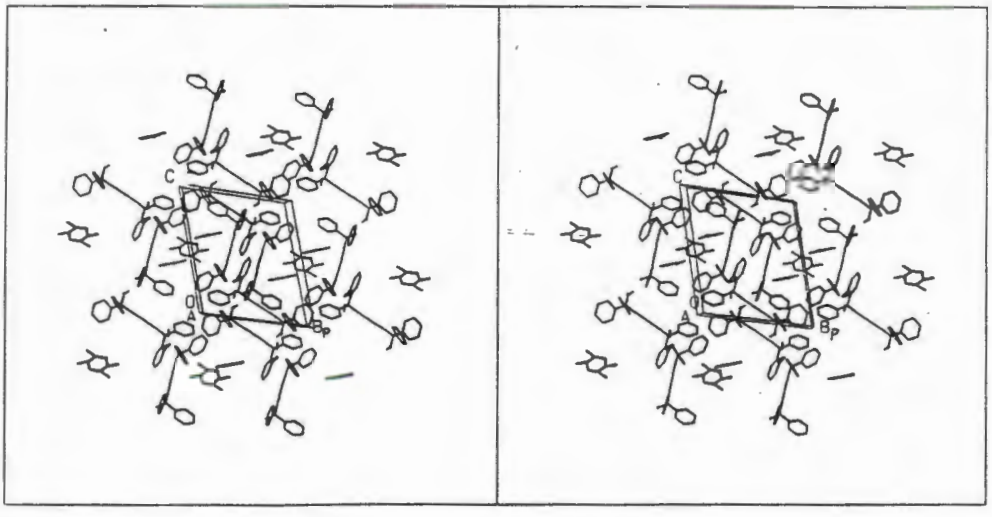

Figure 14

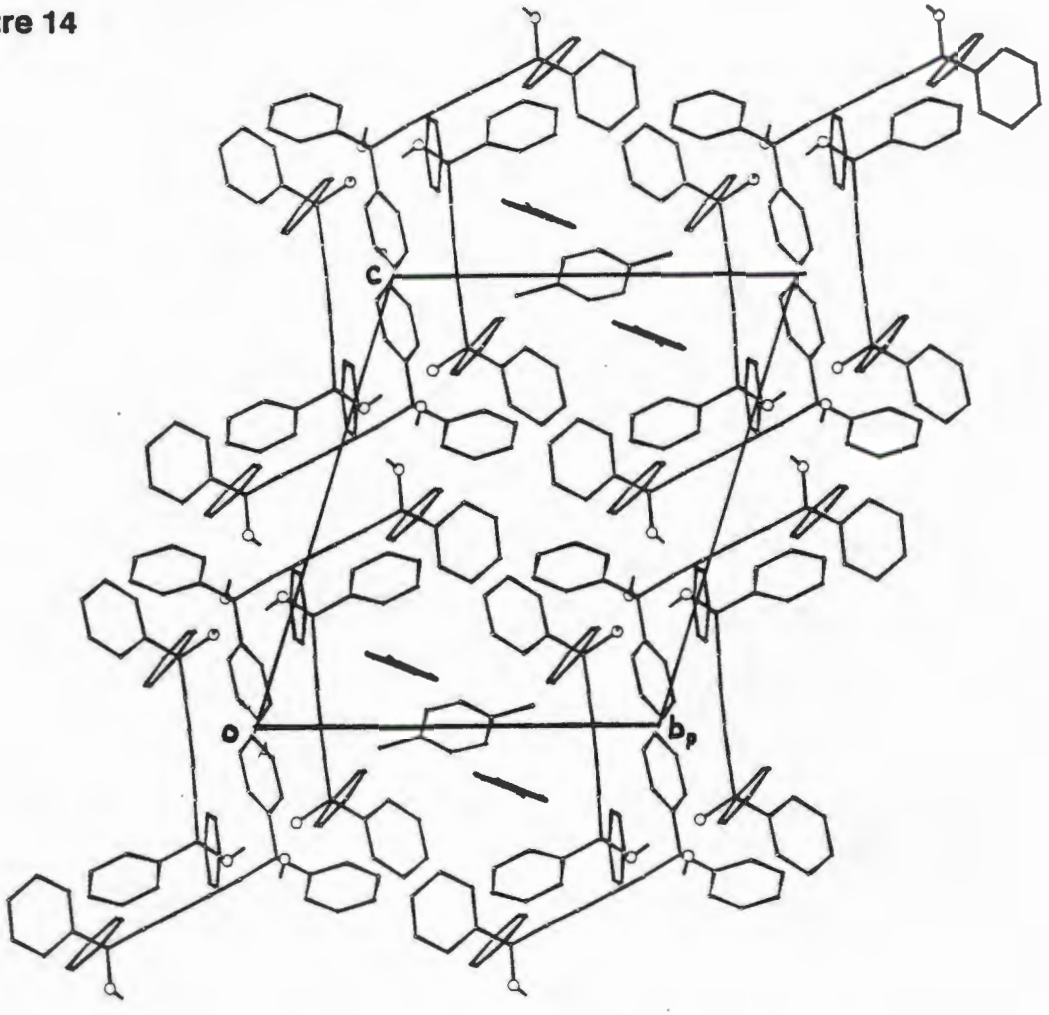

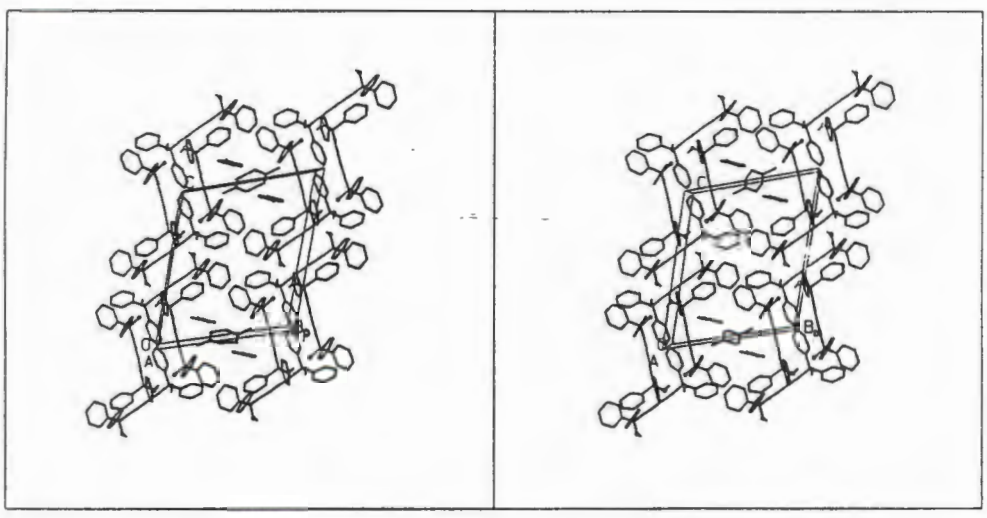

CRYSTAL PACKING

Concave sites created by the molecular axis of host1 molecules are occupied by guests which are trapped as molecules of crystallization in the lattice **(9)**. In order to compare the packing modes of these three isomorphous compounds, packing densities expressed as volume per non-hydrogen atom and occupied volumes, were calculated. If we assume that the volume occupied by one host molecule in the α-phase host1 unit cell ($V_{\alpha/2}$) remains approximately constant in a host-guest structure, then the volume (V_{β}-$V_{\alpha/2}$) can be evaluated. This indicates the volume each guest molecule occupies in the unit cell.

According to the packing factors, the host1-p-xylene structure with the lowest PF value, is the most efficiently packed and has the smallest volume occupied by a guest, ie it exhibits the most complementary van der Waals packing of host and guest constituents. The m-xylene and o-xylene structures are less tightly packed (ie higher PF's) and their guests occupy larger volumes in the host-guest lattice **(10)**. This is as expected, because disorder had to be invoked for some of the guest molecules in the o-xylene and m-xylene structures. Formation of the more stable clathrates appeared to be related to a better steric fit and thus more restricted thermal motion **(11)**.

COMPOUND	Vol. Cell ($Å^3$)	Vβ ($Å^3$)	Vβ-Vα/2 ($Å^3$)	PF ($Å^3$/non-hydrogen atom)
Host1	1110.18		/	17.35
Host1-o-Xylene	2822.25	705.56	150.47	18.57
Host1-m-Xylene	2843.57	710.89	155.80	18.71
Host1-p-Xylene	2816.75	704.19	149.10	18.53

CONFORMATION OF HOST1 MOLECULES

Torsion angles which have been previously defined are as follows:

		H1-o-xylene		H1-m-xylene		H1-p-xylene	
		A	B	A	B	A	B
C2-C1-C21-C12/C16	T_1	5	-18	-9	17	47	-14
C2-C1-C11-C22/C26	T_2	47	44	74	-42	-2	43
C5-C6-C31-C32/C36	T_3	10	16	-8	-17	-74	76
C5-C6-C41-C42/C46	T_4	-67	86	-50	-83	3	17

9 H Hart, L-T W Lin & I Goldberg, *J.Incln.Phenomena*, 2, 1984, 377-389

10 MH Moore, LR Nassimbeni, ML Niven & MW Taylor, *Inorg.Chim.Acta*, 115, 1986, 211-217

11 JL Atwood, JED Davies & DD MacNicol, "*Inclusion Compounds*", Vol 4, 408

* Where A and B refer to the two crystallographically distinct host1 molecules in the asymmetric unit.

Figure 15 represents the torsion angles in bar graph form. The abscissa describes which host molecule in the asymmetric unit, either A or B, as well as which torsion angle is being referred to. Since these compounds are isostructural the similar patterns observed for the three inclusion compounds are to be expected.

Figure 15

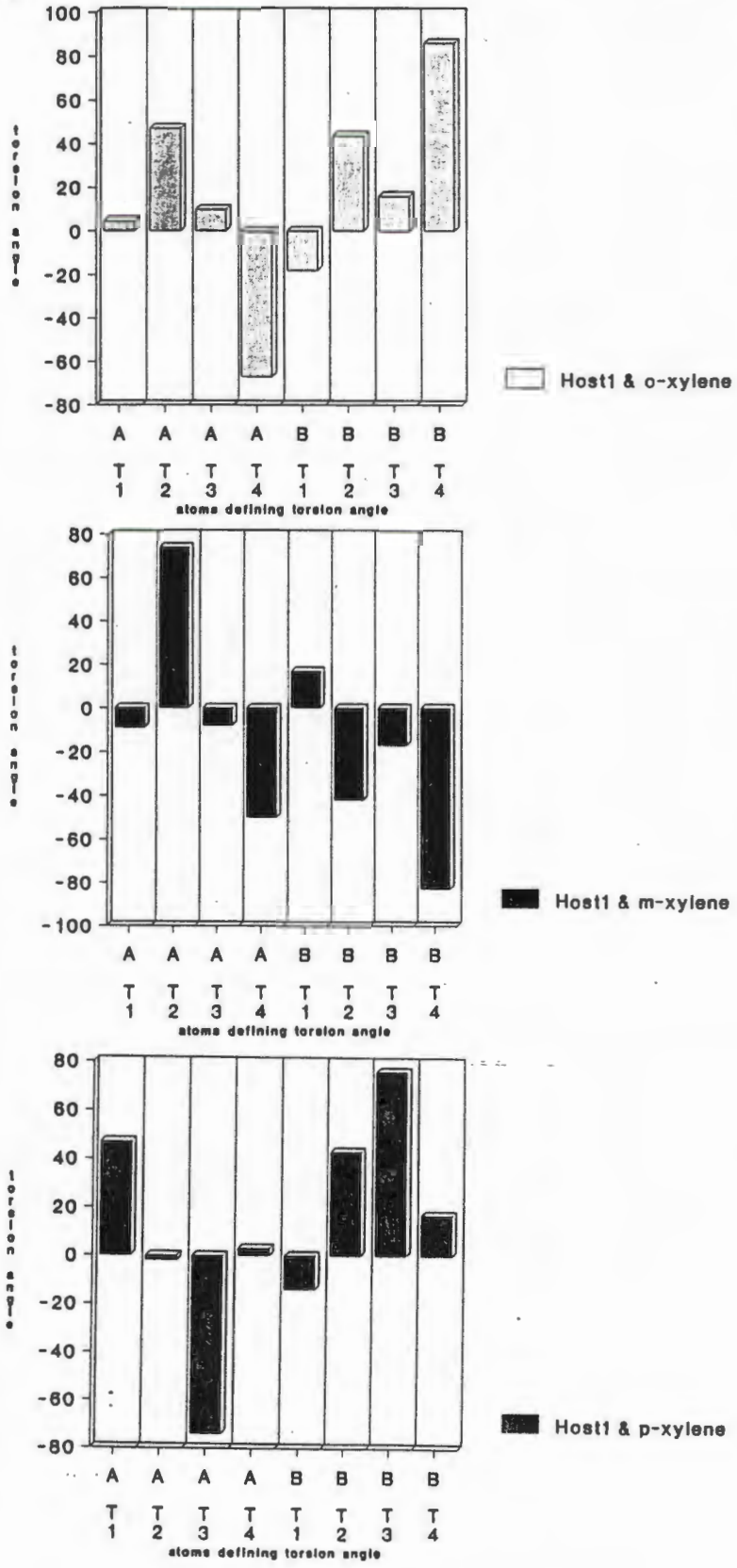

These host1-xylene complexes are host-host coordination assisted inclusion compounds in which the guest molecules are enclathrated and held solely by van der Waals forces. A perspective looking along the molecular backbone of the host1 molecule in these complexes, reveals the gauche character of the host1 hydroxy groups. This is shown in figure 16.

Figure 16

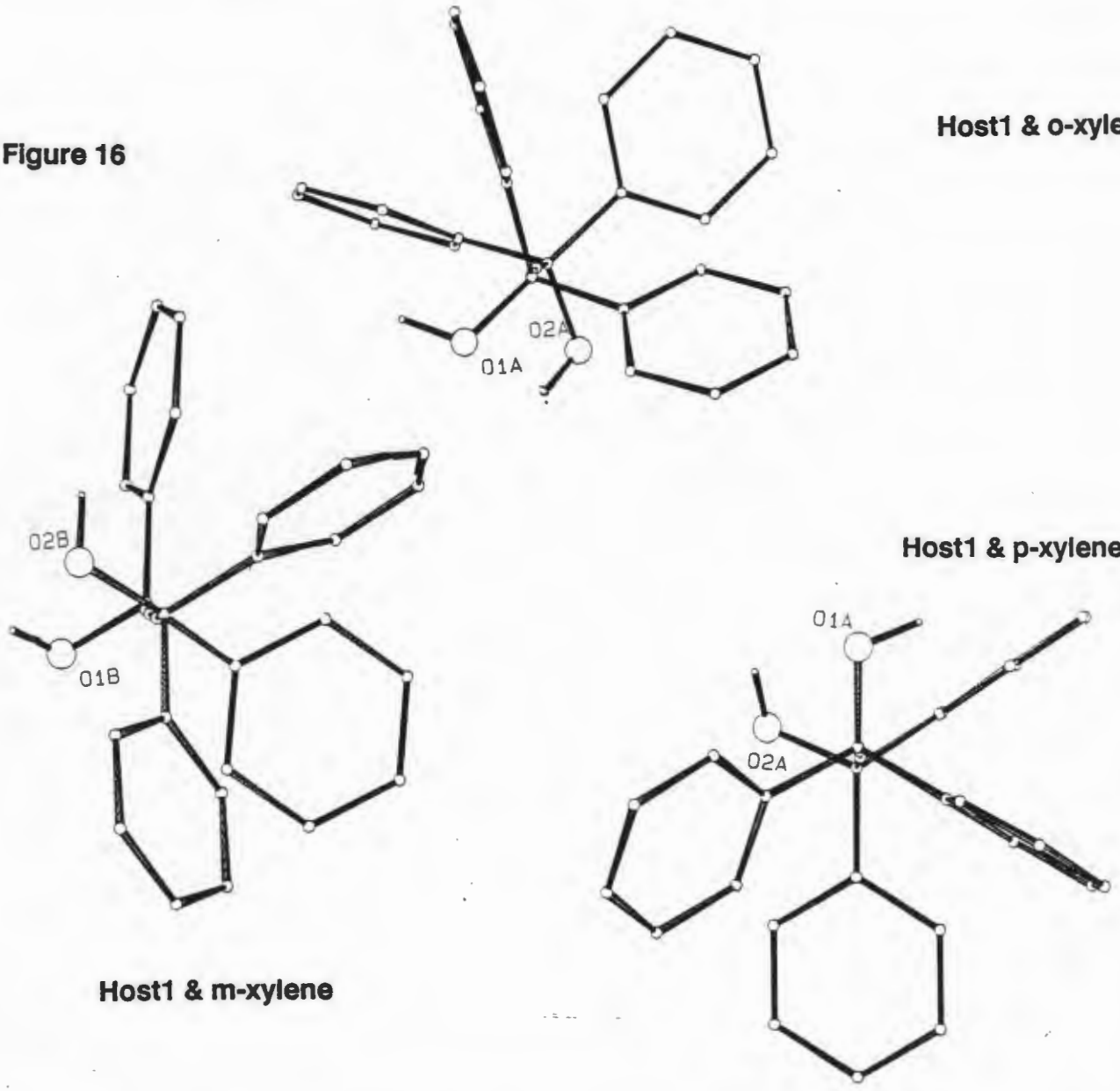

This had also been observed in the case of the host1-cylclohexane compound, in which host-host interaction was the dominant bonding feature. Therefore, the implication is that host1 molecules, in order to form stable host-guest compounds with apolar guests, hydrogen bond to other host1 molecules. In doing this, a host1 molecule is forced to adopt a conformation which is predominantly gauche in character.

THERMAL ANALYSIS

The thermal analysis traces of the host1-xylene compounds may be found in figures 17i, ii and iii. Thermal data is reported in Table 4. The experimental loss of guest from TG correlated stoicheiometrically with the calculated values. Each DSC trace has three endotherms, A, B and C. A corresponds to the desorption of a xylene with recrystallization of α-form host. Endotherm B is pre-melting of host1 due to some lattice rearrangement of host1 which is followed by peak C at the usual melting point.

The difference between the onset temperature and boiling point can again be used as an indication of how firmly the guest is held in the β crystal lattice. This difference indicates greatest stability in the case of the **Host-p-xylene** structure in which there is no guest disorder and the shape of the p-xylene molecule resulted in most efficient packing. The values obtained for $\Delta H(kJmol^{-1})$ from the DSC scans and activation energies from plots of $\log\beta$ versus the inverse of absolute temperature are of the same order for the three compounds with the **Host-p-xylene** having the highest ΔH value. The vapour pressures of the three xylenes are very similar and it would seem that the stability of such a host-guest lattice is governed principally by factors such as the shape and symmetry of the guest entity itself **(12)**.

---

12 F Toda, K Tanaka, Y Wang & G Lee, *Chem.Lett.*, 1986, 109-112

Host1-o-xylene

17(i)

Host1-m-xylene

17(ii)

Host1-p-xylene

17(iii)

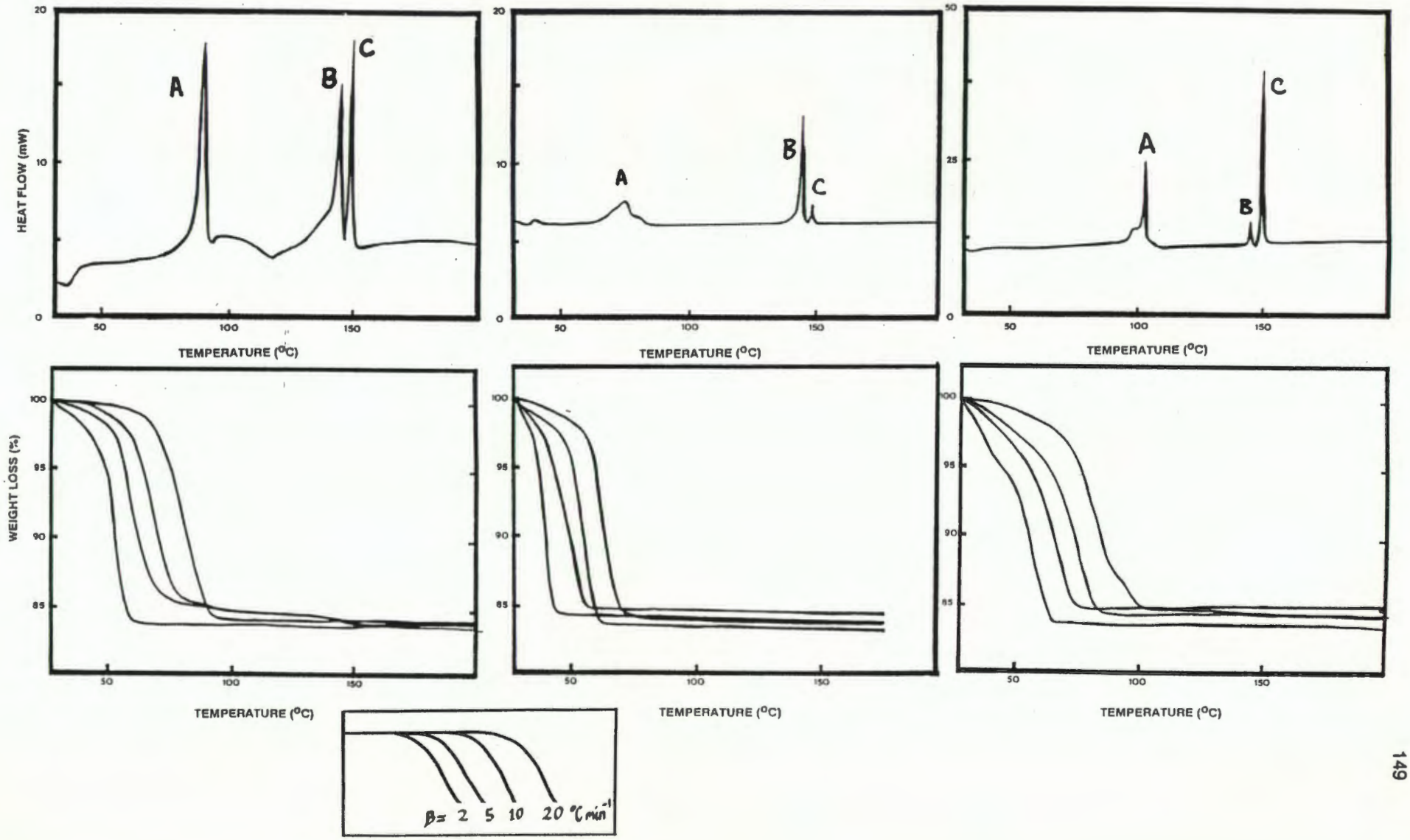

TABLE 4

	Host1 & o-xylene	Host1 & m-xylene	Host1 & p-xylene
H:G	4:3	4:3	4:3
TGA %loss (exptl.)	16.3	16.1	15.6
TGA %loss (calc.)	16.1	16.1	16.1
E_a ($kJmol^{-1}$)	71-78	68-69	62-74
ΔH ($kJmol^{-1}$)	83.1	114.5	92.2
T_b(^oC) **(13)**	144.0	139.3	137.5
T_{on}(^oC)	87.1	66.8	102.0
T_{on}-T_b(^oC)	-56.9	-72.5	-35.5

The % weight losses obtained from TG runs agree well with the calculated values thus confirming the host-guest ratios of 4:3. The slopes calculated from plots of logβ versus the inverse of absolute temperature yield values of activation energies which are approximately the same for the decomposition of the three host1-xylene compounds. This implies that the host-guest compounds have similar thermal stabilities. Although the host1-p-xylene compound would have been expected to exhibit the highest thermal stability, this cannot be deduced from the results because the energy differences are too close together for sensible distinction between them. The enthalpies corresponding to desorption of the xylene are similar but once again there is no definite trend observed. Disappointing though these results might appear with respect to fingerprinting the orders of thermal stabilities for these isomers, they indicated the values of energy to be expected. Further detailed work would be required in order to unambiguously define the thermal decompositions for these isomers.

---

13 CRC Handbook, *op. cit.*

ATOMIC COORDINATES

Table 5

$U_{eq} = (1/3)\Sigma\Sigma U_{ij} a_i a_i^* a_i \cdot a_j$

Fractional atomic coordinates ($x10^4$) and thermal parameters ($Å^2 x10^3$) with e.s.d.'s in parentheses for the Host1-Cyclohexane structure.

Atom	x/a	y/b	z/c	Uequiv/Uiso(*)
O(1)	4896(2)	1793(3)	6419(2)	53(2)
H(1)	4569(21)	1465(43)	6545(40)	81(16)*
O(2)	4201(2)	-1004(3)	2292(2)	55(2)
H(2)	4460(25)	-1247(49)	2814(21)	81(16)*
C(1)	4687(3)	2388(4)	5705(3)	47(2)
C(2)	4496(3)	1760(5)	4960(4)	56(3)
C(3)	4328(3)	1261(5)	4366(4)	55(3)
C(4)	4125(3)	696(5)	3674(4)	57(3)
C(5)	3935(3)	211(5)	3065(4)	57(3)
C(6)	3714(3)	-392(5)	2335(3)	51(2)
C(11)	5242(3)	2996(5)	5705(4)	56(3)
C(12)	5787(5)	2960(9)	6256(8)	156(7)
C(13)	6268(5)	3514(12)	6242(8)	193(8)
C(14)	6221(5)	4168(7)	5700(8)	105(5)
C(15)	5696(7)	4200(13)	5072(13)	259(13)
C(16)	5213(6)	3608(14)	5101(13)	277(12)
C(21)	4154(3)	3010(4)	5752(3)	47(2)
C(22)	4204(4)	3499(6)	6469(5)	84(4)
C(23)	3736(4)	4068(6)	6529(6)	95(4)
C(24)	3206(4)	4189(6)	5862(6)	85(4)
C(25)	3152(4)	3731(7)	5181(5)	87(4)
C(26)	3614(3)	3131(6)	5103(4)	76(3)
C(31)	3542(3)	234(5)	1552(4)	59(2)
C(32)	3963(5)	357(6)	1124(5)	101(5)
C(33)	3819(6)	944(8)	436(7)	131(6)
C(34)	3273(6)	1377(8)	171(6)	121(6)
C(35)	2857(5)	1287(7)	609(7)	110(5)
C(36)	2986(4)	697(6)	1287(5)	85(4)
C(41)	3166(3)	-1003(5)	2359(4)	54(3)
C(42)	2805(4)	-758(6)	2841(5)	83(4)
C(43)	2302(4)	-1319(8)	2823(6)	112(5)
C(44)	2164(4)	-2133(7)	2379(6)	92(4)
C(45)	2524(4)	-2371(6)	1879(5)	88(4)
C(46)	3014(3)	-1813(5)	1882(4)	67(3)
C(1G)	5000(0)	2136(15)	2500(0)	179(8)
C(2G)	5604(8)	2707(13)	2910(13)	133(8)
C(21G)	5547(10)	2707(13)	2383(15)	203(14)
C(3G)	5547(10)	3556(18)	2383(15)	197(13)
C(31G)	5604(8)	3556(18)	2910(13)	225(16)
C(4G)	5000(0)	4202(19)	2500(0)	250(13)

Table 6

Fractional atomic coordinates ($x10^4$) and Thermal Parameters ($Å^2x10^3$) with e.s.d.'s in parentheses for the Host1-1,4-Dioxane structure

Atom	x/a	y/b	z/c	Uequiv/Uiso(*)
C(1)	3159(4)	10307(5)	7447(4)	40(2)
O(1)	3560(3)	9096(4)	6432(3)	51(1)
H(1)	2839(54)	8034(42)	6287(46)	79(16)*
C(2)	3968(5)	10184(5)	8577(4)	46(2)
C(3)	4625(5)	10066(6)	9485(4)	49(2)
C(11)	1279(4)	10020(5)	7434(4)	39(1)
C(12)	336(5)	10481(6)	6621(4)	54(2)
C(13)	-1366(5)	10134(6)	6533(5)	61(2)
C(14)	-2133(5)	9339(6)	7244(5)	59(2)
C(15)	-1205(6)	8871(7)	8049(5)	67(2)
C(16)	490(5)	9203(6)	8138(5)	56(2)
C(21)	3847(5)	12027(5)	7368(4)	42(2)
C(22)	4490(5)	12185(6)	6342(4)	54(2)
C(23)	5044(6)	13739(8)	6269(6)	74(3)
C(24)	5008(7)	15140(8)	7228(7)	85(3)
C(25)	4375(7)	14990(7)	8262(6)	74(2)
C(26)	3811(6)	13450(6)	8329(5)	60(2)
O(1AG)	8445(4)	14012(5)	4540(3)	76(2)
C(1AG)	9119(8)	15298(10)	4072(7)	117(4)
C(2AG)	10863(8)	15628(10)	4229(6)	110(4)
O(1GB)	316(20)	15509(20)	8985(16)	99(1)
O(1BG)	-877(8)	15894(8)	9474(6)	99(1)
C(1GB)	847(11)	16564(9)	10139(8)	113(4)
C(2GB)	-1111(10)	14256(9)	8938(6)	109(4)

Table 7

Fractional atomic coordinates ($x10^4$) and thermal parameters ($Å^2x10^3$) with e.s.d.'s in parentheses for the Host1-o-xylene structure

Atom	x/a	y/b	z/c	Uequiv/Uiso(*)
O(1A)	1949(3)	6725(3)	2081(2)	44(2)
H(1A)	1453(51)	6873(51)	2350(41)	108(25)*
O(2A)	-1841(3)	4668(3)	-2958(2)	48(2)
H(2A)	-1895(45)	4263(31)	-2544(26)	58(16)*
C(1A)	2341(4)	7371(4)	1548(3)	39(3)
C(2A)	1401(5)	6940(4)	651(4)	45(3)
C(3A)	631(5)	6585(4)	-68(4)	45(3)
C(4A)	-234(5)	6224(4)	-907(4)	45(3)
C(5A)	-944(5)	5924(4)	-1643(4)	46(3)
C(6A)	-1767(5)	5571(4)	-2569(3)	43(3)
C(11A)	2526(3)	8390(3)	1958(2)	41(3)
C(12A)	1812(3)	8788(3)	1542(2)	61(4)
C(13A)	1985(3)	9701(3)	1960(2)	82(4)
C(14A)	2870(3)	10216(3)	2796(2)	80(5)
C(15A)	3583(3)	9818(3)	3213(2)	81(4)
C(16A)	3411(3)	8905(3)	2795(2)	73(4)
C(21A)	3513(3)	7437(3)	1524(2)	42(3)

C(22A)	4206(3)	7169(3)	2149(2)	60(4)
C(23A)	5319(3)	7297(3)	2149(2)	72(4)
C(24A)	5733(3)	7694(3)	1524(2)	74(4)
C(25A)	5044(3)	7962(3)	898(2)	74(4)
C(26A)	3932(3)	7834(3)	898(2)	59(3)
C(31A)	-3028(4)	5398(3)	-2666(2)	48(3)
C(32A)	-3270(4)	5709(3)	-1954(2)	68(4)
C(33A)	-4436(4)	5535(3)	-2067(2)	93(6)
C(34A)	-5360(4)	5050(3)	-2891(2)	94(5)
C(35A)	-5119(4)	4738(3)	-3602(2)	91(4)
C(36A)	-3953(4)	4912(3)	-3490(2)	71(4)
C(41A)	-1208(4)	6338(3)	-3035(3)	45(3)
C(42A)	-752(4)	6130(3)	-3649(3)	69(4)
C(43A)	-205(4)	6856(3)	-4038(3)	88(5)
C(44A)	-114(4)	7789(3)	-3814(3)	90(5)
C(45A)	-570(4)	7997(3)	-3200(3)	88(5)
C(46A)	-1117(4)	7271(3)	-2811(3)	68(4)
O(3B)	2044(3)	6679(3)	4286(2)	49(2)
H(3B)	2105(85)	6181(52)	3901(53)	172(39)*
O(4B)	-431(3)	3264(3)	7112(2)	43(2)
H(4B)	1014(52)	3077(57)	6515(19)	119(28)*
C(1B)	816(5)	7050(4)	5191(3)	41(3)
C(2B)	316(5)	6301(4)	5644(3)	46(3)
C(3B)	907(5)	5636(4)	5964(4)	44(3)
C(4B)	488(5)	4886(4)	6348(3)	44(3)
C(5B)	170(5)	4241(4)	6704(3)	44(3)
C(6B)	56(4)	3481(4)	7170(3)	37(3)
C(11B)	4084(4)	7230(3)	5274(2)	44(3)
C(12B)	4566(4)	7684(3)	4694(2)	65(4)
C(13B)	5713(4)	7856(3)	4746(2)	80(4)
C(14B)	6379(4)	7574(3)	5377(2)	75(4)
C(15B)	5899(4)	7120(3)	5957(2)	80(4)
C(16B)	4752(4)	6948(3)	5905(2)	61(4)
C(21B)	2859(4)	8025(3)	5544(2)	41(2)
C(22B)	2559(4)	8552(3)	4972(2)	78(4)
C(23B)	2660(4)	9467(3)	5301(2)	96(5)
C(24B)	3060(4)	9855(3)	6202(2)	71(4)
C(25B)	3360(4)	9329(3)	6775(2)	76(4)
C(26B)	3259(4)	8414(3)	6445(2)	66(4)
C(31B)	740(4)	2531(3)	6790(3)	44(3)
C(32B)	1336(4)	2479(3)	6230(3)	60(3)
C(33B)	1318(4)	1592(3)	5928(3)	79(4)
C(34B)	704(4)	757(3)	6185(3)	83(4)
C(35B)	108(4)	810(3)	6745(3)	100(6)
C(36B)	126(4)	1697(3)	7048(3)	79(5)
C(41B)	1577(3)	3944(3)	8138(3)	42(3)
C(42B)	1328(3)	4502(3)	8697(3)	60(3)
C(43B)	2114(3)	4956(3)	9570(3)	77(5)
C(44B)	3148(3)	4852(3)	9884(3)	87(4)
C(45B)	3396(3)	4294(3)	9325(3)	99(5)
C(46B)	2611(3)	3841(3)	8452(3)	74(4)
C(1X)	2766(13)	8828(12)	8796(8)	174(13)
C(1O)	2131(9)	6881(8)	8226(7)	140(7)
C(1G)	3739(12)	8623(7)	8748(5)	121(7)
C(2G)	3409(9)	7571(7)	8463(5)	98(6)
C(3G)	4231(14)	7278(12)	8398(7)	152(13)
C(4G)	5448(14)	7972(16)	8600(9)	167(12)

C(5G)	5808(12)	8994(16)	8905(9)	172(11)
C(6G)	4925(18)	9287(13)	8960(7)	158(11)
C(1Z)	-951(23)	-761(20)	266(19)	310(12)
C(2Z)	-540(16)	341(14)	599(11)	190(6)
C(3Z)	-250(15)	-768(12)	-247(10)	176(5)
C(4Z)	-1018(22)	-1570(19)	-111(16)	139(8)
C(5Z)	-1355(23)	-377(21)	863(17)	160(9)

Table 8

Fractional atomic coordinates (x10^4) and thermal parameters (Å^{2}x10^3) with e.s.d.'s in parentheses for the Host1 & m-xylene structure

Atom	x/a	y/b	z/c	Uequiv/Uiso(*)
O(1A)	1826(3)	5332(2)	7950(2)	51(2)
H(1A)	1703(44)	5572(35)	7435(20)	75(16)*
O(2A)	-1925(3)	3272(2)	2904(2)	48(2)
H(2A)	-1316(33)	3180(37)	2745(32)	72(16)*
C(1A)	1750(4)	4425(3)	7551(3)	44(2)
C(2A)	935(4)	4075(3)	6630(3)	49(2)
C(3A)	209(4)	3767(3)	5891(3)	49(2)
C(4A)	-634(4)	3411(3)	5053(3)	46(2)
C(5A)	-1390(4)	3059(3)	4316(3)	50(2)
C(6A)	-2309(4)	2621(3)	3425(3)	41(2)
C(12A)	3933(3)	5069(3)	8471(2)	73(3)
C(13A)	5094(3)	5252(3)	8581(2)	88(4)
C(14A)	5334(3)	4962(3)	7862(2)	99(4)
C(15A)	4413(3)	4489(3)	7034(2)	99(5)
C(16A)	3251(3)	4306(3)	6924(2)	68(3)
C(11A)	3010(3)	4596(3)	7641(2)	51(2)
C(22A)	1236(3)	2763(2)	7855(2)	71(3)
C(23A)	708(3)	2041(2)	8243(2)	94(4)
C(24A)	151(3)	2214(2)	8789(2)	102(4)
C(25A)	122(3)	3109(2)	8947(2)	95(4)
C(26A)	650(3)	3832(2)	8560(2)	75(3)
C(21A)	1207(3)	3659(2)	8013(2)	47(2)
C(32A)	-3413(3)	1072(3)	2162(2)	73(3)
C(33A)	-3574(3)	163(3)	1728(2)	88(4)
C(34A)	-2829(3)	-215(3)	2124(2)	104(5)
C(35A)	-1923(3)	316(3)	2954(2)	103(5)
C(36A)	-1762(3)	1225(3)	3388(2)	76(3)
C(31A)	-2507(3)	1602(3)	2992(2)	46(2)
C(42A)	-4160(3)	2852(3)	2834(2)	59(3)
C(43A)	-5268(3)	2721(3)	2829(2)	74(3)
C(44A)	-5705(3)	2292(3)	3426(2)	76(3)
C(45A)	-5033(3)	1995(3)	4030(2)	91(4)
C(46A)	-3924(3)	2126(3)	4037(2)	77(3)
C(41A)	-3488(3)	2555(3)	3439(2)	47(2)
O(1B)	402(3)	6727(2)	7894(2)	45(2)
H(1B)	925(43)	6923(41)	8519(12)	86(18)*
O(2B)	-2004(3)	3330(2)	10710(2)	50(2)
H(2B)	-2067(61)	3843(35)	11071(38)	106(25)*
C(1B)	-774(4)	6504(3)	7846(3)	40(2)
C(2B)	-1173(4)	5751(3)	8304(3)	43(2)
C(3B)	-1483(4)	5104(3)	8655(3)	50(3)
C(4B)	-1900(4)	4366(3)	9040(3)	47(2)

C(5B)	-2303(4)	3704(3)	9359(3)	50(2)
C(6B)	-2782(4)	2961(3)	9803(3)	45(2)
C(12B)	-4502(3)	2334(3)	10321(2)	66(3)
C(13B)	-5630(3)	2176(3)	10289(2)	82(3)
C(14B)	-6301(3)	2465(3)	9675(2)	80(3)
C(15B)	-5844(3)	2910(3)	9092(2)	84(4)
C(16B)	-4717(3)	3068(3)	9124(2)	66(3)
C(11B)	-4046(3)	2780(3)	9738(2)	45(2)
C(22B)	-3249(4)	1604(2)	8524(2)	67(3)
C(23B)	-3369(4)	681(2)	8176(2)	78(4)
C(24B)	-3091(4)	138(2)	8731(2)	73(3)
C(25B)	-2692(4)	518(2)	9636(2)	93(5)
C(26B)	-2572(4)	1441(2)	9984(2)	75(3)
C(21B)	-2850(4)	1984(2)	9429(2)	43(2)
C(32B)	-1377(3)	7499(2)	8780(2)	67(3)
C(33B)	-1377(3)	8382(2)	9082(2)	86(4)
C(34B)	-766(3)	9221(2)	8839(2)	92(4)
C(35B)	-156(3)	9177(2)	8295(2)	114(5)
C(36B)	-156(3)	8293(2)	7993(2)	91(4)
C(31B)	-767(3)	7454(2)	8235(2)	47(2)
C(42B)	-2604(3)	6161(3)	6540(2)	73(3)
C(43B)	-3380(3)	5697(3)	5664(2)	94(4)
C(44B)	-3151(3)	5103(3)	5120(2)	86(4)
C(45B)	-2144(3)	4974(3)	5453(2)	81(3)
C(46B)	-1367(3)	5439(3)	6329(2)	65(3)
C(41B)	-1597(3)	6032(3)	6873(2)	46(2)
C(1G)	-4943(10)	-1465(10)	3804(6)	145(8)
C(2G)	-5445(17)	-2360(9)	3571(7)	225(12)
C(3G)	-6396(18)	-3102(9)	3346(8)	184(12)
C(4G)	-7338(15)	-2891(10)	3396(7)	155(10)
C(5G)	-6961(10)	-1846(10)	3671(5)	127(8)
C(6G)	-5824(8)	-1148(7)	3870(5)	107(5)
C(8G)	-7898(11)	-1580(9)	3694(8)	159(4)
C(9G)	-3726(15)	-675(13)	4017(11)	217(6)
C(1Z)	-669(12)	9174(11)	5061(9)	164(4)
C(2Z)	-629(13)	9926(13)	5529(10)	185(5)
C(3Z)	-75(16)	9176(13)	4474(11)	200(5)
C(1M)	-1548(26)	9128(22)	5870(19)	195(10)
C(2N)	-1166(21)	8206(19)	4777(17)	161(8)

Table 9

Fractional atomic coordinates ($x10^4$) and thermal parameters ($Å^2x10^3$) with e.s.d.'s in parentheses for the Host1-p-xylene structure

Atom	x/a	y/b	z/c	Uequiv/Uiso(*)
O(1A)	4746(1)	8251(1)	2093(1)	45(1)
H(1A)	5401(24)	8193(21)	2228(18)	77(9)*
O(2A)	6494(1)	10310(1)	-2901(1)	48(1)
H(2A)	6151(24)	10695(22)	-2557(18)	74(9)*
C(1A)	5008(2)	7589(2)	1592(1)	37(1)
C(2A)	5517(2)	8026(2)	706(2)	43(1)
C(3A)	5940(2)	8375(2)	-8(2)	46(1)
C(4A)	6429(2)	8750(2)	-842(2)	46(1)
C(5A)	6850(2)	9046(2)	-1566(2)	44(1)
C(6A)	7331(2)	9415(2)	-2482(1)	41(1)
C(11A)	3901(2)	7489(2)	1565(1)	38(1)
C(12A)	3872(2)	7074(2)	971(2)	57(2)

C(13A)	2897(3)	6924(2)	972(2)	72(2)
C(14A)	1956(2)	7184(2)	1559(2)	70(2)
C(15A)	1975(2)	7604(2)	2136(2)	64(2)
C(16A)	2942(2)	7762(2)	2144(2)	51(1)
C(21A)	5834(2)	6565(2)	2036(1)	40(1)
C(22A)	5514(2)	6077(2)	2885(2)	63(1)
C(23A)	6232(3)	5165(2)	3325(2)	79(2)
C(24A)	7275(3)	4742(2)	2918(2)	82(2)
C(25A)	7608(3)	5215(2)	2072(2)	80(2)
C(26A)	6889(2)	6124(2)	1632(2)	60(1)
C(31A)	7562(2)	8626(2)	-2920(1)	47(1)
C(32A)	6870(3)	8761(2)	-3477(2)	71(2)
C(33A)	7083(4)	8035(3)	-3853(3)	96(2)
C(34A)	7978(4)	7158(3)	-3673(3)	98(3)
C(35A)	8676(3)	7011(2)	-3104(3)	90(2)
C(36A)	8468(2)	7744(2)	-2733(2)	66(2)
C(41A)	8394(2)	9643(2)	-2567(2)	44(1)
C(42A)	8864(2)	9473(2)	-1859(2)	61(2)
C(43A)	9826(3)	9702(3)	-1964(2)	80(2)
C(44A)	10328(3)	10082(2)	-2768(3)	79(2)
C(45A)	9869(3)	10267(2)	-3485(2)	77(2)
C(46A)	8898(2)	10049(2)	-3383(2)	64(1)
O(1B)	4608(1)	8371(1)	-5723(1)	45(1)
H(1B)	4069(25)	8821(22)	-6002(19)	73(10)*
O(2B)	3752(1)	11724(1)	-2908(1)	41(1)
H(2B)	4126(21)	11774(18)	-3426(16)	51(7)*
C(1B)	4196(2)	7990(2)	-4827(1)	38(1)
C(2B)	3967(2)	8741(2)	-4393(1)	42(1)
C(3B)	3728(2)	9393(2)	-4074(1)	43(1)
C(4B)	3407(2)	10130(2)	-3686(1)	42(1)
C(5B)	3098(2)	10766(2)	-3342(1)	40(1)
C(6B)	2771(2)	11506(2)	-2873(1)	36(1)
C(11B)	3098(2)	7810(2)	-4766(1)	39(1)
C(12B)	2136(2)	8133(2)	-4214(2)	56(1)
C(13B)	1160(2)	7966(2)	-4192(2)	69(2)
C(14B)	1135(3)	7483(2)	-4719(2)	67(2)
C(15B)	2103(3)	7147(2)	-5264(2)	68(2)
C(16B)	3078(2)	7306(2)	-5287(2)	56(1)
C(21B)	5112(2)	7006(2)	-4438(1)	40(1)
C(22B)	5113(2)	6612(2)	-3558(2)	57(1)
C(23B)	5923(3)	5704(2)	-3210(2)	72(2)
C(24B)	6745(3)	5188(2)	-3732(2)	69(2)
C(25B)	6750(3)	5579(2)	-4608(2)	79(2)
C(26B)	5937(2)	6486(2)	-4967(2)	64(1)
C(31B)	2430(2)	10994(2)	-1911(1)	36(1)
C(32B)	3250(2)	10308(2)	-1400(2)	61(2)
C(33B)	2962(3)	9797(2)	-548(2)	75(2)
C(34B)	1847(3)	9974(2)	-193(2)	69(2)
C(35B)	1032(3)	10661(2)	-695(2)	73(2)
C(36B)	1309(2)	11173(2)	-1548(2)	56(1)
C(41B)	1842(2)	12471(2)	-3250(1)	38(1)
C(42B)	1162(2)	12555(2)	-3797(2)	57(1)
C(43B)	298(3)	13451(2)	-4082(2)	75(2)
C(44B)	103(3)	14253(2)	-3847(2)	74(2)
C(45B)	787(3)	14191(2)	-3316(2)	80(2)
C(46B)	1650(2)	13309(2)	-3022(2)	64(2)
C(1G)	4891(4)	3370(3)	1271(2)	94(3)

C(2G)	5650(5)	2400(3)	1570(2)	105(3)
C(3G)	6740(5)	2236(3)	1653(3)	109(3)
C(4G)	7123(4)	3013(3)	1458(2)	94(2)
C(5G)	6381(4)	3964(3)	1153(2)	90(2)
C(6G)	5290(4)	4150(3)	1060(2)	85(2)
C(1MG)	3692(4)	3591(4)	1169(3)	137(4)
C(2MG)	8307(4)	2819(4)	1584(3)	137(3)
C(11G)	211(6)	4149(5)	-217(4)	115(4)
C(12G)	794(4)	4126(5)	342(3)	119(3)
C(13G)	598(5)	4933(7)	566(3)	121(4)
C(3MG)	442(6)	3222(5)	-474(4)	190(5)

CHAPTER SIX

WEB11 - DIOL HOST COMPOUND

The second diol host compound (4,4'-bisdiphenylhydroxymethyldiphenyl), **WEB11** has the "wheel-and-axle" design but the long molecular axis comprises two phenyl groups:

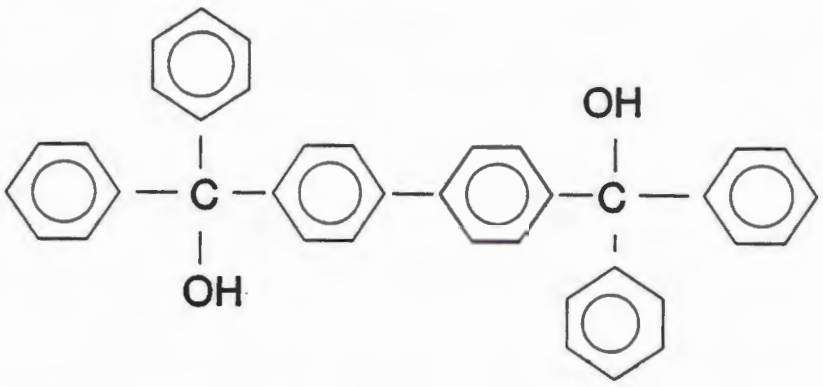

The axis is aromatic in character and has been fundamentally altered from the original form of host1. WEB11 proved to be a more selective host since it captured a smaller variety of molecules as guests.

α -FORMS OF WEB11

The pursuit of host-guest complexes using WEB11 and a variety of different solvents resulted in the discovery of two α-phases. Polymorph (1), space group C2/c, was obtained by evaporating a solution of WEB11 dissolved in diethyl ether; the other polymorph (2), space group $P\bar{1}$, was obtained by evaporating a similar solution of WEB11 and o-xylene. Polymorphs are different crystal forms of the same compound and exhibit different physical and chemical properties including different melting points and spectral properties. Polymorphism is particularly significant with respect to pharmaceuticals, where the polymorph present may alter the dissolution rate, bioavailability and chemical and physical stability. Examples of compounds exhibiting many polymorphic forms are : sulphonamides, barbiturates, steroids (such as progesterone which has five polymorphs) and water which according to Byrn has "eight or nine" **(1)**.

---

1 SR Byrn, "*Solid State Chemistry of Drugs*", Academic Press, New York, 1982, 79

THE STRUCTURE OF WEB11 POLYMORPH (1)

Oscillation and Weissenberg photographs found the following reflection conditions:
hkl: h+k=2n
h0l: l=2n (h=2n)
0k0: (k=2n)
This indicated either C2/c or Cc as a possible space group choice. A structure solution attempted in C2/c using direct methods was successful, the best E-map having a combined figure of merit value of 0.053. The R_E was calculated to be 0.196 for 20 surviving atoms which corresponded exactly to half a molecule of WEB11 and since Z=4 this is as expected. No structure solution was possible in Cc and refinement using a fragment of a molecule of WEB11 proved equally unsuccessful. In the centrosymmetric space group the values of the E-statistics for the 0kl, h0l and hk0 projections and the remainder of the reflections favoured the choice of the centric space group. Convergence during refinement and a low final R of 0.0534 confirmed the choice of space group. The asymmetric unit comprised half a molecule of WEB11 lying on the diad at Wyckoff *e*. The crystal parameters are described in Table 1. The packing of (1) looking along [010] as well as the symmetry operations are illustrated in figure 1. There is no hydrogen bonding between the hydroxy moieties of the WEB11 molecules.

Figure 1

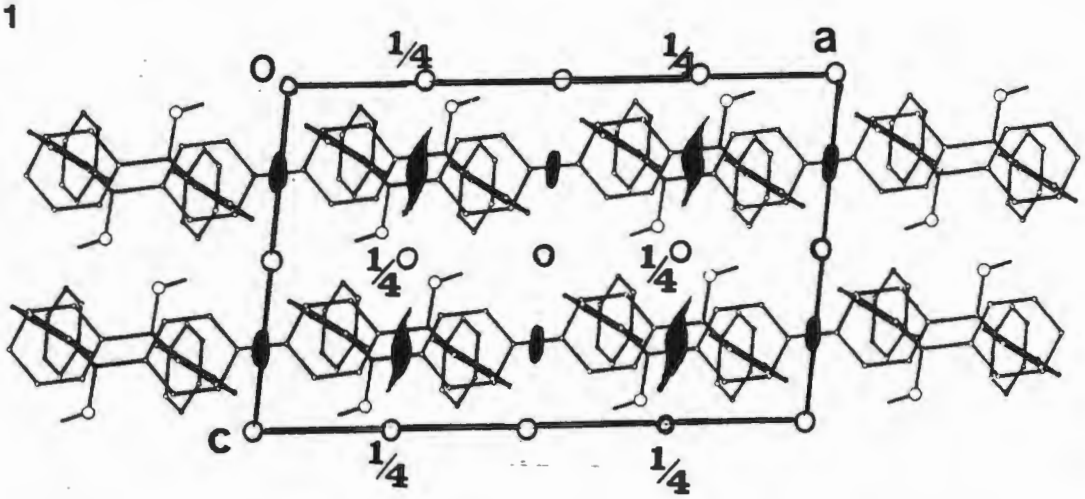

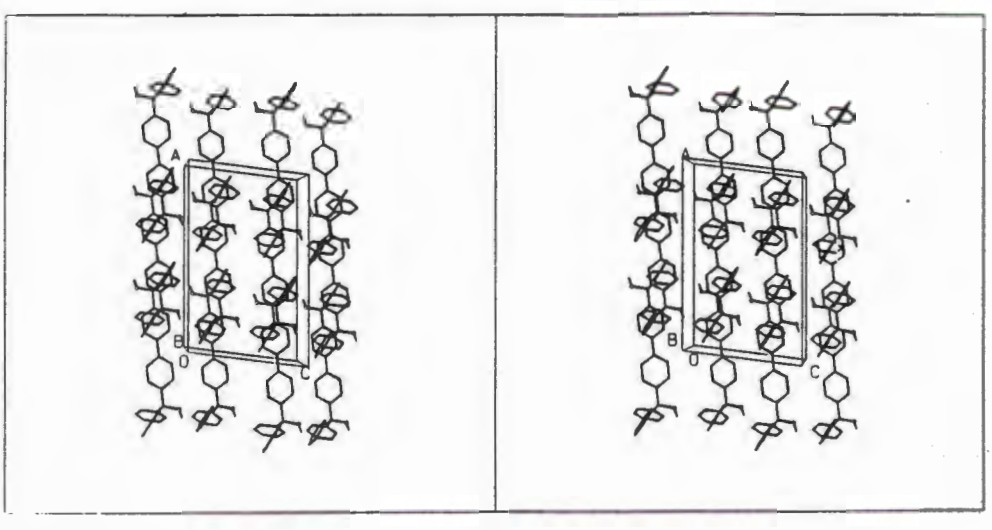

Figure 2 Packing diagrams of WEB11 (1) viewed along [001]
The molecular axes are parallel to one another and align parallel to [1 0 0].

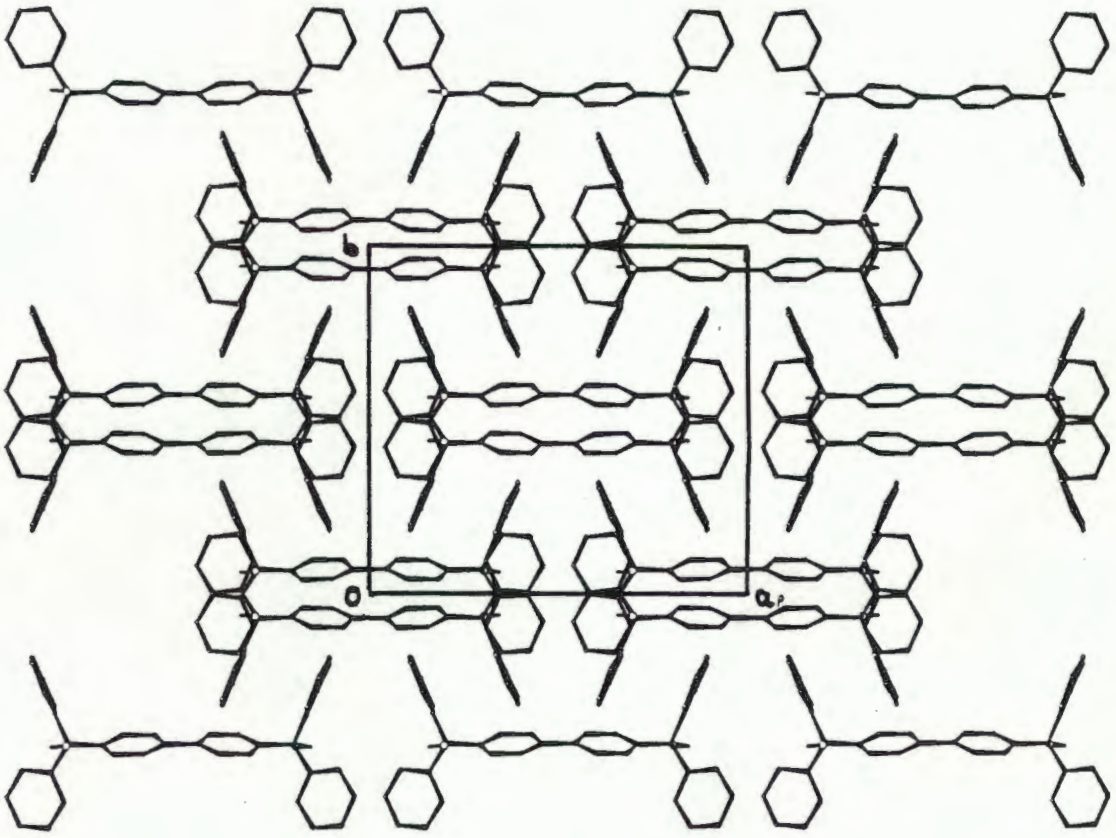

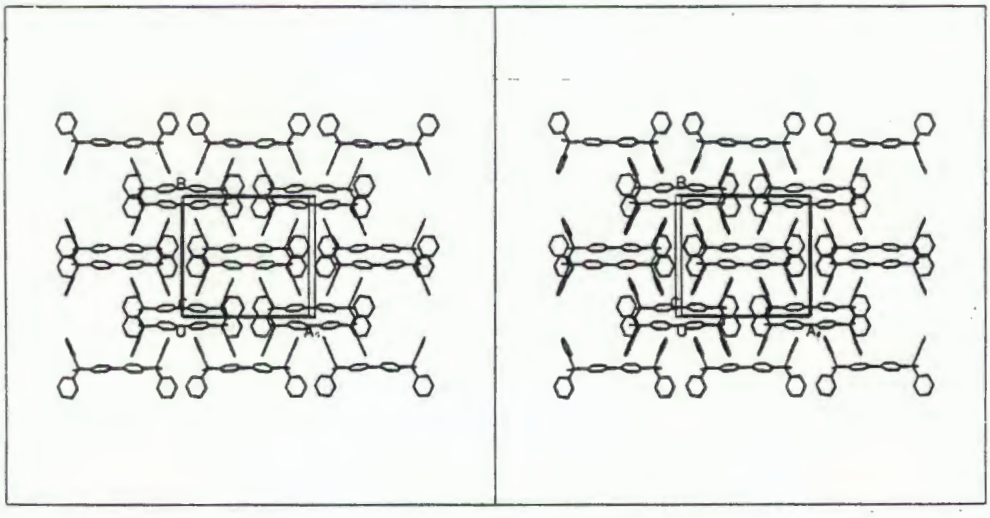

THE STRUCTURE OF WEB11 POLYMORPH (2)

A second α-form was discovered when co-crystallizing WEB11 from o-xylene. No mirror planes were observed in the oscillation and zero level Weissenberg photographs. Thus the possible space groups were P1 or $P\bar{1}$. Mean $|E^2-1|$ statistics pointed to the centric space group as the choice and direct methods was carried out in $P\bar{1}$. The combined figure of merit had a value of 0.056 and the R_E was 0.194 for forty surviving atoms. WEB11 has forty non-hydrogen atoms and one molecule of WEB11 was located in the asymmetric unit. The crystal parameters are described in Table 1. There is one type of host intermolecular hydrogen bond which is illustrated in figure 3. The O1---O2 separation is 2.877 (3)Å, (-x+2,-y+2,-z+1), the O2-H2 hydroxy moiety acting as an acceptor only. The features of this structure are illustrated in figures 4 and 5.

Figure 3

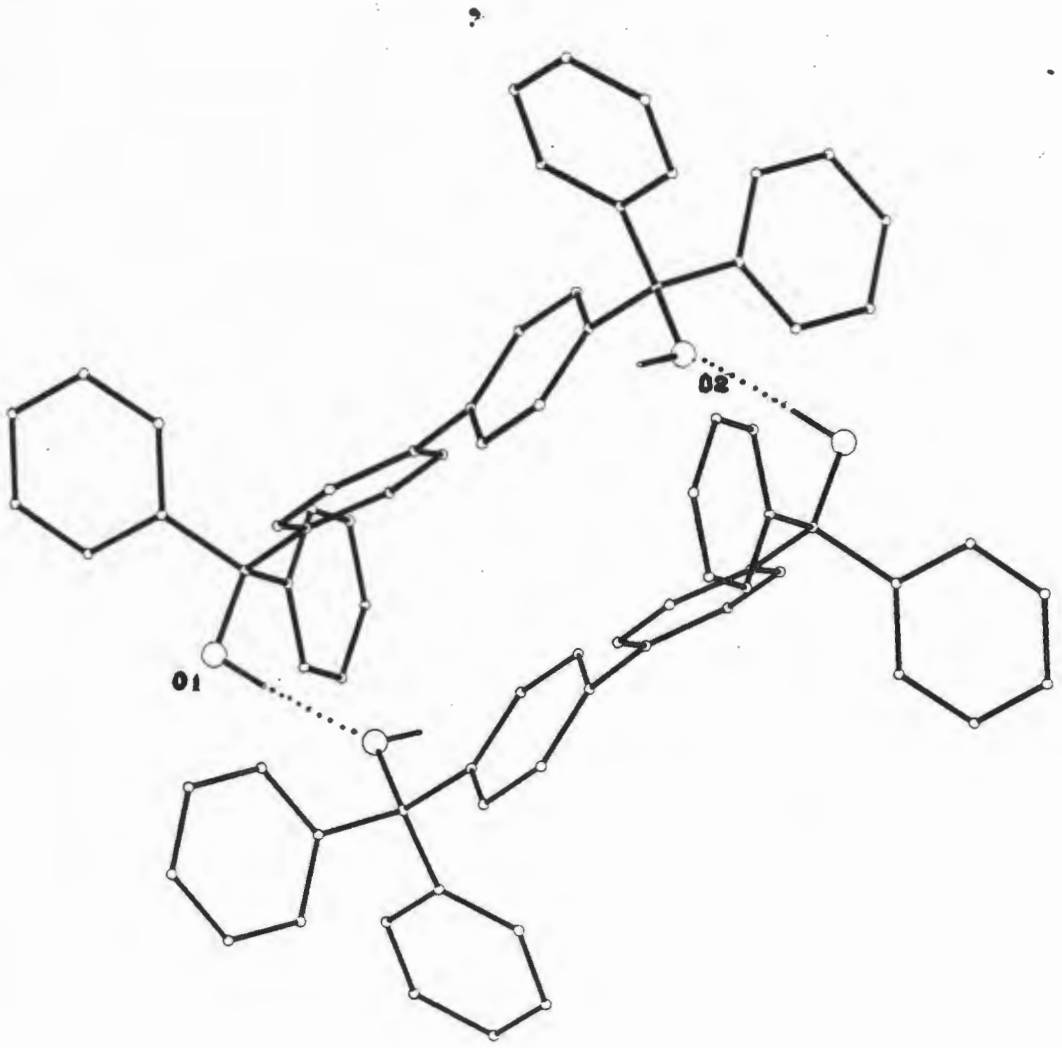

Figure 4 Packing diagrams viewed along [1 0 0]

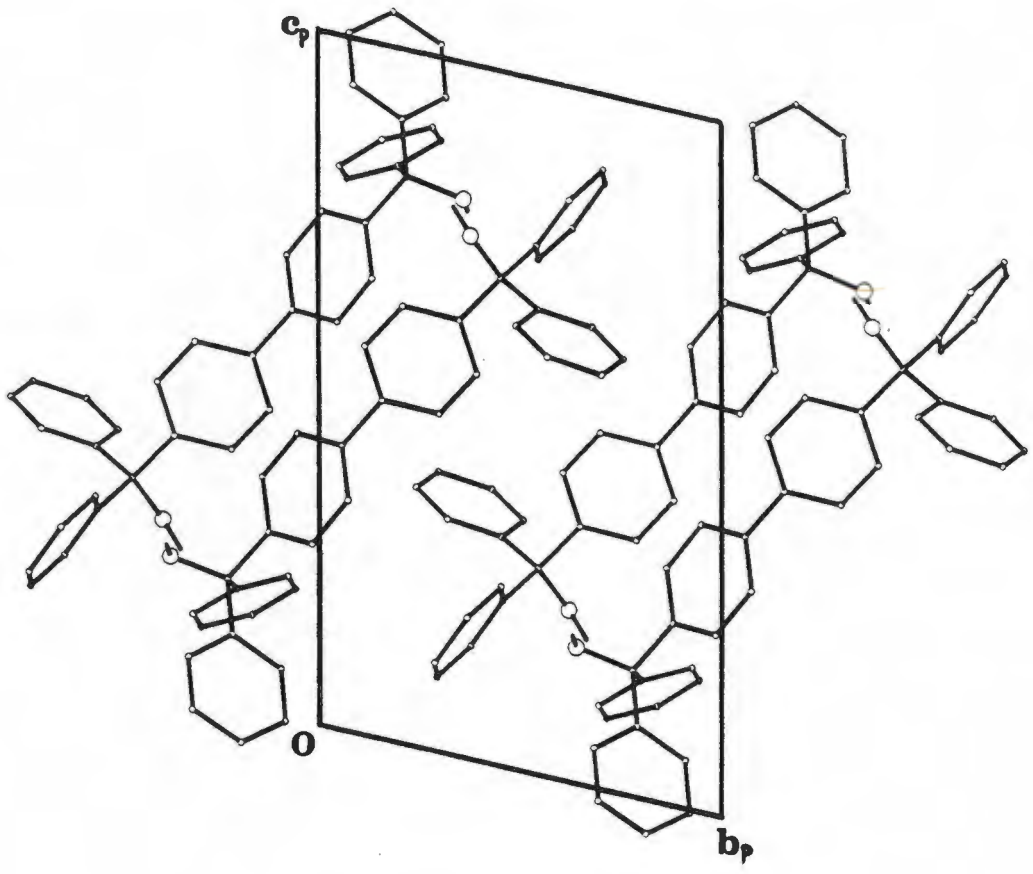

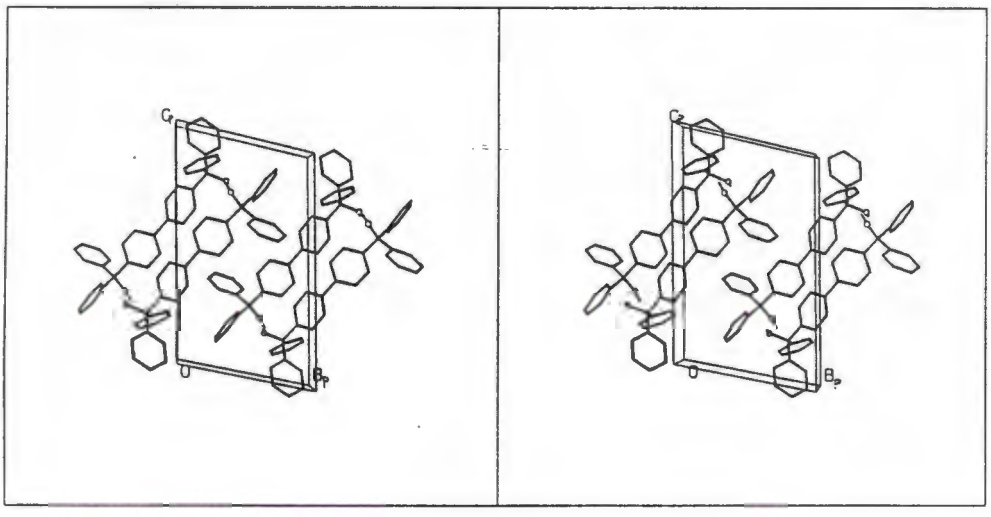

Figure 5 illustrates the crystal packing and shows the way in which the aromatic molecular axes align parallel to one another.

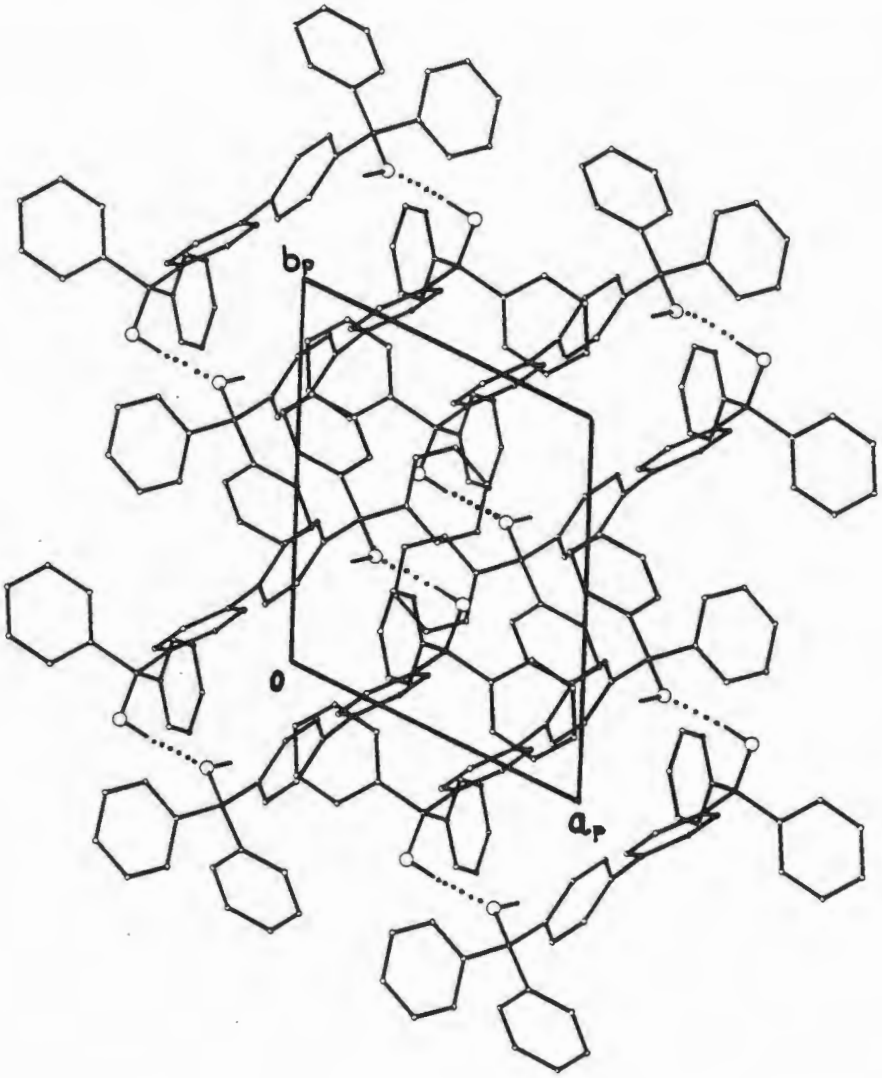

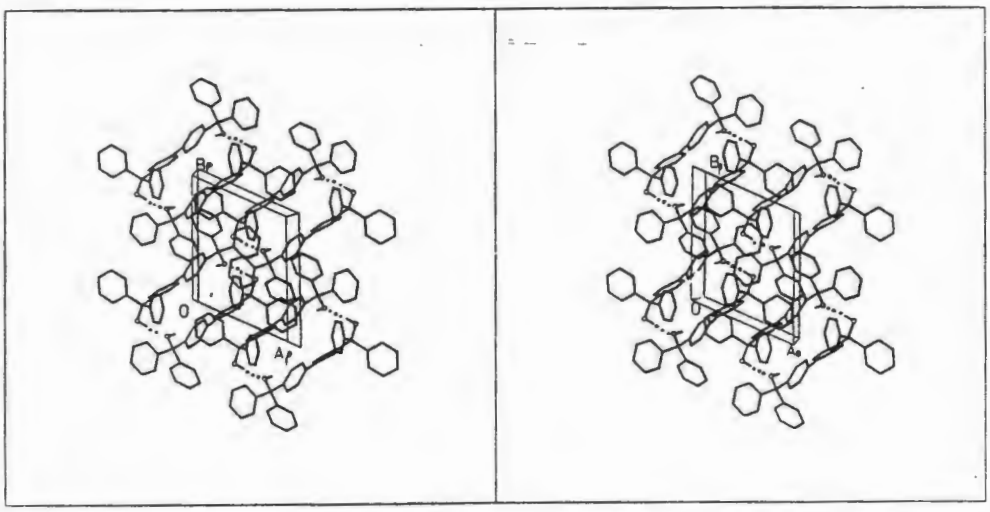

Conformation of the WEB11 host molecules

Torsion angles were examined in order to study differences between molecular conformations of the WEB11 host compounds. The torsion angles are defined as :
- the first carbon atom of the phenyl ring in the molecular axis eg C51;
- the tetrahedral carbon of the carbon chain eg C1; the phenyl carbon, eg C11, which is attached to this latter carbon;
- the ortho carbon in the spacer phenyl group, rings 1-4, see figure 6a. The torsion angles of WEB11 (1) and WEB11 (2) are shown below and are graphically depicted in figure 6b:

	C51-C1-C11-C12/C16	C51-C1-C21-C22/C26	C61-C2-C31-C32/C36	C61-C2-C41-C42/C46
(1)	65	48		
(2)	-68	24	43	-74

Figure 6a

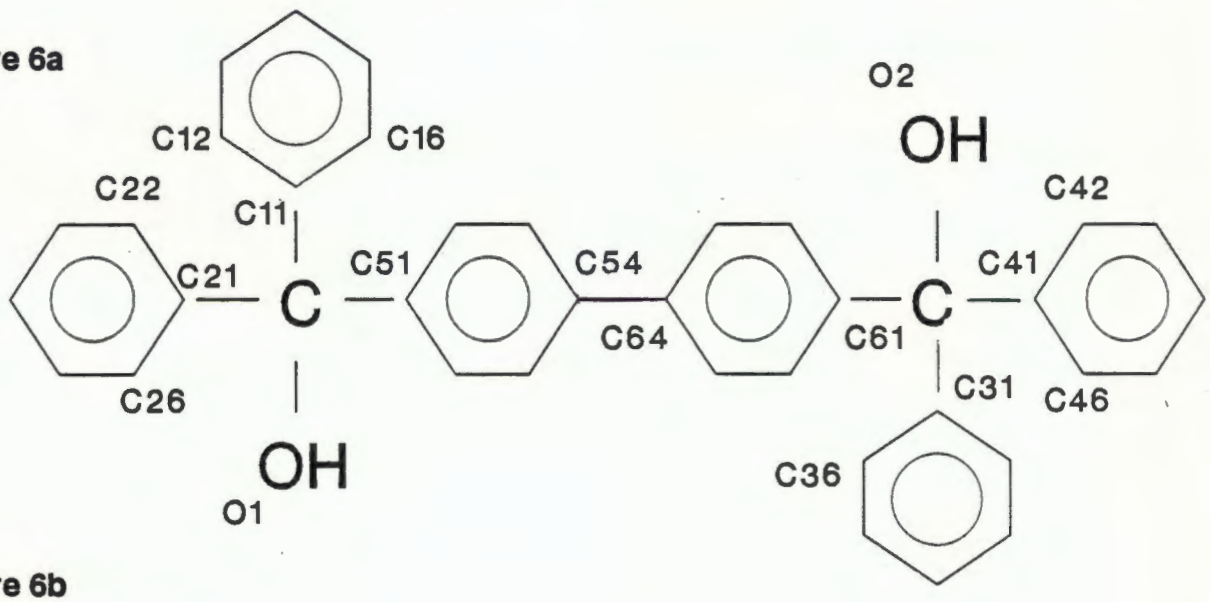

Figure 6b

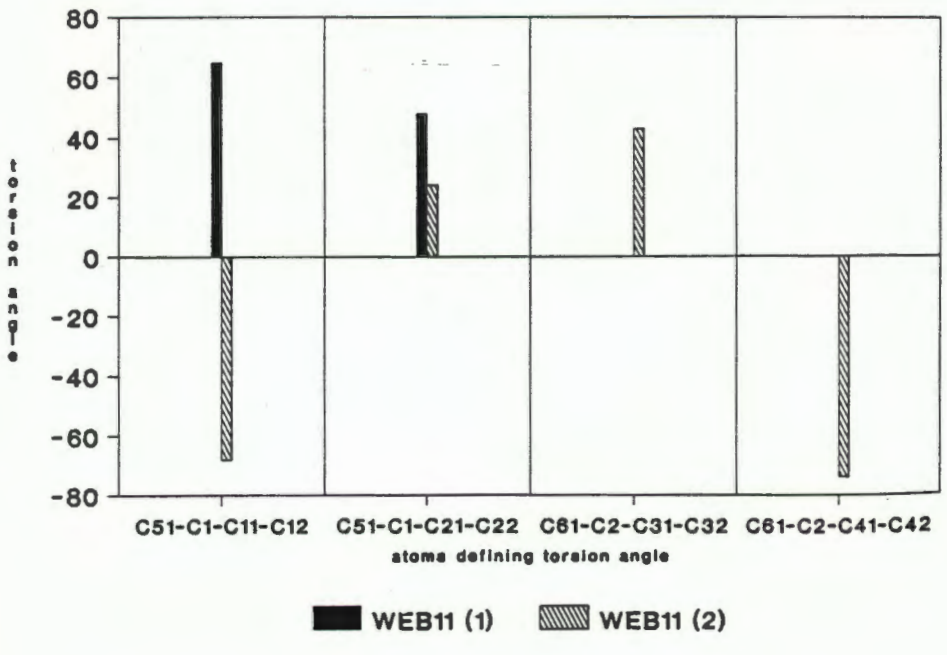

Conformation of the hydroxy moieties was examined by viewing along the length of the molecular axis. Compound (1), figure 6c (i), is shown viewed along C1 and C51 which shows the *trans* conformation of the hydroxy moieties as well as the staggered configuration of the two phenyl rings along the backbone. Compound (2) was similarly viewed, figure 6c (ii) and in this polymorph, the phenyl backbone rings are once again staggered but the hydroxy moieties are almost eclipsed having adopted a *cis* conformation in order to achieve the host-host interaction evident in this crystal form.

Figure 6c (i)

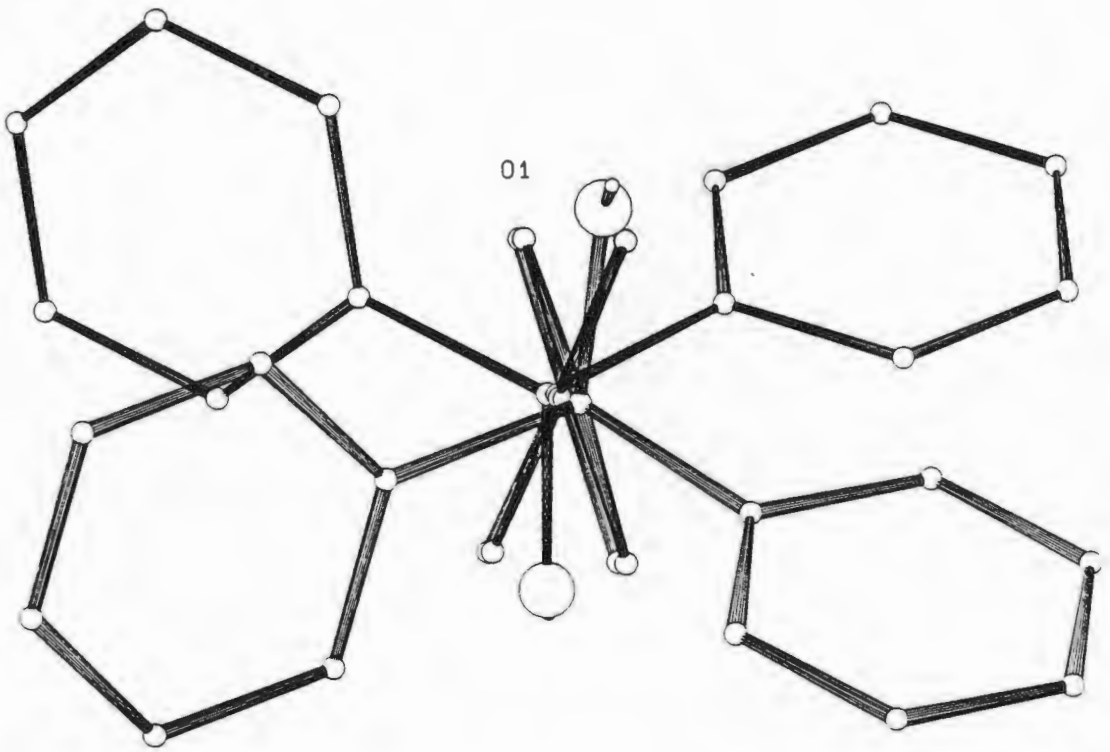

Figure 6c (ii)

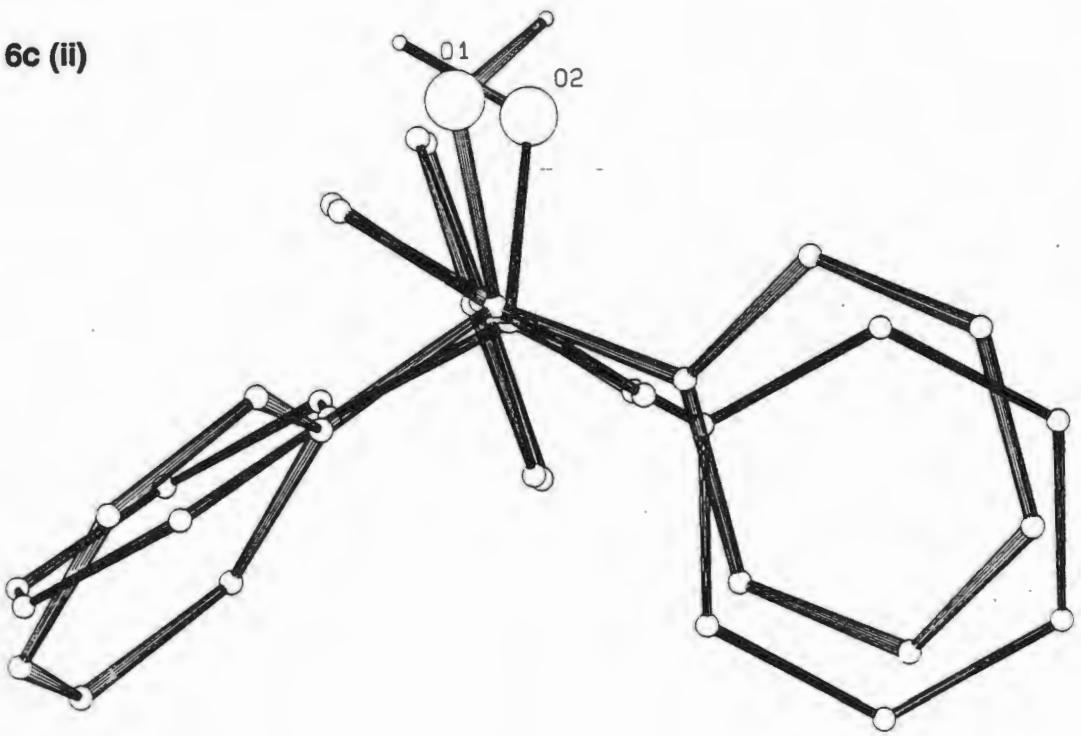

TABLE 1 CRYSTAL DATA AND EXPERIMENTAL DETAILS FOR WEB11 POLYMORPHS.

Compound	**(1)**	**(2)**
Molecular formula	$C_{38}H_{30}O_2$	$C_{38}H_{30}O_2$
Molecular weight($gmol^{-1}$)	518.65	518.65
Space group	C2/c	$P\bar{1}$
a (Å)	16.827(2)	8.807(2)
b (Å)	15.212(3)	10.687(6)
c (Å)	10.708(2)	16.263(3)
α (°)	90	100.97(3)
β (°)	97.01(1)	91.47(2)
γ (°)	90	113.02(3)
Z	4	2
V ($Å^3$)	2721(1)	1375(1)
D_c (gcm^{-3})	1.27	1.25
D_m (gcm^{-3})	1.22(4)	1.23(3)
$\mu(MoK_\alpha)$ (cm^{-1})	0.41	0.40
F(000)	1096	548
Data collection (21°C)		
Crystal dimensions (mm)	0.28x0.31x0.47	0.38x0.44x0.47
Range scanned θ (°)	1-25	1-23
Range of indices *h,k,l*	±20,+18,+12	±9,±11,+17
Reflections for lattice parameters no.,θ range (°)	24,15-17	24,16-17
Instability of standard reflections (%)	2.9	9.0
Scan mode	(ω-2θ)	(ω-2θ)
Scan width in(°)	(0.85+0.35tanθ)	(0.60+0.35tanθ)
Vertical aperture length (mm)	4	4
Aperture width (mm)	(1.12+1.05tanθ)	(1.12+1.05tanθ)
Number of reflections collected (unique)	2072	3462
Number of reflections observed with $I_{rel}>2\sigma I_{rel}$	1593	2930
Final refinement		
Number of parameters	186	370
R	0.053	0.046
wR	0.057	0.054
w	$(\sigma^2(F_O)+0.001F_O^2)^{-1}$	$(\sigma^2(F_O)+0.001F_O^2)^{-1}$
S	3.23	0.71
Max. shift/e.s.d.	0.166	0.002
Max. height in difference electron density map ($eÅ^{-3}$)	0.23	0.21
Min. height in difference electron density map ($eÅ^{-3}$)	-0.30	-0.25

THERMAL ANALYSIS

DSC is a useful technique for detecting the existence of polymorphs because differences in melting point as well as phase changes can be detected **(2)**. A schematic DSC trace is shown in figure 7. The first endotherm corresponds to desorption of any guest which is followed by a small pre-melting endotherm due to a lattice rearrangement of the host compound.

Figure 7

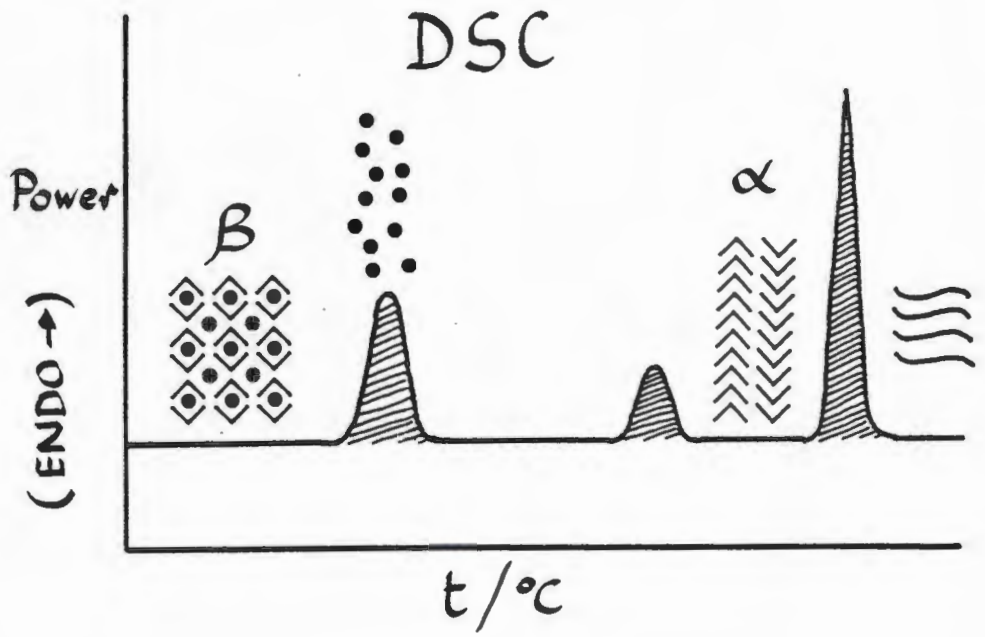

The DSC traces are shown in figure 8. The polymorphs differ in melting point by seven degrees. The C2/c form (1) is represented by the broken line. It melts at 186.8^{o}C and has an enthalpy of melting of 36.6kJmol^{-1}. The decomposition shows a thermal event, possibly a lattice rearrangement prior to the melt. Compound (2) melts at 180.4^{o}C and has an enthalpy of melting of 49.7kJmol^{-1}.

---

2 SR Byrn, "*Solid State Chemistry of Drugs*", Academic Press, New York, 1982, 135

Figure 8

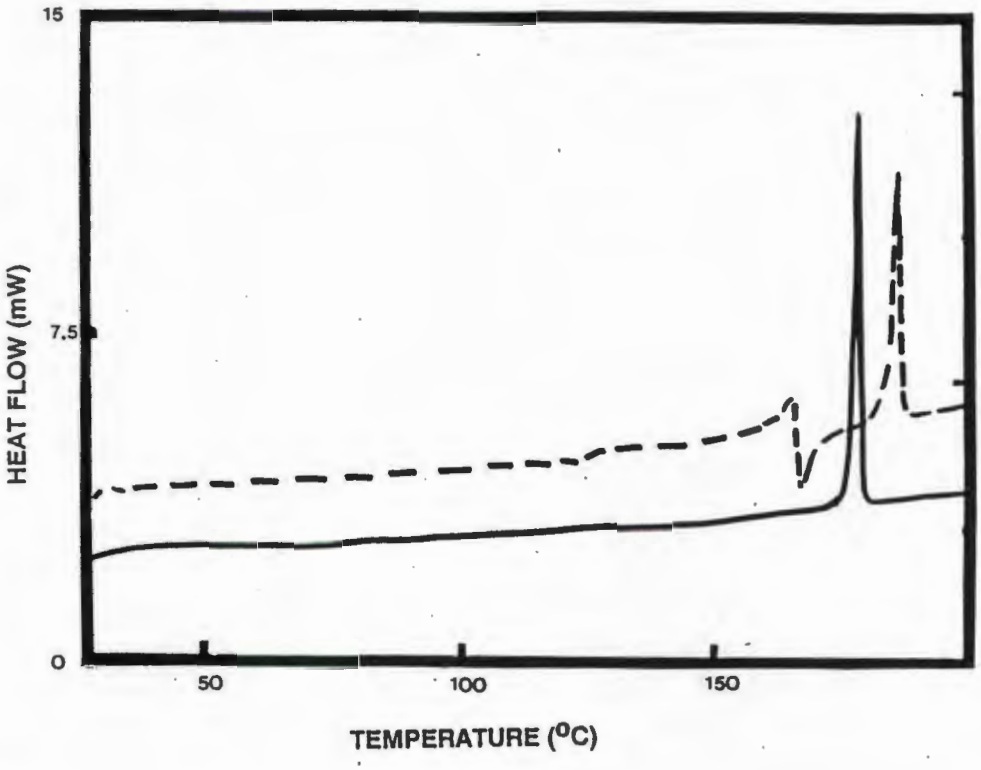

DISCUSSION

The two different forms of WEB11 differ both in their crystal packing as well as their thermal properties. Compound (1) is monoclinic and contains no stabilization due to hydrogen bonding despite the fact that it melts at a higher temperature than (2). The latter, on the other hand, is triclinic and fundamentally different because hydrogen bonding influences its packing motif. The crystal packing of compounds (1) and (2) both shows that alignment of the molecular axes occurs. Polymorph (1) has a PF of 17.00 $Å^3$/non-hydrogen atom and contains no hydrogen bonding between host molecules. Polymorph (2) has a PF of 17.18 $Å^3$/non-hydrogen atom which implies that the molecules of WEB11 are slightly less efficiently packed in this form, although this structure has the added stabilisation due to hydrogen bonding contributions. The difference in packing factors is, however, not dramatic.

Certain factors have been observed to favour or to permit the formation of polymorphic forms, one of the most notable being the flexibility of the molecule, *ie*. the number of degrees of freedom it possesses. A more flexible molecule is able to adopt many possible conformations which may result in polymorph formation. The manner in which a polymorphic crystal is grown is of paramount importance. For instance, the polarity of

the solvent and rate of cooling of the mother liquor will stabilize a certain conformer, ie. favour the existence of one polymorphic molecular arrangement as opposed to another. The observed crystal structure corresponds to only one of several minima in the free energy surface **(3)**. Since the differences in lattice energy between polymorphs are very small- in the region of ~~1-2 kcal mol^{-1}~~ 4–8 kJ mol^{-1} **(4)**, the optimum chemical and energy environments required to achieve a specific form, are extremely difficult to define.

Desiraju describes polymorph formation in terms of crystal formation which is mediated via the influence of weak and numerous intermolecular forces operating within a temperature dependent entropy framework **(5)**. Thus, the formation of each polymorph of a compound is governed by specific conditions of temperature, pressure and solvent, and the form obtained need not correspond to a unique energy minimum. Desiraju states that " even though weak intermolecular forces may be involved in stabilising crystal structures, at least one set of forces may be sufficiently directionally specific to steer all polymorphic modifications of a given compound towards a particular crystal structure type, if not to a unique energy minimum" **(6)**. Thus the occurrence of polymorphs reflects the alternative ways in which molecules arrange so as to exist in a free energy minimum in a crystal, but how this is attained may not necessarily be known with certainty.

---

3 GR Desiraju, "*Crystal Engineering*", Elsevier Press, Amsterdam, 1989, Chapter 10
M Pierrot (Ed), "*Structure and Properties of Molecular Crystals*", Elsevier, Amsterdam, 1990, Chapter 4

4 J Bernstein, "*Crystal Forces and Molecular Conformation*", presented at the International School of Crystallography, 9th Course, Erice, Italy, 21 March-1 April, 1983

5 SR Byrn, "*Solid State Chemistry of Drugs*", op. cit., 285

6 GR Desiraju, "*Crystal Engineering*", op. cit., 287

WEB10 - AN UNSUCCESSFUL HOST COMPOUND

WEB10 (4,4'-bisdiphenylmethyldiphenyl), is a compound with the fundamental "wheel-and-axle" design: it has a long molecular axis with bulky groups at either end but no hydrogen bond acceptors present. WEB10 is illustrated below.

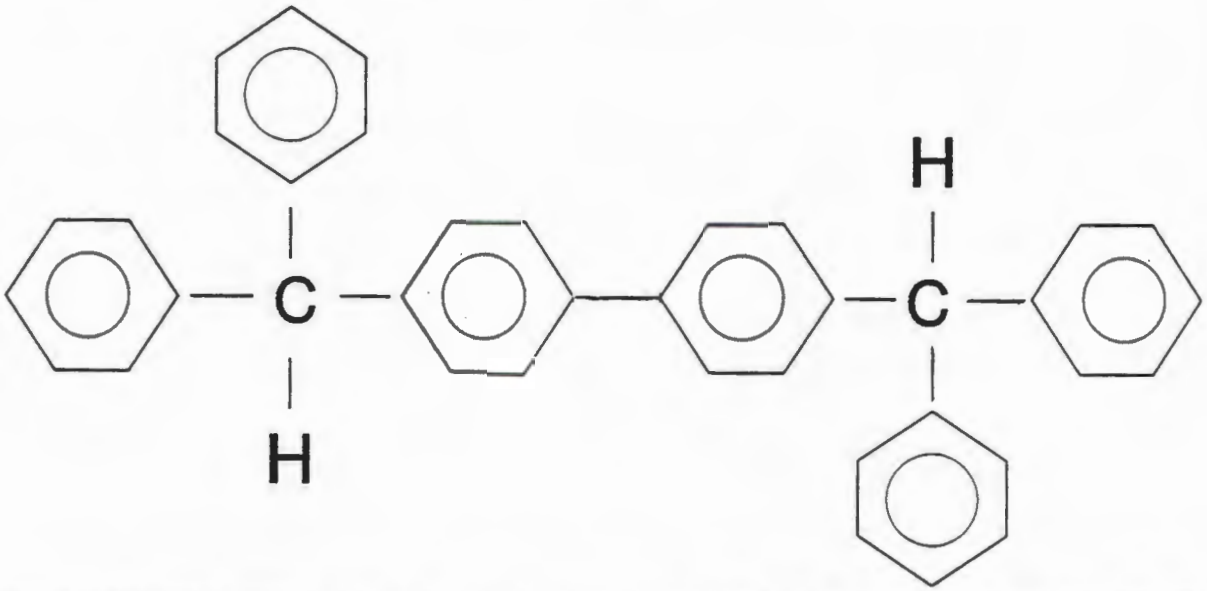

WEB10 did not function as a host molecule - it was unable to trap any guest molecules at all. Co-crystallization with many possible guests was attempted, but absence of weight loss in the TG traces showed that none had been captured.

Guests tried were: acetone, benzophenone, methyl ethyl ketone, diethyl ketone, acetophenone and propiophenone. In order to attempt to include apolar components, ortho, meta and para-xylene, α- and β-napthol, benzene and naphthalene were all tried as possible guests. It would appear that the loss in functionality, combined with sufficient conformational freedom in the aromatic backbone, rendered the "wheel-and-axle" host compound WEB10 unable to include molecular species as guests.
Oscillation and Weissenberg photography indicated that the α-form of WEB10 had crystallized in a monoclinic space group. The intensity data exhibited the non-extinction reflection conditions: h0l: h+l =2n; (h00: h=2n); (00l: l=2n); 0k0: k=2n which are consistent with the space group $P2_1/n$ and in which the structure was solved using direct methods.
Details of the crystal parameters may be found in Table 2. WEB10 has a packing factor of 18.09 $Å^3$/non-hydrogen atom and is therefore less tightly packed than the two WEB11 α-forms (17.00 and 17.18 $Å^3$/non-hydrogen atom).

Figure 9 illustrates the crystal packing obtained for WEB10. The projection is viewed along [010].

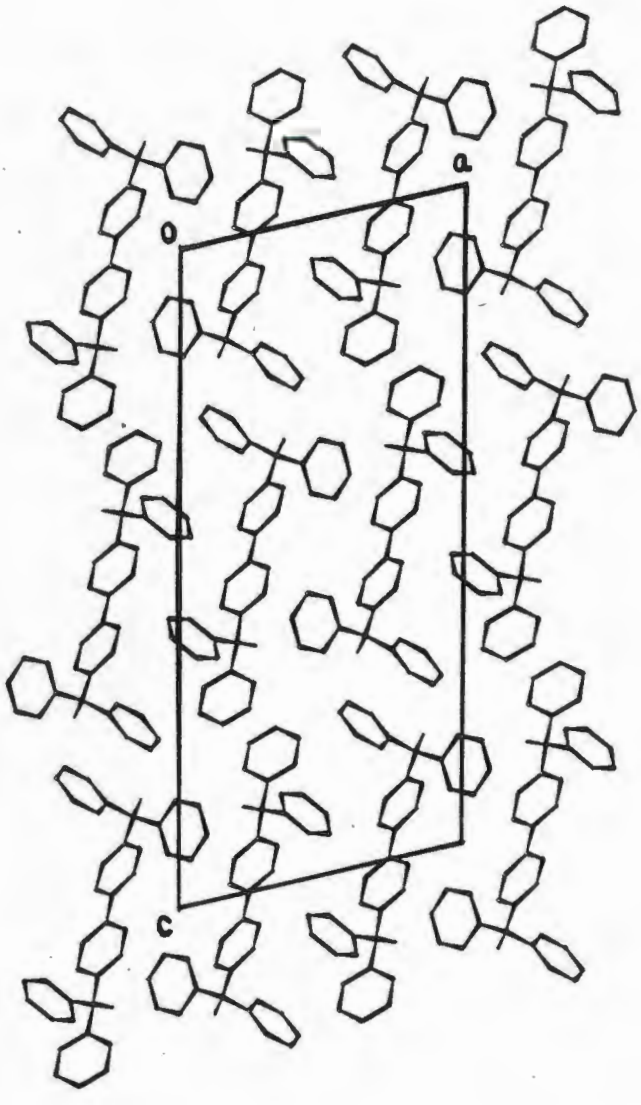

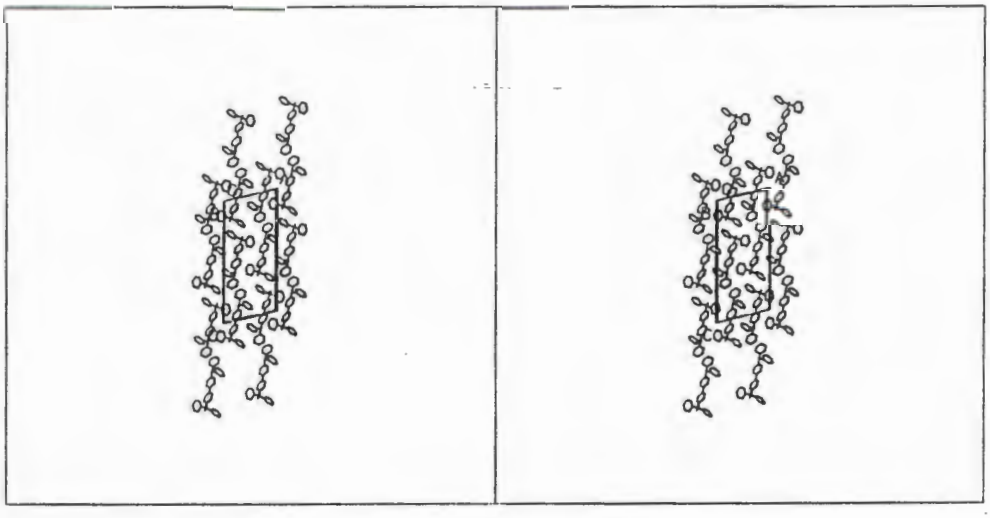

The DSC trace of the α-form of WEB10, figure 10, shows that melting occurs at 163^{o}C.

Figure 10

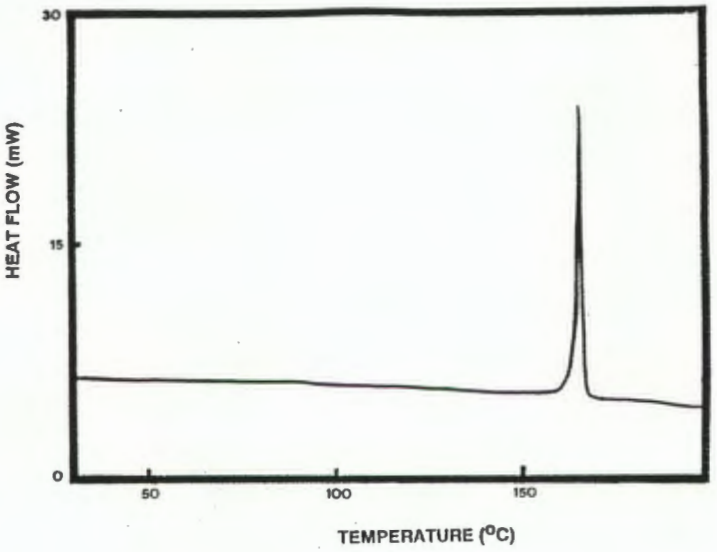

The torsion angles were chosen as was previously described and are graphically depicted in figure 11. The estimated standard deviations are less than one degree.

C51-C1-C11-C12/C16	C51-C1-C21-C22/C26	C61-C2-C31-C32/C36	C61-C2-C41-C42/C46
67	27	21	87

Figure 11

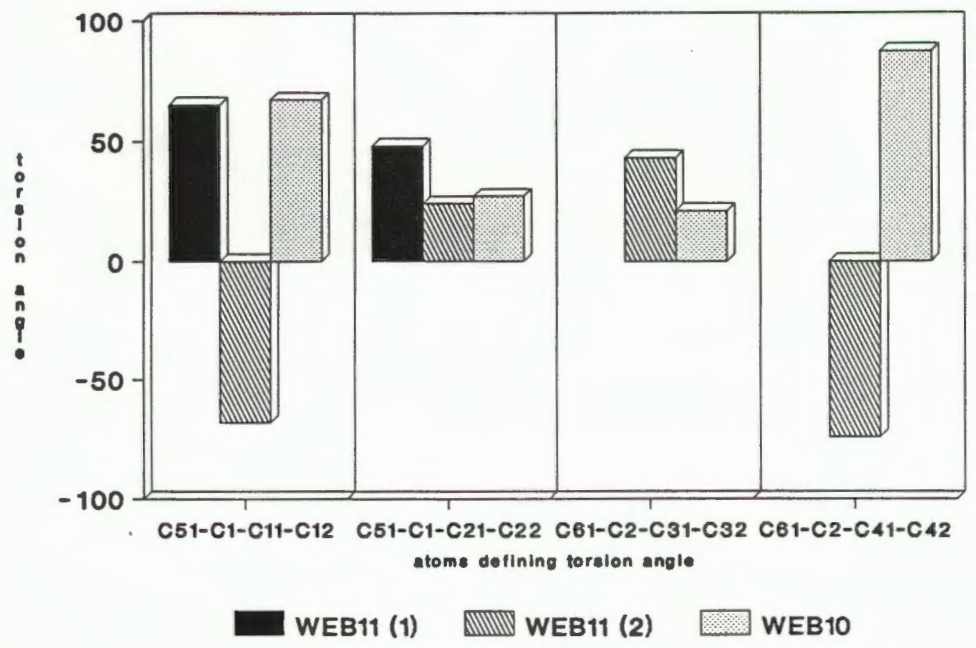

TABLE 2 CRYSTAL DATA AND EXPERIMENTAL DETAILS FOR WEB10 STRUCTURE.

Compound	**WEB10**
Molecular formula	$C_{38}H_{30}$
Molecular weight ($gmol^{-1}$)	486.66
Space group	$P2_1/n$
a (Å)	12.781(3)
b (Å)	7.773(2)
c (Å)	28.405(17)
β (°)	103.05(3)
Z	4
V ($Å^3$)	2749(2)
D_c (gcm^{-3})	1.18
D_m (gcm^{-3})	1.16(1)
$\mu(MoK_\alpha)$ (cm^{-1})	0.15
F(000)	484
Data collection (21°C)	
Crystal dimensions (mm)	0.38x0.38x0.47
Range scanned θ (°)	1-25
Range of indices *h,k,l*	±15,+9,+33
Reflections for lattice parameters no.,θ range (°)	24,16-17
Instability of standard reflections (%)	0.8
Scan mode	(ω-2θ)
Scan width in(°)	(0.80+0.35tanθ)
Vertical aperture length (mm)	4
Aperture width (mm)	(1.12+1.05tanθ)
Number of reflections collected (unique)	3874
Number of reflections observed with $I_{rel} > 2\sigma I_{rel}$	2712
Final refinement	
Number of parameters	352
R	0.055
wR	0.054
w	$(\sigma^2(F_o)+0.001F_o^2)^{-1}$
S	1.44
Max. shift/e.s.d.	0.002
Max. height in difference electron density map ($eÅ^{-3}$)	0.15
Min. height in difference electron density map ($eÅ^{-3}$)	-0.22

THE STRUCTURE OF THE WEB11-ACETONE (1:2) INCLUSION COMPOUND

STRUCTURE SOLUTION

X-ray photography showed the diffraction pattern to contain the following reflection conditions :

hkl	no conditions
0kl	l=2n
h0l	no conditions
hk0	h+k=2n
h00	(h=2n)
0k0	(k=2n)
00l	(l=2n)

The data collection indicated that the space group was either $Pc2_1n$ or Pcmn and these were appropriately transformed to the standard settings of $Pna2_1$ (space group no. 33) and Pnma (space group no. 62) respectively. A direct methods calculation performed in the centrosymmetric space group failed to give an automatic solution : the combined figure of merit was 0.33 and the R_E value 0.507 for 24 surviving atoms. Peaks which were generated in the E-map could not be sensibly interpreted and bond lengths lay outside the usual ranges.

An attempt was made to solve the structure in Pnma by hand. From convergence maps that were obtained using SHELX76 **(7)**, three origin-defining reflections that satisfied the parity rules were chosen and an additional six reflections for multisolution were chosen. All of these were chosen on the basis of their high E and α values. These reflections were then used to generate phases and produce E-maps. However this attempt failed and a chemically feasible model was not obtained.

Since a solution could not be found in Pnma, automatic direct methods was performed in the non-centrosymmetric space group $Pna2_1$. An R_E of 0.232 for 46 surviving atoms was obtained, WEB11 has forty non-hydrogen atoms and acetone has four. One WEB11 host molecule and two crystallographically distinct acetone molecules with acceptable bond lengths and angles were obtained in the asymmetric unit. Subsequent refinement was successfully carried out and very few correlation matrix elements greater than 0.5 were obtained. The z coordinate of one atom was fixed because the origin lies along a two-fold screw axis. An attempt to carry out a refinement in Pnma using a WEB11 host molecular fragment input on a centre of symmetry, proved unsuccessful.

---

7 SHELX76 GM Sheldrick in "*Computing in Crystallography*", op. cit.

Figure 12 shows the way in which two acetone molecules hydrogen bond to one WEB11 molecule : O1GA---O1 = 2.873Å, (½-x,-½+y,½+z) and O1GB---O2 = 3.002Å, (-x,-y,½+z).

Figure 12

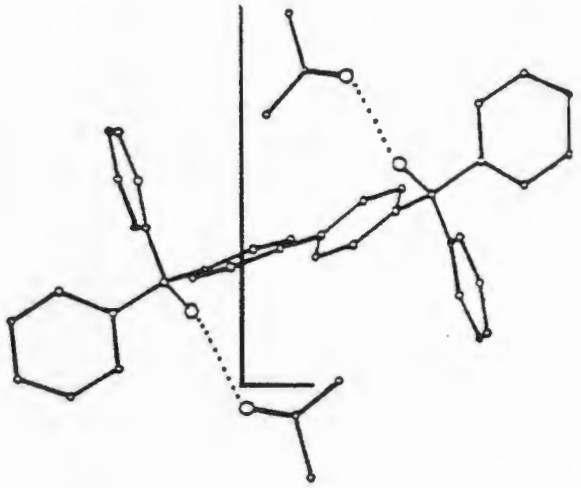

Crystal packing viewed along [010] is illustrated in figure 13.

Figure 13

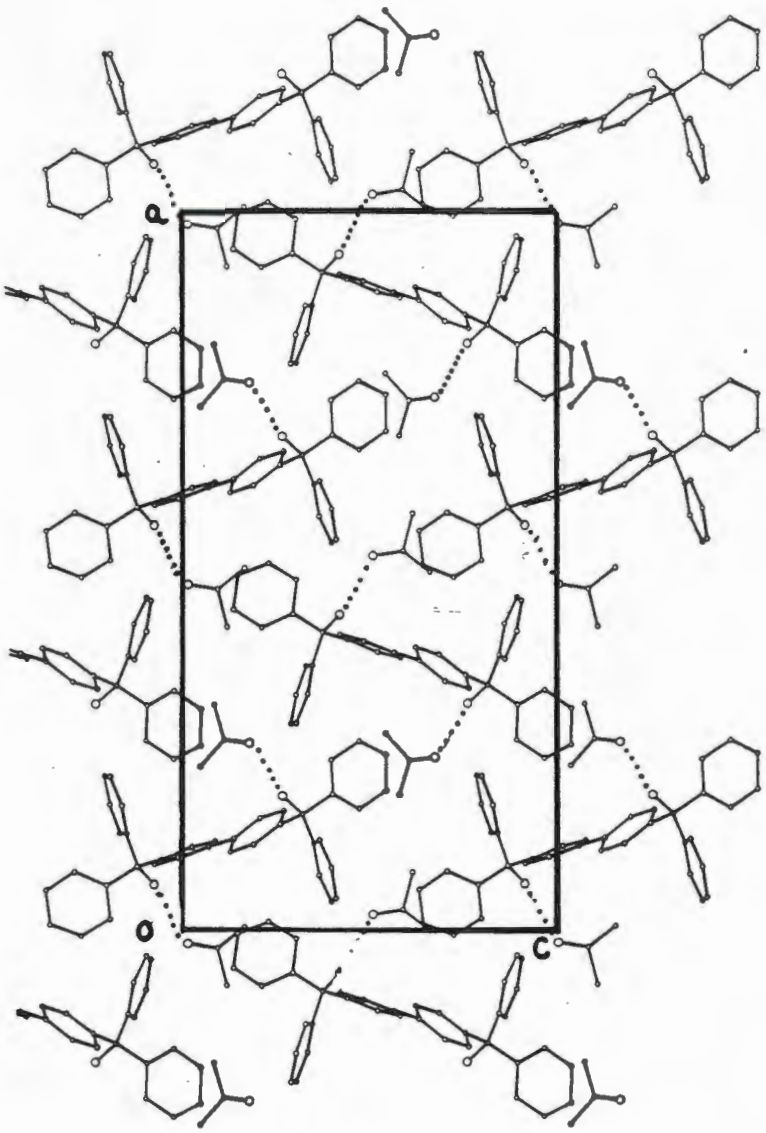

Figure 14 (i) illustrates a stereoscopic view along [0 1 0] of the WEB11 crystal packing. Figure 14 (ii) illustrates the location of the guest molecules plotted with van der Waals radii. OPEC showed that the guests lay in cavities and not channels in contrast to the Host1-acetone structure which was discussed in Chapter 3. Details of the intensity data collection and crystal parameters may be found in Table 3.

Figure 14 (i)

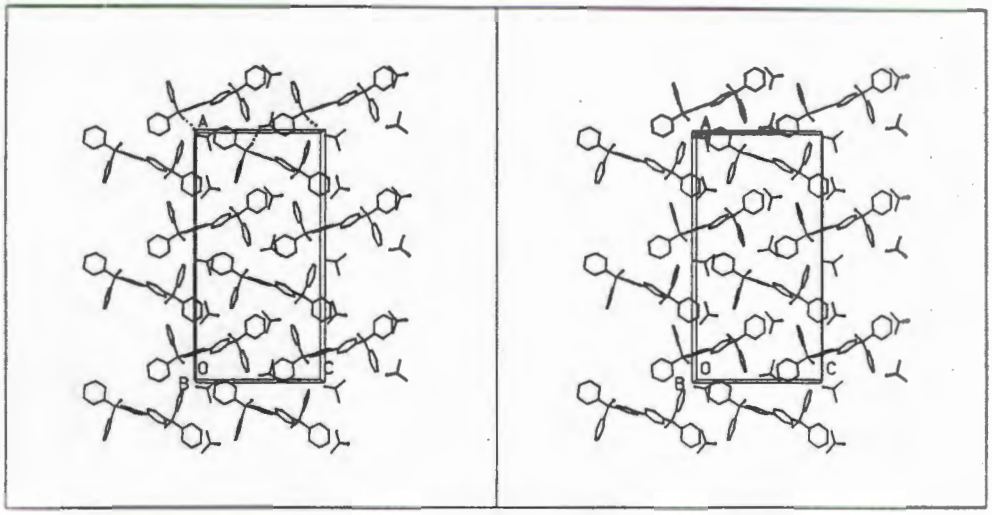

Figure 14 (ii)

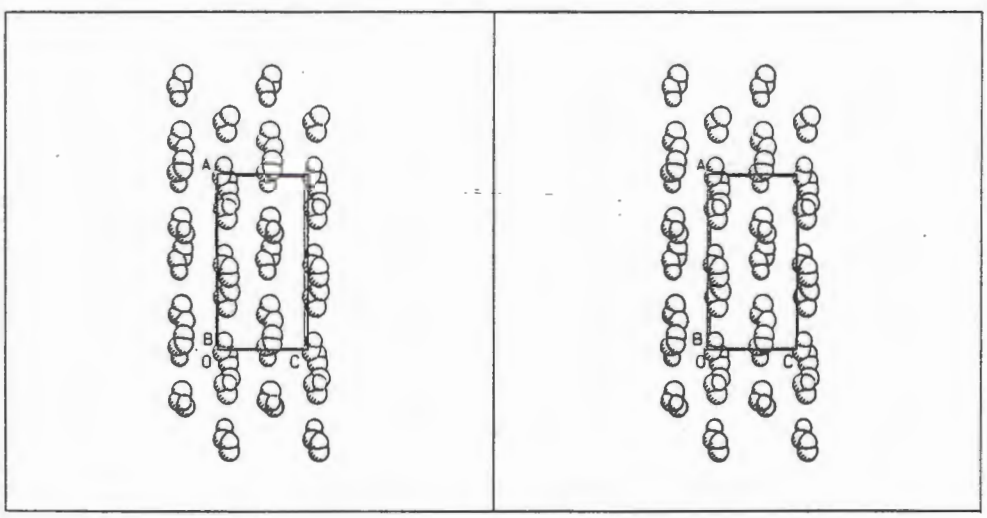

Conformation of the WEB11 molecule in the WEB11-actone (1:2) compound

The torsion angles will be discussed later and were found to be as follows:

C51-C1-C11-C12/C16	C51-C1-C21-C22/C26	C61-C2-C41-C42/C46	C61-C2-C31-C32/C36
30(1)	-78(1)	-70(1)	-38(1)

The conformation of the hydroxy moieties and the orientation of the molecular backbone phenyl rings may be seen by looking along the molecular axis of a WEB11 molecule which is shown below:

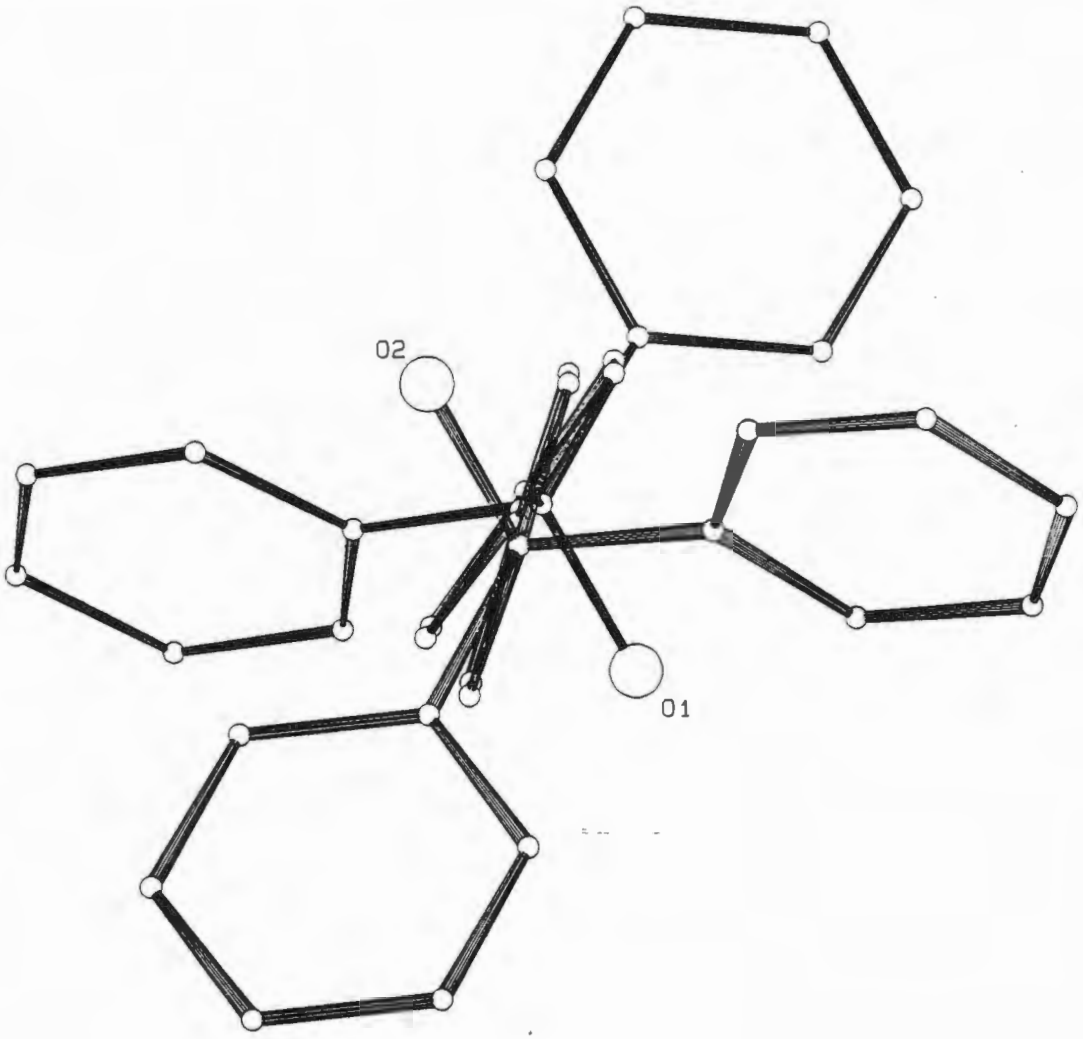

The hydroxy groups have a *trans* conformation and the backbone phenyl rings are almost parallel to one another.

TABLE 3 CRYSTAL DATA AND EXPERIMENTAL DETAILS FOR WEB11 & ACETONE.

Compound	**WEB11 & Acetone**
Molecular formula	$C_{38}H_{30}O_2.2C_3H_6O$
Molecular weight ($gmol^{-1}$)	634.81
Space group	$Pna2_1$
a (Å)	29.169(6)
b (Å)	8.046(1)
c (Å)	15.235(2)
Z	4
V ($Å^3$)	3576(1)
D_c (gcm^{-3})	1.18
D_m (gcm^{-3})	1.17(3)
$\mu(MoK_\alpha)$ (cm^{-1})	0.39
F(000)	1316
Data collection (21°C)	
Crystal dimensions (mm)	0.31x0.38x0.41
Range scanned θ (°)	1-25
Range of indices *h,k,l*	+9,±18,+34
Reflections for lattice parameters no.,θ range (°)	24,16-17
Instability of standard reflections (%)	-6.9
Scan mode	(ω-2θ)
Scan width in(°)	(0.80+0.35tanθ)
Vertical aperture length (mm)	4
Aperture width (mm)	(1.12+1.05tanθ)
Number of reflections collected (unique)	2681
Number of reflections observed with $I_{rel} > 2\sigma I_{rel}$	1954
Final refinement	
Number of parameters	352
R	0.075
wR	0.080
w	$(\sigma^2(F_o)+0.005F_o^2)^{-1}$
S	1.60
Max. shift/e.s.d.	0.14
Max. height in difference electron density map ($eÅ^{-3}$)	0.31
Min. height in difference electron density map ($eÅ^{-3}$)	-0.25

THERMAL ANALYSIS

The thermal traces are shown in figure 15. The DSC trace of the WEB11-acetone compound exhibits a complex decay. There are three endotherms evident in the DSC trace, A, B and C. A and B correspond to desorption of the acetone and collapse of the host-guest complex. Endotherm A occurs at 70°C and has a ΔH value of 43.8kJmol^{-1}. Endotherm B occurs at 90°C and has ΔH of melting of 33.3kJmol^{-1}. The sharp endotherm, C, occurs at 165°C due to the melting of WEB11 and has a ΔH of 42kJmol^{-1}. This is some 20°C lower than was obtained for the melting of α-form of WEB11 (2) possibly because another polymorph of WEB11 has formed. The % weight loss obtained from TG is 18.0% which agrees well with the calculated value of 18.3%. From plots of log β versus the inverse of absolute temperature, activation energies for guest desorption were found to lie in the range 92-105kJmol^{-1} **(8)**.

Figure 15

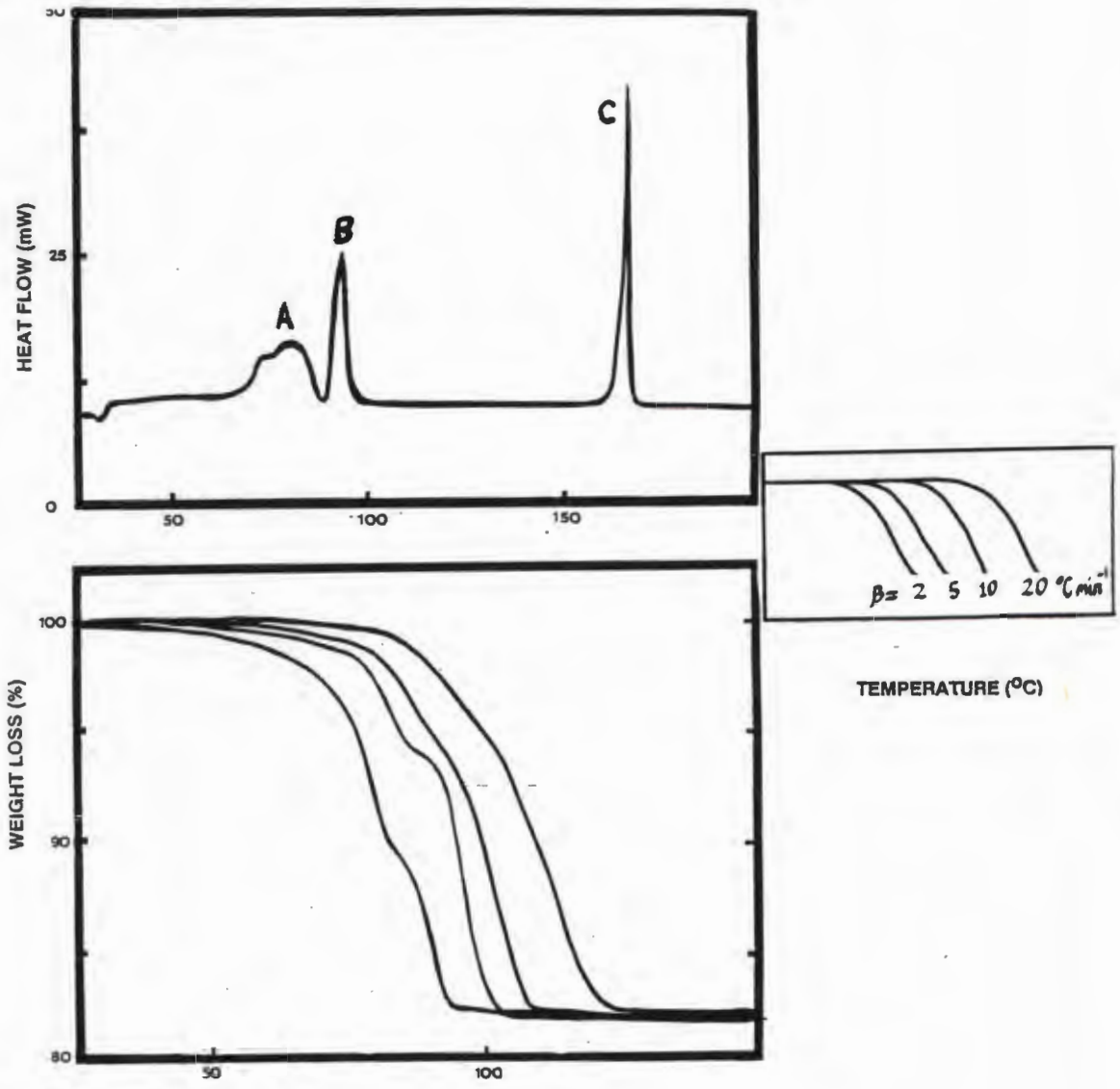

8 JH Flynn & LA Wall, *Polymer Letters*, Vol. 4, 1966, 323-328

THE STRUCTURE OF THE WEB11-1,4-DIOXANE (1:2) INCLUSION COMPOUND

WEB11 co-crystallized with 1,4-dioxane in a 1:2 host-guest ratio. X-ray oscillation and Weissenberg photographs showed it to be monoclinic. The crystal reflection data exhibited the following non-extinction conditions:

hkl: no conditions

h0l: h+l=2n

(h00: h=2n)

(00l: l=2n)

0k0: k=2n

Solving in $P2_1/n$ yielded a best solution with a combined figure of merit of 0.078 and R_E of 0.241 for 25 surviving atoms. The asymmetric unit contained a molecule of WEB11 lying on a centre of symmetry at Wyckoff *c* and one molecule of dioxane in a general position. Two guests hydrogen bond to one WEB11 molecule with an O---O separation of 2.780(4)Å.

Figure 16 the crystal packing of WEB11-dioxane viewed along [0 1 0]

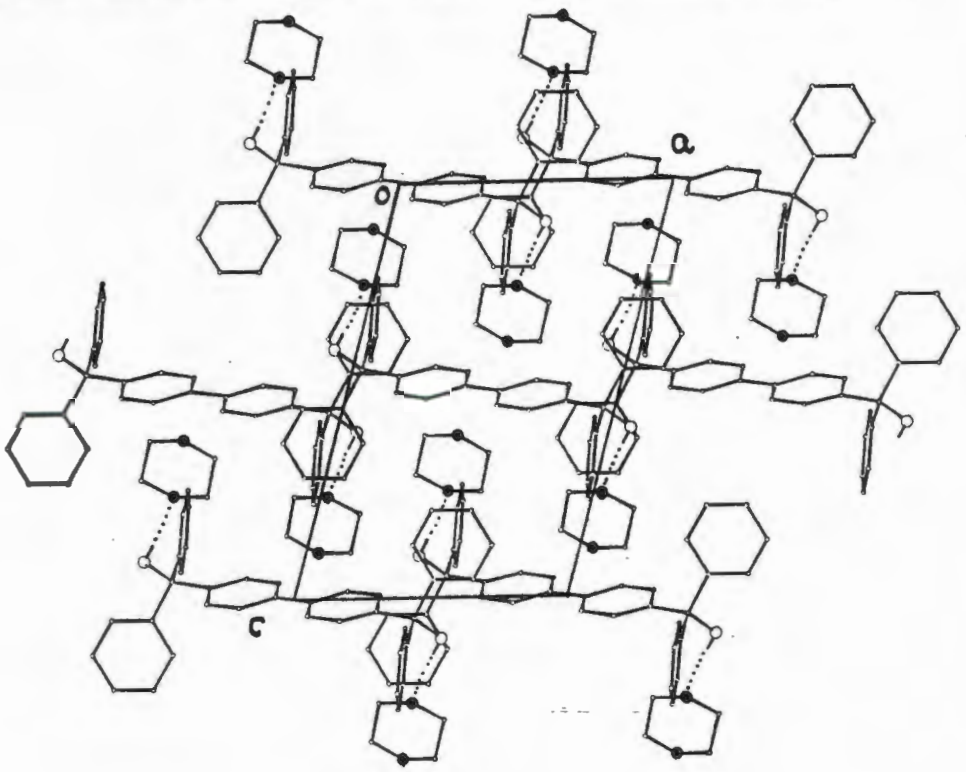

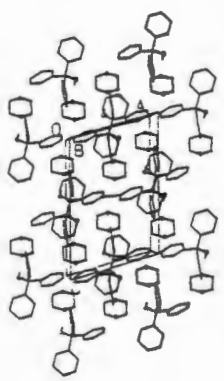

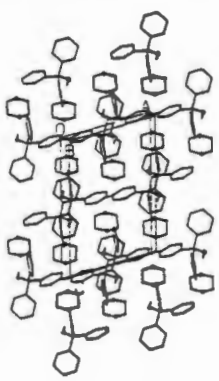

Figure 17 the packing motif viewed along [0 0 1]

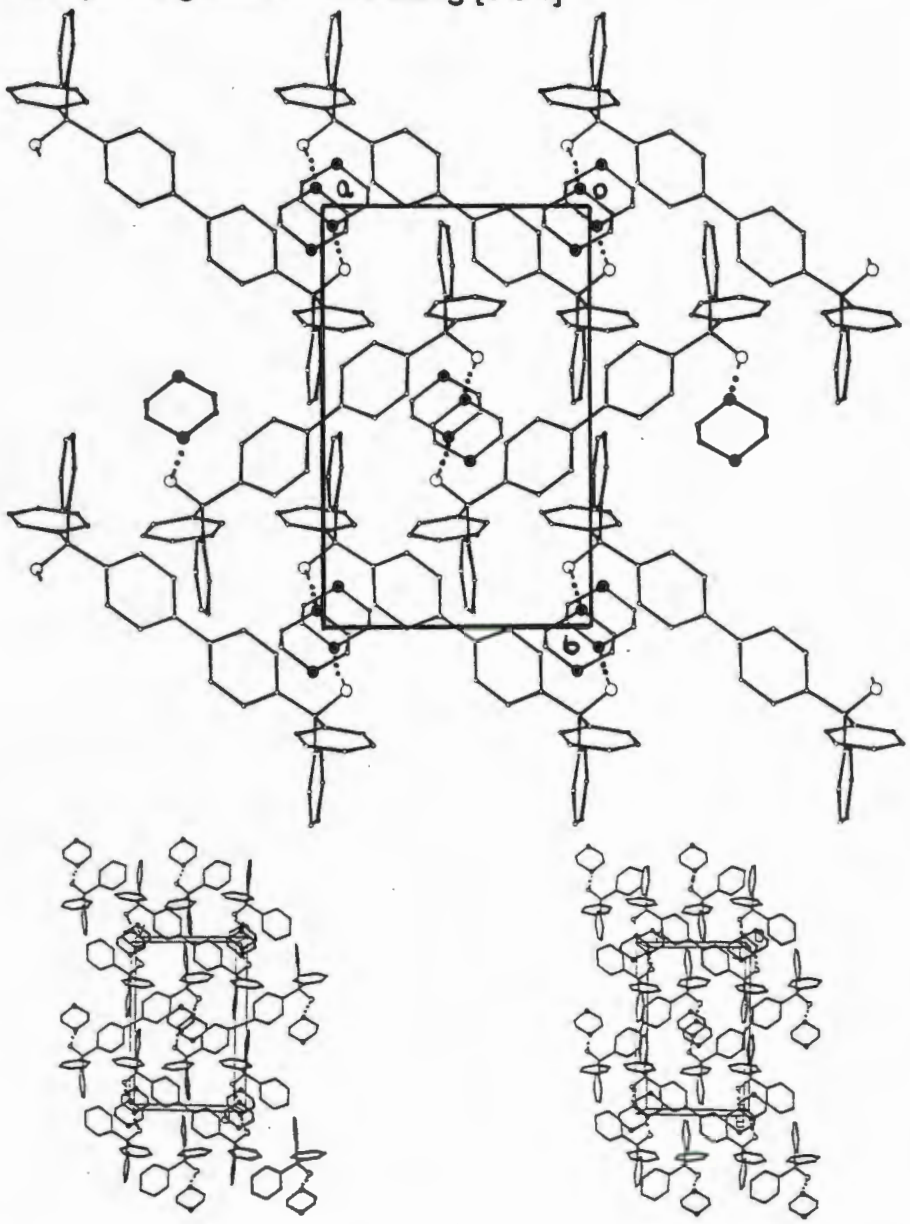

Figure 18 the chair conformation adopted by 1,4-dioxane guest in the WEB11 inclusion compound.

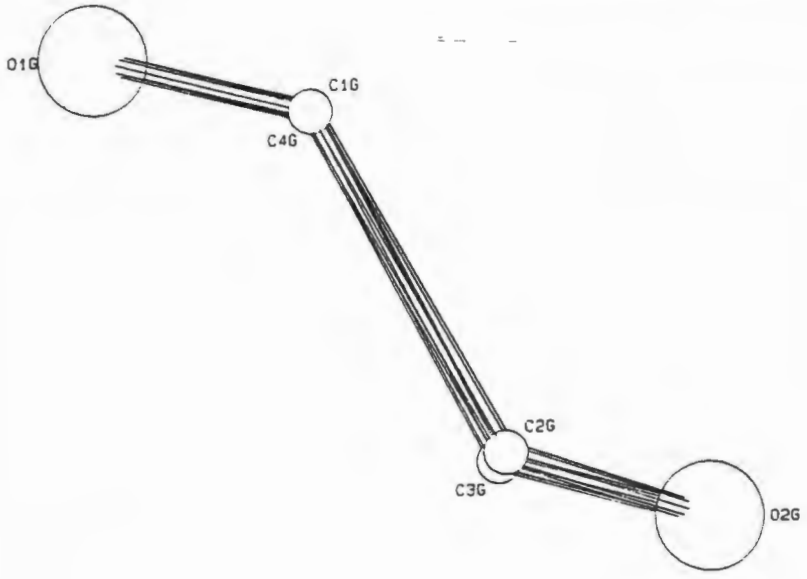

Despite the fact that a centrosymmetric location for a molecule such as WEB11 would appear to be disfavoured due to close contacts between the ortho hydrogens of the phenyl ring backbone(see figure 19) two examples of centrosymmetric WEB11 host molecules were found. This is not anomalous if the famous example of the structure of biphenyl is considered. Biphenyl crystallises in the monoclinic cell $P2_1/a$, $Z=2$ so that a molecule of biphenyl is required to lie on a crystallographic centre of symmetry. Thus it is necessary that the two rings are coplanar **(9)** which occurs due to stability achieved by favourable stacking of the molecules. The non-bonded distance between the ortho hydrogen atoms in the biphenyl structure is 2.07Å whereas this distance is shorter in the WEB11 & dioxane structure at a value of 1.99Å implying that there is more strain in this example. Correspondingly the bonded distance between the two phenyl rings has a value of 1.507Å for the biphenyl but a lower value of 1.481Å for the WEB11-dioxane structure. The biphenyl system provides a large number of examples where higher energy conformations are stabilised by packing forces **(10)**. The alignment of the molecular axes of the WEB11 host molecules in this inclusion compound constitutes stacking of the phenyl backbone rings.

Figure 19

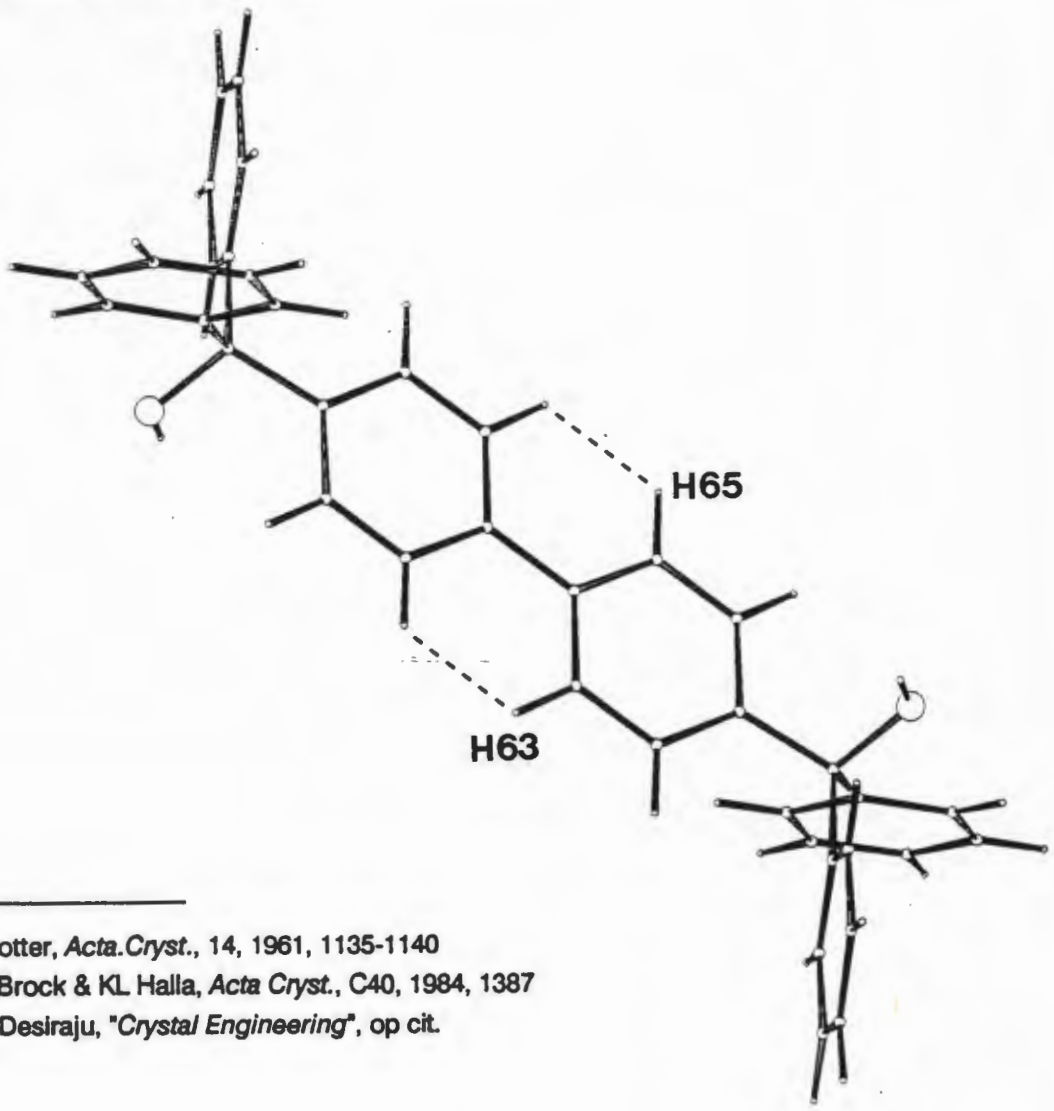

---

9 J Trotter, *Acta.Cryst.*, 14, 1961, 1135-1140

10 CP Brock & KL Halla, *Acta Cryst.*, C40, 1984, 1387
GR Desiraju, "*Crystal Engineering*", op cit.

The torsion angles had estimated standard deviations and were found to have the following values:

C51-C1-C11-C12/C16	C51-C1-C21-C22/C26
28	80

An illustration of the conformation adopted by a WEB11 molecule in the dioxane inclusion compound is shown below. The coplanarity of the phenyl rings in the molecular rings is evident.

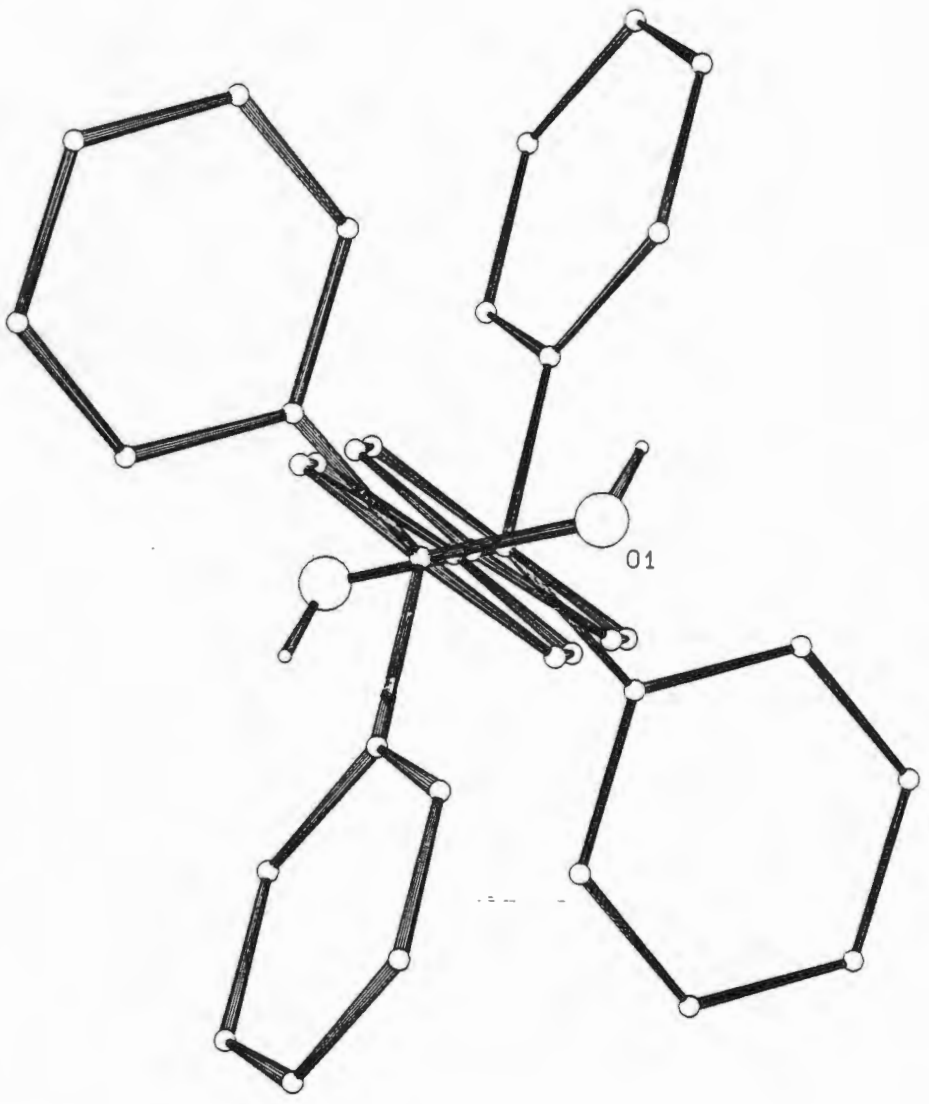

The program OPEC located guest cavities which had dimensions of 7.55Å x 11.6Å, at y=0.5 and at y=1, these are shown in figure 20 (i) and (ii) respectively.

Figure 20 WEB11 & dioxane - an ædiculate host-guest compound

(i)

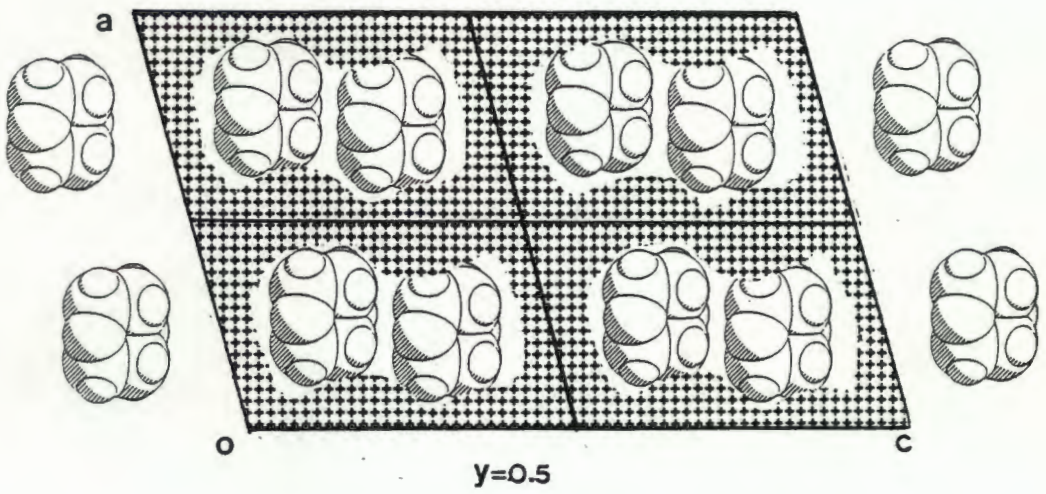

(ii)

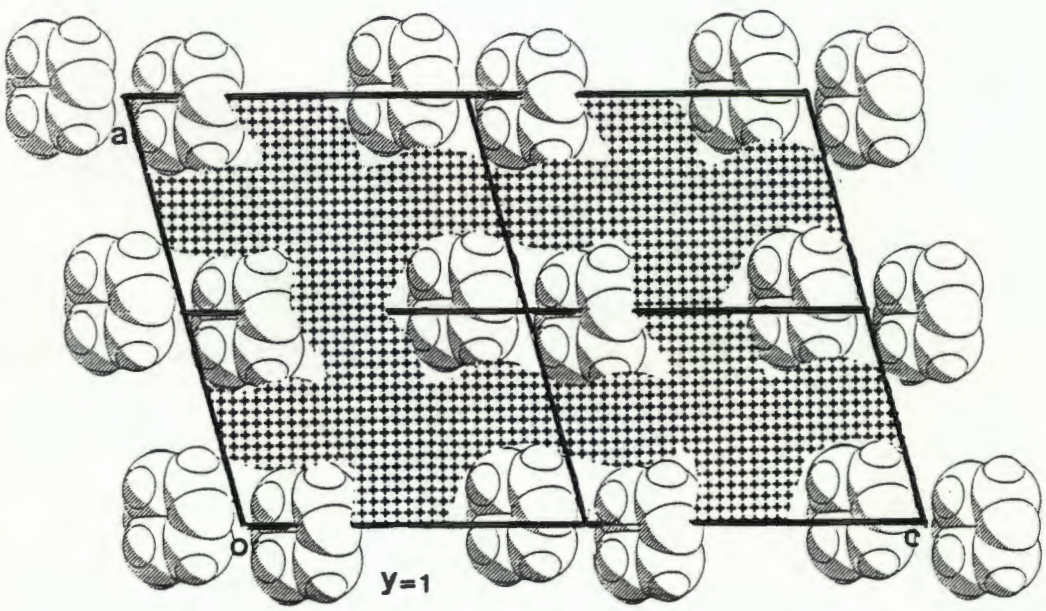

THERMAL ANALYSIS

There is stoicheiometric loss of guest observed in the TG trace which is shown in figure 21. The calculated percentage loss is 25.4 % and the experimental percentage loss 23.4%. The activation energy range obtained from plots of logβ versus the inverse of absolute temperature was 136-163kJmol^{-1} for the decomposition, see figure 22. The DSC profile shows that there is desorption of the guest at 112^{o}C which is followed by the melt of WEB11 at T_{on}=155.9^{o}C. This is approximately thirty degrees lower than the melting points that were measured for the alpha forms of WEB11, and once again it is possible that a lattice rearrangement of α-form WEB11 is taking place to form a new polymorph of WEB11 with its own unique melting point.

Figure 21

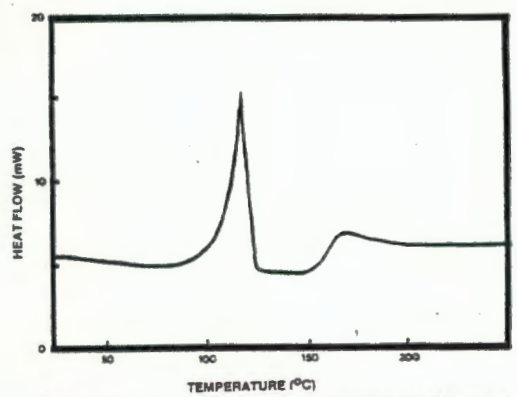

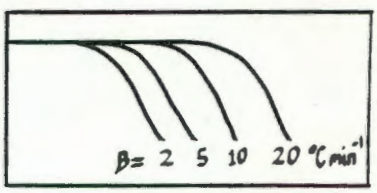

Figure 22

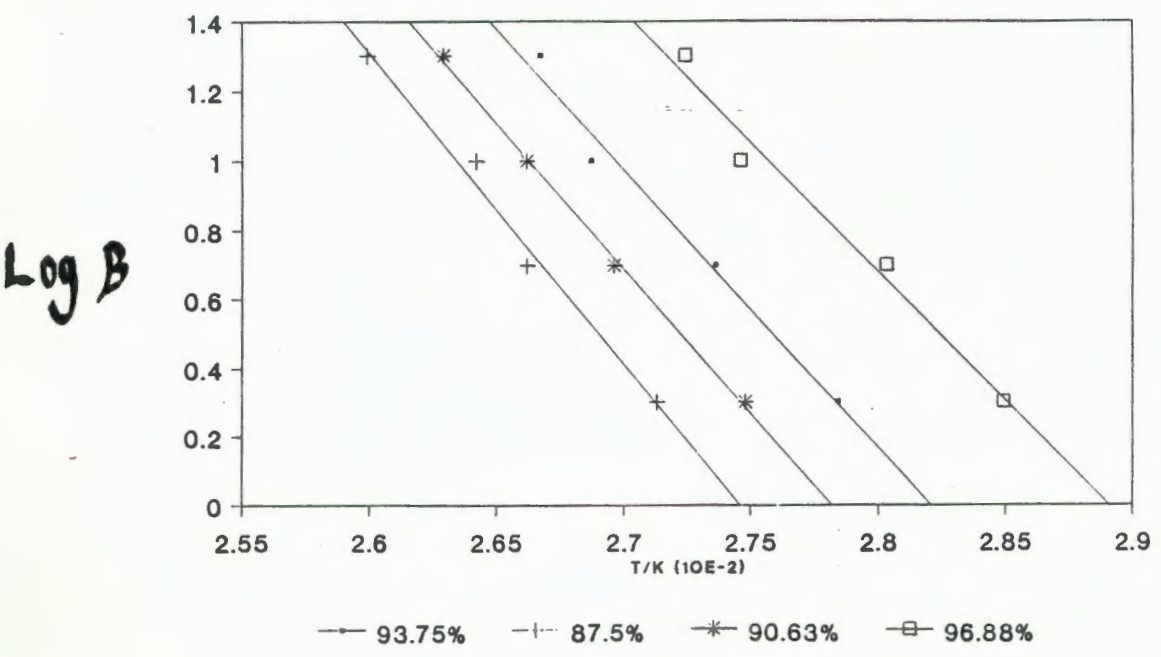

TABLE 4 CRYSTAL DATA AND EXPERIMENTAL DETAILS FOR WEB11-1,4-DIOXANE.

Compound	**WEB11-1,4-dioxane**
Molecular formula	$C_{38}H_{30}O_2 \cdot 2C_4H_8O_2$
Molecular weight ($gmol^{-1}$)	654.80
Space group	$P2_1/n$
a (Å)	9.434(2)
b (Å)	14.152(5)
c (Å)	14.503(1)
β (°)	105.36(1)
Z	2
V ($Å^3$)	1866(1)
D_c (gcm^{-3})	1.22
D_m (gcm^{-3})	1.20(2)
$\mu(MoK_\alpha)$ (cm^{-1})	0.44
F(000)	836
Data collection (21°C)	
Crystal dimensions (mm)	0.38x0.38x0.44
Range scanned θ (°)	1-25
Range of indices *h,k,l*	±11,+16,+17
Reflections for lattice parameters no.,θ range (°)	24,16-17
Instability of standard reflections (%)	35.3
Scan mode	(ω-2θ)
Scan width in(°)	(0.85+0.35tanθ)
Vertical aperture length (mm)	4
Aperture width (mm)	(1.12+1.05tanθ)
Number of reflections collected (unique)	2712
Number of reflections observed with $I_{rel} > 2\sigma I_{rel}$	1989
Final refinement	
Number of parameters	240
R	0.060
wR	0.065
w	$(\sigma^2(F_o)+0.001F_o^2)^{-1}$
S	1.72
Max. shift/e.s.d.	0.51
Max. height in difference electron density map ($eÅ^{-3}$)	0.22
Min. height in difference electron densitymap ($eÅ^{-3}$)	-0.31

THE STRUCTURE OF THE WEB11-ACETOPHENONE (1:1) INCLUSION COMPOUND

X-ray photography found no symmetry other than $\bar{1}$ and direct methods calculations were carried out in $P\bar{1}$. The E-statistics favoured the choice of the centric space group and the combined figure of merit for the best solution was 0.044. The R_E value was 0.257 and a molecule of WEB11 at a crystallographic centre of symmetry, Wyckoff *f* as well as one acetophenone molecule were located. The phenyl rings of the molecular backbone are coplanar and the non-bonded distance between the ortho hydrogen atoms is 2.05Å. The hydroxy functions of the host are hydrogen bonded to the carbonyl functions of the acetophenone (O---O = 2.872Å). The position of the hydroxyl hydrogen could not be refined and it was thus not included in the final model. All non-hydrogen atoms were refined anisotropically and the positions of all hydrogens were calculated and refined with linked temperature factors. A description of the data collection and crystal parameters may be found in Table 5. The temperature factors of the guest atoms as well as those of the backbone phenyl ring were consistently higher than the remainder of the host molecule. These factors coupled with the residual electron density of approximately ½ an electron per $Å^3$ in the region of the backbone phenyl ring only allowed the value of the final R to converge to a value of 0.132.
The packing in the crystal may be viewed along [1 0 0] in figure 23. Alignment and stacking of the backbone phenyl rings may be seen.

Figure 23

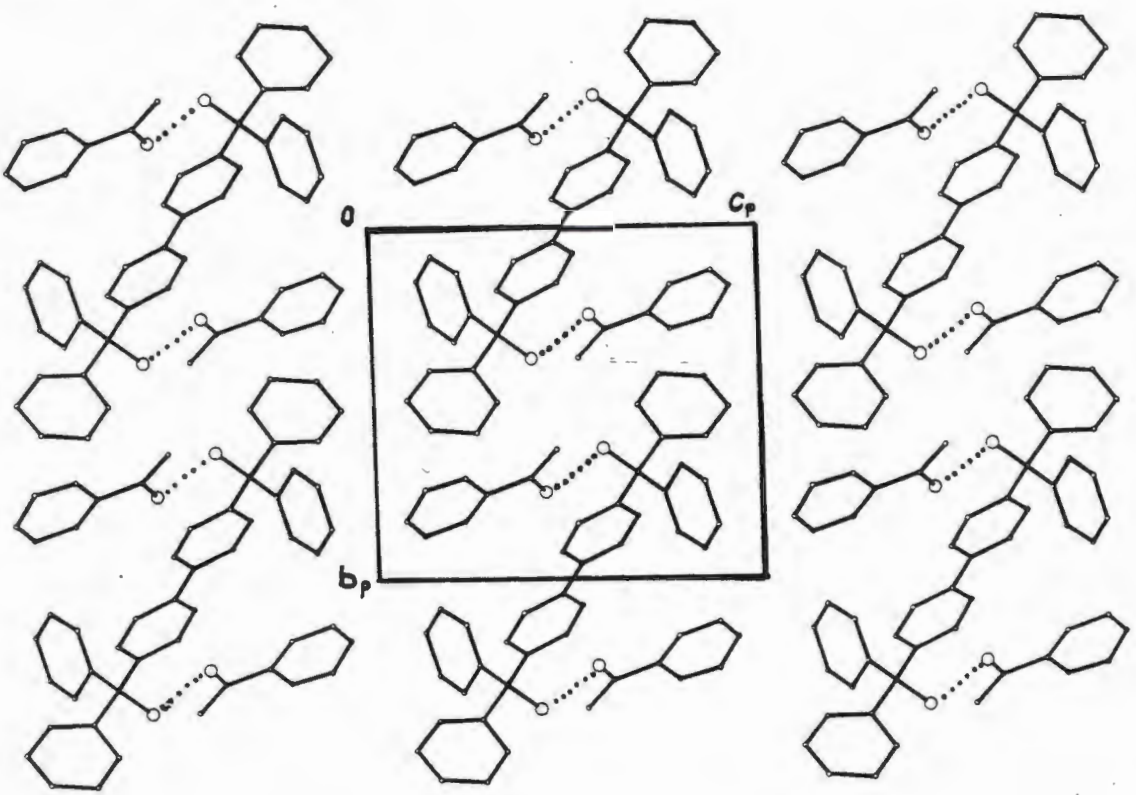

Figure 24 The packing of WEB11-acetophenone viewed along [0 0 1], the molecular backbones align parallel to one another

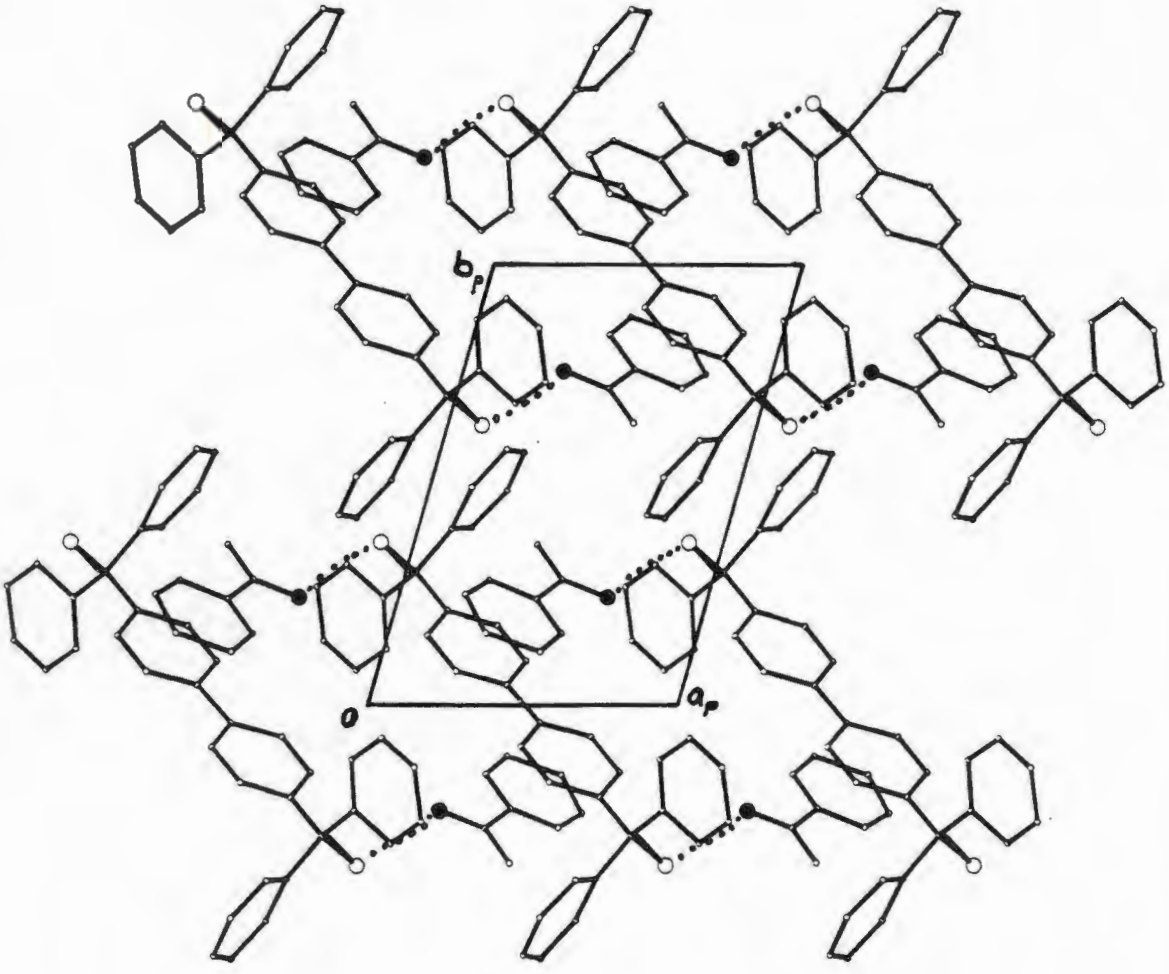

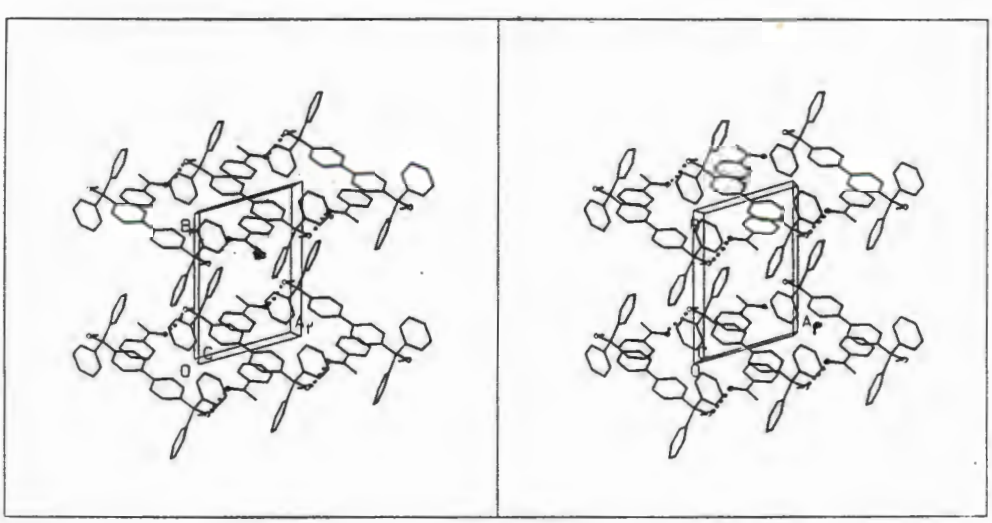

THERMAL ANALYSIS (figure 25)

There is stoicheiometric loss of guest observed in the TG: the calculated % loss = 31.7% and experimental % loss = 32.8%. The DSC trace exhibits a single endotherm corresponding to the melt of the complex, (T_{on} = 72.5, enthalpy of melting = 55 kJmol^{-1}).

Figure 25

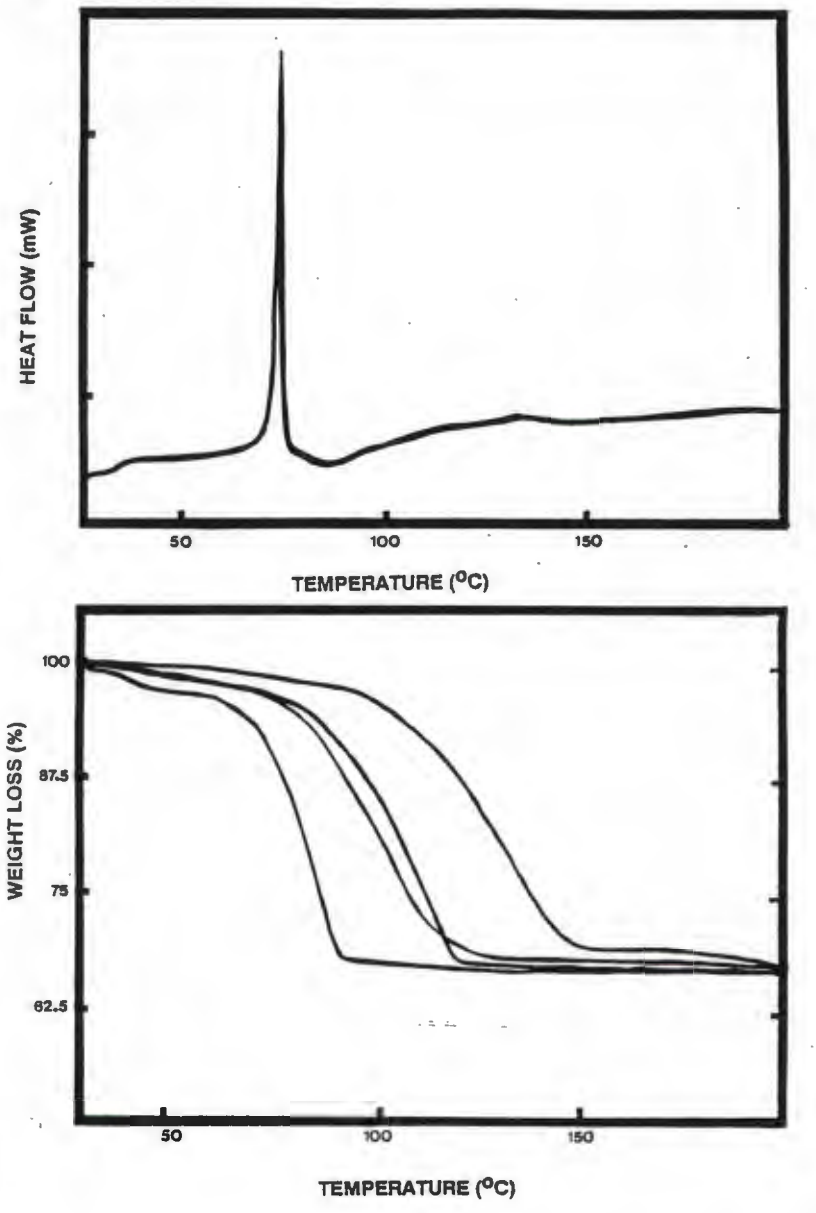

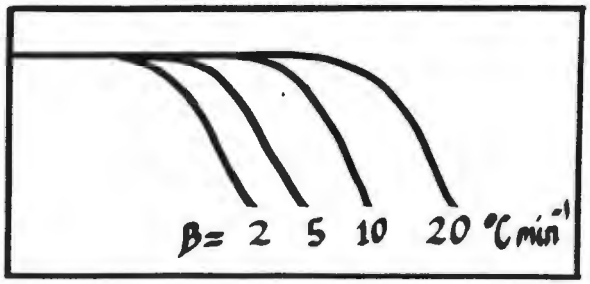

TABLE 5 CRYSTAL DATA AND EXPERIMENTAL DETAILS FOR WEB11-ACETOPHENONE STRUCTURE.

Compound	**WEB11-Acetophenone**
Molecular formula	$C_{38}H_{30}O_2.2C_8H_8O$
Molecular weight ($gmol^{-1}$)	758.95
Space group	$P\bar{1}$
a (Å)	8.005(6)
b (Å)	11.464(3)
c (Å)	12.338(3)
α (°)	85.14(2)
β (°)	76.89(4)
γ (°)	73.71(4)
Z	1
V ($Å^3$)	1058(1)
D_c (gcm^{-3})	1.19
D_m (gcm^{-3})	1.17(2)
$\mu(MoK_\alpha)$ (cm^{-1})	0.40
F(000)	402
Data collection (21°C)	
Crystal dimensions (mm)	0.31x0.38x0.47
Range scanned θ (°)	1-25
Range of indices *h,k,l*	±9,±13,+14
Reflections for lattice parameters no.,θ range (°)	24,16-17
Instability of standard reflections (%)	4.0
Scan mode	(ω-2θ)
Scan width in(°)	(0.85+0.35tanθ)
Vertical aperture length (mm)	4
Aperture width (mm)	(1.12+1.05tanθ)
Number of reflections collected (unique)	2992
Number of reflections observed with $I_{rel}>2\sigma I_{rel}$	2105
Final refinement	
Number of parameters	256
R	0.132
wR	0.137
w	$(\sigma^2(F_o)+0.001F_o^2)^{-1}$
S	13.98
Max. shift/e.s.d.	0.145
Max. height in difference electron density map ($eÅ^{-3}$)	0.53
Min. height in difference electron density map ($eÅ^{-3}$)	-0.55

TORSION ANGLES OF WEB11-KETONE STRUCTURES

The torsion angles of the WEB11 host-guest coordination assisted compounds as well as WEB10 are illustrated in bar graph form in figure 26. As was the case in Host1, the phenyl rings do not finely adjust in order to capture a guest but act as steric barriers for the formation of channels and cavities. The phenyl rings also play a minor stabilizing role with respect to van der Waals interactions in the host-guest crystal.

Figure 26

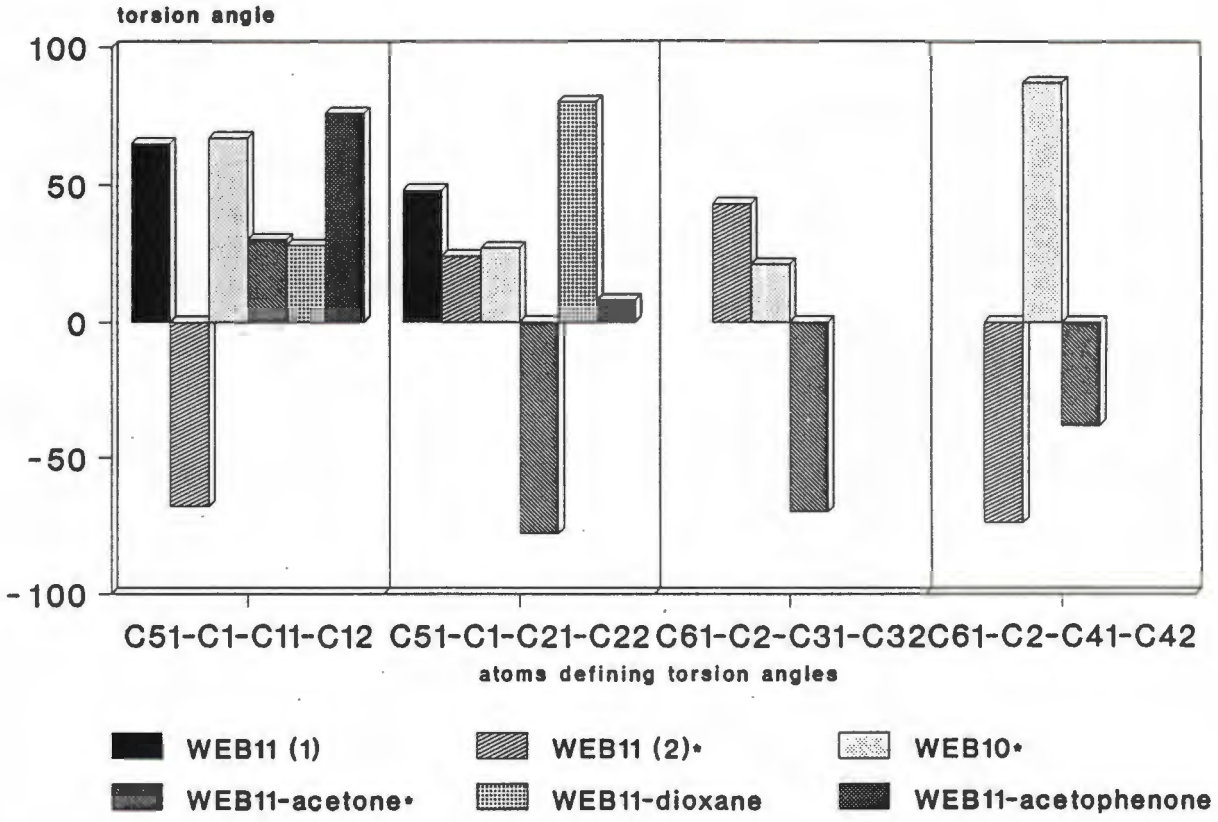

* the asymmetric unit comprises one molecule of WEB11

THE STRUCTURE OF WEB11-p-XYLENE (2:3½) INCLUSION COMPOUND

The only xylene isomer to be included by WEB11 was p-xylene. X-ray photography found the space group to be monoclinic. Structure solution was carried out by direct methods in $P2_1/n$. The mean $|E^2-1|$ statistics were close to the theoretical values expected for centric space groups. The combined figure of merit had a value of 0.202 and the R_E was 0.302 for 99 surviving atoms. The host-guest ratio was found to be 2:3½. One xylene guest molecule lay at a centre of symmetry, Wyckoff *a*. The structure was refined using blocked matrix least-squares analysis. The temperature factors of the guest were consistently higher than those of the host and owing to the large number of parameters, only the host and the two guests with the lowest temperature factors, were treated anisotropically. The hydroxyl hydrogen atoms were all successfully located and refined as constrained to their parent carbon atoms. Details of the data collection and the crystal parameters may be found in Table 6.
The hydroxy moieties of four WEB11 host molecules interact to from hydrogen bonded tetramers which are shown below.

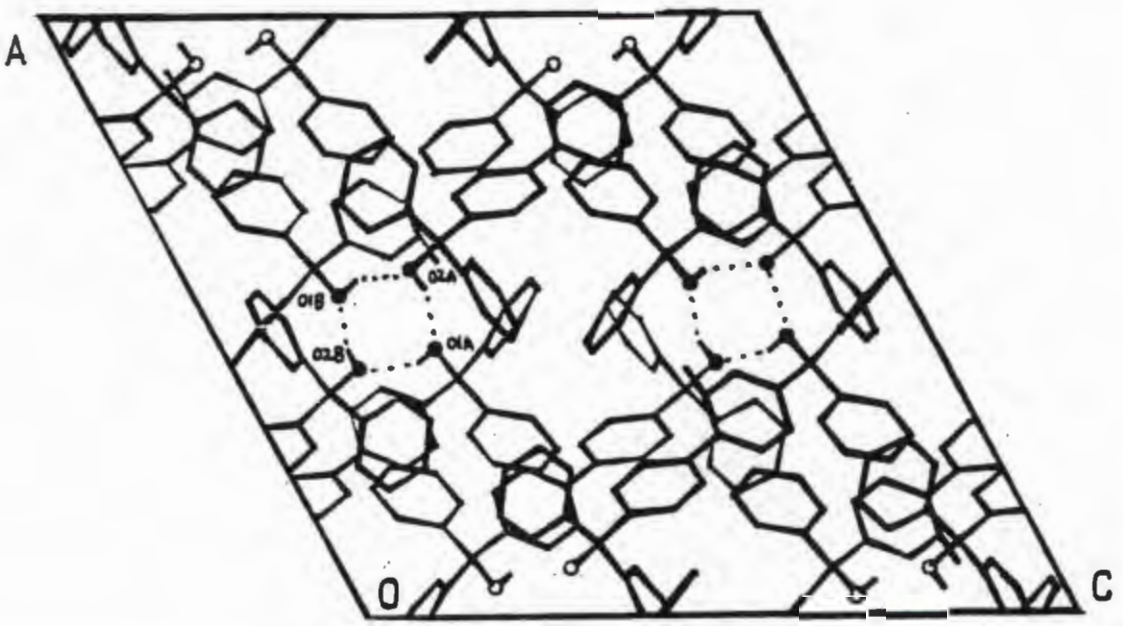

The oxygen-to-oxygen hydrogen bonding distances are:

O2A---O1A = 2.913(6)Å (x+1½,1½-y,1½+z)
O1A---O2B = 2.799(6)Å (x+½,1½-y,½+z)
O1B---O2A = 2.860(6)Å (x+½,1½-y,½+z)
O2B---O1B = 2.875(6)Å (x+½,1½-y,½+z)

Figure 27 illustrates the packing viewed along [0 1 0] of this inclusion compound, with the guests omitted for the purposes of clarity.

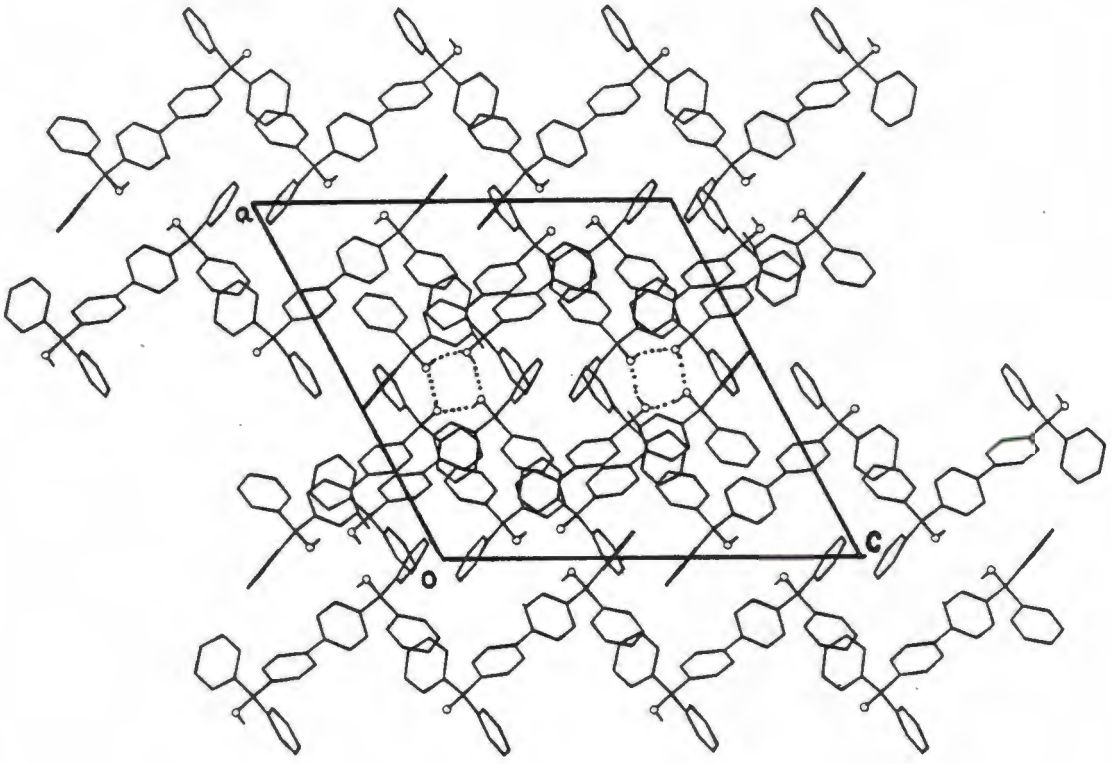

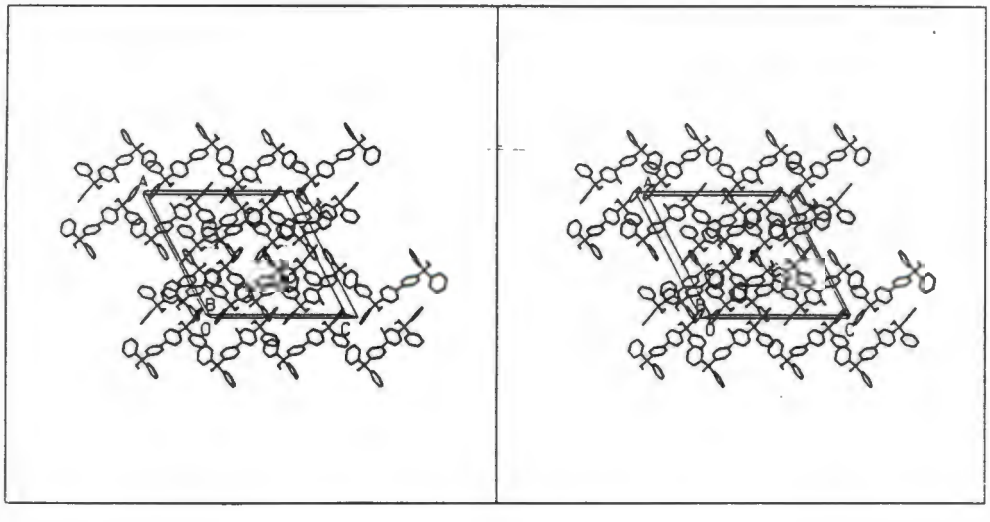

Figure 28 (i) shows how the WEB11 host molecules pack in a herringbone motif viewed along [1 0 0], with the guests omitted.

28 (i)

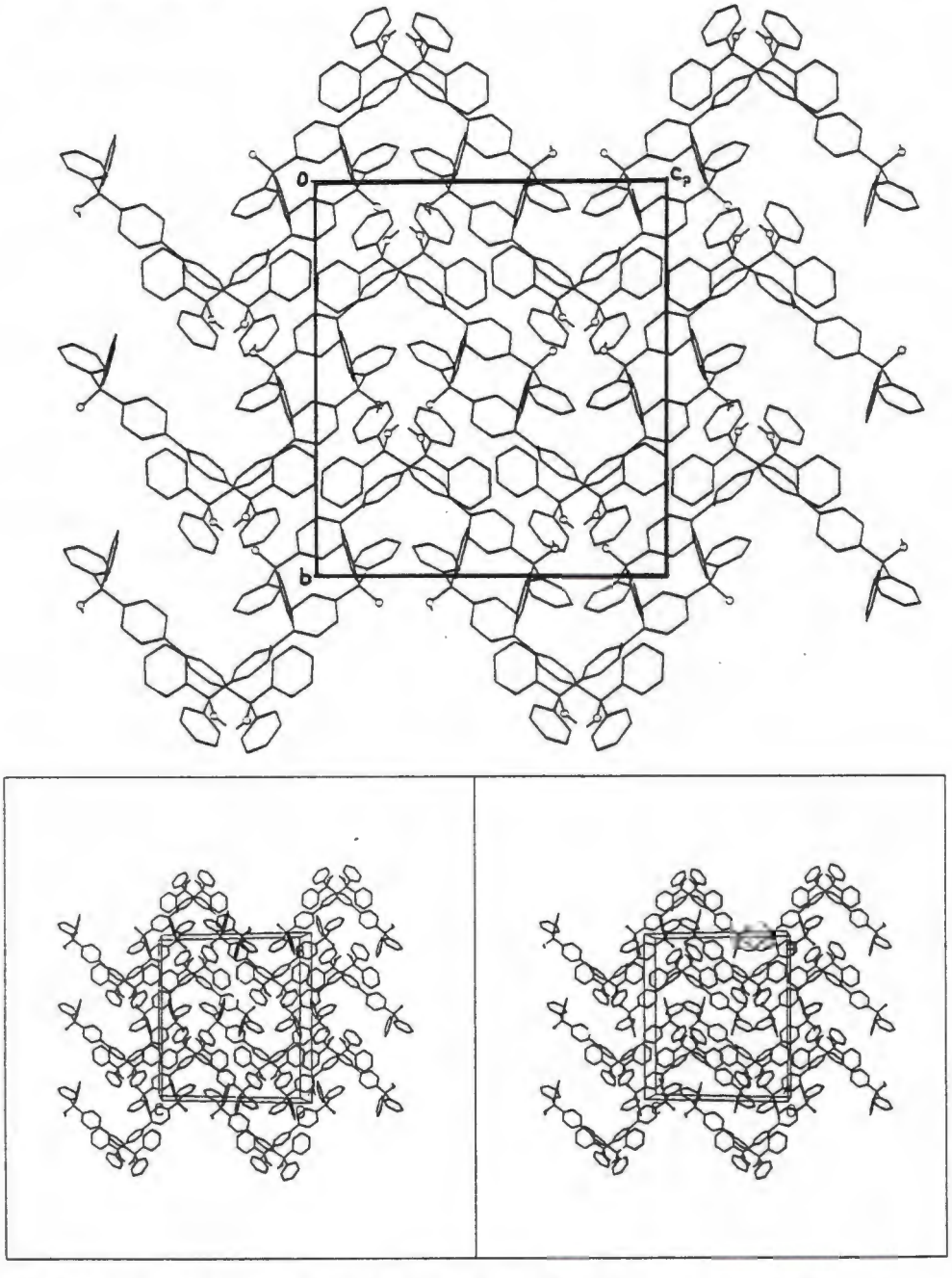

Figure 28 (ii) shows a stereoscopic view of the guests along [1 0 0].

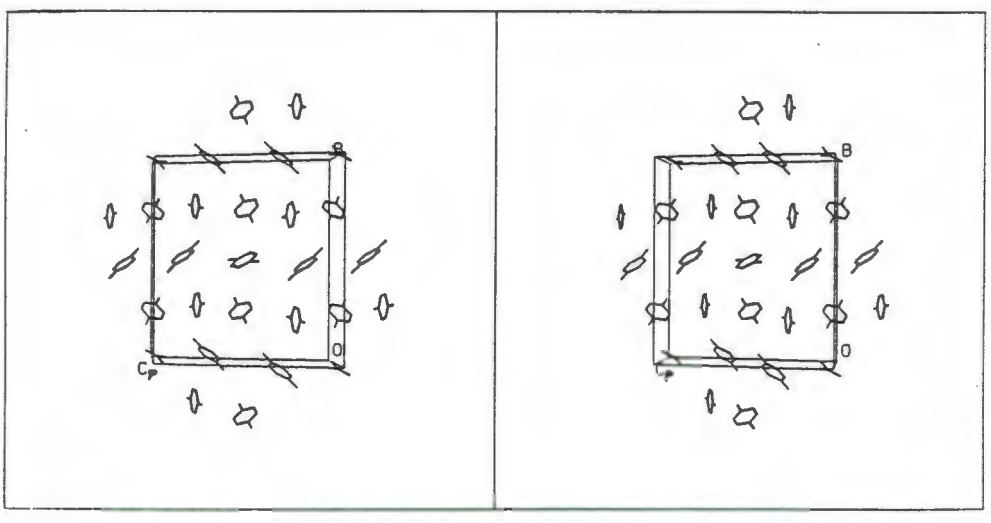

The packing of guests E, F, H and I viewed along [0 0 1] is illustrated in figures 29i, 29ii, 29iii, 29iv.

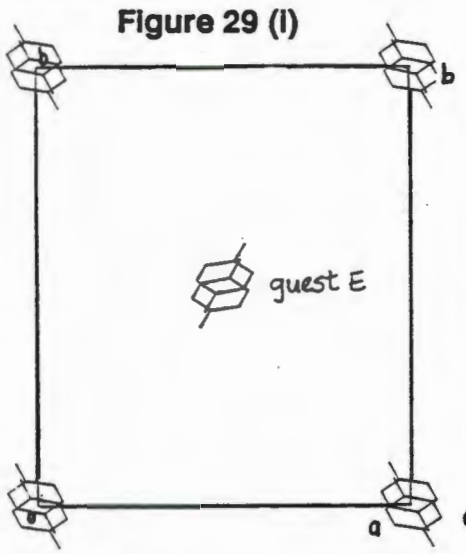

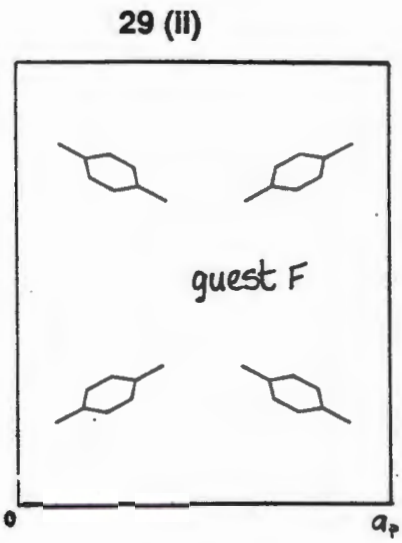

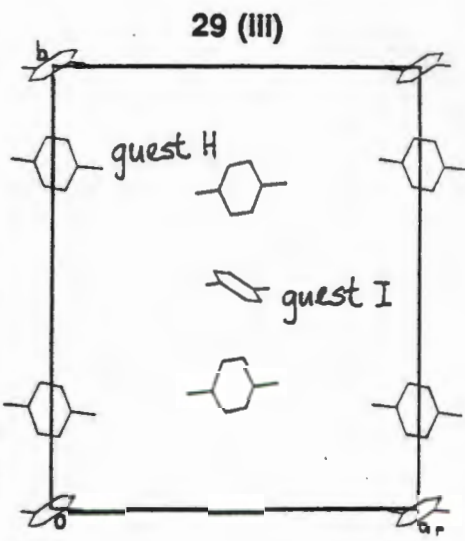

Figure 29 (iv) View along [0 0 1] of the packing of all the guests.

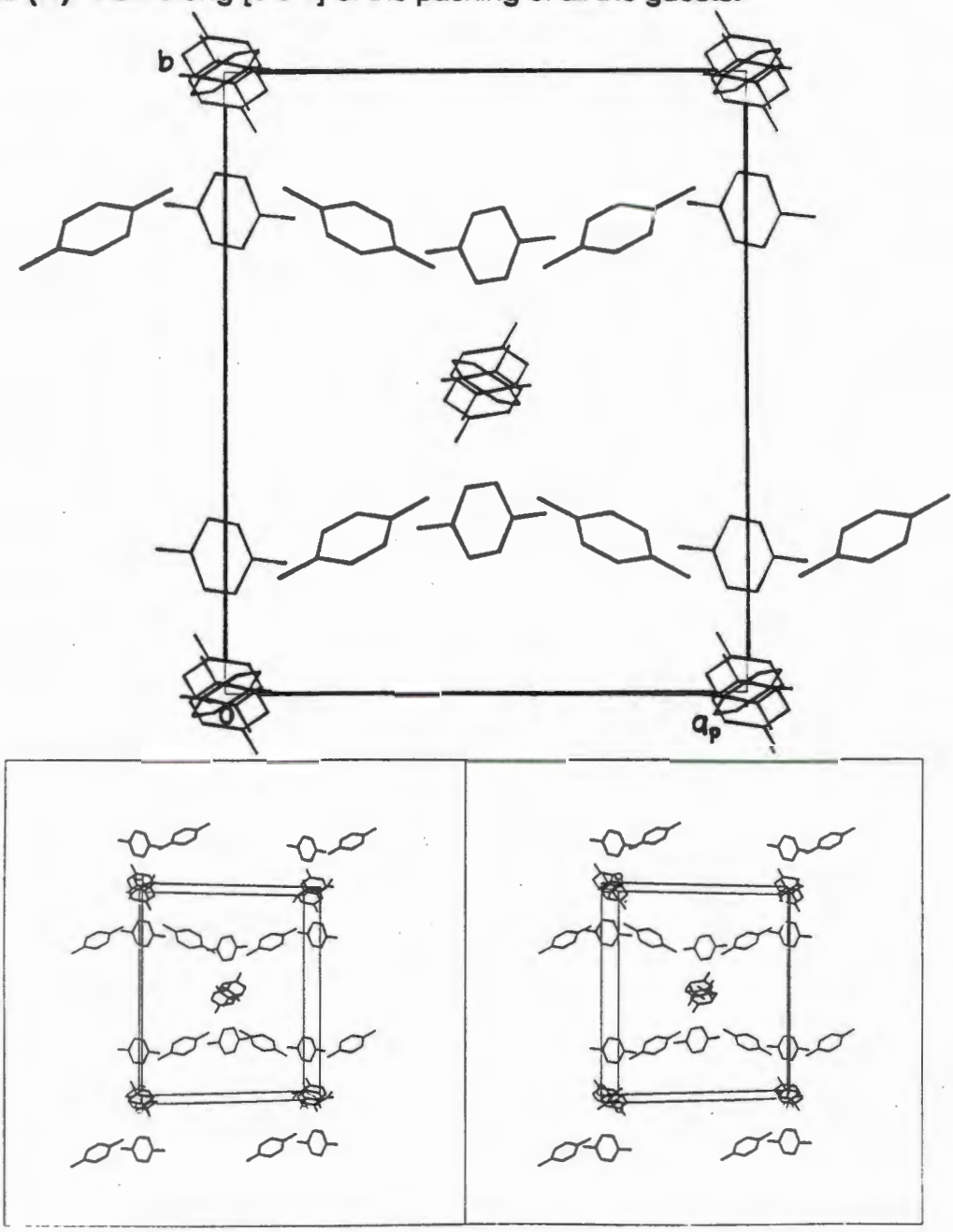

Guests E and I lie in channels running parallel to c. This is illustrated in the packing diagram below in which the host molecules exhibit van der Waals radii.

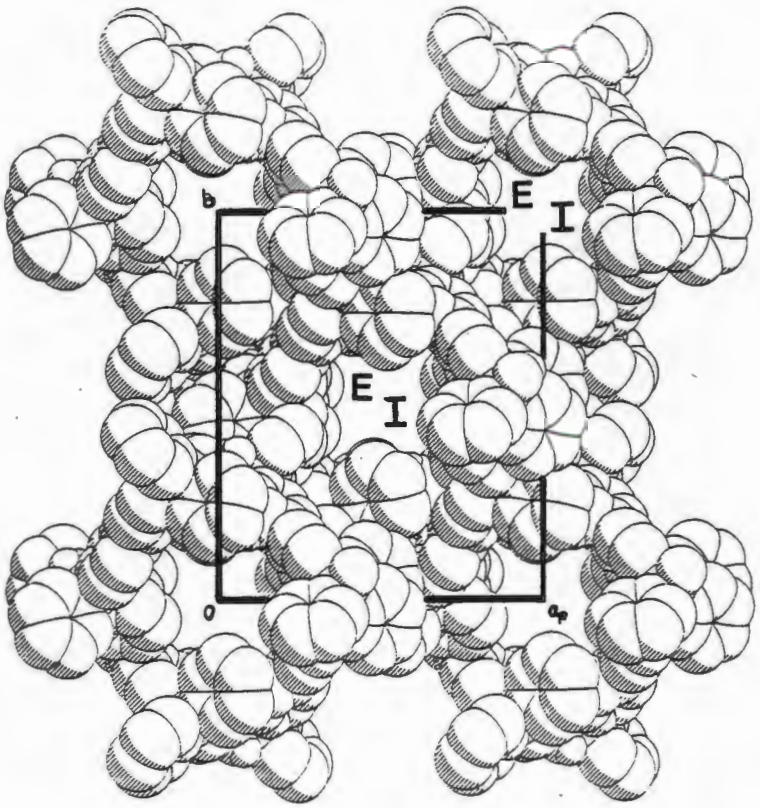

Guest molecules H and F lie in channels running along [1 0 1] at b values of 0.25 and 0.75 respectively.

viz.

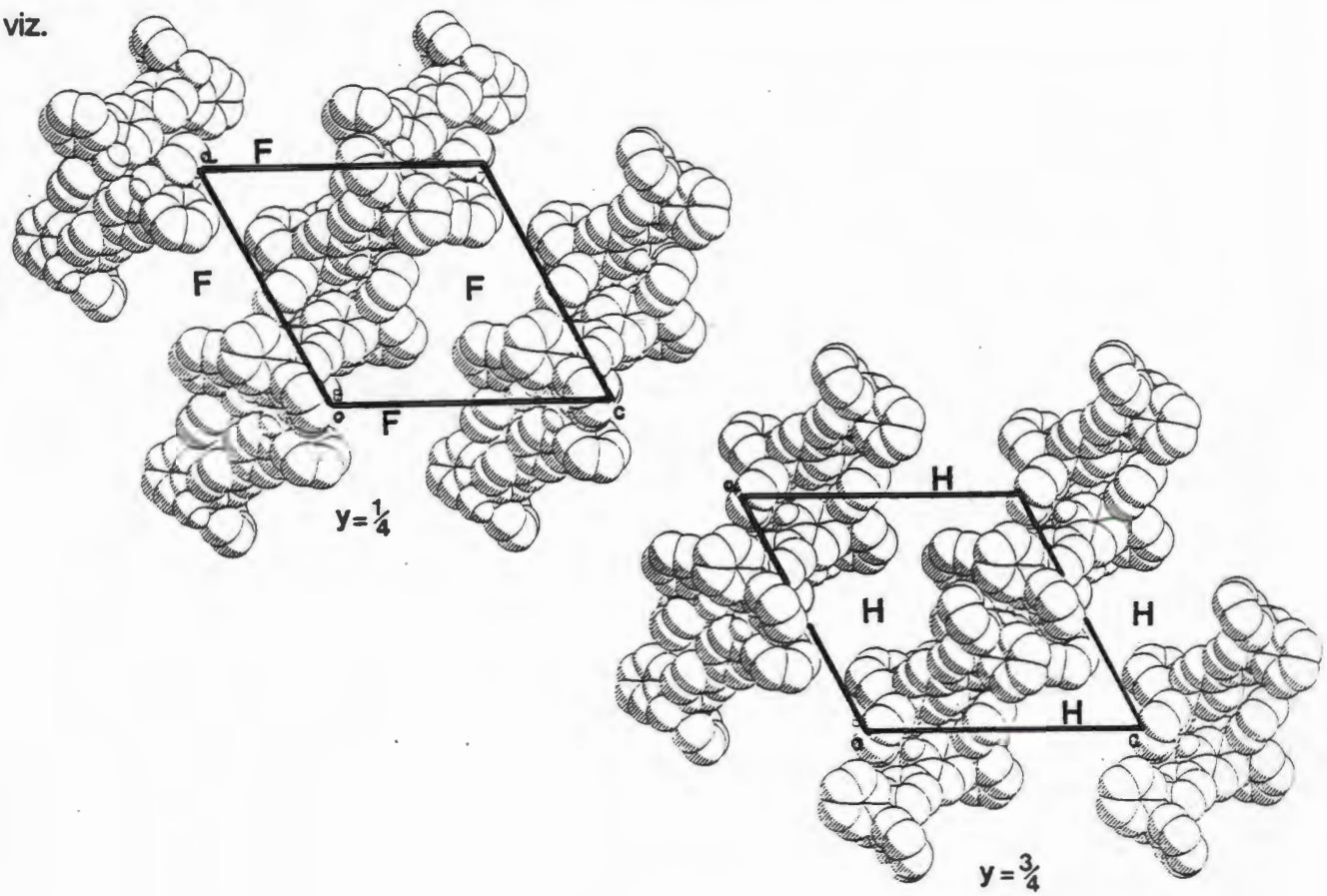

The torsion angles chosen as previously defined were found to be:

	C51-C1-C11-C12/C16	C51-C1-C21-C22/C26	C61-C2-C31-C32/C36	C61-C2-C41-C42/C46
A	25(1)	73(1)	-73(1)	-18(1)
B	73(1)	13(1)	-79(1)	-11(1)

where A and B are the two molecules of WEB11 comprising the asymmetric unit.

Figures 30 (i) and (ii) illustrate the gauche conformation of the hydroxy moieties on the molecules of WEB11. The WEB11-p-xylene complex is an example of a host-host coordination assisted inclusion compound. The guests are held in place by van der Waals forces. In order to permit interaction between the molecules of WEB11, the hydroxyl groups adopt a gauche conformation.

Figure 30

(i)

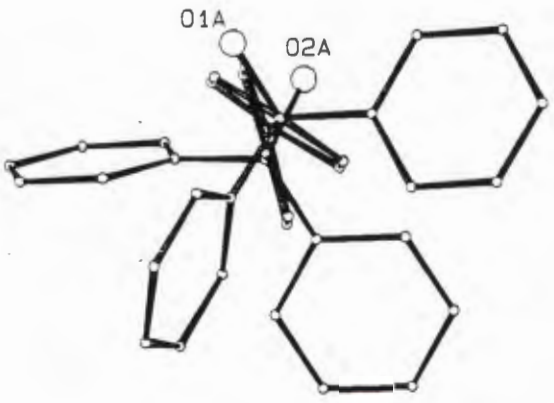

(ii)

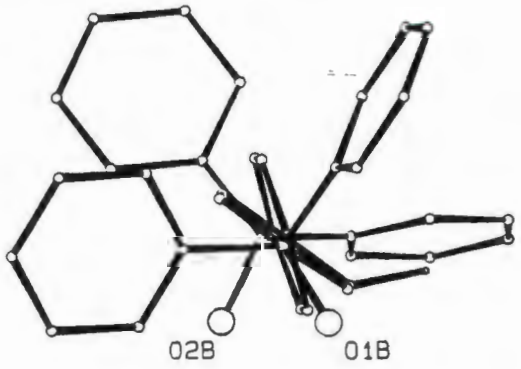

THERMAL ANALYSIS (FIGURE 31)

The stoicheiometry of this host-guest compound was confirmed since the experimental % guest loss of 26.2% correlated closely with the calculated value of 26.4%. The TG trace shows a two step decay. The plots of logβ versus the inverse of absolute temperature, shown in figure 32, were curved which is indicative of a complex decomposition mechanism. The DSC trace also indicates a complicated thermal decay: the endotherm A at T_{on}=75.2°C corresponds to desorption of the guest. At 165°C, there is a small endotherm B which is followed by another larger one, C, at about 182°C. These two endotherms probably correspond to the melting of different polymorphs of WEB11.

Figure 31

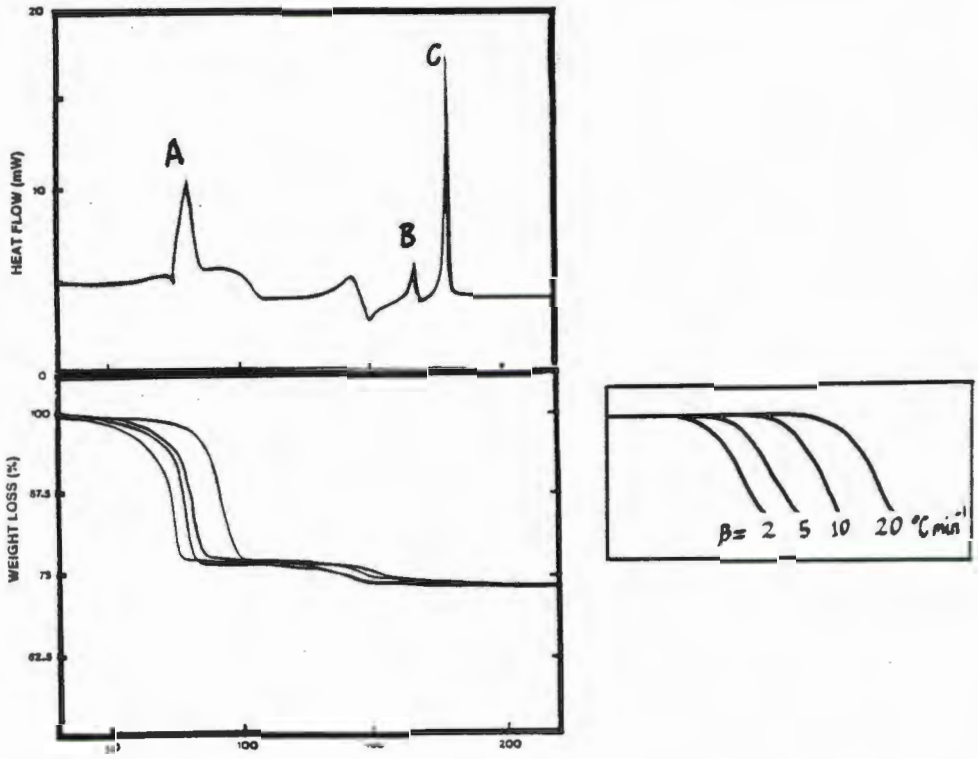

Figure 32

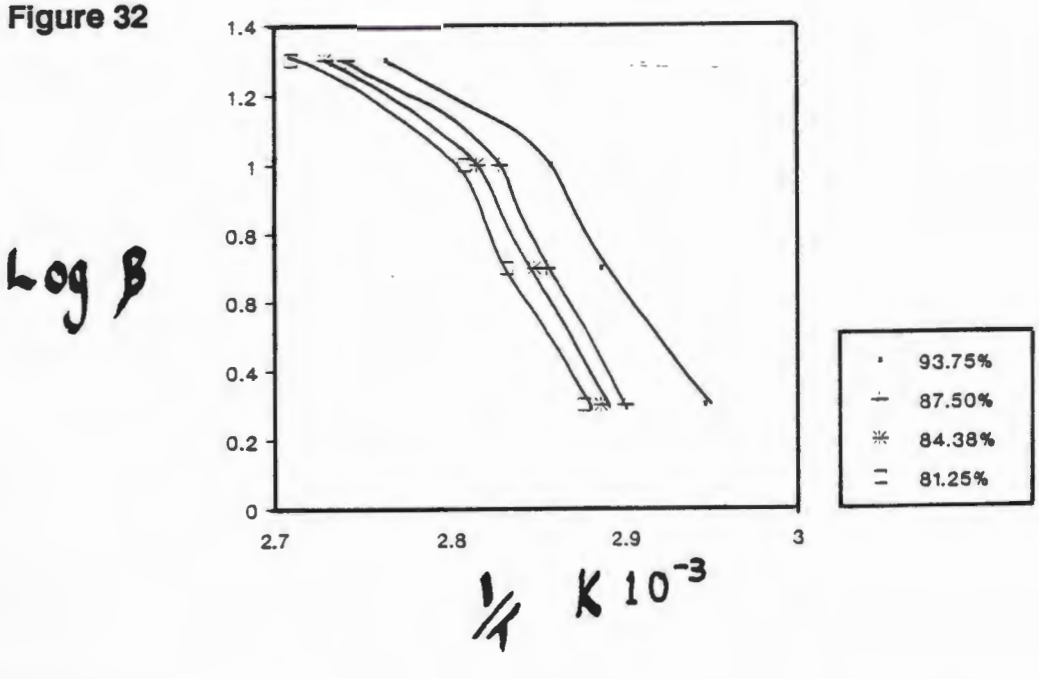

TABLE 6 CRYSTAL DATA AND EXPERIMENTAL DETAILS FOR WEB11-p-XYLENE STRUCTURE.

Compound	WEB11-p-Xylene
Molecular formula	$2C_{38}H_{30}O_2.3½C_8H_{10}$
Molecular weight ($gmol^{-1}$)	1408.89
Space group	$P2_1/n$
a (Å)	20.354(3)
b (Å)	21.142(4)
c (Å)	21.327(4)
α (°)	90
β (°)	117.92(1)
γ (°)	90
Z	4
V ($Å^3$)	8109(3)
D_c (gcm^{-3})	1.15
D_m (gcm^{-3})	1.15(2)
$\mu(MoK_\alpha)$ (cm^{-1})	0.71
F(000)	3004
Data collection (21°C)	
Crystal dimensions (mm)	0.38x0.38x0.44
Range scanned θ (°)	1-23
Range of indices *h,k,l*	+23,±22
Reflections for lattice parameters no.,θ range (°)	24,16-17
Instability of standard reflections (%)	-0.3
Scan mode	(ω-2θ)
Scan width in(°)	(0.75+0.35tanθ)
Vertical aperture length (mm)	4
Aperture width (mm)	(1.12+1.05tanθ)
Number of reflections collected (unique)	8592
Number of reflections observed with $I_{rel} > 2\sigma I_{rel}$	5226
Final refinement	
Number of parameters	894
R	0.072
wR	0.077
w	$(\sigma^2(F_o)+0.001F_o^2)^{-1}$
S	2.80
Max. shift/e.s.d.	0.51
Max. height in difference electron density map ($eÅ^{-3}$)	0.46
Min. height in difference electron density map ($eÅ^{-3}$)	-0.33

ATOMIC COORDINATES

TABLE 7

$U_{eq} = (1/3)\Sigma\Sigma U_{ij} a_i a_i^* a_i \cdot a_j$

Fractional atomic coordinates ($x10^4$) and thermal parameters ($Å^2 x10^3$) with e.s.d.'s in parentheses for WEB11 (1) C2/c

Atom	x/a	y/b	z/c	Uequiv
O(1)	3024(1)	643(1)	723(2)	50(1)
C(1)	2980(1)	694(2)	2050(2)	39(1)
C(11)	3327(1)	1577(2)	2577(2)	40(1)
C(12)	3601(2)	2197(2)	1805(3)	54(1)
C(13)	3906(2)	2991(2)	2285(3)	66(1)
C(14)	3922(2)	3181(2)	3532(3)	62(1)
C(15)	3647(2)	2575(2)	4318(3)	61(1)
C(16)	3347(2)	1772(2)	3849(3)	53(1)
C(21)	3426(2)	-107(2)	2658(3)	41(1)
C(22)	3103(2)	-938(2)	2404(3)	55(1)
C(23)	3504(2)	-1687(2)	2855(3)	64(1)
C(24)	4246(2)	-1620(2)	3562(3)	62(1)
C(25)	4580(2)	-807(2)	3798(3)	61(1)
C(26)	4173(2)	-52(2)	3350(3)	50(1)
C(51)	2087(1)	674(2)	2186(2)	37(1)
C(52)	1527(2)	961(2)	1206(2)	40(1)
C(53)	718(2)	964(2)	1328(2)	40(1)
C(54)	436(1)	702(2)	2432(2)	35(1)
C(55)	1002(2)	425(2)	3416(2)	38(1)
C(56)	1807(2)	409(2)	3300(2)	40(1)

TABLE 8

Fractional atomic coordinates ($x10^4$) and thermal parameters ($Å^2 x10^3$) with e.s.d.'s in parentheses for WEB11 Compound (2) P1

Atom	x/a	y/b	z/c	Uequiv
O(1)	4183(2)	6400(1)	1949(1)	43(1)
C(1)	4700(2)	7788(2)	1815(1)	35(1)
O(2)	12768(2)	13758(2)	7519(1)	45(1)
C(2)	12225(3)	14519(2)	7018(1)	37(1)
C(11)	5529(2)	7907(2)	1002(1)	36(1)
C(12)	5921(3)	9091(2)	675(1)	42(1)
C(13)	6635(3)	9192(2)	-68(1)	49(1)
C(14)	6966(3)	8102(2)	-504(1)	51(1)
C(15)	6583(3)	6924(2)	-192(1)	51(1)
C(16)	5876(3)	6824(2)	556(1)	44(1)
C(21)	3107(2)	8025(2)	1702(1)	37(1)
C(22)	1732(3)	6960(2)	1208(1)	48(1)
C(23)	310(3)	7165(3)	1044(2)	57(1)
C(24)	223(3)	8416(3)	1377(2)	59(1)
C(25)	1567(3)	9464(3)	1879(2)	55(1)
C(26)	3003(3)	9272(2)	2035(1)	45(1)
C(31)	11512(3)	15402(2)	7598(1)	39(1)
C(32)	10003(3)	15452(2)	7416(1)	47(1)
C(33)	9464(3)	16314(3)	7967(2)	59(1)
C(34)	10423(3)	17110(3)	8712(2)	62(1)
C(35)	11903(3)	17045(3)	8899(2)	59(1)

C(36)	12466(3)	16210(2)	8354(1)	52(1)
C(41)	13769(3)	15424(2)	6670(1)	38(1)
C(42)	14040(3)	16769(2)	6595(2)	52(1)
C(43)	15402(3)	17536(2)	6222(2)	62(1)
C(44)	16495(3)	16986(3)	5927(2)	64(1)
C(45)	16237(3)	15649(3)	6002(2)	65(1)
C(46)	14873(3)	14876(2)	6363(1)	51(1)
C(51)	5836(2)	8797(2)	2600(1)	35(1)
C(52)	7359(3)	9856(2)	2574(1)	40(1)
C(53)	8314(3)	10739(2)	3310(1)	42(1)
C(54)	7786(3)	10592(2)	4093(1)	39(1)
C(55)	6266(3)	9505(2)	4123(1)	43(1)
C(56)	5307(3)	8645(2)	3389(1)	41(1)
C(61)	10975(3)	13476(2)	6275(1)	37(1)
C(62)	10731(3)	13903(2)	5547(1)	46(1)
C(63)	9673(3)	12975(2)	4858(1)	46(1)
C(64)	8821(3)	11576(2)	4867(1)	40(1)
C(65)	9049(3)	11159(2)	5597(1)	58(1)
C(66)	10109(3)	12092(2)	6287(1)	57(1)

TABLE 9

Fractional atomic coordinates ($x10^4$) and thermal parameters ($Å^2x10^3$) with e.s.d.'s in parentheses for WEB10

Atom	x/a	y/b	z/c	Uequiv/Uiso(*)
C(1)	7044(2)	6455(3)	1185(1)	45(1)
H(1)	7717(21)	5861(34)	1297(9)	57(8)*
C(6)	8408(2)	14094(4)	-1526(1)	48(1)
H(2)	8674(19)	13322(35)	-1757(9)	55(8)*
C(11)	6833(2)	7537(3)	1603(1)	45(1)
C(12)	7646(2)	8611(4)	1851(1)	61(1)
C(13)	7501(3)	9593(4)	2237(1)	72(1)
C(14)	6552(3)	9534(4)	2382(1)	69(1)
C(15)	5737(3)	8499(4)	2138(1)	62(1)
C(16)	5873(2)	7507(3)	1751(1)	50(1)
C(21)	6235(2)	4992(3)	1054(1)	42(1)
C(22)	6341(2)	3567(3)	1357(1)	52(1)
C(23)	5607(2)	2257(4)	1274(1)	59(1)
C(24)	4736(2)	2333(4)	886(1)	59(1)
C(25)	4625(2)	3720(4)	581(1)	57(1)
C(26)	5367(2)	5046(4)	662(1)	50(1)
C(31)	9338(2)	15312(3)	-1315(1)	47(1)
C(32)	9905(2)	16034(4)	-1627(1)	63(1)
C(33)	10729(2)	17178(5)	-1468(1)	75(1)
C(34)	11005(3)	17636(4)	-992(2)	80(2)
C(35)	10468(3)	16919(4)	-674(1)	75(1)
C(36)	9633(2)	15756(4)	-832(1)	58(1)
C(41)	7462(2)	15075(4)	-1826(1)	55(1)
C(42)	6844(3)	14320(5)	-2239(1)	81(2)
C(43)	5969(3)	15192(7)	-2515(2)	109(2)
C(44)	5700(3)	16774(8)	-2384(2)	105(2)
C(45)	6303(3)	17549(6)	-1982(1)	92(2)
C(46)	7182(2)	16713(5)	-1703(1)	72(1)
C(51)	7174(2)	7562(3)	761(1)	42(1)
C(52)	8000(2)	7264(4)	536(1)	69(1)
C(53)	8153(2)	8273(4)	158(1)	70(1)
C(54)	7483(2)	9651(3)	-13(1)	45(1)

C(55)	6649(2)	9951(3)	214(1)	47(1)
C(56)	6499(2)	8932(3)	594(1)	47(1)
C(61)	8110(2)	12927(4)	-1147(1)	48(1)
C(62)	7331(3)	13310(5)	-905(1)	93(2)
C(63)	7125(3)	12266(5)	-545(1)	96(2)
C(64)	7679(2)	10768(3)	-413(1)	46(1)
C(65)	8445(3)	10385(4)	-662(1)	82(2)
C(66)	8648(3)	11435(4)	-1021(1)	81(2)

TABLE 10

Fractional atomic coordinates ($x10^4$) and thermal parameters ($Å^2x10^3$) with e.s.d.'s in parentheses for the WEB11-Acetone compound

Atom	x/a	y/b	z/c	Uequiv
O(1)	1854(2)	7011(7)	2652(0)	47(2)
C(1)	1599(3)	5890(9)	3171(6	40(3)
O(2)	615(2)	-4472(7)	-818(5)	51(2)
C(2)	870(3)	-3213(10)	-1276(6)	36(2)
C(12)	1229(2)	8570(6)	3649(6)	51(3)
C(13)	856(2)	9509(6)	3940(6)	64(4)
C(14)	433(2)	8747(6)	4080(6)	68(4)
C(15)	381(2)	7047(6)	3930(6)	68(4)
C(16)	754(2)	6108(6)	3639(6)	51(3)
C(11)	1178(2)	6870(6)	3499(6)	37(3)
C(22)	2362(2)	5528(8)	3965(5)	56(3)
C(23)	2623(2)	5022(8)	4684(5)	70(4)
C(24)	2410(2)	4321(8)	5414(5)	67(4)
C(25)	1934(2)	4125(8)	5426(5)	80(4)
C(26)	1673(2)	4631(8)	4708(5)	69(4)
C(21)	1887(2)	5333(8)	3977(5)	39(3)
C(32)	1717(2)	-3062(6)	-1679(6)	63(4)
C(33)	2120(2)	-3809(6)	-1976(6)	83(5)
C(34)	2129(2)	-5511(6)	-2149(6)	94(6)
C(35)	1735(2)	-6467(6)	-2024(6)	83(5)
C(36)	1332(2)	-5720(6)	-1727(6)	59(3)
C(31)	1323(2)	-4018(6)	-1555(6)	45(3)
C(42)	800(2)	-2628(9)	-2928(5)	67(4)
C(43)	539(2)	-2148(9)	-3652(5)	82(5)
C(44)	81(2)	-1694(9)	-3541(5)	73(4)
C(45)	-116(2)	-1722(9)	-2706(5)	76(5)
C(46)	146(2)	-2202(9)	-1982(5)	57(4)
C(41)	604(2)	-2655(9)	-2093(5)	49(3)
C(51)	967(3)	-1808(9)	-615(6)	38(3)
C(52)	898(3)	-129(9)	-802(6)	45(3)
C(53)	996(3)	1082(10)	-161(6)	42(3)
C(54)	1161(3)	675(9)	652(6)	36(3)
C(55)	1232(3)	-1022(9)	807(6)	45(3)
C(56)	1148(3)	-2210(10)	179(7)	46(3)
C(61)	1461(3)	4408(9)	2588(6)	34(2)
C(62)	1638(3)	2843(9)	2658(7)	42(3)
C(63)	1541(3)	1655(10)	2032(6)	47(3)
C(64)	1266(2)	1944(8)	1317(6)	30(2)
C(65)	1073(3)	3545(9)	1261(6)	42(3)
C(66)	1171(3)	4716(9)	1874(7)	45(3)
O(1GA)	2395(3)	521(9)	6743(6)	77(2)
C(1GA)	2348(4)	-152(13)	6052(7)	62(3)

C(2GA)	1873(6)	-818(22)	5777(13)	125(5)
C(3GA)	2754(6)	-310(20)	5422(12)	115(5)
O(1GB)	197(4)	3089(13)	5112(8)	116(3)
C(1GB)	293(4)	3019(13)	5899(8)	69(3)
C(2GB)	766(6)	2463(19)	6164(11)	106(4)
C(3GB)	-22(7)	3353(24)	6609(14)	140(6)

TABLE 11

Fractional atomic coordinates ($x10^4$) and thermal parameters ($Åx10^3$) with e.s.d.'s in parentheses for the WEB11-1,4-Dioxane structure

Atom	x/a	y/b	z/c	Uequiv/Uiso(*)
O(1)	785(2)	8540(1)	6005(2)	46(1)
H(1)	509(42)	8867(23)	6514(20)	81(13)*
C(1)	-397(3)	7936(2)	5516(2)	38(1)
C(11)	-30(3)	7659(2)	4584(2)	43(1)
C(12)	-1118(4)	7519(3)	3736(3)	58(1)
C(13)	-743(6)	7235(3)	2910(3)	75(2)
C(14)	708(7)	7103(3)	2937(4)	84(2)
C(15)	1787(5)	7237(3)	3770(4)	76(2)
C(16)	1421(4)	7506(2)	4595(3)	55(1)
C(21)	-424(3)	7052(2)	6128(2)	38(1)
C(22)	-632(3)	6154(2)	5752(2)	46(1)
C(23)	-581(4)	5374(2)	6337(3)	56(1)
C(24)	-324(4)	5482(3)	7303(3)	58(2)
C(25)	-135(4)	6373(3)	7694(3)	63(2)
C(26)	-183(4)	7155(2)	7120(2)	57(1)
C(61)	-1834(3)	8502(2)	5334(2)	38(1)
C(62)	-3091(3)	8189(2)	5538(2)	44(1)
C(63)	-4329(3)	8770(2)	5406(2)	45(1)
C(64)	-4346(3)	9693(2)	5065(2)	36(1)
C(65)	-3087(3)	9979(2)	4819(3)	52(1)
C(66)	-1868(3)	9402(2)	4944(3)	54(1)
O(1G)	318(3)	9559(2)	7548(2)	77(1)
O(2G)	486(3)	11011(2)	8881(2)	98(2)
C(1G)	-878(5)	10158(4)	7536(4)	122(3)
C(2G)	-819(6)	10569(4)	8441(5)	123(3)
C(3G)	1672(5)	10434(4)	8873(4)	119(3)
C(4G)	1648(5)	10043(4)	7962(5)	119(3)

TABLE 12

Fractional atomic coordinates ($x10^4$) and thermal parameters (A^2x10^3) with e.s.d.'s in parentheses for the WEB11-Acetophenone structure

Atom	x/a	y/b	z/c	Uequiv
O(1)	1101(7)	6338(5)	5893(4)	50(2)
C(1)	-298(9)	6980(6)	6773(6)	37(3)
C(11)	-1099(9)	5993(7)	7429(6)	36(3)
C(12)	-1672(12)	5999(8)	8538(8)	57(4)
C(13)	-2495(15)	5126(10)	9117(9)	74(5)
C(14)	-2760(15)	4279(10)	8545(10)	75(5)
C(15)	-2199(14)	4236(9)	7414(11)	77(5)
C(16)	-1349(11)	5114(7)	6838(8)	55(4)

C(21)	518(10)	7559(7)	7503(7)	45(3)
C(22)	-122(12)	8786(8)	7790(8)	59(4)
C(23)	691(15)	9266(11)	8454(9)	4(5)
C(24)	2145(17)	8551(14)	8856(10)	85(6)
C(25)	2781(14)	7350(13)	8571(10)	82(6)
C(26)	2019(12)	6870(9)	7924(8)	62(4)
C(51)	-1673(9)	7899(6)	6258(7)	39(3)
C(52)	-3493(11)	8201(8)	6747(7)	57(3)
C(53)	-4739(10)	9007(8)	6286(7)	54(3)
C(54)	-4349(9)	9578(6)	5246(6)	35(3)
C(55)	-2503(11)	9295(9)	4790(9)	76(4)
C(56)	-1259(11)	8480(9)	5238(8)	64(4)
O(1G)	3230(8)	7583(6)	4429(6)	70(3)
C(1G)	4857(12)	7194(7)	4072(8)	52(4)
C(2G)	6028(13)	6362(8)	4701(9)	67(4)
C(12G)	4391(7)	8401(6)	2323(6)	71(5)
C(13G)	5026(7)	8787(6)	1244(6)	96(6)
C(14G)	6829(7)	8369(6)	748(6)	115(8)
C(15G)	7993(7)	7564(6)	1330(6)	120(8)
C(16G)	7358(7)	7177(6)	2409(6)	87(5)
C(11G)	5556(7)	7596(6)	2904(6)	47(3)

TABLE 13

Fractional atomic coordinates ($x10^4$) and thermal parameters ($Å^2x10^3$) with e.s.d.'s in parentheses for the WEB11-p-xylene structure

Atom	x/a	y/b	z/c	Uequiv/Uiso(*)
O(1A)	531(2)	6397(2)	2037(2)	42(2)
H(1A)	807(4)	6095(3)	2398(3)	146(35)*
O(2A)	4215(2)	9328(2)	6792(2)	41(2)
H(2A)	4620(3)	9072(3)	6842(4)	113(28)*
C(1A)	1016(3)	6826(2)	1932(3)	38(2)
C(2A)	3775(3)	9730(2)	6185(3)	37(2)
C(12A)	641(2)	7892(2)	1289(2)	57(3)
C(13A)	174(2)	8260(2)	707(2)	70(4)
C(14A)	-445(2)	7986(2)	143(2)	57(3)
C(15A)	-595(2)	7345(2)	161(2)	59(3)
C(16A)	-128(2)	6977(2)	743(2)	53(3)
C(11A)	491(2)	7250(2)	1307(2)	36(3)
C(22A)	1926(2)	5937(2)	2178(2)	72(4)
C(23A)	2432(2)	5594(2)	2042(2)	90(5)
C(24A)	2565(2)	5768(2)	1480(2)	82(5)
C(25A)	2191(2)	6283(2)	1053(2)	83(4)
C(26A)	1685(2)	6625(2)	1189(2)	60(3)
C(21A)	1553(2)	6452(2)	1751(2)	42(3)
C(32A)	3571(2)	10376(2)	7063(2)	55(3)
C(33A)	3125(2)	10733(2)	7267(2)	69(4)
C(34A)	2369(2)	10804(2)	6804(2)	69(4)
C(35A)	2057(2)	10518(2)	6138(2)	71(4)
C(36A)	2500(2)	10161(2)	5933(2)	56(3)
C(31A)	3258(2)	10089(2)	6396(2)	41(3)
C(42A)	4929(2)	9935(1)	6065(2)	48(3)
C(43A)	5378(2)	10324(1)	5898(2)	60(3)
C(44A)	5186(2)	10956(1)	5721(2)	69(4)
C(45A)	4544(2)	11200(1)	5711(2)	73(4)

C(46A)	4093(2)	10811(1)	5877(2)	59(4)
C(41A)	4287(2)	10178(1)	6054(2)	40(3)
C(51A)	1451(3)	7228(2)	2599(3)	35(2)
C(52A)	1169(3)	7339(2)	3072(3)	41(3)
C(53A)	1538(3)	7731(2)	3650(3)	40(3)
C(54A)	2193(3)	8032(2)	3782(3)	38(3)
C(55A)	2483(3)	7904(3)	3322(3)	44(3)
C(56A)	2122(3)	7508(2)	2744(3)	42(3)
C(61A)	3343(3)	9296(2)	5536(3)	35(3)
C(62A)	3270(3)	9436(2)	4881(3)	40(3)
C(63A)	2890(3)	9027(3)	4312(3)	44(3)
C(64A)	2570(3)	8475(2)	4386(3)	36(3)
C(65A)	2628(3)	8348(3)	5051(3)	45(3)
C(66A)	3008(3)	8751(2)	5619(3)	43(3)
O(1B)	-366(2)	6517(2)	2965(2)	40(2)
H(1B)	-662(4)	6251(3)	2563(3)	139(33)*
O(2B)	-4160(2)	9334(2)	-1763(2)	43(2)
H(2B)	-4545(3)	9107(3)	-1717(4)	134(31)*
C(1B)	-825(3)	6959(2)	3105(3)	38(3)
C(2B)	-3765(3)	9780(2)	-1192(3)	37(2)
C(12B)	-1515(2)	6735(2)	3827(2)	57(3)
C(13B)	-2040(2)	6391(2)	3935(2)	73(4)
C(14B)	-2428(2)	5898(2)	3477(2)	72(4)
C(15B)	-2292(2)	5747(2)	2911(2)	80(5)
C(16B)	-1768(2)	6090(2)	2803(2)	63(3)
C(11B)	-1379(2)	6583(2)	3261(2)	38(3)
C(22B)	-291(2)	7999(2)	3759(2)	48(3)
C(23B)	215(2)	8329(2)	4357(2)	63(4)
C(24B)	741(2)	8000(2)	4946(2)	63(3)
C(25B)	760(2)	7341(2)	4936(2)	57(3)
C(26B)	254(2)	7009(2)	4338(2)	50(3)
C(21B)	-271(2)	7339(2)	3749(2)	35(3)
C(32B)	-4177(2)	10818(2)	-879(2)	59(3)
C(33B)	-4667(2)	11167(2)	-729(2)	73(4)
C(34B)	-5303(2)	10882(2)	-768(2)	73(4)
C(35B)	-5449(2)	10247(2)	-957(2)	61(3)
C(36B)	-4958(2)	9896(2)	-1107(2)	54(3)
C(31B)	-4323(2)	10182(2)	-1068(2)	38(3)
C(42B)	-2554(2)	10280(2)	-1037(2)	57(3)
C(43B)	-2167(2)	10649(2)	-1296(2)	69(3)
C(44B)	-2543(2)	10925(2)	-1967(2)	71(4)
C(45B)	-3306(2)	10831(2)	-2378(2)	69(4)
C(46B)	-3693(2)	10461(2)	-2119(2)	56(3)
C(41B)	-3318(2)	10186(2)	-1449(2)	42(3)
C(51B)	-1252(3)	7384(2)	2454(3)	36(3)
C(52B)	-969(3)	7501(3)	1981(3)	44(3)
C(53B)	-1339(3)	7898(2)	1408(3)	44(3)
C(54B)	-1989(3)	8211(2)	1292(3)	37(2)
C(55B)	-2255(3)	8090(3)	1775(3)	50(3)
C(56B)	-1897(3)	7688(3)	2336(3)	47(3)
C(61B)	-3271(3)	9399(2)	-524(3)	37(3)
C(62B)	-3185(3)	9550(3)	144(3)	44(3)
C(63B)	-2755(3)	9175(3)	727(3)	46(3)
C(64B)	-2392(3)	8638(2)	679(3)	37(3)
C(65B)	-2457(3)	8501(2)	16(3)	44(3)
C(66B)	-2881(3)	8872(2)	-569(3)	44(3)
C(1EG)	4683(5)	4436(4)	2074(5)	86(5)

C(2EG)	4197(4)	4703(4)	1445(5)	93(5)
C(3EG)	4440(5)	5058(4)	1062(5)	95(5)
C(4EG)	5167(5)	5170(3)	1257(5)	83(5)
C(5EG)	5665(4)	4894(4)	1883(5)	95(5)
C(6EG)	5427(5)	4535(4)	2291(4)	93(5)
C(1ME)	4412(5)	4048(4)	2511(5)	130(7)
C(2ME)	5447(6)	5590(4)	840(6)	137(8)
C(1FG)	6773(5)	2806(3)	-163(5)	82(5)
C(2FG)	7402(5)	2909(3)	490(4)	83(5)
C(3FG)	8054(4)	2618(4)	662(4)	84(5)
C(4FG)	8126(4)	2197(3)	201(5)	80(4)
C(5FG)	7500(5)	2103(4)	-456(5)	89(5)
C(6FG)	6836(5)	2399(4)	-621(4)	88(4)
C(1MF)	6043(5)	3124(4)	-362(6)	131(7)
C(2MF)	8853(5)	1870(5)	395(6)	141(7)
C(1HG)	5636(4)	7282(4)	2301(4)	93(2)
C(2HG)	5335(4)	7812(4)	2412(4)	108(3)
C(3HG)	4770(5)	7755(5)	2590(4)	117(3)
C(4HG)	4512(5)	7194(5)	2653(5)	116(3)
C(5HG)	4810(5)	6618(5)	2548(4)	120(3)
C(6HG)	5399(4)	6689(4)	2374(4)	105(3)
C(1MH)	6314(6)	7334(5)	2118(6)	159(4)
C(2MH)	3869(7)	7110(6)	2864(7)	204(5)
C(1IG)	5437(5)	4960(4)	4619(5)	122(3)
C(2IG)	5245(6)	4700(4)	5662(5)	129(3)
C(6IG)	4379(5)	5316(4)	4746(5)	117(3)
C(1MI)	4158(7)	5055(6)	5824(7)	193(5)

CHAPTER SEVEN

CONCLUSION

The inclusion properties of three host compounds have been investigated. By virtue of their shape these host compounds are described as "wheel-and-axle" host compounds. They comprise bulky phenyl groups which are attached to either end of a relatively thin molecular axis as well as hydroxy groups as peripheral functional sensors. The latter provide effective multiple binding sites for other polar functions owing to their ability to donate as well as to accept hydrogen bonds. The molecular axis had been incorporated in the host design with the aim of creating molecules capable of higher molecular organisation in the crystal packing.

HOST1

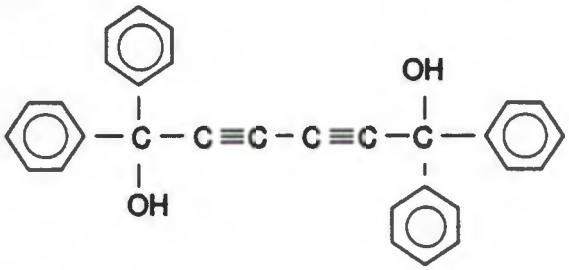

WEB11

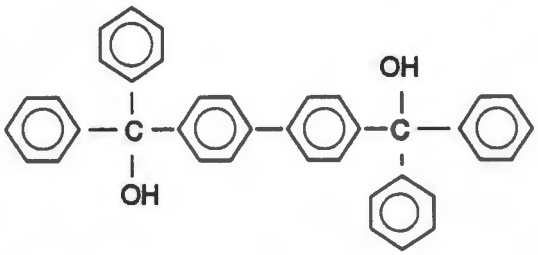

WEB10

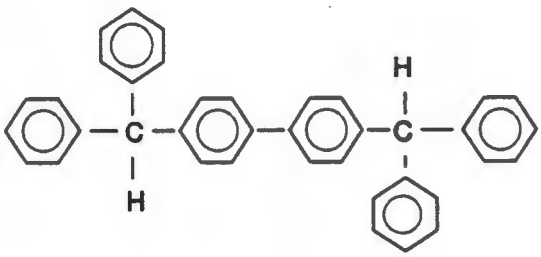

Host1 was found to form host-guest hydrogen bonded inclusion compounds with polar guests. In these compounds the host1 hydroxy moieties adopted a *trans* conformation, and the guests were located either in channels, or else in cavities. Polar guests of higher vapour pressures formed tubulato-clathrates, and those of lower vapour pressures, æediculato-clathrates. 1,4-Dioxane, a weaker hydrogen bond acceptor, formed a tubulato-clathrate with host1 in which one of the two guest molecules was hydrogen

bonded to the host, the other being held in place by van der Waals forces.

Host1 and apolar guest formed host-host coordination assisted inclusion compounds in which intermolecular host hydrogen bonded networks entrapped guest molecules by van der Waals forces and steric barriers. In order to achieve this the host1 hydroxy groups adopted a gauche conformation. This implies that the drive to form hydrogen bond is dominant in inclusion compound formation and overrides destabilisation resulting from a less favourable host conformation. Host-host hydrogen bonding interactions often resulted in the formation of tetrameric networks because co-operative hydrogen bonds are more energetically favoured than isolated ones. Crystal packing of the tetrameric entities is stabilized by van der Waals forces resulting from host-host interaction. Host1 was thus found to include a wide variety of guests differing in shape, size and polarity by hydrogen bonding either to other host1 molecules, or else to polar guests. Thus the ability of host1 to hydrogen bond both dominates and directs its inclusion behaviour and guest selectivity.

The location of the hydroxy groups in α-phase host1 was found to be important with respect to the gas-solid and solid-solid reaction in which hydroxy groups exposed on the bc plane of α-form host1 permit one-dimensional attack by incoming guest species. The mechanism of a solid-solid reaction involving host1 and benzophenone was investigated. Scanning electron microscopy showed that the surface area of the reactant was of crucial importance while the molecular structure suggested a possible mechanism. The external habit of the form of α-phase host1 proved to play a pivotal role in the propagation of the solid phase reaction. The porosity evident in the habit of host1 grown from acetone and vacuum dried, provided access to reactive sites within the crystal which were effectively protected in the habit of α host1 grown from ether. Turbulence was necessary to propagate the reaction by encouraging migration of reacting guest particles along grain boundaries and lattice imperfections. Contrary to initial preconceptions, vapour phase diffusion was determined not be a dominant factor influencing the rate determining step although its effect may be implemented if the solid reactants are heated together.

WEB11 has a molecular backbone comprised of two phenyl rings. In comparison to host1, guest inclusion was found to be more selective since a smaller number of guest molecules as well as the para isomer only of xylene, were included. Polymorphism requires a molecule to contain some degrees of molecular freedom so that the possibility of adopting different conformations and molecular arrangements in the crystal state exists. The relative flexibility of the WEB11 axis not only resulted in two α forms but also

appeared to introduce a degree of guest selectivity. The axis of WEB11 must influence crystal formation by means of stacking arrangements and significant van der Waals interactions. Formation of host-host hydrogen bonds involving WEB11 host molecules resulted in a gauche conformation of the hydroxy moieties in inclusion compounds in which the guest was apolar, for example p-xylene. Hydrogen bonds are directed forces are the major influence governing the form of the host-guest arrays. In WEB11, the influence of functionality works in conjunction with the van der Waals forces arising from the aromatic backbone, although the tradeoff between van der Waals forces and directional interactions is not fully understood **(11)**.
Pre-eminence of hydrogen bond formation in the formation host-guest inclusion compounds for these "wheel-and-axle" host compounds, is supported by the behaviour of WEB10. In a molecule of WEB10, the "wheel-and-axle" shape is retained but the functionality is absent. This "host" compound was not able to include any molecular species as guests, for example apolar aromatic compounds. This implies that van der Waals interactions alone are insufficient stabilizing forces in the formation of inclusion compounds with the "wheel-and-axle" hosts studied.

Thermal analysis proved to be a very useful investigative technique since precise stoicheioimetries could be determined and insight into the manner of decomposition and strength of host-guest binding could be derived. TG was used to detect the presence and concentration of guest species present in host-guest inclusion compounds. It was also employed to study the guest release behaviour as a function of weight loss. DSC proved useful to fingerprint the melting of host-guest compounds as a function of enthalpic values. The temperature at which a guest desorbed served as a method to examine the strength with which the guest species is held in the β-lattice. Optical observation of the thermal decomposition showed formation of new phases which could be correlated with DSC and TG results and proof of new phases was provided by X-ray powder diffraction. In order to improve the correlation of crystal energies with thermal parameters in further work, DSC sample preparation technique with respect to controlling crystallite size should be improved so that more precise values of the enthalpies of the guest release reaction can be obtained.
The techniques of TG and DSC have not been widely used to examine inclusion compounds but the results obtained are encouraging and justify further use of these techniques as analytical as well as investigative tools in the field of host-guest chemistry.

---

11 GR Desiraju, "*Crystal Engineering*", op. cit., 109